Amino-acid-derived, pH-responsive polyelectrolytes

Dissertation

Zur Erlangung des akademischen Grades

Eines Doktors der Naturwissenschaften (Dr. rer. nat.)

In der Bayreuther Graduiertenschule für Mathematik und Naturwissenschaften

(BayNAT)

Der Universität Bayreuth

vorgelegt von

Jonas De Breuck

aus Sint-Niklaas

Bayreuth, 2025

Der experimentelle Teil der vorliegenden Arbeit wurde in der Zeit von Dezember 2022 bis Dezember 2025 in Bayreuth am Lehrstuhl nachhaltige und funktionale Polymere unter Betreuung von Frau Prof. Dr. Meike Nicole Leiske angefertigt.

Vollständiger Abdruck der von der Bayreuther Graduiertenschule für Mathematik und Naturwissenschaften (BayNAT) der Universität Bayreuth genehmigten Dissertation zur Erlangung des akademischen Grades eines Doktors der Naturwissenschaften (Dr. rer. nat.)

Form der Dissertation: Kumulative Dissertation

Dissertation eingereicht am: 22. Januar 2026

Zulassung durch das Leitungsgremium:19. Februar 2026

Wissenschaftliches Kolloquium:14. Juli 2026

Amtierender Direktor: Prof. Dr. Jürgen Senker

Prüfungsausschuss:

JProf. Dr. Meike Leiske	(Gutachterin)
Prof. Dr. André Gröschel	(Gutachter)
Prof. Dr. Georg Papastavrou	(Vorsitz)
JProf. Dr. Hannah Kurz	

List of Publications

The most important results of my thesis are summarized and presented in the form of 3 manuscripts, 2 of which have been published in peer-reviewed journals. The following papers are the subject to this thesis:

[I] Jonas De Breuck, Michael Streiber, Michael Ringleb, Dennis Schröder, Natascha Herzog, Ulrich S. Schubert, Stefan Zechel, Anja Traeger, Meike N. Leiske
Amino-Acid-Derived Anionic Polyacrylamides with Tailored Hydrophobicity–Physicochemical Properties and Cellular Interactions
ACS Polymers Au, **2024**, 4, 3, 222-234

[II] Jonas De Breuck, Valérie Jérôme, Ruth Freitag, Meike N. Leiske
Zwitterionic Amino-Acid-Derived Polyacrylamides with a Betaine Twist – Synthesis and Characterization
Macromolecular Rapid Communications, **2025**, 46, 2400623

[III] Jonas De Breuck, Theresa M. Lutz, Christian Jahns, Jonas Debbeler, Valérie Jérôme, Ruth Freitag, Anja Traeger, Meike N. Leiske
Impact of the polymer side-chain chemistry on interactions of amino-acid-derived polyelectrolytes with cells
Submitted to Journal of Material Chemistry B, currently under peer-review

During my thesis, I was involved in further collaborations and co-authored the following peer-reviewed publications. As these publications are not in the focus of this thesis, they will not be discussed further:

[I] Anne-Catherine Lehnen, Sergio Kogikoski Jr., Till Stensitzki, Ahmad AlSawaf, Alain M. Bapolisi, Martin Wolff, Jonas De Breuck, Henrike M. Müller-Werkmeister, Salvatore Chiantia, Ilko Bald, Meike N. Leiske and Matthias Hartlieb
Anisotropy in Antimicrobial Bottle Brush Copolymers and Its Influence on Biological Activity
Advanced Functional Materials, **2024,** 34, 2312651

[II] Cevin P. Braksch, Anne-Catherine Lehnen, Alain M. Bapolisi, Johannes Gurke, Jonas De Breuck, Meike N. Leiske and Matthias Hartlieb
Staphylococcus aureus selective antimicrobial polymers based on an arginine-derived monomer
Journal of Polymer Science, **2024,** 62, 1, 132-145

[III] Amphiphilic Zwitterionic Bioderived Block Copolymers from Glutamic Acid and Cholesterol – Ability to Form Nanoparticles and Serve as Vectors for the Delivery of 6-Mercaptopurine
Meike N. Leiske, Christopher Kuenneth, Jonas De Breuck, Bruno G. De Geest and Richard Hoogenboom
Macromolecular Chemistry and Physics, **2023**, 224, 2300200

[IV] Theresa M. Lutz, Cevin P. Braksch, Jonas De Breuck, Matthias Hartlieb and Meike N. Leiske
Bio-inspired, Zwitterionic Copolymers with Amphiphilic Character
Macromolecular Rapid Communications, **2025**, 2401099

Finally, I contributed to the preparation of a review article published in a peer-reviewed journal. Portions of this publication have been incorporated into this thesis and are cited accordingly:

[I] Theresa M. Lutz, Jonas De Breuck, Sahar Salehi, Meike N. Leiske
Smart, Bio-Inspired Polymers and Bio-Based Molecules Modified by Zwitterionic Motifs to Design Next-Generation Materials for Medical Applications
Advanced Functional Materials, **2025**, e13765

Summary

Drug carriers increase the therapeutic efficiency by reaching intracellular targets that remain inaccessible to small drug molecules; however, efficient intracellular delivery remains a key challenge for therapeutic as the plasma membrane strongly limits passive diffusion of proteins, peptides, and nucleic acids. Typically, active internalization such as transporters-mediated uptake or endocytosis are necessary. As a result, ideal carrier materials remain colloidally stable and show low-fouling characteristics in biological media such as blood, while still showing association to target cells or transporters and promoting cellular uptake in a controlled, stimulus-dependent manner. Ideally, complex and costly targeting ligands are not required. This dissertation addresses such material-design concepts by developing and systematically studying **amino-acid-derived, pH-responsive polyelectrolytes.** The established polymers and their investigated structure–property–function relationships provide information about smart molecular design to control protein interactions, membrane association, and cellular uptake.

Amino acids are unique, bio-inspired building blocks for the design of functional polymers: they introduce chirality, offer tunable hydrophobicity and aromaticity, and contain ionizable, functional groups. On the one hand, their biomimetic character should reduce unspecific fouling and on the other hand opportunities for selective interactions with proteins/transporters and cell membranes are created. Across all three parts of this work, reversible addition–fragmentation chain-transfer (RAFT) polymerization and post-polymerization modification (PPM) are used to generate well-defined polymer libraries with different physicochemical properties resulting in tailored cell interactions.

In the *first publication*, a synthetic strategy is established to acquire **chiral, amino-acid-derived polybetaines**, which combine both, the zwitterionic and low-fouling characteristics of polybetaines and the tunable chirality and diversity of side-chain moieties based on amino-acid-derived polyzwitterions. Using methylated lysine as a model system, the study demonstrates that permanent positive charges broaden the pH range over which the polymers remain zwitterionic and moderately increase hydrophobicity, which has an impact on protein interactions. Importantly, cytocompatibility remains high, indicating that the introduction of quaternary ammonium groups does not compromise biological toxicity. This work provides the synthetic and conceptual foundation for the subsequent studies.

The *second publication* expands this platform to a series of **amino-acid-derived anionic polyacrylamides**, synthesized *via* PPM of an activated ester precursor. By systematically varying side-chain hydrophobicity using different α-amino acids, *e.g.*, glycine and leucine, the degree of polymerization and mass distribution are preserved. Although pK_a values remain nearly constant across the series, hydrophobicity significantly impacts both protein complexation and cell association. More hydrophobic anionic polymers showed stronger interactions with positively charged proteins such as lysozyme and display a distinctive, slow, however, pronounced accumulation at the cell membrane which is an uncommon, yet interesting, behavior for anionic polymers. These findings reveal design features in hydrophobicity, which inversely correlated with charge density due increasing alkyl side-chain, to facilitate controlled membrane interactions without inducing cytotoxicity.

Building on this, the *third publication* **combines zwitterionic and anionic polymers** to create a standardized library, enabling direct comparisons of charge state, hydrophobicity, and aromaticity. The polyzwitterions exhibited low hydrophobicity and minimal protein-fouling, while anionic, aromatic polymers showed reverse properties (strong hydrophobicity and polymer-protein interactions). These trends could be transferred to the biological scale as polyzwitterions are non-interacting with cells, whereas anionic, hydrophobic polymers — especially the one containing an aromatic group —display rapid and substantial cell association and internalization. Uptake studies reveal that these cell interactions are based on active cellular processes but are not strongly dependent on specific amino-acid-transporters, suggesting more general membrane-mediated entry pathways. Confocal microscopy confirmed pronounced intracellular localization for hydrophobic anionic polymers, supporting their potential as pH-responsive carriers capable of engaging with the endosomal pathway.

Together, the three publications focus on amino-acid-derived polyacrylamides, in which amino acids or amino-acid-like moieties are introduced as side-chains either directly by the monomer design before synthesis or *via* PPM of activated ester prepolymers. Consequently, a coherent structure–property characterization analysis for the obtained amino-acid-derived polyelectrolytes is established to summarize the association of side-chain hydrophobicity, charge distribution, and aromaticity. This information can be used to systematically tune polymers and control their pH-response, protein interaction characteristics, and cellular uptake.

This dissertation provides not only a synthetic pathway strategy and a versatile, bio-inspired building block toolbox, but also an initial understanding of how amino-acid-derived polyelectrolytes behave at biological interfaces. These insights serve as the basis for designing next-generation pH-responsive polymers with tailored intracellular delivery capabilities and selective interactions with cancer cells, without relying on external targeting ligands.

Zusammenfassung

Arzneistoffträger können die therapeutische Wirksamkeit erhöhen, indem sie den Zugang zu intrazellulären Zielstrukturen ermöglichen, die für kleine Wirkstoffmoleküle nicht zugänglich sind; dennoch stellt eine effiziente intrazelluläre Abgabe weiterhin eine wesentliche Herausforderung in der Entwicklung moderner Therapeutika dar. Ursache hierfür ist die ausgeprägte Barrierefunktion der Plasmamembran, die die passive Diffusion von Proteinen, Peptiden und Nukleinsäuren stark limitiert. Folglich sind energieabhängige Internalisierungsprozesse, wie transportervermittelte Aufnahme oder endozytotische Mechanismen, erforderlich, um eine zelluläre Aufnahme zu gewährleisten. Zur Überwindung dieses Problems werden Trägermaterialien benötigt, die in biologischen Medien kolloidal stabil und kaum Fouling-anfällig sind. Des Weiteren sollten diese Materialien spezifisch mit Zellen wechselwirken können, von der Zelle aufgenommen werden und schließlich Stimuli-responsiv und somit kontrolliert intrazellulär freigesetzt werden können. Idealerweise kann hier auf den Einsatz komplexer und kostspieliger Targeting-Liganden verzichtet werden. Diese Dissertation befasst sich mit solchen Materialdesign-Konzepten, indem sie aus **Aminosäuren modifizierte, pH-responsive Polyelektrolyte** entwickelt und systematisch untersucht. Die etablierten Polymere und ihre Struktur–Eigenschaft–Funktions-Beziehungen liefern Informationen über intelligentes Moleküldesign zur Steuerung der Proteininteraktionen, Zellmembranassoziation und zellulärer Aufnahme.

Aminosäuren sind einzigartige, bio-basierte Bausteine für das Design funktionaler Polymere: Sie implementieren Chiralität, ermöglichen eine einstellbare Hydrophobie und Aromatizität und führen ionisierbare Gruppen ein. Ihr biomimetischer Charakter reduziert unspezifisches Protein-Fouling und schafft zugleich Möglichkeiten für die selektive Wechselwirkung mit Proteinen/Transportern und Zellmembranen. In allen drei Kapiteln dieser Dissertation werden die Polymere mittels reversible Additions-Fragmentierungs-Kettenübertragung (RAFT)-Polymerisation und Post-Polymerisations-Modifikationen (PPM) Hergestellt, um Polymerbibliotheken zu erzeugen, die Eigenschaften zur Zellinteraktion und den physikochemischen Charakteristika enthalten.

In der *ersten Publikation* wird eine Synthesestrategie etabliert, um **chirale, aminosäurebasierte Polybetaine** zu bilden, die sowohl die zwitterionischen und geringen Bio-Fouling Eigenschaften von Polybetainen als auch die Chiralität und Vielfalt der Seitenkettenreste basierend auf aminosäure-abgeleitete polyzwitterionen kombinieren. Um nur ein Modellsystem zu nennen: Bei Verwendung von methyliertem Lysin, ermöglichen die permanenten positiven Ladungen, dass diese Polymere über einen weiten pH-Bereich zwitterionisch bleiben. Des Weiteren bleibt die Hydrophobie dieses Polymers weitestgehend konstant, was positive Auswirkungen auf Proteininteraktionen hat. Darüber hinaus ermöglicht die Einführung des quartären Ammoniumzentrums im Polymer, dass die Toxizität gegenüber Zellen nicht negativ beeinträchtigt wird. Die Ergebnisse aus dieser Arbeit liefren die synthetische und konzeptionelle Grundlage für die nachfolgenden Studien.

Die *zweite Publikation* erweitert die Polymerbibliothek um eine Reihe von **aminosäurebasierten, anionischen Polyacrylamiden**. Diese werden mittels PPM aus einem aktivierten Ester-Vorläufer synthetisiert. Durch systematische Variation der Seitenketten-Hydrophobie mithilfe von α-Aminosäuren,

z. B. Glycin und Leucin, bleibt der Polymerisationsgrad und die Massenverteilung konstant. Während die pKa Werte der einzelnen Polymere dieser Bibliothek nahezu konstant sind, beeinflusst ihre Hydrophobizität sowohl die Proteinkomplexierung als auch die Zellassoziation signifikant. Hydrophobere, anionische Polymere hingegen zeigten stärkere Wechselwirkungen mit positiv geladenen Proteinen wie Lysozym und eine charakteristische, langsame, jedoch ausgeprägte Akkumulation an der Zellmembran auf, ein für anionische Polymere ungewöhnliches Verhalten. Diese Resultate belegen, dass bestimmte Designmerkmale hinsichtlich Hydrophobie und Ladungsdichte kontrollierte Membraninteraktionen ermöglichen, ohne Zytotoxizität zu induzieren.

Darauf aufbauend **kombiniert** die *dritte Publikation* **zwitterionische und anionische Polymere** in einer gemeinsamen Bibliothek für den direkten Vergleich von Ladungszustand, Hydrophobie und Aromatizität. Die zwitterionischen Polymere zeigten geringe Hydrophobie und geringes Protein-Fouling, während anionische, aromatische Polymere ein umgekehrtes Verhalten (ausgeprägte Hydrophobie und Polymer-Protein-Interaktion) aufwiesen. Diese Trends konnten auf die biologische Ebene übertragen werden: Zwitterionische Polymere zeigten kaum Wechselwirkungen mit Zellen, wohingegen anionische, hydrophobe Polymere – insbesondere das Polymer mit aromatischen Gruppen – eine erhöhte Zellassoziation und Internalisierung aufwiesen. Zellinteraktionsstudien belegen, dass diese Wechselwirkungen auf aktiven, zellulären Prozessen basieren, jedoch unabhängig von spezifischen Aminosäuretransportern sind. Dies legt nahe, dass die intrazelluläre Aufnahme der Polymere über membranvermittelte Eintrittswege stattfindet. Konfokale Mikroskopie festigt dies, durch die intrazelluläre Lokalisation hydrophober anionischer Polymere im Zytosol und untermauert damit das Potenzial der pH-responsiven, polymerer Trägermaterialien.

Alle drei Publikationen befassen sich mit aminosäurebasierten Polyacrylamiden, bei denen Aminosäuren oder aminosäureähnliche Motive als Seitenketten entweder direkt über das Monomer Design oder über PPM einer aktivierten Ester-Vorstufe des Polymers eingeführt werden. Folglich wird eine kohärente Struktur–Eigenschaft-Charakterisierungsanalyse aus den synthetisierten, aminosäurebasierten Polyelektrolyten abgeleitet, um die Assoziation von Seitenketten-Hydrophobie, Ladungsverteilung und Aromatizität zusammenzufassen. Diese Informationen können genutzt werden, um Polymere systematisch zu variieren und ihre pH-Response, Proteininteraktionseigenschaften und zelluläre Internalisierung gezielt zu steuern.

Damit liefert diese Dissertation nicht nur Synthesestrategien für aminosäure-basierte Polymere und eine vielseitige, bio-inspirierte Baustein-Bibliothek zur Polymerisation und Postmodifikation, sondern auch ein grundsätzliches Verständnis dafür, wie sich aminosäure-basierte Polyelektrolyte an biologischen Grenzflächen verhalten. Diese Erkenntnisse bilden die Grundlage für das Design pH-responsiver Polymere der nächsten Generation mit maßgeschneiderten, intrazellulären Freisetzungseigenschaften und selektiven Interaktionen mit Krebszellen – ohne auf externe Ziel-Liganden angewiesen zu sein.

Table of Contents

List of Publications ..... **I**

Summary ..... **III**

Zusammenfassung ..... **V**

List of abbreviations ..... **IX**

1 Introduction **1**

1.1 Rationale 1

1.2 Polyelectrolytes 2

1.2.1 Synthesis of polyelectrolytes 3

1.2.2 Polymer properties 12

1.2.3 Applications 18

1.3 References 24

2 Objective **47**

3 Synopsis **51**

3.1 Overview of the Thesis 51

3.2 Zwitterionic Amino-Acid-Derived Polyacrylamides with a Betaine Twist 54

3.3 Amino-Acid-Derived Anionic Polyacrylamides with Tailored Hydrophobicity 60

3.4 Impact of the Polymer Side-Chain Chemistry on Interactions of Amino-Acid-Derived Polyelectrolytes with Cells 65

4 Publications **73**

4.1 Individual contributions to joint publications 73

4.2 Zwitterionic Amino-Acid-Derived Polyacrylamides with a Betaine Twist – Synthesis and Characterization 76

4.3 Amino-Acid-Derived Anionic Polyacrylamides with Tailored Hydrophobicity–Physicochemical Properties and Cellular Interactions 106

4.4 Impact of the polymer side-chain chemistry on interactions of amino-acid-derived polyelectrolytes with cells 138

5 Danksagung **215**

List of abbreviations

AAT	Amino acid transporter
Abu	Aminobutyric acid
Ala	L-alanine
ASCT	Alanine-serine-cysteine transporter
ATRP	Atom transfer radical polymerization
Boc-Lys-OH	Boc-Lysine-OH
BSA	Bovine serum albumin
BzlSer	O-Benzyl-L-serine
CD	Circular dichroism
CLSM	Confocal laser scanning microscopy
CTA	Chain transfer agent
Cy5	Cyanine-5
d_h	Hydrodynamic diameter
DLS	Dynamic light scattering
DNA	Deoxyribonucleic acid
(D)PBS	(Dubelcco's) phosphate buffer solution
EPR	Enhanced permeability and retention
FTIR	Fourier transform infrared
Glu	Glutamate / Glutamic Acid
Gly	Glycine
HEA	Hydroxyethyl acrylate
HEAAm	Hydroxyethyl acrylamide
HEMA	Hydroxyethyl methacrylate
HEMAA	*N*-(2-hydroxyethyl)methacrylamide
HPLC	High-Performance Liquid Chromatography
LAT	L-Type amino acid transporter
Lys	L-lysine
MFI	Mean fluorescence intensity
MPC	2-Methacryloyloxyethyl phosphorylcholine
MTT	3-(4,5-di methyl thiazol-2-yl)-2,5-diphenyltetrazolium bromide
NAM	*N*-Acryloylmorpholine
NAS	*N*-Acryloyloxysuccinimide
NMR	Nucleic magnetic resonance
Nva	Norvaline

PAA	Poly(acrylic acid)
PB	Polybetaine
PC	Phosphatidylcholine
PCB(s)	Polycarboxybetaine(s)
PDMAEMA	Poly(2-(dimethylamino)ethyl methacrylate)
PEG	Poly(ethylene glycol)
PEI	Polyethyleneimine
PPFPMA	Poly(pentafluorophenyl methacrylate)
PPFPA	Poly(pentafluorophenyl acrylate)
P_I	Isoelectric point
pK_a	Negative logarithm of the acid dissociation constant
PMPC	Poly(methacryloyloxyethyl phosphorylcholine)
PPM	Post-polymerization modification
RAFT	Reversible addition–fragmentation chain transfer
RDPR	Reversible-deactivation radical polymerization
RNA	Ribonucleic acid
SEC	Size-exclusion chromatography
r_x	Reactivity ratios
t_{ret}	Polymeric retention times
X_n	Degree of polymerization
Z	Zeta
Đ	Dispersity
δ	Chemical shift

1 Introduction

1.1 Rationale

Cancer cells and tissue show some abnormal behavior as compared to healthy tissue, *e.g.*, acidic pH in their micro-environment, high level of glutathione, and hypoxic called biomarkers for cancer cells.[1] Breast cancer is one of the most prevalent cancers among women and ranks second in cancer-related mortality after lung cancer. According to global cancer statistics, breast cancer has become the most common tumor worldwide, with approximately 2.26 million new cases and 685,000 deaths reported in 2020.[2] However, achieving effective chemotherapy remains challenging due to factors such as insufficient drug accumulation at the tumor site (*i.e.* therapeutic efficiency), rapid systemic clearance, dose-limiting toxicity and side effects.[3]

To address these limitations, active research over the past six decades has focused on designing drug carriers to improve the solubility and bioavailability of hydrophobic drugs in drug delivery applications.[4–6] Great achievements were made in applying carriers for various pharmaceuticals such as drugs, antibodies, peptides, enzymes, with improved delivery and efficacy.[7] One example being lipid-based approaches where bioavailability of drugs is enhanced, therefore improving the therapeutic efficiency.[8,9] Nevertheless, several disadvantages exist, such as drug leakage, low drug loading capacity and poor stability in case of liposomes.[10] Therefore, polymer-based nanoparticles were utilized in numerous studies to enhance oral bioavailability and to achieve rapid absorption of poorly soluble drugs.[11] Despite substantial progress in design of drug carriers, nonspecific biofouling remains a major challenge, hindering the performance of therapeutic systems.[12,13] Biofouling refers to the spontaneous and undesirable adsorption of biomolecules and cells onto material surfaces – such as polymer-based nanoparticles – which can lead to drug carrier or device failure. When, in the first fouling step, non-specific proteins adhere to the material surface, they form a protein corona that alters surface properties, triggers immune recognition, and accelerates clearance by the reticuloendothelial system.[14] This process results in reduced circulation time, premature drug release, and potential adverse immune responses. Therefore, it is crucial to develop drug carriers which can resist nonspecific biofouling for improving drug delivery efficiency and biocompatibility.

In recent years, poly(ethylene glycol) (PEG) achieved great attention due its exploitation of the enhanced retention permeation (EPR) effect as it allowed accumulation of its nanocarriers at cancerous cells.[15] Owing to the nonionic, hydrophilic, and water-soluble nature of PEG polymer, it was widely used as antifouling material.[16] However, PEGylated nanoparticles lose their long circulation property after repeated intravenous injection because of the accelerated blood clearance phenomenon where anti-PEG immunoglobulin antibodies are created.[17–20] In addition, PEG shells can hinder the desired interaction between nanocarriers and cell membranes, which reduces the endocytosis and endosomal escape efficiency of drugs.[21,22] Furthermore, PEG is reported to be easily destroyed by oxidation in the presence of transition metal ions and oxygen, which severely impairs the antifouling property of PEG during prolonged usage or storage.[23–25] Therefore, it is urgently needed to develop alternative materials to address the physiological barriers during drug delivery and further enhance the therapeutic efficiency.

Biobased nanoparticles have emerged as a pivotal component in modern drug delivery, attracting considerable attention in recent years. Derived from natural sources or synthesized to mimic biological structures, these materials offer distinct advantages for therapeutic applications. Their inherent biocompatibility and versatility enable precise, targeted drug delivery, minimizing off-target effects and thereby improving treatment efficacy and patient outcomes.[26] In particular, within cancer therapy, biobased nanomaterials show remarkable potential for selective drug delivery and targeting. By functionalizing their surfaces with specific recognition molecules, they can be engineered to identify and bind selectively to cancer cells, allowing drugs to be delivered directly to malignant tissues while sparing healthy ones and enhancing overall therapeutic effectiveness.[27] The structural diversity of polyelectrolytes which can be based on biobased materials – such as amino acids – bring a broad range of functionalities beyond nonspecific biofouling, which might give different bioactive functionality and, therefore, would be an useful platform for drug delivery applications due their biocompatibility and molecular versatility.[28,29]

While structural modifications of the therapeutically active drugs are limited to not compromise their therapeutic efficiency, (polymeric) drug carriers can be tailored regarding their size[30], shape[31,32], hydrophilicity[33], surface chemistry[34] or stimuli-responsiveness[35,36]. This, together with recent research developments and the continuous lack of tissue specific medications for cancer treatment leads to an urgent need for further exploration of these treatments to not only improve the therapeutic success but also to reduce the severe side effects in patients.[37] In this regard, polyelectrolytes have proven to be an interesting platform to design tailored drug carriers in order to tackle the issues towards tissue specific drug delivery.[38]

1.2 Polyelectrolytes

According to the IUPAC nomenclature, a polyelectrolyte is defined as a “polymer composed of macromolecules in which a substantial portion of the constitutional units contains ionic or ionizable groups, or both.”.[38] generally, polyelectrolytes can be classified into four different categories: (i) polyanions, which contain anionic groups; (ii) polycations, which contain cationic groups; (iii) polyampholytes, which contain both anionic and cationic groups; and (iv) polyzwitterions, a unique type of polyampholyte in which anionic and cationic groups are present in each monomer unit (Fig 1).[39] Due to the high charge density and complex interactions with their surroundings, polyelectrolytes exhibit unique properties that makes them interesting polymer group to investigate.

It is well established that cellular uptake of positively charged polymers (*e.g.* nanoparticles) is preferred over those comprising a negative charge.[40] However, both are susceptible to biofouling equally in physiological environment. Thus, utilizing the antifouling property of polyzwitterions can improve the therapeutic efficacy of drug carriers. The pH-dependent surface charge can be modulated to introduce longer circulation times while the surface charge conversion ability can increase cellular uptake by cancer cells due either positive charge or increase in hydrophobicity upon stimulation by the inherently different properties of cancer cells compared to normal cells.[41–43]

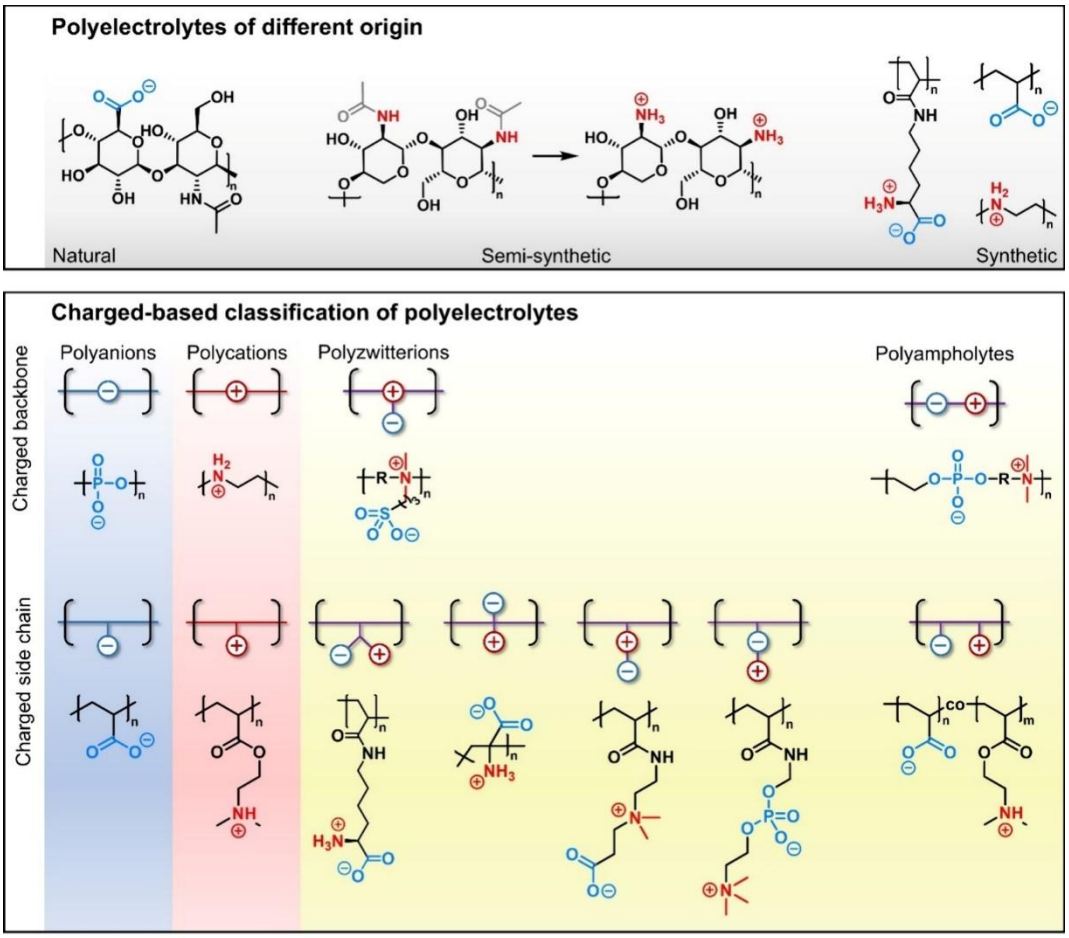


Figure 1. Schematic structures and examples of different polyelectrolytes and representative chemical structures of exemplary polymers. Cationic charges are highlighted in red ad anionic ones are highlighted in blue. Adapted and used with permission under a Creative Commons CC_BY 4.0 license from ref 39. Copyright 2025 Biomacromolecules.

The diverse applications and interactions of polyelectrolytes create a vital area of research as will be discussed throughout this introduction. In this chapter we will dive deeper into their synthetic routes, properties and applications for which they have shown very promising results. However, polycations and polyampholytes will be mentioned briefly for the sake of comprehensiveness and completeness, as they are not part of the research in this work. Polyanions and polyzwitterions will be discussed in more detail, as they are directly relevant to the scope of this work.

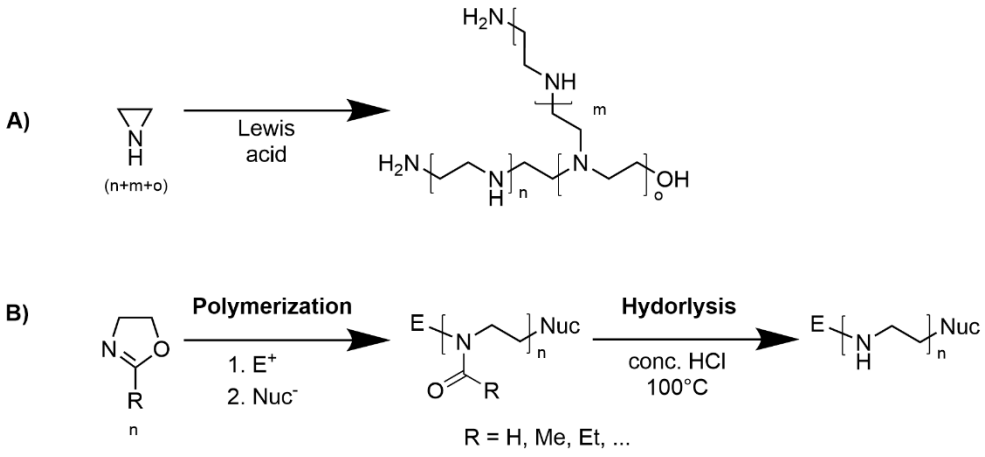
1.2.1 Synthesis of polyelectrolytes

In general, polyelectrolytes can be either of (semi)synthetic or of natural origin.[39] Examples of natural polyelectrolytes are polysaccharides[44], gelatin[45], proteins[46], and (deoxy)ribonucleic acid (DNA/RNA)[47] which can be modified for various applications[48]. Apart from them, all polyelectrolytes follow a synthetic or semi-synthetic approach[49]. In the following part, the synthetic approaches of polyelectrolytes are discussed with emphasis on the approaches which are more frequently used during this work. Additionally, some part will largely be inspired by the review 'Smart, Bio-Inspired Polymers and Bio-Based Molecules Modified by Zwitterionic Motifs to Design Next-Generation Materials for Medical Applications'[50] to which I contributed by discussing the synthetic approaches towards polyzwitterions (see §1.2.1.3).

1.2.1.1 Polycations

The preparation of polycations *via* ionic polymerization techniques, generally, requires the use of protecting groups to mask potentially interfering moieties. In contrast to ionic polymerizations, radical polymerization techniques feature a higher tolerance toward functional groups.[51] For example, monomers with pendant tertiary amines are perfectly suitable for radical polymerizations. In contrast, primary and secondary amines need to be protected with protecting groups as described above to enable RAFT polymerization, which is sensitive to aminolysis of the chain transfer agent (CTA).[51] The polymerization of, *e.g.*, protected amino acid-derived monomers to obtain amino acid-derived polycations was performed by De *et al.*[52] In the following section, additional, synthetic strategies for commonly used polycations in polymer nanomedicine are briefly outlined to provide a comprehensive overview of polyelectrolytes, despite polycations not being part of the practical scope of this thesis, the polymerization methods are described in more detail in §1.2.1.2 to avoid repetition.

For decades, polyethyleneimine (PEI) was considered the golden standard for polymeric gene transfection. It can by synthesized from ethyleneimine (aziridine) or 2-oxazoline monomers, leading to branched or linear polymeric backbones, respectively.[53] The polymerization of aziridine was investigated by Zomlefer *et al.* and proceeds *via* the cationic ring opening of aziridine, leading inevitably to branched chains with primary, secondary, and tertiary amino groups.[54] The general mechanism is initiated by an electrophilic attack of a Lewis acid (or protons) on an aziridine monomer (Scheme 1A). The generated active aziridinium ion is easily attacked by a nucleophilic species to yield the ring opened product. In the case of aziridine as the nucleophile, the resulting product contains a secondary amino group and a new aziridinium species at the terminus. Multiple consecutive attacks of aziridine results in the linear propagation of the chain. However, the secondary (and tertiary) amino groups generated during polymerization may also react and consequently lead to branched structures[55]. Synthesis of linear PEI is performed by cationic ring-opening polymerization of a 2-oxazoline yielding the corresponding acylated linear PEI (Scheme 1B)[56–58]. The obtained polymer was further subject to acidic[59,60] or alkaline hydrolysis[61] to yield the desired linear PEI.



Scheme 1: Synthesis of polyethyleneimines:
A) Branched poly(ethylene imine) *via* polymerization of aziridine
B) Linear poly(ethylene imine*) via* polymerization of substituted 2-oxazolines

Poly(β-amino ester)s were introduced in 2000.[62] They are synthesized *via* a one-pot, atom-economic Michael addition of amines to acrylates, without production of any side products. This synthesis route provides a convenient way to construct an enormous library of polymers with different structures for potential modifications and applications.[63]

Poly(L-Lysine) is a synthetic biopolymer which is commonly synthesized *via* three different routes: (i) solid phase peptide synthesis[64], (ii) ring-opening polymerization[65,66] and (iii) chemo-enzymatic synthesis.[39] The technique of choice depends on the requirements of the product as each technique yields different molar mass (distribution) and purity.[39]

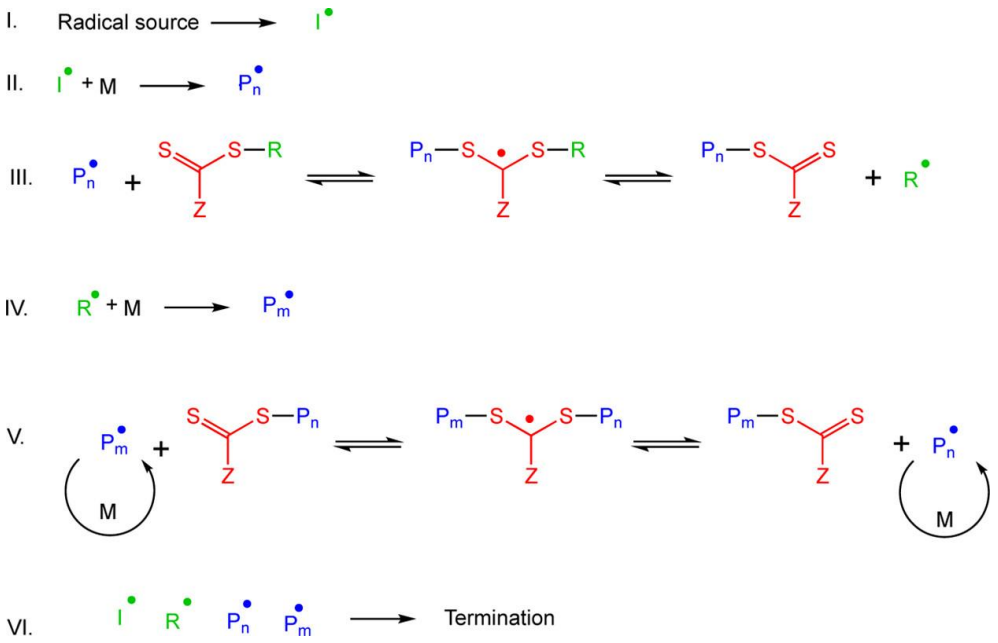
Poly(*N*-isopropylacrylamide) and other poly(meth)acrylates featuring tertiary amines have gained attention due to their responsiveness to pH and temperature and their potential to act as gene delivery vectors, facilitating endosomal release while maintaining considerably high biocompatibility.[67–69] These polymers are generally prepared in a straightforward manner *via* radical polymerization techniques (atom transfer reversible polymerization (ATRP) or RAFT polymerization).[70,71] However, synthesis *via* anionic polymerization[72] was also established in the past.

1.2.1.2 Polyanions

- Radical polymerization

Polyacrylic acid (PAA) finds its applications in numerous fields such as drug delivery[73], superabsorbers[74,75] and adhesive hydrogels[76]. PAA is commonly prepared using radical polymerization techniques, *e.g.*, free radical polymerization[77] or in a more controlled manner *via* reversible-deactivation radical polymerization (RDRP) if polymers with a narrow dispersity (Đ) are required.[78] From all RDRP methods, RAFT polymerization[79] is the most suitable for our purposes as it features a high tolerance towards functional groups and as a result compatible with carboxylate functional groups and acidic reaction conditions (*f.e.* acidic deprotection conditions).[80,81]

RAFT polymerization was first reported in 1998 and since then has grown into one of the most versatile and powerful techniques used for the synthesis of polymers.[82–84] This RDRP has an equilibrium between dormant and active chains which is maintained by degenerative transfer.[85] The RAFT polymerization mechanism is depicted in Scheme 2. First, the initiator decomposes into radicals **(step I)** which subsequently generate monomer radicals with formation of propagating radicals **(step II)**. The propagating radicals add to the RAFT agent (*e.g.* CTA), which is favored compared to chain growth due to the highly reactive C=S bond (**steps III)**, entering an equilibrium between active and dormant species **(steps V)**. The core of the RAFT process lies in degenerate chain transfer steps, involving the reversible exchange of the functional chain end group. Typically, the end group is a thiocarbonylthio moiety (Z–C(=S)–S–R) which promotes fast chain transfer between dormant chains (Z–C(=S)–S–P_n) and propagating radicals ($P_m^{\bullet}$). For efficient control, the addition–fragmentation equilibrium ($P_m^{\bullet}$ + Z–C(=S)–S–P_n ↔ $P_n^{\bullet}$ + Z–C(=S)–S–P_m) must proceed faster than monomer propagation ($P_n^{\bullet}$ + M), ensuring that less than one monomer unit is incorporated per activation cycle.[51] This provides equal probability for all chains to grow and allows for the production of narrow Đ polymers.[86]



Scheme 2: Proposed Mechanism of Reversible Addition−Fragmentation Chain Transfer Polymerization. Used with permission from Ref 51. Copyright 2017 Macromolecules

Generally looking for optimal control in RAFT polymerization requires choosing an appropriate CTA for the monomer(s) and reaction conditions. The Z and R groups both play a critical role as they determine the rate of addition and fragmentation and therefore control efficiency of chain transfer and the likelihood of retardation or inhibition. The Z-group is chosen to tune the thiocarbonylthio reactivity and stabilizes the intermediate radical, thereby setting the rates/selectivity of addition and fragmentation. The role of the R-group is much more subtle and affects the RAFT through its influence on the radical addition to the CTA, since the S-R group influences the C=S activity in a similar way to a S-alkyl Z group. Secondly, fragmentation from the intermediate formed should go fast, therefore the R-group must be a sufficient leaving group to fragment, and lastly, R• must rapidly reinitiate propagation **(step IV)** to ensure all chains are initiated in the same time frame to prevent retardation and obtain a narrow molecular weight distribution. Thus, the R-group needs to keep a fine balance between radical stability and steric effects or differently the R-group must form a radical stable enough to be formed, and reactive enough so that it can add to a monomer. Typically, good R-groups are groups that mimic monomer radicals or thermal initiators such as azobisisobutyronitrile.[51,87] As a result, The CTA is tailored in a way that all polymer chains can maintain a similar degree of polymerization (X_n) at any given time, resulting in polymers with low Đ.

Additionally, however of less importance for this work, one can perform end-group modifications by exploiting the versatility of the polymer chain end functionalization. The thiocarbonylthio end-group can be reduced to a thiol, by either hydrolysis or aminolysis which enables a number of nucleophilic or radical functionalizations, *e.g.*, dye labeling.[88] In our purposes, however, the thermal and chemical stability of the RAFT end group is of greater importance, as aminolysis and hydrolysis can still occur under certain conditions, and subsequent side reactions, such as the formation of disulfide bridges between polymer chains may take place following thiol generation. The most effective process for complete removal of the thiocarbonylthio group is either thermolysis or radical-induced transformation. The last one provides both end-group removal and functionalization.[89] The process uses the reactivity of the thiocarbonylthio

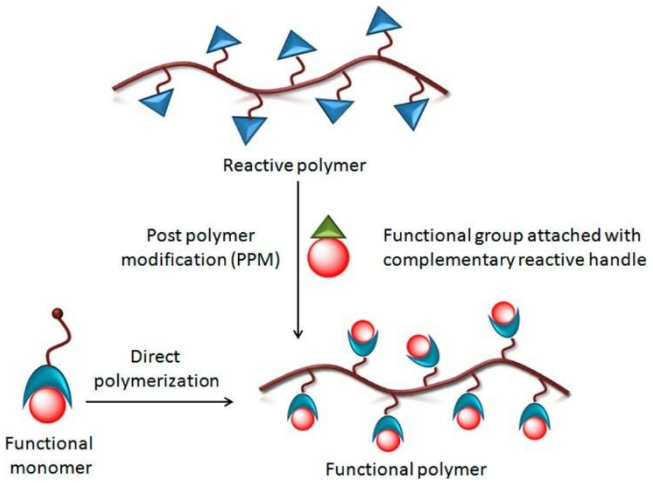
group towards a radical generated *in situ* followed by its fragmentation. In the absence of monomer but in the presence of either a radical trap (*e.g.*, radical initiator) or hydrogen donor, the radical is trapped by a functional group or hydrogen, respectively.[89,90]

Similar to PAA, other polyacrylic acids[91] can be obtained by radical polymerization of commercially available monomers such as methacrylic acid[92] or synthesized like ethyl and propyl acrylic acid[93]. Anionic polyacrylamides can also be obtained by radical polymerization, using their synthesized monomeric equivalents with[94] or without[95,96] protecting groups. For example, various amino-acid-containing monomers can be prepared by the reaction of (meth)acryloyl chloride with amino acids such as phenylalanine[97,98], alanine[99] and proline[100] which can be directly polymerized by RAFT to obtain well-defined amino-acid-derived polyanions.[101]

By using protecting groups, one can also polymerize the precursor *tert*-butyl acrylate, with subsequent acidic hydrolysis, *via* nitroxide mediated polymerization[102] or ATRP which are also RDRP reactions.[103–105] Here, a precursor monomer is often required as ATRP is incompatible with carboxylic acids, as carboxylic acids tend to complex the cupper catalyst.[103,106] However, successful ATRP of amino acid vinyl monomers comprising carboxylic acids has also been demonstrated.[107,108] In the case of nitroxide mediated polymerization was found that broadening during polymerization of acrylic acid happened, due creation of dead chain as the acid groups degraded the nitroxide end groups and, therefore, polymerization of the precursor is a more viable option.[102]

- Post-polymerization modification (PPM)

Despite the versatility of direct polymerization methods, the synthesis of the functional monomers often requires multiple synthetic steps[52] or is even impossible to obtain. Therefore it can become impractical to obtain a targeted polymer *via* direct polymerization. This limitation, together with possible incompatibility of functional groups with the opted polymerization method or limited solubility of the monomers[109] can be circumvented by using the PPM approach as a robust alternative strategy (Scheme 3).[42,110] In this approach a prepolymer is functionalized through a post-polymerization reaction to yield the polymer with the desired side-chain functionality without the hurdle of making the monomer resembling structure. The most attractive prepolymers for these reactions have an activated ester functionality in the side-chain as it combines a robust prepolymer with reliable and controllable amide formation.[110] Although, it should be noted that PPM procedures with non-activated ester functional groups are also reported using coupling agents such as 1,5,7-Triazabicyclodec-5-ene[42] or 4-(4,6-dimethoxy-1,3,5-triazin-2-yl)-4-methyl-morpholinium chloride.[111] Additional advantages of this approach is that at the same time any additional functional group can simultaneously be incorporated, *e.g.*, i) to track the distribution of the final polymer in the body *via* fluorescent dyes or radioactive labels[112–115], ii) to further stabilize the self-assembled structures by core-crosslinking[113,114] or iii) to introduce active targeting units.[114,115] Further, the synthesis of polymer libraries with identical X_n and Đ but different functional side-chains is nearly impossible without the PPM approach. Using this approach, one can prepare these libraries, even on a high throughput level,[116,117] from the same prepolymer which allows us to draw conclusions on structure-property relationships which are detrimental in this work.



Scheme 3: Schematic Representation for the Synthesis of Functional Polymer by PPM and Direct Polymerization. Used with permission from Ref 110. Copyright 2016 American Chemical Society

Using RAFT polymerization, one can synthesize narrowly distributed prepolymers without using any copper complexes from acrylate monomers such as pentafluorophenyl (meth)acrylate (PFP(M)A) or *N*-acryloyloxysuccinimide (NAS). Moreover, polymerization using RAFT is favorable due to its tolerance towards the side-chain functional groups of these activated esters. The prepolymers should first be characterized before modification and functionalization by controlled aminolysis reactions. Generally, activated ester polymers are ideal prepolymers if their solubility is given in various organic solvents. This is particularly important, when classical macromolecular characterization methods need to be applied, *e.g.* size-exclusion chromatography (SEC). While this is not fully provided by the polymeric NAS-based activated ester, although being the oldest and the most regularly employed monomer.[118,119] The polymeric PFP(M)A, first described by Théato *et al*.,[120] commonly features higher hydrolytic stability and enhanced solubility in a wider range of organic solvents.[120,121] Therefore, polymeric PFPA is a more versatile although also more expensive candidate for controlled synthesis and well-defined characterization.[122] Reactive precursor homo and block copolymers prepared thereof are generally well-soluble in typical organic solvents for SEC analyses.[120] Additionally, the pentafluorophenylate leaving group facilitates subsequent reaction monitoring by ^{19}F-nucleic magnet resonance (NMR).[123] Théato *et al.* showed that the aminolysis of PPFP(M)A with primary amines reaches 100% conversion.[120] It is, however, important to note that water-free conditions are crucial to avoid any partial hydrolysis of the reactive ester block during the aminolysis, as a study by Zentel *et al*. showed partial hydrolysis with 3% water content in the reaction solvent.[122]

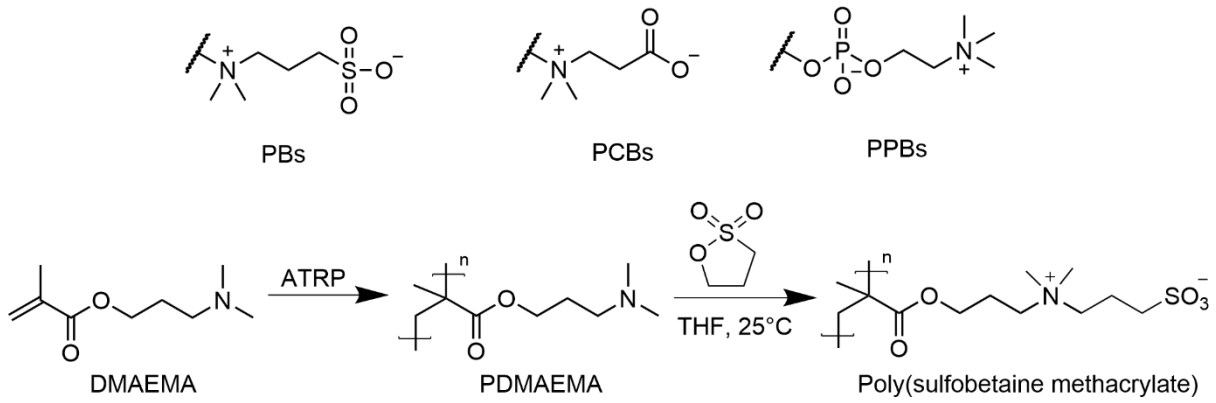
Another solution to solubility issues of NAS is its copolymerization which offers a powerful strategy to combine the desirable properties of two distinct polymers into a single polymer. In this context, the copolymerization of NAS with hydrophilic comonomers, such as *N*-acryloylmorpholine (NAM), can yield water-soluble reactive polymers.[110] Therefore, the kinetic studies of NAS with aqueous soluble NAM during both free radical copolymerization and controlled RAFT polymerization were previously performed. The reactivity ratios (r_X) during free radical copolymerization, initiated by azobisisobutyronitrile in 1,4-dioxane at 60°C, were determined to be $r_{NAS} = 0.63 \pm 0.03$ and $r_{NAM} = 0.75 \pm 0.01$, indicating that the NAM/NAS pair copolymerizes in a statistical way with a very low compositional drift.[124] The kinetic study of NAM/NAS pair copolymerization using RAFT in the presence of tert-

butyldithiobenzoate as CTA showed similar kinetic behavior as the free radical copolymerization of the pair.[125] As PNAM, is a non-ionic hydrophilic polymer, it has shown low toxicity, unspecific cell association and a low incidence of provoking immunological reactions *in vivo*. Different NAM/NAS monomer ratios can give statistical distributed copolymers which can be used as pre-polymers to synthesize antifouling polyanions with tunable charge densities. The incorporation of NAM in different ratios can tune the surface characteristics and therefore potentially its behavior *in vitro* and later *in vivo*.[126–128]

1.2.1.3 Polyzwitterions

Within the broader family of polyelectrolytes, polyzwitterions contain oppositely charged cationic and anionic groups along the chain or side-chain of one macromolecule. To this end, the charge stoichiometry of the resulting polymers can be equal or an excess of one type of charge.[129] Polyampholytes, on the other hand, contain opposite charges on separate repeating units distributed throughout the chain (Fig 1).[130] Polyampholytes can be synthesized in an alternating, statistical, or block-like manner where on the other hand polyzwitterions contain zwitterionic units within one repeating unit. McCormick *et al.* wrote an extensive review on the synthesis of polyzwitterions up to 2002[131] while Kudaibergenov *et al.* published a chapter on the synthesis, characterization, and application around the subclass polybetaines in 2006.[132] Laschewsky published the last synthesis specific review about polyzwitterions in 2014.[133] Like others, our group published a review about polyzwitterions which goes more in depth on other aspects of this interesting polymer class, such as its potential towards medical applications in our case. In this introduction, a comprehensive overview of the synthesis towards these polymers is also given for the sake of completeness.[50]

Most polyzwitterions that have been studied in biological environments are polysulfobetaines, polycarboxybetaines (PCBs), and polyphosphobetaines which is why the whole category is often referred to as polybetaines (PBs) (Scheme 4).[134] Furthermore, zwitterionic betaines are frequently found in nature as well, *e.g.*, in microorganisms, plants, and animals.[135] In the human body, betaines are not part of the protein synthesis itself, but rather serve to post-modify biomolecules with methyl groups during transmethylation mechanisms.[135] There are many examples of how the zwitterionic betaines are obtained where alkylation of amines is the most performed coupling reaction.[131,133] In detail, tertiary amines such as 2-(dimethylamino)ethyl methacrylate contain target sites for chemical functionalization with lactones *via* ring opening alkylation to obtain CB monomers.[136,137] In addition, reactions with 2-alkoxy-2-oxo1,3,2dioxaphospholanes[138] and sultones[139–141] allow for the covalent linkage of phosphate and sulfate group to obtain phosphobetaine and sulfobetaine, respectively. Polymerization of zwitterionic betaine monomer derivates can be achieved using free radical polymerization[142], reversible deactivation radical polymerization[143], ring opening metathesis polymerization[136,144] or step-growth polymerization[145] (although applied rarely). Also here, the PPM approach has also proven itself helpful to synthesize polyzwitterions. One prominent example is the PPM of poly(2-(dimethylamino)ethyl methacrylate) (PDMAEMA) *via* ring opening of sultones[146–148] and 2-oxo-dioxaphopholanes[149,150].

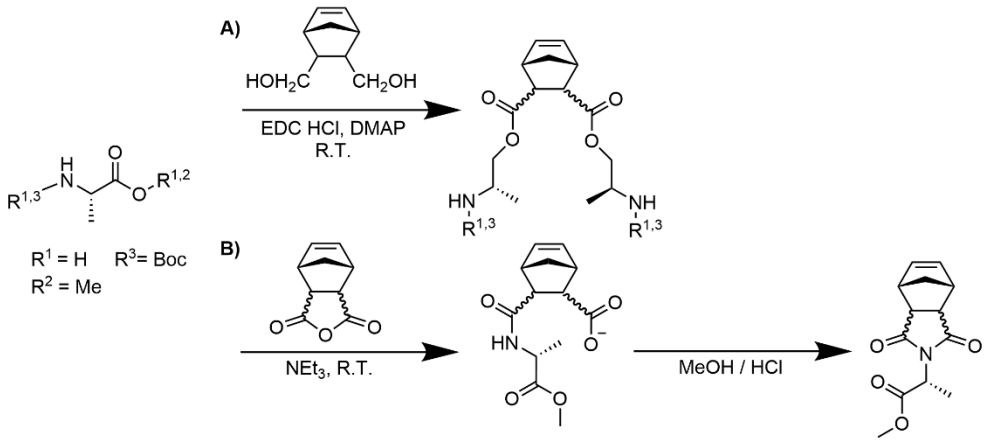


Scheme 4: Structures of polybetaines (top) and ATRP of DMAEMA followed by PPM of PDMAEMA using 1,3-propanesultone in THF at 25°C (bottom).

There are also phospholipids in the human body carrying zwitterionic charges – namely phosphatidylcholine (PC), phosphatidylethanolamine and phosphatidylserine. A general trend in synthesis is the formation of polymerous analogues, in this case of phospholipid-based ones. For example, Nakaya et al.[138] reported that various phospholipid analogous monomers made from starting compounds such as 2-chloro-2-oxo-1,3,2-dioxaphospholane. It was now possible to synthesize vinylic monomers and polymers carrying phospholipid analogues in both, the side and the main chain. The most commonly used vinylic analogue, 2-methacryloyloxyethyl-phosphorylcholine (MPC), is commercially available and can be easily polymerized *via* various radical polymerization techniques.[151–154] Alternatively, phospholipid moieties can be integrated by end-group functionalization using PPM[155], modified *via* the CTA in a RAFT synthesis[156] or by an initiator in ATRP[157,158]. Moreover, step growth polymerization was performed to obtain PC polymer analogues by the reaction of diisocyanates with zwitterionic diols[159] or dibrome with a zwitterionic dichloride.[145]

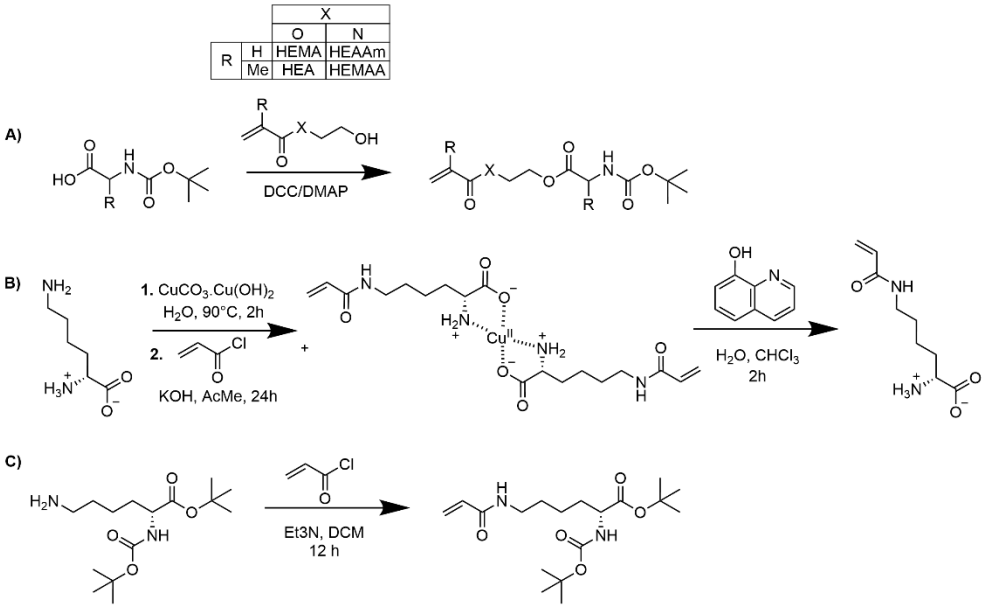
In nature, zwitterionic amino acids can be defined as organic acid molecules that also carry at least one amino group. If one of the amino groups is attached to the α-carbon (relative to the carboxylic group), the amino acid will be an α-amino acid.[160] In addition, a specific side-chain can be connected to the carbon atom which differs depending on the amino acid. The side-chain opens a toolbox providing further charge, by other carboxylic (*e.g.*, glutamic acid, aspartic acid) and amino moieties (*e.g.*, lysine, arginine, histidine) or contributing to a hydrophilic (*e.g.*, serine, cysteine) / hydrophobic character (*e.g.* glycine, alanine, leucine).[161] Proteinogenic amino acids, which are amino acids that are incorporated into proteins, offer a huge range of building blocks, which are well-known to be found in different classes of biomolecules.[162] Typically, the formation of those long chain structures in the human body occurs during a condensation reaction. Of course, the resulting biomolecules are degradable by hydrolysis *(i.e.*, proteolysis) as well to reconstitute single amino acids again.[163] The condensation pathway is problematic for the formation of polyzwitterions as the zwitterionic head groups are covalently linked. To assist in the synthesis of amino acid functionalized monomers and their polymerization, Kempe *et al.* wrote a guideline towards synthetic strategies to obtain both main-chain as well as side-chain amino acid functional polymers.[164] To produce zwitterionic materials, it is aimed at having the charged moieties of amino acids as a side-chain and linking them *via* residue groups. Several modification strategies work towards monomers to obtain side-chain amino acid functionalized polymers, such as first: amino-acid-

functionalized[165,166] or amino-acid-like norbornenes (*e.g.*, polymerized *via* ring-opening metathesis polymerization)[167] with electrostatically charged structures. They can be obtained by a Steglich coupling of the amino acid α-carboxylic moiety with 5-norbonene-2,3-endo,endo-dimethanol[168] (Scheme 5A) or reaction of the amino acid α-amino moiety with 5-norbonene-2,3-endo,endodicarboxylic anhydride (Scheme 5B) to create (novel) molecular zwitterionic structures.[169]



Scheme 5:Synthesis of amino acid-derived norbornene monomers. A) bis-functional ester norbornenes. B) monofunctional imide norbornenes. (EDC.HCl: 1-Ethyl-3-(3-dimethylaminopropyl)carbodiimid-hydrochlorid; DMAP: 4-Dimethylaminopyridin; R.T.: room temperature; NEt_3: triethylamine; MeOH: methanol)

Secondly, amino acid-derived poly(meth)acrylamide or poly(meth)acrylates (*e.g.*, polymerized *via* radical polymerization)[170] can be made to obtain protein or peptide mimicking structures. Various synthetic strategies are known to obtain these monomers. The first synthetic strategy is *via* Steglich esterification where the unprotected carboxylic acid of a (protected) amino acid is conjugated to a commercially available hydroxy-functionalized vinyl monomers, such as, 2-hydroxylethyl acrylate (HEA), 2-hydroxyethyl methacrylate (HEMA), 2-hydroxyethyl acrylamide (HEAAm) or *N*-(2-hydroxyethyl)methacrylamide (HEMAA) to obtain an acrylic, methacrylic, arcylamidic or methacrylamidic monomer, respectively.[170,171] Scheme 6A shows an example for the Steglich esterification method. The second strategy is a substitution reaction of activated vinyl compounds (eg. acryloylchloride) with the remaining free functional group (*f.e.* ε-amine group for lysine) after chelation of the α-amine and carboxylic acid group of the amino acid (Scheme 6B).[36,172,173] The acyl substitution is followed by a decomplexation step. This strategy has been used to synthesize monomers made from lysine[172], serine[36] and ornithine[173,174]. The last and most employed strategy to make amino acid-based monomers is reaction between the free amine of an amino acid with (meth)acryloyl chloride where the side group is protected in case it is not orthogonal towards the reactivity of the amine (scheme 6C).[175] In this approach the (possibly) protected groups and carboxylic acid group of the amino acid are preserved which therefore more often results in anionic monomers.[98]



Scheme 6: Synthesis of amino acid-derived (meth)acrylate monomers. A) Steglich esterification of amino acid with 2-hydroxylethyl acrylate (HEA), 2-hydroxyethyl methacrylate (HEMA), 2-hydroxyethyl acrylamide (HEAAm) or *N*-(2-hydroxyethyl)methacrylamide (HEMAA). B) substitution reaction after Cu-complexation. C) direct substitution of acryloyl chloride with amino acid having protection groups.

Alternatively one can obtain amino acid functionalized polymers by the PPM approach, already discussed in §1.3.1.1.2 using *e.g.*, amidation of activated esters[110], amino acid-derived monomer synthesis allows the formation of highly diverse classes of zwitterionic molecules[164].

1.2.2 Polymer properties

Polymers offer the opportunity of unlimited architecture designs with chemical variation, scalability and simple storage conditions.[176] Herein, chemical variation enables to tune and introduce material properties including hydrophobicity, stimulus responsiveness, and phase-transition behavior. Such control can be achieved by adjusting parameters such as the X_n, Đ, and microstructure or more directly through the choice of molecular building blocks (*i.e.* monomers). As shown in the previous chapter, amino acids and other charged compounds form attractive starting materials, as they provide straightforward access to polymers with well-defined cationic, anionic or zwitterionic polymers that yield specific polymer properties.

1.2.2.1 Polycations

Polycations are well known for their ability to condense biological anions (*e.g.*, DNA, RNA, or proteins) through electrostatic interactions to form polyplexes (Fig 2). The nanoscale polyplexes are described by their ratio of cationic (*e. g.* nitrogen (N)) moieties and anionic (*e. g.* phosphate (P)) moieties. Polyplexes with N:P ratio > 1 have net cationic charges which facilitate the transfection of these biomolecules into target cells as non-viral transfer systems and make them interesting as polymeric antimicrobials.[177–179] However, toxicity and immunogenicity remain major concerns associated with cationic moieties, representing a key barrier to the clinical translation of such delivery systems. The mechanism responsible for its toxicity is poorly understood, although two main pathways have been proposed: a surfactant-like disruption of the cell membrane[180] and acid-catalyzed hydrolysis of phospholipids.[181,182] In this context, Thanou *et al.* systematically studied the effect of molar mass on cytotoxicity for PEI and

poly(L-lysine). The study showed a clear correlation between higher molar mass and increased membrane damage. Using liposome hydrolysis experiments, they further demonstrated that hydrolysis of phospholipids could act as the initial step of toxicity, potentially opening a non-endocytic entry route into cells.[183]

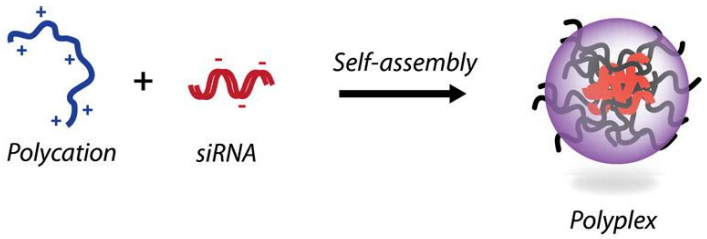


Figure 2: Formation of Polyplexes. Used with permission from Ref 184. Copyright 2012 Elsevier

Polycations typically interact with biological membranes through (1) hydrophobic interactions between hydrophobic moieties in amphiphilic polycations and lipid bilayers, (2) hydrogen bonding between polymer donor groups and PC head groups[185], and (3) electrostatic attraction between their positive charges and the negatively charged cell surface[186]

After transfection through the cell membrane, polyplexes need to overcome or escape the lysosomal entrapment. Overcoming lysosomal entrapment may happen when polyplexes are internalized by fusion. If endocytic internalization happens, it is important to escape the lysosome vesicles to prevent recycling or enzymatic degradation and to transport the genetic material closer to its site of action.[187] Escape can be assisted by polycations, however different theories are proposed for the mechanism behind it. The proton sponge effect was used to explain the highly efficient transfection performance of PEI.[188] Here, their efficiency is believed to rely on the protonation of the amino groups within the endosome caused by adenosine triphosphatase-driven proton accumulation following passive chloride influx and osmotic swelling. The extensive endosome swelling should eventually cause rupture.[188] The ability of cationic polymers to act as a “proton sponge’” was also proven by other cationic polymers with high buffer capacities over a broad pH range including polyamidoamine[189] and PDMAEMA.[190] More recent research, such as mathematical calculations[191–193] and transmission electron microscopy imaging[194,195] studies indicated a endosomal release through “membrane-pore” or “nanoscale hole” formation. In summary, endosomal escape happens by a charge-driven polyplex-membrane interaction leading to local membrane destabilization/nanoscale hole formation where the polyplex can be released into the cytoplasm. Important to notice is that here the endosome is kept intact during and after escape compared to the “proton sponge” theory.[196] Furthermore, one proposed that the endosomal release was supported by membrane disruption or nanoscale pore formation of dissociated free polycations.[180]

After successful endosomal escape, the cargo needs to be released from its carrier and transported to its site of action. In case of various RNA types, like small interfering RNA and messenger RNA, the release within the cytoplasm is sufficient to enable interaction with the RNA-induced silencing complex in order to exert their silencing activity.[197] In contrast, plasmid DNA has to cover a relatively long distance through the cytoplasm to reach the nucleus. Thereby increasing the chance of enzymatic degradation by nucleases.[198] Furthermore, naked DNA moves by Brownian motion and therefore highly inefficient depending on the site of release as well as the size of DNA.[199,200] As polycations are electrostatically

bound to the biological anions, difficulties can occur during release. Therefore, biodegradable polycations are a good option however the primary challenge with these kinds of polymers is balancing their degradation rate with their therapeutic efficacy.[39]

Poly(β-amino esters) are an example of biodegradable polyesters and first introduced for gene delivery by Langer *et al.*[62] Their ester bonds in the backbone structure undergo hydrolysis in aqueous conditions, making poly(β-amino esters) less toxic than other non-degradable cationic polymers. This allows a higher amount of polymer to be used without concerns of toxicity.[201] Hydrophilic degradation facilitates fast release of the cargo, although there are different features that can be tuned to control the rate of degradation, including molar mass and hydrophobicity.[202,203] Schubert *et al.* showed that introducing hydrophobic groups making amphiphilic polymers, results in polymers that outperform pure polycations.[204]

1.2.2.2 Polyanions

Polyanions are often formed of polycarboxylates, that are negatively charged at the physiological pH value of blood (pH = 7.4) and, consequently, making them repulsive to the negatively charged cell membranes.[205] To this end, the pH response of polyanions (*i.e.*, the pK_a-value) often takes place at physiologically relevant pH values (*i.e.*, pH = 4–6).[205] Below the pK_a, they lose their charge which increases membrane interaction of polyanions due higher hydrophobicity. Consequently, the pH-dependent endosomal activity of polyanions is generally considered less harmful, as they are unlikely to be internalized into cells *via* translocation of the synthetic bilayer, which often causes cell disruption.[206] Internalization of polyanions only happens when lipid membranes are faced with polyanions, which also contain enough hydrophobic groups.[207] The polymers often prefer incorporation into the bilayer over self-association.[208,209] Here, the additional hydrophobic forces were shown to be critical to enable the binding of anionic polymer to neutral and even negatively charged lipid bilayers.[207] This is extremely interesting in the preparation of a pH-sensitive delivery system design to exhibit maximum activity under acidic conditions and minimal membrane perturbation where properly tuning of hydrophilic/hydrophobic balance of polyanions could be sufficient. As interactions such as hydrogen bonding, ionization and chemical composition of the polymer (*e.g.* presence of alkyl groups, backbone stiffness) can influence the conformation of polyelectrolytes[208], interesting research has been done towards optimalization of carboxylic acid and hydrophobic units in both homo- as copolymers.

Leroux *et al.* studied different methacrylic acid copolymers for their pH dependent conformational changes. They found that the pH responsiveness depended on copolymer's composition. It interestingly showed that enough hydrophobic ethyl acrylate units and sufficient low pH/high protonation was needed for efficient membrane destabilization (*e.g.* endosomal escape).[91] A similar trend was observed by Murthy *et al.* where the more hydrophobic poly(propyl acrylic acid) had higher hemolytic activity at lower pH while being not active at pH 7.4, outperforming the less hydrophobic poly(ethyl acrylic acid).[93] Conversely, excessive polymer hydrophobicity lead to high microphage cytotoxicity at a neutral pH value.[91] This is probably caused by the globule configuration adopted by the polymer in the solution.

Slater *et al.* and *Chen et al*. modified poly(L-lysine iso-phthalamide) *via* PPM to adjust the hydrophobic/hydrophilic balance and enhance endosomal membrane destabilization. Slater *et al.*[210]

achieved this by incorporating varying amounts of hydrophobic amino acids, yielding 'pseudo-peptides,' while Chen *et al.* introduced long aliphatic chains, resulting in 'comb-like' polymer architectures.[211] These long aliphatic chains should act as hydrophobic anchors, mimicking membrane proteins that contain covalently attached long-chain fatty acids and therefore enhance the polymer-membrane interaction.[212] Incorporation of amino acids generally shifted onset pH where hydrophobic association started to higher values with a higher effect for more hydrophobic incorporated amino acids (L-phenylalanine) compared to less hydrophobic (L-valine).[210] Incorporation of long aliphatic chains modulated the pH-responsive conformation, hydrodynamic size, and hemolytic activity of the polymers. At endosomal pH, these modifications induced complete hemolysis compared to only 0.5% for unmodified poly(L-lysine iso-phthalamide), while maintaining low toxicity at physiological pH.[211]

1.2.2.3 Polyzwitterions

Polyzwitterions are polymers that consist of oppositely charged cationic and anionic groups along the chain or side-chain. The charge stoichiometry between the polyions can be equal, or can be weighted towards anionic or cationic character.[131] Such polymers are typically stimuli-responsive, switching between properties depending on their environment, and therefore are considered as 'smart' adaptive materials.

The property usually depends on its environment. The pH will influence the ionization of the polymer for which the isoelectric point (P_I) is a characteristic value of each polymer at which it is electrically neutral.[131,213] The P_I can easily theoretically be calculated, when the polymer contains an equal balance of cationic and anionic groups, using:[214]

$$P_I = \frac{pK_a + pK_b}{2}$$

With: P_I ; the isoelectric point

pK_a the negative logarithm of the acid dissociation constant

pK_b the negative logarithm of the base dissociation constant

Generally, the polymer is in its most hydrophobic state, and often insoluble, at this point because intramolecular interactions dominate forcing a globule conformation. Above and below this point, repulsion between charges dominate yielding a coiled polymer that behaves in a similar manner as a polyanion or cation.[213] The anionic and cationic properties of zwitterionic molecules can reduce nanoparticles aggregation by reducing the effective nanoparticle surface energy while also simultaneously increasing the circulation time and cellular uptake *in vivo*.[40] This effect can be enhanced by the use of pH-sensitive zwitterionic moieties capable of adjusting the zeta (ζ)-potential in response to the microenvironment.[40]

This can be achieved by choosing the right anionic and cationic groups in a polyzwitterion to get the P_I at the pH, that is desired. For designing pH-sensitive polyzwitterions, ideally, both the cationic and anionic groups should not be subject to protonation/deprotonation, *i.e.*, they should be zwitterionic over a large pH range. This can be achieved by employing inherently quenched ionic species, such as quaternized nitrogen groups as basic moieties, and/or strongly acidic/basic groups, whose strength is reflected in their Negative logarithm of the acid dissociation constant (pK_a) value.[133] Anionic groups,

such as, phosphates, sulfonates ,and carboxylates dominate the field of polyzwitterions.[50,131,133] Phosphoric acid has typically pK_a of 2.12 and sulfuric acid of 1.9.[215] Hence, these groups stay fully deprotonated over a very broad pH range, thereby satisfying the above defined conditions very well. In case of carboxylates, however, the situation is less straightforward, as their acidity is modulated by the distance between the carboxyl group and the cationic site. In the case of the ammoniocarboxylates, pK_a values of 1.8, 3.3, 4.0 and 4.2 were reported, by Weers *et al.,* where the number of methylene groups between the ionic sites increase from 1 to 4, respectively.[216] This is due to the strong electron withdrawing effect of the ammonium group, which levels off with higher number of methylene groups (≥ 4), resulting in pK_a values of about 4.5. Under physiological conditions (pH ≈ 7.4), the moderate acidity of a carboxylate will not endanger the zwitterionic state. However in other, more acidic environments (*f.e.* in the endosomes), deprotonation of the anionic site may be partially or even fully suppressed, turning the supposed polyzwitterion into a polycation which are known to be membrane disruptive (§1.2.2.1).[197]

The most often employed cationic groups in polyzwitterions contain nitrogen, as quaternized ammonium groups, or of protonated amines.[133] Quaternized ammonium groups are often opted for as they can't be deprotonated. For aliphatic amines, the pK_a of the protonated form typically ranges from 8 to 11[215], following the trend primary > secondary > tertiary amines, due to stabilization from $N–H^+$ bond hydration. However, steric hindrance weakens their base strength by limited solvation.[217] Functional derivatives such as aminoethanol or amino acids have pK_a's of 9.5 and ± 8,[218] respectively, and are influenced by combined effects of substituents. Some of the most important are polar (inductive) effects[219], resonance[220,221], electrical repulsion[218], solvation[219] and steric effects[222]. For example, for ethylamine and amino ethanol, the effects that play are a small electron-donating effect of the ethyl group and the net repulsion between the hydrogens bound to the nitrogen are strongly reduced due addition of a substituent – the ethyl group – compared to ammonia. Therefore, the basic strength of ethylamine is 28 times stronger than ammonium. However, the electron-attracting power of the hydroxy group in aminoethanol is relatively large, making it only 7 times stronger than ammonium.[218]

Besides the choice of anionic and cationic groups, the zwitterionic properties are also dependent on other parameters such as orientation and strength of the dipole moment, the spacing between the ions, and composition of the backbone. The strength and orientation of the dipole moment - itself dependent on ion orientation[223], composition and spacing between ions[224] - play a major role in explaining the behavior of zwitterions in solution.[225] Straightforward conclusions about the interactions of polyelectrolytes are not easy as multiple parameters such as polyelectrolyte, counterions, co-ions, and solvent, but also interactions, like intra- and interchain interactions, long-range electrostatic interaction, hydrophobic interaction, and entropic force, have to be simultaneously considered.[226] For example, Muthukumar M. *et al.* found that the aggregation behavior between polyzwitterions with different orientations in dipole moment was drastically different. However, it should be noted that this could also be related to internal factors such as the presence of hydrophobic groups on the phosphate ion on only one of both studied polymers.[223] Wei *et al.* studied the fouling, and therefore hydration, properties of CBs with different spacing between their ions. It was shown that stronger hydration was achieved with larger spacing due to stronger ionization. However, the increased dipole moment also promotes

electrostatic and dipole–dipole interactions which can induce biofouling. They therefore concluded that zwitterionic materials with shorter ionic distances should be designed if excellent fouling resistance wants to be achieved.[224]

Leiske *et al.* showed the importance of the polymer backbone as this parameter also influences physicochemical properties and interactions with cells. This was done by synthesizing a glutamate (Glu)-derived monomer library with an acrylate, methacrylate, acrylamide and methacrylamide group. These polymers have shown that backbone chemistry influences the pH-responsiveness (*i.e.* pK_a and P_I) as well as their hydrophilicity and stability against hydrolysis in aqueous media.[170]

Besides the huge potential zwitterionic moieties offer to modify their properties, their effectiveness in improving protein stability was already discovered in the early 1980s when glycine, betaine, and proline were found to improve solvation of protein molecules.[227,228] Further development in the field of polyzwitterions advanced the understanding of its resistance towards protein absorption.[131,142,229,230] The strong resistance of polyzwitterions to foulant attachment arises from their high density of charged groups, which strongly binds a hydration layer *via* electrostatic interactions (ionic solvation) in solution.[231] This layer forms an energy barrier that biomolecules must surmount to contact the zwitterion.[232] Since the ionic solvation is stronger/more stable than the hydrogen bonding responsible for hydration layers in non-ionic polymers (*e.g.*, PNAM or PEG), polyzwitterions exhibit superior low-fouling properties[233,234] - especially in saline environments[231] - compared to the more conventional non-ionic systems[233]. Additionally, for long term applications, it is demonstrated that PEG is susceptible to oxidative damage in the presence of oxygen and transition metal ions, which significantly worsens its antifouling properties and loses its function in biological media as already mentioned (§1.1).[23–25] At last, we can conclude that polyzwitterions possess the unique dual-functionally, by being able to resist protein absorption/cell adhesion on the one hand and functionality which can be used for targeting of cells[235,236], immobilization of ligands[237] or other modification (Fig 3).

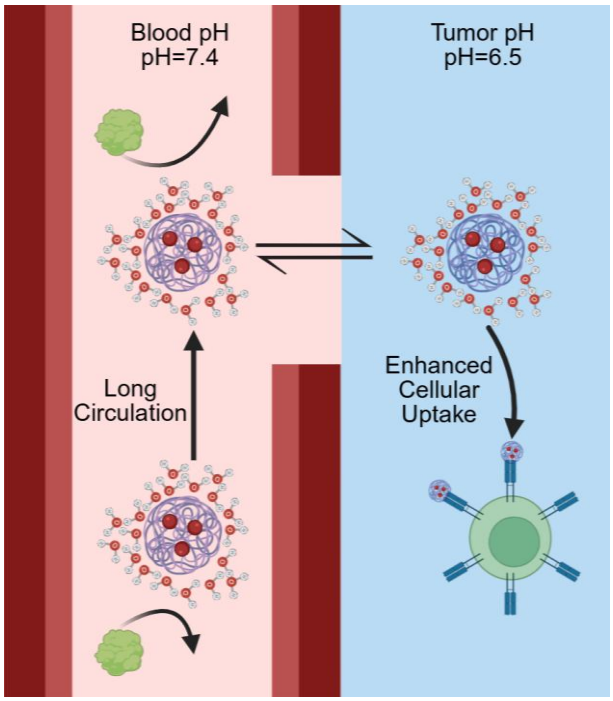


Figure 3: Overview of dual-functionality of *polyzwitterion*s. Created with BioRender.

1.2.3 Applications

1.2.3.1 Zwitterionic polymers in biomedical applications

Most recently Lutz *et al.* wrote an extensive review to highlight the various medical applications polyzwitterions could be designed for (Fig 4).[50] As a short overview, it was discussed that low-biofouling coatings would benefit from highly charged nature of zwitterions due their high degree of hydration could form steric hindrance for undesired protein fouling or other undesired interactions[238] as attachment onto artificial materials could stimulate colonization**,** biofilm development and finally cause infections and tissue inflammation[239]. Studies from Jiang *et al.* showed that the levels of protein attachment is lower than the detection limit of surface plasmon resonance measurements in case of polysulfobetaines or PCBs (< 0.3 ng cm^{-2}).[237,240] They have also interestingly shown that the method of attachment plays a role in surface coverage, as the ‘‘grafting to’’ method, where the polymer is synthesized first, followed by covalent attachment to the surface using an anchoring group, results in poorer surface coverage than the ‘‘grafting from’’ method[241], where the polymer is grown directly from the surface. However, both methods have been reported to be used in preparing surfaces.[241]

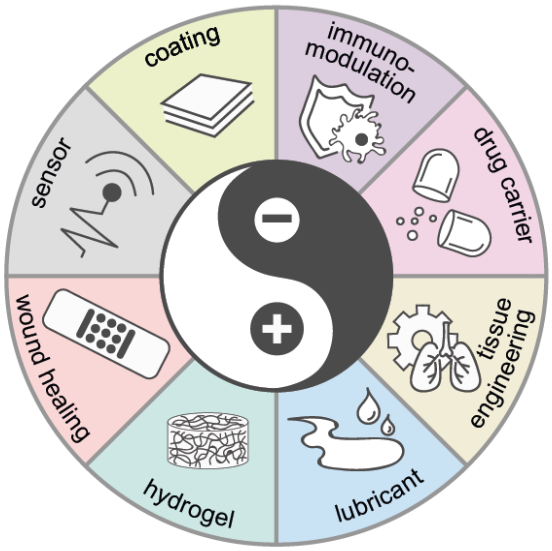


Figure 4: overview of medical applications of polyzwitterions. Reused with permission under a Creative Commons CC_BY 4.0 license from Ref 50. Copyright 2025 Wiley

The water binding properties can also be sourced for lubrication for joints as they are exposed to a lot of friction.[242,243] To obtain the required mechanical characteristics that remain joint functionality, articular cartilage consisting of extracellular matrix *i.e.* collagen[244], (glycosylated)proteins[245], chondrocytes[245], and the main components of synovial fluid – namely lubricin[246], hyaluronic acid and zwitterionic lipids (*e.g.,* PC)[247] – are suitable for friction and wear reduction by both boundary and hydration lubrication[247].

In tissue engineering, polyzwitterions often serve purpose for their hydration, low-biofouling, immunological activity as well as the support of cell adhesion and embedding. The latter combined with the capability of making hydrogels expands the versatility and application of zwitterionic hydrogels for tissue engineering applications, beside bone regeneration.[248] More particularly, research towards artificial microvascular systems is promising.[249,250] Looking at wound healing applications, a wide range of polyzwitterions, based on hydrogels and in the form of adhesive patches[251], interact with tissue surfaces *via* hydrogen bonds, dipole–dipole, and electrostatic interactions. In addition, those non-covalent forces provide the formed adhesive matrix with cohesion properties.[252] Maintaining the balance of zwitterionic motifs within the material is an important demand, *i.e.*, the overall number of zwitterions present must be either below or above a certain threshold, depending on the material composition and required properties depending on the type of wound (post operative or not)[253]. Generally, hydrogels are created for a multitude of purposes going from lubricants for joints[247], coatings[239], patches for wound healing, bone regeneration[254] and sensors to connect cell signaling with bioelectronics[255], but can also have potential applications for the treatment of dry eye syndrome.[256] One of the most successful zwitterionic synthetic polymers is poly(methacryloyloxyethyl phosphorylcholine) (PMPC), whose zwitterionic chemical structure is inspired by the phosphorylcholine moiety of cell membrane components.[257,258] Covering material surfaces with PMPC renders the surfaces biocompatible without any interactions with proteins and cells.

Worldwide, many people suffer from chronic diseases that lack effective treatment. In the case of inflammatory bowel disease,[259] current research can only alleviate the symptoms, however, cannot cure the disease. Conventional drug therapies are based on amino salicylates, corticosteroids, and/or biologics, but may cause unwanted side effects and affect quality of life.[260] These limitations highlight the need for alternative therapeutic strategies that improve tolerability. Even though fully synthetic alternatives are hardly available in literature, there are many semi-synthetic, zwitterionic based materials that hold the potential to be applied.[261,262] These polyzwitterions, obtained by sequential RAFT polymerization of lysine-, mannose, and selenocystamine based monomers, have proven anti-inflammatory properties. These polyzwitterion helps interact with the macrophage cell membrane *via* hydrogen bonds and electrostatic interactions, therefore enhancing the binding affinity of surface-bound receptors with mannose.[263]

Zwitterionic polymers, such as PMPC, could be used as biosensors as they combine multiple desired characteristics at the same time to connect two worlds, namely, bioelectronics and cells. This is done by either initiating specific cell processes or measuring cellular activities.[264,265] Besides biomedical applications, polyzwitterions can also be applied for other applications. Such as polyzwitterion surface coatings that can be used as anti-icing coating by reducing the freezing point of surface adjacent solutions.[266] Further applications of polyzwitterions-based surface coatings include bio separation and functionalization of nanoparticles onto porous structures for liquid chromatography.[267]

1.2.3.2 Drug therapy

Drug therapy is one of the most promising strategies towards disease treatment, as wide range of small molecules, nucleic acids, proteins, and peptides are discovered.[268,269] However the therapeutic efficiency of free drugs is often limited by instability, short half-life in blood[270] or poor cellular uptake.[271–273] Polymer drug carriers form a promising solution to circumvent these limitations. The core task of those carriers, having either entrapped drug molecules or conjugate-chemically bound drug molecules, is the targeted delivery of drugs to specific sites of action in the body.[15] Due to the solubility of these carriers in the physiological environment and hindrance of physiological barriers after administrations, side effects, such as blood clearance, nonspecific tissue/cell localization, endosomal trapping come unwillingly with introducing carriers.[274] PEG is very well known for its ability to increase blood circulation time, although due to their lack of targeting ability and already discussed issues (§ 1.2.2.3, §1.1). Zwitterionic polymers have come up as an appealing alternative for PEG due to their already discussed pH-responsiveness, solubility and resistance towards non-specific protein absorption (§1.2.2.3). Furthermore, polyzwitterions show negligible accelerated blood clearance phenomenon after administration.[275,276] The ability of polyzwitterions to prolong circulation time makes them viable for applications such as polyzwitterion-conjugated surfaces, and zwitterionic membrane coatings which are just highlighted and extensively described in reviews (Fig 5).[233,241,277] This antifouling property can also be used for drug carriers which only need to have high resistance to nonspecific protein absorption as alternative to PEG. As a result, PCBs were prepared as drug carriers to target cancer based on the EPR effect.[278] In parallel to zwitterionic systems, pH-responsive polyanions (often poly(carboxylate)-based) have been explored to improve the therapeutic efficiency.[208] More specifically, because the pH-dependent endosomal activity of polyanions is generally considered less harmful, compared to

polycations, as they are unlikely to be internalized into cells *via* translocation of the synthetic bilayer, which often causes cell disruption (§1.2.2.2). The polyanions are commonly designed by combining a pH-responsive carboxylic acid unit with a hydrophobic unit, leading to protonation at endosomal pH, which promotes a transition toward a more hydrophobic, membrane-associating state.[279] At the same time, the polymer performance depends on balancing hydrophobicity (to promote membrane disruption at pH ~ 4–6) against aqueous solubility and biocompatibility, since excessive hydrophobic character can drive aggregation and/or toxicity.[91] Anionic polypeptides such as poly(Glu) are an example of a polyanionic platform reported to be water-soluble, biodegradable, and non-toxic, and they have been widely explored in biomedical formulations including drug delivery constructs.[280] While polyanions seem to be promising materials for intracellular drug delivery, considerably less is known compared to polyzwitterions making them an interesting polymer class to investigate.

Generally, polymeric carriers having stimulus-responsive properties - *f.e.* change in properties upon change in pH[281], present ions[282] or functional groups tagged on the outer walls of proteins[283] attracted the interest of many researchers because they are more efficient in drug delivery and releasing drug loads at the diseased sites within the desired period. Additionally, polymeric carriers are often tailored to their purpose by having different architectures.[241] Due to the attractive properties of polyzwitterions towards drug therapy and, more generally, biomedical applications. Extensive research was pursued and consequently various reviews were published over the past years.[15,29,284]

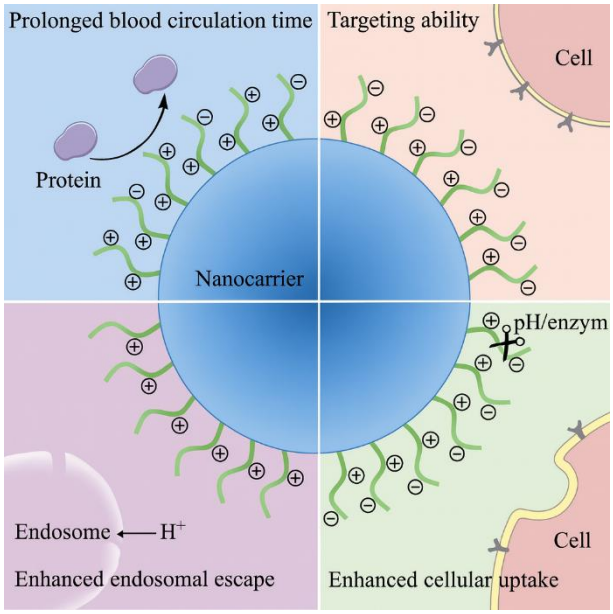


Figure 5: Overview of barriers polyzwitterions can tackle as drug carrier. Adapted with permission from Ref 29. Copyright 2023 Elsevier

For protein therapeutics, it has been shown that polyzwitterions, through the formation of polymer–protein conjugates, can promote protein folding *via* hydrophobic interactions, thereby enhancing the thermal stability of the protein.[285] Combined with their ability to prolong circulation time, such conjugates can be used for therapeutic protein delivery. Self-assembly of polyzwitterions and copolymers into nano aggregates has become a widely explored strategy for therapeutic delivery. These nanocarriers can enhance the solubility of poorly soluble drugs, improve pharmacokinetic profiles and reduce cytotoxicity toward normal tissues. For example, a PMPC and poly(butylmethacrylate) copolymer was synthesized

as nanocarrier for a poorly soluble anticancer drug, improving solubility, long-term stability and antitumor efficacy.[286] However these approaches improve blood circulation time and stability, they still face nonspecific tissue localization, poor cellular uptake, and endosome trapping as hindrances that reduce the accumulation of drugs in target action sites.[287]

To enhance the accumulation of drugs in target action sites, design of active targeting strategies could be developed. One being the attachment of a pilot molecule, *e.g.*, peptides[288], aptamers[289], or sugars[290], onto the nanomedicine bearing the polyzwitterions that have no targetability against a specific cell. Some zwitterionic have also specific target ability due to their biomimetic structure. So is the internalization of PMPC polymerosomes mediated by class B scavenger receptors which are overexpressed by cancer cells compared to normal oral cells. Therefore, opening up the opportunity to exploit this overexpression on cancer cells to use these polymersomes to target tumors.[281] Betaine is a methyl derivative of glycine and plays an important role in cellular osmoregulation and metabolism of human physiology.[291] More importantly, betaine is a specific substrate of the Na^+/Cl^- betaine/ γ-aminobutyric acid transporter, that is expressed at blood-brain barrier and mediates the transport of betaine.[292] The monomer of PCBs has a similar structure compared to betaine. Therefore, PCBs can pass the blood-brain barrier *via* the Na^+/Cl^- betaine/ γ-aminobutyric acid transporter.[293] It has also been shown that betaine and its derivatives can penetrate through intestinal epithelial cell layer, which is one of the key players of intestinal adsorption, by uptake through the proton-assisted amino acid transporter 1.[294] Betain-based microstructures were also directly compared to non-ionic PEG methacrylate-based microstructures on their tissue penetration. This study showed that PCB-based microstructures showed efficient cellular uptake into cancer cells, enabling them to be penetrated deeper into the cancer spheroid *via* the transcytosis pathway (Fig 6). Additionally, incorporation of only 10 mol % of those PCB into the non-ionic microstructures improved its tumor permeability, revealing the importance of zwitterionic nature in tumor penetration.[143]

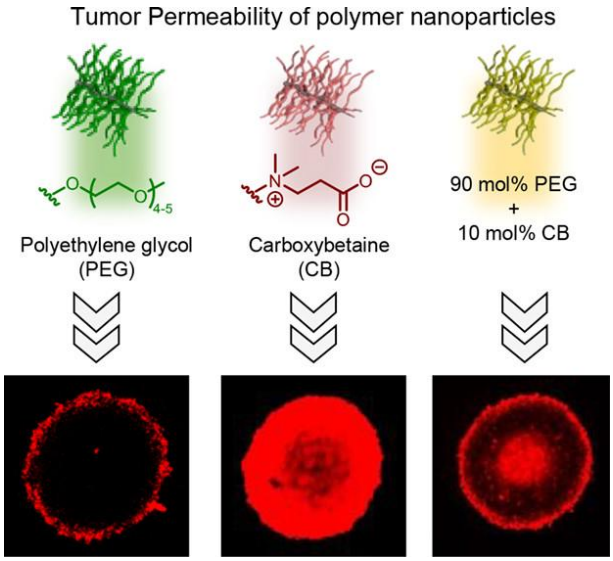


Figure 6: Confocal laser scanning microscopy (CLSM) images at approximately middle depth of the CT26 tumor cell spheroids incubated with cyanine-5 (Cy5)-labeled microstructures for 3 h in a culture medium with PEG (left), PCB (middle) and PEG_{90}-*block*-PCB (right). Reused with permission from Ref 143. Copyright 2022 American Chemical Society

Zwitterionic amino acids, consisting of an α-amino group as the cationic moiety and an α-carboxyl group as the anionic counterpart, are often employed as polyzwitterions with targetability for the recognition of amino acid transporters (AATs), such as the L-type large neutral amino acid transporter (LAT) 1 and the alanine-serine-cysteine transporter (ASCT) 2, which are typically overexpressed in many cancer cells compared to normal tissues.[295–297] Some nanomedicines targeting these AATs have been developed. For instance, Yamada et al. conjugated Glu to the side-chain of poly(L-lysine) as a recognition motif for ASCT2 on BxPC-3 cancer cells.[298] In another study, Leiske *et al.* copolymerized Glu-modified acrylate with *O*-benzyl-L-serine (BzlSer) acrylate with a tailored copolymer ratio of both comonomers. Here, the Glu moieties introduced a high degree of cytocompatibility and cellular specificity, *i.e.*, showing association to different cancer cell lines, but not with nontumor fibroblasts.[299] While on the other hand BzlSer was introduced as it is a known amino acid receptor antagonist.[300] The copolymer with 25 mol% BzlSer revealed to have specific cytotoxicity to cancer cells while leaving fibroblast unaffected for over 3 days.[299] In addition, Fujii *et al.* studied methacrylamide polyzwitterions with glutamine in the side-chain were also actively internalized into cancer cells. As the AAT-mediated endocytosis inhibitor, BzlSer, and exocytosis inhibitor did not affect tumor permeability, it was concluded that penetration depended on the intercellular pathway via cell-cell tight junctions.[301]

Stimuli-responsive charge conversion strategy can achieve surface charge conversion from neutral to positive, enhancing cellular uptake while maintaining the long blood circulation.[302] Some polyzwitterions have been found to have charge-transforming property which is a suitable strategy for cancer therapy as the pH of tumor tissue is lower than that in blood an normal tissue.[41] For example, PMPC could accelerate the doxorubicin release at pH 5.5 as the conformation of PMPC was affected by salts in the solution through ionic interaction. Consequently, poly(ε-caprolactone)-PMPC micelles showed better therapeutic efficacy than doxorubicin-loaded poly(ε-caprolactone)-PEG micelles.[303]

After endosomal uptake/engulfment, drugs and its carriers are often trapped inside the endosomes and end up in the lysosome, where they will be enzymatically degraded. This would drastically decrease the therapeutic efficiency which makes endosomal escape crucial as already discussed for gene delivery (§ 1.2.2.1). Besides polycation drug carriers[304], polyzwitterionic drug carriers that can undergo pH-dependent charge conversion would help in the escape by nanopore formation or membrane rupture.[305]

1.3 References

(1) Raza, A.; Rasheed, T.; Nabeel, F.; Hayat, U.; Bilal, M.; Iqbal, H. M. N. Endogenous and Exogenous Stimuli-Responsive Drug Delivery Systems for Programmed Site-Specific Release. *Mol. 2019, Vol. 24, Page 1117* **2019**, *24* (6), 1117.

(2) Sung, H.; Ferlay, J.; Siegel, R. L.; Laversanne, M.; Soerjomataram, I.; Jemal, A.; Bray, F. Global Cancer Statistics 2020: Globocon Estimates of Incidence and Mortality Worldwide for 36 Cancers in 185 Countries. *CA. Cancer J. Clin.* **2021**, *71* (3), 209–249.

(3) Patil, J.; Pawde, D. M.; Bhattacharya, S.; Srivastava, S. Phospholipid Complex Formulation Technology for Improved Drug Delivery in Oncological Settings: A Comprehensive Review. *AAPS PharmSciTech 2024 255* **2024**, *25* (5), 91.

(4) Yun, Y. H.; Lee, B. K.; Park, K. Controlled Drug Delivery: Historical Perspective for the next Generation. *J. Control. Release* **2015**, *219*, 2–7.

(5) Barenholz, Y.; Amselem, S.; Goren, D.; Cohen, R.; Gelvan, D.; Samuni, A.; Golden, E. B.; Gabizon, A. Stability of Liposomal Doxorubicin Formulations: Problems and Prospects. *Med. Res. Rev.* **1993**, *13* (4), 449–491.

(6) Huynh, L.; Leroux, J. C.; Allen, C. Enhancement of Docetaxel Solubility via Conjugation of Formulation-Compatible Moieties. *Org. Biomol. Chem.* **2009**, *7* (17), 3437–3446.

(7) Allen, T. M.; Cullis, P. R. Drug Delivery Systems: Entering the Mainstream. *Science (80-.).* **2004**, *303* (5665), 1818–1822.

(8) Holm, R.; Kuentz, M.; Ilie-Spiridon, A. R.; Griffin, B. T. Lipid Based Formulations as Supersaturating Oral Delivery Systems: From Current to Future Industrial Applications. *Eur. J. Pharm. Sci.* **2023**, *189*, 106556.

(9) Davis, D. A.; Peng, H. H.; Williams, R. O. Lipid-Based Formulations. *AAPS Adv. Pharm. Sci. Ser.* **2022**, *50*, 253–285.

(10) Xu, L.; Wang, X.; Liu, Y.; Yang, G.; Falconer, R. J.; Zhao, C. X. Lipid Nanoparticles for Drug Delivery. *Adv. NanoBiomed Res.* **2022**, *2* (2).

(11) Mishra, D.; Hubenak, J. R.; Mathur, A. B. Nanoparticle Systems as Tools to Improve Drug Delivery and Therapeutic Efficacy. *J. Biomed. Mater. Res. - Part A* **2013**, *101* (12), 3646–3660.

(12) Barcellona, M. N.; Johnson, N.; Bernards, M. T. Characterizing Drug Release from Nonfouling Polyampholyte Hydrogels. *Langmuir* **2015**, *31* (49), 13402–13409.

(13) Lichtenberg, J. Y.; Ling, Y.; Kim, S. Non-Specific Adsorption Reduction Methods in Biosensing. *Sensors* **2019**, *19* (11), 2488.

(14) Uwaezuoke, O. J.; Kumar, P.; Pillay, V.; Choonara, Y. E. Fouling in Ocular Devices: Implications for Drug Delivery, Bioactive Surface Immobilization, and Biomaterial Design. *Drug Deliv. Transl. Res. 2021 115* **2021**, *11* (5), 1903–1923.

(15) Harijan, M.; Singh, M. Zwitterionic Polymers in Drug Delivery: A Review. *J. Mol. Recognit.* **2022**, *35* (1), e2944.

(16) Lin, C. C.; Anseth, K. S. PEG Hydrogels for the Controlled Release of Biomolecules in Regenerative Medicine. *Pharm. Res. 2008 263* **2008**, *26* (3), 631–643.

(17) Ishida, T.; Ichihara, M.; Wang, X. Y.; Kiwada, H. Spleen Plays an Important Role in the Induction of Accelerated Blood Clearance of PEGylated Liposomes. *J. Control. Release* **2006**, *115* (3), 243–250.

(18) Ishida, T.; Maeda, R.; Ichihara, M.; Irimura, K.; Kiwada, H. Accelerated Clearance of PEGylated Liposomes in Rats after Repeated Injections. *J. Control. Release* **2003**, *88* (1), 35–42.

(19) Ishida, T.; Harada, M.; Xin, Y. W.; Ichihara, M.; Irimura, K.; Kiwada, H. Accelerated Blood Clearance of PEGylated Liposomes Following Preceding Liposome Injection: Effects of Lipid Dose and PEG Surface-Density and Chain Length of the First-Dose Liposomes. *J. Control. Release* **2005**, *105* (3), 305–317.

(20) Ibrahim, M.; Ramadan, E.; Elsadek, N. E.; Emam, S. E.; Shimizu, T.; Ando, H.; Ishima, Y.; Elgarhy, O. H.; Sarhan, H. A.; Hussein, A. K.; Ishida, T. Polyethylene Glycol (PEG): The Nature, Immunogenicity, and Role in the Hypersensitivity of PEGylated Products. *J. Control. Release* **2022**, *351*, 215–230.

(21) Kaasgaard, T.; Mouritsen, O. G.; Jørgensen, K. Screening Effect of PEG on Avidin Binding to Liposome Surface Receptors. *Int. J. Pharm.* **2001**, *214* (1–2), 63–65.

(22) Romberg, B.; Hennink, W. E.; Storm, G. Sheddable Coatings for Long-Circulating Nanoparticles. *Pharm. Res. 2007 251* **2007**, *25* (1), 55–71.

(23) Barz, M.; Luxenhofer, R.; Zentel, R.; Vicent, M. J. Overcoming the PEG-Addiction: Well-Defined Alternatives to PEG, from Structure–Property Relationships to Better Defined Therapeutics. *Polym. Chem.* **2011**, *2* (9), 1900.

(24) Herold, D. A.; Keil, K.; Bruns, D. E. Oxidation of Polyethylene Glycols by Alcohol Dehydrogenase. *Biochem. Pharmacol.* **1989**, *38* (1), 73–76.

(25) Shen, M.; Martinson, L.; Wagner, M. S.; Castner, D. G.; Ratner, B. D.; Horbett, T. A. PEO-like Plasma Polymerized Tetraglyme Surface Interactions with Leukocytes and Proteins: In Vitro and in Vivo Studies. *J. Biomater. Sci. Polym. Ed.* **2002**, *13* (4), 367–390.

(26) Erduran, M.; Çankaya, N.; Yalcin, S. Biobased Nanomaterials in Drug Delivery. *Biobased Nanomater. Appl. Biomed. Food Ind. Agric. Environ. Sustain.* **2024**, 173–222.

(27) Hossain, N.; Chowdhury, M. A.; Kchaou, M.; Alam, A.; Rahman, M. M. Scope of Bio-Based Nanoparticle Targeted through the Cancer Zone to Deactivate Cancer Affected Cells. *Chem. Phys. Impact* **2023**, *6*, 100180.

(28) De Geest, B. G.; Sukhorukov, G. B.; Möhwald, H. The Pros and Cons of Polyelectrolyte Capsules

in Drug Delivery. *Expert Opin. Drug Deliv.* **2009**, *6* (6), 613–624.

(29) Li, M.; Zhang, W.; Li, J.; Qi, Y.; Peng, C.; Wang, N.; Fan, H.; Li, Y. Zwitterionic Polymers: Addressing the Barriers for Drug Delivery. *Chinese Chem. Lett.* **2023**, *34* (11), 108177.

(30) Sprouse, D.; Jiang, Y.; Laaser, J. E.; Lodge, T. P.; Reineke, T. M. Tuning Cationic Block Copolymer Micelle Size by PH and Ionic Strength. *Biomacromolecules* **2016**, *17* (9), 2849–2859.

(31) Rampersaud, S.; Fang, J.; Wei, Z.; Fabijanic, K.; Silver, S.; Jaikaran, T.; Ruiz, Y.; Houssou, M.; Yin, Z.; Zheng, S.; Hashimoto, A.; Hoshino, A.; Lyden, D.; Mahajan, S.; Matsui, H. The Effect of Cage Shape on Nanoparticle-Based Drug Carriers: Anticancer Drug Release and Efficacy via Receptor Blockade Using Dextran-Coated Iron Oxide Nanocages. *Nano Lett.* **2016**, *16* (12), 7357–7363.

(32) Culver, K. S. B.; Shin, Y. J.; Rotz, M. W.; Meade, T. J.; Hersam, M. C.; Odom, T. W. Shape-Dependent Relaxivity of Nanoparticle-Based T1 Magnetic Resonance Imaging Contrast Agents. *J. Phys. Chem. C* **2016**, *120* (38), 22103–22109.

(33) Bianco, A.; Kostarelos, K.; Prato, M. Making Carbon Nanotubes Biocompatible and Biodegradable. *Chem. Commun.* **2011**, *47* (37), 10182–10188.

(34) Kocbek, P.; Obermajer, N.; Cegnar, M.; Kos, J.; Kristl, J. Targeting Cancer Cells Using PLGA Nanoparticles Surface Modified with Monoclonal Antibody. *J. Control. Release* **2007**, *120* (1–2), 18–26.

(35) De Jongh, P. A. J. M.; Mortiboy, A.; Sulley, G. S.; Bennett, M. R.; Anastasaki, A.; Wilson, P.; Haddleton, D. M.; Kempe, K. Dual Stimuli-Responsive Comb Polymers from Modular N-Acylated Poly(Aminoester)-Based Macromonomers. *ACS Macro Lett.* **2016**, *5* (3), 321–325.

(36) Maji, T.; Banerjee, S.; Biswas, Y.; Mandal, T. K. Dual-Stimuli-Responsive l -Serine-Based Zwitterionic UCST-Type Polymer with Tunable Thermosensitivity. *Macromolecules* **2015**, *48* (14), 4957–4966.

(37) Kayl, A. E.; Meyers, C. A. Side-Effects of Chemotherapy and Quality of Life in Ovarian and Breast Cancer Patients. *Curr. Opin. Obstet. Gynecol.* **2006**, *18* (1), 24–28.

(38) Park, J. H.; Lee, S.; Kim, J. H.; Park, K.; Kim, K.; Kwon, I. C. Polymeric Nanomedicine for Cancer Therapy. *Prog. Polym. Sci.* **2008**, *33* (1), 113–137.

(39) Traeger, A.; Leiske, M. N. The Whole Is Greater than the Sum of Its Parts – Challenges and Perspectives in Polyelectrolytes. *Biomacromolecules* **2024**, *26* (1), 5–32.

(40) Yuan, Y. Y.; Mao, C. Q.; Du, X. J.; Du, J. Z.; Wang, F.; Wang, J. Surface Charge Switchable Nanoparticles Based on Zwitterionic Polymer for Enhanced Drug Delivery to Tumor. *Adv. Mater.* **2012**, *24* (40), 5476–5480.

(41) Lee, E. S.; Gao, Z.; Bae, Y. H. Recent Progress in Tumor PH Targeting Nanotechnology. *J. Control. Release* **2008**, *132* (3), 164–170.

(42) Leiske, M. N.; Singha, R.; Jana, S.; De Geest, B. G.; Hoogenboom, R. Amidation of Methyl Ester-Functionalised Poly(2-Oxazoline)s as a Powerful Tool to Create Dual PH- and Temperature-Responsive Polymers as Potential Drug Delivery Systems. *Polym. Chem.* **2023**, *14* (17), 2034–2044.

(43) Nakamura, Y.; Nasu, M.; Shindo, Y.; Oka, K.; Citterio, D.; Hiruta, Y. Effect of the Side Chain Composition of Mixed-Charge Polymers on PH-Selective Cell–Membrane Interactions. *Polym. J.* **2023**, 1–10.

(44) Zong, A.; Cao, H.; Wang, F. Anticancer Polysaccharides from Natural Resources: A Review of Recent Research. *Carbohydr. Polym.* **2012**, *90* (4), 1395–1410.

(45) Alipal, J.; Mohd Pu'ad, N. A. S.; Lee, T. C.; Nayan, N. H. M.; Sahari, N.; Basri, H.; Idris, M. I.; Abdullah, H. Z. A Review of Gelatin: Properties, Sources, Process, Applications, and Commercialisation. *Mater. Today Proc.* **2021**, *42*, 240–250.

(46) Karplus, M.; McCammon, A. dynamics of proteins: elements and function. *Ann. Rev. Biochem* **1983**, *53*, 263–293.

(47) Blackburn, G.; Egli, M.; Gait, M.; Watts, J. *Nucleic Acids in Chemistry and Biology*; Blackburn, G. M., Egli, M., Gait, M. J., Watts, J. K., Eds.; RSC, 2022.

(48) Parmentier, L.; D'Haese, S.; Carpentier, N.; Dmitriev, R. I.; Van Vlierberghe, S. Bottom-Up Extrusion-Based Biofabrication of the Osteoid Niche. *Macromol. Biosci.* **2024**, *24* (4), 2300395.

(49) Rinaudo, M. Polyelectrolytes Derived from Natural Polysaccharides. *Monomers, Polym. Compos. from Renew. Resour.* **2008**, 495–516.

(50) Lutz, T. M.; De Breuck, J.; Salehi, S.; Leiske, M. N. Smart, Bio-Inspired Polymers and Bio-Based Molecules Modified by Zwitterionic Motifs to Design Next-Generation Materials for Medical Applications. *Adv. Funct. Mater.* **2025**, e13765.

(51) Perrier, S. *50th Anniversary Perspective*: RAFT Polymerization—A User Guide. *Macromolecules* **2017**, *50* (19), 7433–7447.

(52) Bauri, K.; Roy, S. G.; Pant, S.; De, P. Controlled Synthesis of Amino Acid-Based PH-Responsive Chiral Polymers and Self-Assembly of Their Block Copolymers. *Langmuir* **2013**, *29* (8), 2764–2774.

(53) Demeneix, B.; Behr, J. P. Polyethylenimine (PEI). *Adv. Genet.* **2005**, *53*, 215–230.

(54) Jones, G. D.; Langsjoen, A.; Neumann, S. M.; Zomlefer, J. The polymerization of ethylenimine.. *J. Org. Chem.* **1944**, *09* (2), 125–147.

(55) Jäger, M.; Schubert, S.; Ochrimenko, S.; Fischer, D.; Schubert, U. S. Branched and Linear Poly(Ethylene Imine)-Based Conjugates: Synthetic Modification, Characterization, and Application. *Chem. Soc. Rev.* **2012**, *41* (13), 4755.

(56) Kagiya, T.; Narisawa, S.; Maeda, T.; Fukui, K. Ring-Opening Polymerization of 2-Substituted 2-

Oxazolines. *J. Polym. Sci. Part B Polym. Lett.* **1966**, *4* (7), 441–445.

(57) Seeliger, W.; Aufderhaar, E.; Diepers, W.; Feinauer, R.; Nehring, R.; Thier, W.; Hellmann, H. Recent Syntheses and Reactions of Cyclic Imidic Esters. *Angew. Chemie Int. Ed. English* **1966**, *5* (10), 875–888.

(58) Tomalia, D. A.; Sheetz, D. P. Homopolymerization of 2-Alkyl- and 2-Aryl-2-Oxazolines. *J. Polym. Sci. Part A-1 Polym. Chem.* **1966**, *4* (9), 2253–2265.

(59) Tanaka, R.; Ueoka, I.; Takaki, Y.; Kataoka, K.; Saito, S. High Molecular Weight Linear Polyethylenimine and Poly(N-Methylethylenimine). *Macromolecules* **1983**, *16* (6), 849–853.

(60) Lambermont-Thijs, H. M. L.; Van Der Woerdt, F. S.; Baumgaertel, A.; Bonami, L.; Du Prez, F. E.; Schubert, U. S.; Hoogenboom, R. Linear Poly(Ethylene Imine)s by Acidic Hydrolysis of Poly(2-Oxazoline)s: Kinetic Screening, Thermal Properties, and Temperature-Induced Solubility Transitions. *Macromolecules* **2009**, *43* (2), 927–933.

(61) Saegusa, T.; Ikeda, H.; Fujii, H. Crystalline Polyethylenimine. *Macromolecules* **1972**, *5* (1), 108–108.

(62) Lynn, D. M.; Langer, R. Degradable Poly(-Amino Esters): Synthesis, Characterization, and Self-Assembly with Plasmid DNA. *J. Am. Chem. Soc*. **2000,** *122*, 10761-10768.

(63) Liu, Y.; Li, Y.; Keskin, D.; Shi, L. Poly(β-Amino Esters): Synthesis, Formulations, and Their Biomedical Applications. *Adv. Healthc. Mater.* **2019**, *8* (2), 1801359.

(64) Jaradat, D. M. M. Thirteen Decades of Peptide Synthesis: Key Developments in Solid Phase Peptide Synthesis and Amide Bond Formation Utilized in Peptide Ligation. *Amin. Acids* **2017**, *50* (1), 39–68.

(65) Lagrille, O.; Danger, G.; Boiteau, L.; Rossi, J. C.; Taillades, J. Process Improvement in Amino Acid N-Carboxyanhydride Synthesis by N-Carbamoyl Amino Acid Nitrosation. *Amin. Acids 2008 362* **2008**, *36* (2), 341–347.

(66) Vayaboury, W.; Giani, O.; Cottet, H.; Deratani, A.; Schué, F. Living Polymerization of α-Amino Acid N-Carboxyanhydrides (NCA) upon Decreasing the Reaction Temperature. *Macromol. Rapid Commun.* **2004**, *25* (13), 1221–1224.

(67) Gao, Y. J.; Qiao, Z. Y.; Wang, H. Polymers with Tertiary Amine Groups for Drug Delivery and Bioimaging. *Sci. China Chem. 2016 598* **2016**, *59* (8), 991–1002.

(68) Kujawa, P.; Aseyev, V.; Tenhu, H.; Winnik, F. M. Temperature-Sensitive Properties of Poly(N-Isopropylacrylamide) Mesoglobules Formed in Dilute Aqueous Solutions Heated above Their Demixing Point. *Macromolecules* **2006**, *39* (22), 7686–7693.

(69) Paul, T. J.; Strzelczyk, A. K.; Feldhof, M. I.; Schmidt, S. Temperature-Switchable Glycopolymers and Their Conformation-Dependent Binding to Receptor Targets. *Biomacromolecules* **2020**, *21* (7), 2913–2921.

(70) Convertine, A. J.; Ayres, N.; Scales, C. W.; Lowe, A. B.; McCormik, C. L. Facile, Controlled, Room-Temperature RAFT Polymerization of N-Isopropylacrylamide†. *Biomacromolecules* **2004**, *5* (4), 1177–1180.

(71) Masci, G.; Giacomelli, L.; Crescenzi, V. Atom Transfer Radical Polymerization of N-Isopropylacrylamide. *Macromol. Rapid Commun.* **2004**, *25* (4), 559–564.

(72) Ito, M.; Ishizone, T. Living Anionic Polymerization of N-Methoxymethyl-N-Isopropylacrylamide: Synthesis of Well-Defined Poly (N-Isopropylacrylamide) Having Various Stereoregularity. *J. Polym. Sci. Part A Polym. Chem.* **2006**, *44* (16), 4832–4845.

(73) Dalei, G.; Das, S. Polyacrylic Acid-Based Drug Delivery Systems: A Comprehensive Review on the State-of-Art. *J. Drug Deliv. Sci. Technol.* **2022**, *78*, 103988.

(74) Chen, Y.; Tan, H. min. Crosslinked Carboxymethylchitosan-g-Poly(Acrylic Acid) Copolymer as a Novel Superabsorbent Polymer. *Carbohydr. Res.* **2006**, *341* (7), 887–896.

(75) Lin, J.; Wu, J.; Yang, Z.; Pu, M. Synthesis and Properties of Poly(Acrylic Acid)/Mica Superabsorbent Nanocomposite. *Macromol. Rapid Commun*. **2001**, 22, 6, 422-424

(76) Zhang, X.; Wan, H.; Lan, W.; Miao, F.; Qin, M.; Wei, Y.; Hu, Y.; Liang, Z.; Huang, D. Fabrication of Adhesive Hydrogels Based on Poly (Acrylic Acid) and Modified Hyaluronic Acid. *J. Mech. Behav. Biomed. Mater.* **2022**, *126*, 105044.

(77) Kabanov, V. A.; Topchiev, D. A.; Karaputadze, T. M.; Mkrtchian, L. A. Kinetics and Mechanism of Radical Polymerization of Weak Unsaturated Acids in Aqueous Solutions. *Eur. Polym. J.* **1975**, *11* (2), 153–159.

(78) Lai, J. T.; Filla, D.; Shea, R. Functional Polymers from Novel Carboxyl-Terminated Trithiocarbonates as Highly Efficient RAFT Agents. *Macromolecules* **2002**, *35* (18), 6754–6756.

(79) Llauro, M. F.; Loiseau, J.; Boisson, F.; Delolme, F.; Ladavière, C.; Claverie, J. Unexpected End-Groups of Poly(Acrylic Acid) Prepared by RAFT Polymerization. *J. Polym. Sci. Part A Polym. Chem.* **2004**, *42* (21), 5439–5462.

(80) Millard, P. E.; Barner, L.; Stenzel, M. H.; Davis, T. P.; Barner-Kowollik, C.; Müller, A. H. E. RAFT Polymerization of N-Isopropylacrylamide and Acrylic Acid under γ-Irradiation in Aqueous Media. *Macromol. Rapid Commun.* **2006**, *27* (11), 821–828.

(81) Chaduc, I.; Crepet, A.; Boyron, O.; Charleux, B.; D'Agosto, F.; Lansalot, M. Effect of the PH on the RAFT Polymerization of Acrylic Acid in Water. Application to the Synthesis of Poly(Acrylic Acid)-Stabilized Polystyrene Particles by RAFT Emulsion Polymerization. *Macromolecules* **2013**, *46* (15), 6013–6023.

(82) Chiefari, J.; Chong, Y. K.; Ercole, F.; Krstina, J.; Jeffery, J.; Le, T. P. T.; Mayadunne, R. T. A.; Meijs, G. F.; Moad, C. L.; Moad, G.; Rizzardo, E.; Thang, S. H. Living Free-Radical Polymerization by Reversible Addition-Fragmentation Chain Transfer: The RAFT Process. *Macromolecules* **1998**, *31*, 5559–5562.

(83) Corpart, P.; Charmot, D.; Zard, S. Z.; Biadatti, T.; Michelet, D. Method for Block Polymer Synthesis by Controlled Radical Polymerisation, 1998. US patent, USOO6153705A

(84) Tam Phuong, L.; Moad, G.; Rizzardo, E.; San Hoa, T. Polymerization with Living Characteristics, 1998. WIPO patent, WO 98/01478

(85) Ouchi, M.; Terashima, T.; Sawamoto, M. Transition Metal-Catalyzed Living Radical Polymerization: Toward Perfection in Catalysis and Precision Polymer Synthesis. *Chem. Rev.* **2009**, 109, 4963-5050

(86) Moad, G.; Rizzardo, E.; Thang, S. H. Radical Addition–Fragmentation Chemistry in Polymer Synthesis. *Polymer (Guildf).* **2008**, *49* (5), 1079–1131.

(87) Keddie, D. J.; Moad, G.; Rizzardo, E.; Thang, S. H. RAFT Agent Design and Synthesis. *Macromolecules* **2012**, *45* (13), 5321–5342.

(88) Willcock, H.; O'Reilly, R. K. End Group Removal and Modification of RAFT Polymers. *Polym. Chem.* **2010**, *1* (2), 149–157.

(89) Moad, G.; Rizzardo, E.; Thang, S. H. End-Functional Polymers, Thiocarbonylthio Group Removal/Transformation and Reversible Addition-Fragmentation-Chain Transfer (RAFT) Polymerization. *Polym. Int.* **2011**, *60* (1), 9–25.

(90) Perrier, S.; Takolpuckdee, P.; Mars, C. A. Reversible Addition−Fragmentation Chain Transfer Polymerization: End Group Modification for Functionalized Polymers and Chain Transfer Agent Recovery. *Macromolecules* **2005**, *38* (6), 2033–2036.

(91) Yessine, M.-A.; Lafleur, M.; Meier, C.; Petereit, H.-U.; Leroux, J.-C. Characterization of the Membrane-Destabilizing Properties of Different PH-Sensitive Methacrylic Acid Copolymers. *Biochim. Biophys. Acta - Biomembr.* **2003**, *1613* (1–2), 28–38.

(92) Chaduc, I.; Lansalot, M.; D'Agosto, F.; Charleux, B. RAFT Polymerization of Methacrylic Acid in Water. *Macromolecules* **2012**, *45* (3), 1241–1247.

(93) Murthy, N.; Robichaud, J. R.; Tirrell, D. A.; Stayton, P. S.; Hoffman, A. S. The Design and Synthesis of Polymers for Eukaryotic Membrane Disruption. *J. Control. Release* **1999**, *61* (1–2), 137–143.

(94) Leer, K.; Reichel, L. S.; Kimmig, J.; Richter, F.; Hoeppener, S.; Brendel, J. C.; Zechel, S.; Schubert, U. S.; Traeger, A. Optimization of Mixed Micelles Based on Oppositely Charged Block Copolymers by Machine Learning for Application in Gene Delivery. *Small* **2024**, *20* (6), 2306116.

(95) Hoke, D. I.; Robins, R. D. Preparation and Polymerization of 3-acrylamido-3-methylbutanoic Acid. *J. Polym. Sci. Part A-1 Polym. Chem.* **1972**, *10* (11), 3311–3315.

(96) Yaşayan, G.; Redhead, M.; Magnusson, J. P.; Spain, S. G.; Allen, S.; Davies, M.; Alexander, C.; Fernández-Trillo, F. Well-Defined Polymeric Vesicles with High Stability and Modulation of Cell Uptake by a Simple Coating Protocol. *Polym. Chem.* **2012**, *3* (9), 2596.

(97) Mori, H.; Matsuyama, M.; Sutoh, K.; Endo, T. RAFT Polymerization of Acrylamide Derivatives Containing L-Phenylalanine Moiety. *Macromolecules* **2006**, 39, 4351-4360.

(98) Mori, H.; Sutoh, K.; Endo, T. Controlled Radical Polymerization of an Acrylamide Containing L-Phenylalanine Moiety via RAFT. *Macromolecules* **2005**, *38* (22), 9055–9065.

(99) Mori, H.; Matsuyama, M.; Endo, T. Assembled Structures and Chiroptical Properties of Amphiphilic Block Copolymers Synthesized by RAFT Polymerization of N-Acryloyl-L-Alanine A. *Macromol. Chem. Phys.* **2008**, *209* (20), 2100–2112.

(100) Mori, H.; Kato, I.; Matsuyama, M.; Endo, T. RAFT Polymerization of Acrylamides Containing Proline and Hydroxyproline Moiety: Controlled Synthesis of Water-Soluble and Thermoresponsive Polymers. *Macromolecules* **2008**, *41* (15), 5604–5615.

(101) Mori, H.; Endo, T. Amino-Acid-Based Block Copolymers by RAFT Polymerization. *Macromol. Rapid Commun.* **2012**, *33* (13), 1090–1107.

(102) Lessard, B.; Marić, M. Effect of an Acid Protecting Group on the “Livingness” of Poly(Acrylic Acid-Ran-Styrene) Random Copolymer Macroinitiators for Nitroxide-Mediated Polymerization of Styrene. *Macromolecules* **2008**, *41* (21), 7881–7891.

(103) Davis, K. A.; Matyjaszewski, K. Atom Transfer Radical Polymerization of Tert-Butyl Acrylate and Preparation of Block Copolymers. *Macromolecules* **2000**, *33* (11), 4039–4047.

(104) Plamper, F. A.; Becker, H.; Lanzendörfer, M.; Patel, M.; Wittemann, A.; Ballauff, M.; Müller, A. H. E. Synthesis, Characterization and Behavior in Aqueous Solution of Star-Shaped Poly(Acrylic Acid). *Macromol. Chem. Phys.* **2005**, *206* (18), 1813–1825.

(105) Fischer, H. The Persistent Radical Effect: A Principle for Selective Radical Reactions and Living Radical Polymerizations. *Chem. Rev.* **2001**, *101* (12), 3581–3610.

(106) Feng, L.; Zhao, F. B.; Liu, Z. L.; Sun, J. P.; Hu, J. W. Synthesis of Optically Active Polymers Bearing Amino Acid Moieties by Atom Transfer Radical Polymerization. *Chinese Chem. Lett.* **2007**, *18* (7), 875–878.

(107) Chung, I.-D.; Britt, P.; Xie, D.; Harth, E.; Mays, J. Synthesis of Amino Acid-Based Polymers via Atom Transfer Radical Polymerization in Aqueous Media at Ambient Temperature. *Chem. Commun.* **2005**, No. 8, 1046.

(108) Rafiee, Z. Controlled Radical Polymerization of an Acrylamide Containing L-Alanine Moiety via ATRP. *Amin. Acids 2015 482* **2015**, *48* (2), 437–443.

(109) Laschewsky, A.; Zerbe, I. Polymerizable and Polymeric Zwitterionic Surfactants: 1. Synthesis and Bulk Properties. *Polymer (Guildf).* **1991**, *32* (11), 2070–2080.

(110) Das, A.; Theato, P. Activated Ester Containing Polymers: Opportunities and Challenges for the Design of Functional Macromolecules. *Chem. Rev.* **2016**, *116* (3), 1434–1495.

(111) Van Guyse, J. F. R.; Mees, M. A.; Vergaelen, M.; Baert, M.; Verbraeken, B.; Martens, P. J.;

Hoogenboom, R. Amidation of Methyl Ester Side Chain Bearing Poly(2-Oxazoline)s with Tyramine: A Quest for a Selective and Quantitative Approach. *Polym. Chem.* **2019**, *10* (8), 954–962.

(112) Herth, M. M.; Barz, M.; Moderegger, D.; Allmeroth, M.; Jahn, M.; Thews, O.; Zentel, R.; Rösch, F. Radioactive Labeling of Defined HPMA-Based Polymeric Structures Using [18F]FETos for In Vivo Imaging by Positron Emission Tomography. *Biomacromolecules* **2009**, *10* (7), 1697–1703.

(113) Kramer, S.; Kim, K. O.; Zentel, R. Size Tunable Core Crosslinked Micelles from HPMA-Based Amphiphilic Block Copolymers. *Macromol. Chem. Phys.* **2017**, *218* (19), 1700113.

(114) De Coen, R.; Vanparijs, N.; Risseeuw, M. D. P.; Lybaert, L.; Louage, B.; De Koker, S.; Kumar, V.; Grooten, J.; Taylor, L.; Ayres, N.; Van Calenbergh, S.; Nuhn, L.; De Geest, B. G. PH-Degradable Mannosylated Nanogels for Dendritic Cell Targeting. *Biomacromolecules* **2016**, *17* (7), 2479–2488.

(115) Wang, W.; Lee, J. Y.; Kil, J.; Kim, T.; Lee, D. C.; Kharbash, R.; Nam, Y.; Li, S. Near-Infrared Fluorescent Nanoparticles from Reactive Polymers for Bioimaging. *ACS Appl. Polym. Mater.* **2025**, *7* (15), 10177–10190.

(116) Siegwart, D. J.; Whitehead, K. A.; Nuhn, L.; Sahay, G.; Cheng, H.; Jiang, S.; Ma, M.; Lytton-Jean, A.; Vegas, A.; Fenton, P.; Levins, C. G.; Love, K. T.; Lee, H.; Cortez, C.; Collins, S. P.; Li, Y. F.; Jang, J.; Querbes, W.; Zurenko, C.; Novobrantseva, T.; Langer, R.; Anderson, D. G. Combinatorial Synthesis of Chemically Diverse Core-Shell Nanoparticles for Intracellular Delivery. *Proc. Natl. Acad. Sci. U. S. A.* **2011**, *108* (32), 12996–13001.

(117) Panda, S.; Eaton, E. J.; Muralikrishnan, P.; Stelljes, E. M.; Seelig, D.; Leyden, M. C.; Gilkey, A. K.; Barnes, J. T.; Morrissey, D. V.; Sarupria, S.; Moriarity, B. S.; Reineke, T. M. Machine Learning Reveals Amine Type in Polymer Micelles Determines MRNA Binding, In Vitro, and In Vivo Performance for Lung-Selective Delivery. *JACS Au* **2025**, *5* (4), 1845–1861.

(118) Batz, H. G.; Franzmann, G.; Ringsdorf, H. Pharmakologisch Aktive Polymere, 5. Modellreaktionen Zur Umsetzung von Pharmaka Und Enzymen Mit Monomeren Und Polymeren Reaktiven Estern. *Die Makromol. Chemie* **1973**, *172* (1), 27–47.

(119) Ferruti, P.; Bettelli, A.; Feré, A. High Polymers of Acrylic and Methacrylic Esters of N-Hydroxysuccinimide as Polyacrylamide and Polymethacrylamide Precursors. *Polymer (Guildf).* **1972**, *13* (10), 462–464. h

(120) Eberhardt, M.; Mruk, R.; Zentel, R.; Théato, P. Synthesis of Pentafluorophenyl(Meth)Acrylate Polymers: New Precursor Polymers for the Synthesis of Multifunctional Materials. *Eur. Polym. J.* **2005**, *41* (7), 1569–1575.

(121) Theato, P. Synthesis of Well-Defined Polymeric Activated Esters. *J. Polym. Sci. Part A Polym. Chem.* **2008**, *46* (20), 6677–6687.

(122) Mohr, N.; Barz, M.; Forst, R.; Zentel, R. A Deeper Insight into the Postpolymerization Modification

of Polypenta Fluorophenyl Methacrylates to Poly(N-(2-Hydroxypropyl) Methacrylamide). *Macromol. Rapid Commun.* **2014**, *35* (17), 1522–1527.

(123) Boyer, C.; Davis, T. P. One- Pot Synthesis and Biofunctionalization of Glycopolymers via RAFT Polymerization and Thiol–Ene Reactions. *Chem. Commun.* **2009**, No. 40, 6029–6031.

(124) D'Agosto, F.; Charreyre, M.-T.; Veron, L.; Llauro, M.-F.; Pichot, C. Kinetic Study of Free-Radical Solution Copoly- Merization OfN-Acryloylmorpholine with an Activated Ester-Type Monomer,N-Acryloxysuccinimide. *Macromol. Chem. Phys.* **2001**, *202* (9), 1689–1699.

(125) Favier, A.; D'Agosto, F.; Charreyre, M. T.; Pichot, C. Synthesis of N-Acryloxysuccinimide Copolymers by RAFT Polymerization, as Reactive Building Blocks with Full Control of Composition and Molecular Weights. *Polymer (Guildf).* **2004**, *45* (23), 7821–7830.

(126) Torchilin, V. P.; Trubetskoy, V. S.; Whiteman, K. R.; Caliceti, P.; Ferruti, P.; Veronese, F. M. New Synthetic Amphiphilic Polymers for Steric Protection of Liposomes in Vivo. *J. Pharm. Sci.* **1995**, *84* (9), 1049–1053.

(127) Sartore, L.; Peroni, I.; Ferruti, P.; Latini, R.; Bernasconi, R. Synthesis and Pharmacokinetic Behaviour of Ester Derivatives of 4-Isobutylphenyl-2-Propionic Acid (Ibuprofen) with End-Hydroxylated Poly(N-Vinyl Pyrrolidinone) and Poly(N-Acryloyl Morpholine) Oligomers. *J. Biomater. Sci. Polym. Ed.* **1997**, *8* (10), 741–754.

(128) Jo, Y. S.; Van Der Vlies, A. J.; Gantz, J.; Antonijevic, S.; Demurtas, D.; Velluto, D.; Hubbell, J. A. RAFT Homo- and Copolymerization of N-Acryloyl-Morpholine, Piperidine, and Azocane and Their Self-Assembled Structures. *Macromolecules* **2008**, *41* (4), 1140–1150.

(129) Hess, M.; Jones, R. G.; Kahovec, J.; Kitayama, T.; Kratochvíl, P.; Kubisa, P.; Mormann, W.; Stepto, R. F. T.; Tabak, D.; Vohlídal, J.; Wilks, E. S. Terminology of Polymers Containing Ionizable or Ionic Groups and of Polymers Containing Ions (IUPAC Recommendations 2006). *Pure Appl. Chem.* **2006**, *78* (11), 2067–2074.

(130) Dobrynin, A. V.; Colby, R. H.; Rubinstein, M. Polyampholytes. *J. Polym. Sci. Part B Polym. Phys.* **2004**, *42* (19), 3513–3538.

(131) Lowe, A. B.; McCormick, C. L. Synthesis and Solution Properties of Zwitterionic Polymers. *Chem. Rev.* **2002**, *102* (11), 4177–4190.

(132) Kudaibergenov, S.; Jaeger, W.; Laschewsky, A. Polymeric Betaines: Synthesis, Characterization, and Application. *Adv. Polym. Sci.* **2006**, *201* (1), 157–224.

(133) Laschewsky, A. Structures and Synthesis of Zwitterionic Polymers. *Polymers (Basel).* **2014**, *6* (5), 1544–1601.

(134) Blackman, L. D.; Gunatillake, P. A.; Cass, P.; Locock, K. E. S. An Introduction to Zwitterionic Polymer Behavior and Applications in Solution and at Surfaces. *Chemical Society Reviews*. RSC **2019**, 757–770.

(135) Craig, S. A. S. Betaine in Human Nutrition. *Am. J. Clin. Nutr.* **2004**, *80* (3), 539–549.

(136) Rankin, D. A.; Lowe, A. B. New Well-Defined Polymeric Betaines: First Report Detailing the Synthesis and ROMP of Salt-Responsive Sulfopropylbetaine- and Carboxyethylbetaine-Exo-7-Oxanorbornene Monomers. *Macromolecules* **2007**, *41* (3), 614–622.

(137) Hahn, M.; Görnitz, E.; Dautzenberg, H. Synthesis and Properties of Ionically Modified Polymers with LCST Behavior. *Macromolecules* **1998**, *31* (17), 5616–5623.

(138) Nakaya, T.; Li, Y. J. Phospholipid Polymers. *Prog. Polym. Sci.* **1999**, *24* (1), 143–181.

(139) SchAnemann, E.; Koc, J.; Karthaüser, J. F.; Ozcan, O.; Schanzenbach, D.; Schardt, L.; Rosenhahn, A.; Laschewsky, A. Sulfobetaine Methacrylate Polymers of Unconventional Polyzwitterion Architecture and Their Antifouling Properties. *Biomacromolecules* **2021**, *22* (4), 1494–1508.

(140) Monroy Soto, V. M.; Galin, J. C. Poly(Sulphopropylbetaines): 1. Synthesis and Characterization. *Polymer.* **1984**, *25* (1), 121–128.

(141) Ghosh, R.; Wong, W.-W.; Reimers, T.; Radzanowski, A.; Correa Ruiz, J.; Coughlin, E. B. Amphiphilic–Zwitterionic Block Polymers. *Polym. Chem.* **2024**, *15* (7), 622–630.

(142) Bonte, N.; Laschewsky, A. Zwitterionic Polymers with Carbobetaine Moieties. *Polymer.* **1996**, *37* (10), 2011–2019.

(143) Fujii, S.; Takano, S.; Nakazawa, K.; Sakurai, K. Impact of Zwitterionic Polymers on the Tumor Permeability of Molecular Bottlebrush-Based Nanoparticles. *Biomacromolecules* **2022**, *23* (7), 2846–2855.

(144) Davis, E.; Caparco, A. A.; Steinmetz, N. F.; Pokorski, J. K. Poly(Oxanorbornene)-Protein Conjugates Prepared by Grafting-to ROMP as Alternatives for PEG. *Macromol. Biosci.* **2024**, *24* (2), 2300255.

(145) Iwasaki, Y.; Nakabayashi, N.; Ishihara, K. Synthesis of Novel Phospholipid Polymers by Polycondensation. *Macromol. Rapid Commun* **2000**, *21*, 287–290.

(146) Lowe, A. B.; Billingham, N. C.; Armes, S. P. Synthesis and Properties of Low-Polydispersity Poly(Sulfopropylbetaine)s and Their Block Copolymers. *Macromolecules* **1999**, *32* (7), 2141–2148.

(147) Daumann, K.; May, P.; Brückerhoff, J.; Ulbricht, M. Synthesis of Well-Defined Cross-Linkable Zwitterionic Macromolecular Building Blocks for Hydrogels. *React. Funct. Polym.* **2018**, *131*, 251–257.

(148) Housni, A.; Zhao, Y. Gold Nanoparticles Functionalized with Block Copolymers Displaying Either LCST or UCST Thermosensitivity in Aqueous Solution. *Langmuir* **2010**, *26* (15), 12933–12939.

(149) Sugiyama, K.; Shiraishi, K. Synthesis and Properties of Macromonomers Carrying Phosphatidylcholine Analogous and Azobenzene Moieties. *Die Makromol. Chemie* **1989**, *190*

(10), 2381–2390.

(150) Charalabidis, D.; Pitsikalis, M.; Hadjichristidis, N. Model Linear and Star-Shaped Polyisoprenes with Phosphatidylcholine Analogous End-Groups. Synthesis and Association Behavior in Cyclohexane.

(151) Liu, W.; Wan, Y.; Wang, X.; Li, Y.; Gao, B.; Zhang, Y.; Wang, K.; Feng, Y. "Synergistic Anticoagulant and Endothelial Regeneration Strategy" Based on Mussel-Inspired Phospholipid Copolymer Coating and Bioactive Zeolitic Imidazolate Frameworks-90 to Maintain the Patency of CoCr Stent. *Int. J. Biol. Macromol.* **2024**, *280*, 135842.

(152) Imbia, A. S.; Ounkaew, A.; Mao, X.; Zeng, H.; Liu, Y.; Narain, R. Mussel-Inspired Polymer-Based Coating Technology for Antifouling and Antibacterial Properties. *Langmuir* **2024**, *40* (21), 10957–10965.

(153) Thedrattanawong, C.; Zhang, M.; Zhang, Z.; Song, X.; Zhu, J.; Tian, X.; Li, J.; Wen, Y. Synthesis and Characterization of Lipid-Polyzwitterion Diblock Copolymers for Optimizing Micelle Formation to Enhance Anticancer Drug Delivery in 2D and 3D Cell Cultures. *Biomacromolecules* **2025**, *26* (2), 1032–1043.

(154) Wen, J.; Liu, K.; Bu, Y.; Zhang, Y.; Zheng, Y.; He, J.; Huang, Y.; Hu, D.; Wang, K. An Injectable and Antifouling Hydrogel Prevents the Development of Abdominal Adhesions by Inhibiting the CCL2/CCR2 Interaction. *Biomaterials* **2024**, *311*, 122661.

(155) Berger, M.; Toussaint, F.; Ben Djemaa, S.; Maquoi, E.; Pendeville, H.; Evrard, B.; Jerôme, C.; Leblond Chain, J.; Lechanteur, A.; Mottet, D.; Debuigne, A.; Piel, G. Poly(N-Methyl-N-Vinylacetamide): A Strong Alternative to PEG for Lipid-Based Nanocarriers Delivering SiRNA. *Adv. Healthc. Mater.* **2024**, *13* (8), 2302712.

(156) Schiazza, L. Amphiphilic Polymers: Structure-Activity Relationship between Their Properties and Interactions with Cell Membranes, University of Nottingham, **2022**.

(157) Hu, M.; Zheng, R.; Pan, Q.; Peng, C.; Zhang, X.; He, W.; Yao, W.; Li, Y. Targeted and PH-Sensitive Polyzwitterionic Liposomes for Oral Anticancer Drug Delivery. *Particuology* **2025**, *98*, 13–20.

(158) Li, Y.; Cheng, Q.; Jiang, Q.; Huang, Y.; Liu, H.; Zhao, Y.; Cao, W.; Ma, G.; Dai, F.; Liang, X.; Liang, Z.; Zhang, X. Enhanced Endosomal/Lysosomal Escape by Distearoyl Phosphoethanolamine-Polycarboxybetaine Lipid for Systemic Delivery of SiRNA. *J. Control. Release* **2014**, *176* (1), 104–114.

(159) Tan, H.; Liu, J.; Li, J.; Jiang, X.; Xie, X.; Zhong, Y.; Fu, Q. Synthesis and Hemocompatibility of Biomembrane Mimicing Poly(Carbonate Urethane)s Containing Fluorinated Alkyl Phosphatidylcholine Side Groups. *Biomacromolecules* **2006**, *7* (9), 2591–2599.

(160) Amaya-Farfan, J.; Bertoldo Pacheco, M. T. AMINO ACIDS | Properties and Occurrence. *Encycl. Food Sci. Nutr.* **2003**, 181–192.

(161) Cole, A. S.; Eastoe, J. E. The Amino Acids. *Biochem. Oral Biol.* **1988**, 33–43.

(162) Fichtner, M.; Voigt, K.; Schuster, S. The Tip and Hidden Part of the Iceberg: Proteinogenic and Non-Proteinogenic Aliphatic Amino Acids. *Biochim. Biophys. Acta - Gen. Subj.* **2017**, *1861* (1), 3258–3269.

(163) Raju, T. S. Proteolysis of Proteins. *Co□ Post-Translational Modif. Ther. Antibodies Proteins* **2019**, 183–202.

(164) Leiske, M. N.; Kempe, K. A Guideline for the Synthesis of Amino-Acid-Functionalized Monomers and Their Polymerizations. *Macromol. Rapid Commun.* **2022**, *43* (2), 1–24.

(165) Sutthasupa, S.; Terada, K.; Sanda, F.; Masuda, T. Ring-Opening Metathesis Polymerization of Amino Acid-Functionalized Norbornene Derivatives. *J. Polym. Sci. Part A Polym. Chem.* **2006**, *44* (18), 5337–5343.

(166) Sutthasupa, S.; Sanda, F.; Masuda, T. Ring-Opening Metathesis Polymerization of Amino Acid-Functionalized Norbornene Diamide Monomers: Polymerization Behavior and Chiral Recognition Ability of the Polymers. *Macromol. Chem. Phys.* **2008**, *209* (9), 930–937.

(167) Sutthasupa, S.; Shiotsuki, M.; Sanda, F. Recent Advances in Ring-Opening Metathesis Polymerization, and Application to Synthesis of Functional Materials. *Polym. J.* **2010**, *42* (12), 905–915.

(168) Sutthasupa, S.; Sanda, F.; Masuda, T. ROMP of Norbornene Monomers Carrying Nonprotected Amino Groups with Ruthenium Catalyst. *Macromolecules* **2009**, *42* (5), 1519–1525.

(169) Biagini, S. C. G.; Bush, S. M.; Gibson, V. C.; Mazzariol, L.; North, M.; Teasdale, W. G.; Williams, C. M.; Zagotto, G.; Zamuner, D. The Synthesis of N-Norbornenyl-Amino Acids and Esters: Monomers for the Preparation of Well Defined Polymers. *Tetrahedron* **1995**, *51* (26), 7247–7262.

(170) Leiske, M. N.; De Geest, B. G.; Hoogenboom, R. Impact of the Polymer Backbone Chemistry on Interactions of Amino-Acid-Derived Zwitterionic Polymers with Cells. *Bioact. Mater.* **2023**, *24* (January), 524–534.

(171) Sun, H.; Gao, C. Facile Synthesis of Multiamino Vinyl Poly(Amino Acid)s for Promising Bioapplications. *Biomacromolecules* **2010**, *11* (12), 3609–3616.

(172) Dinda, P.; Anas, M.; Banerjee, P.; Mandal, T. K. Dual Thermoresponsive Boc-Lysine-Based Acryl Polymer: RAFT Kinetics and Anti-Protein-Fouling of Its Zwitterionic Form. *Macromolecules* **2022**, *55* (10), 4011–4024.

(173) Nagaoka, S.; Shundo, A.; Satoh, T.; Nagira, K.; Kishi, R.; Ueno, K.; Iio, K.; Ihara, H. Method for a Convenient and Efficient Synthesis of Amino Acid Acrylic Monomers with Zwitterionic Structure. *Synth. Commun.* **2005**, *35* (19), 2529–2534.

(174) Liu, Q.; Li, W.; Singh, A.; Cheng, G.; Liu, L. Two Amino Acid-Based Superlow Fouling Polymers: Poly(Lysine Methacrylamide) and Poly(Ornithine Methacrylamide). *Acta Biomater.* **2014**, *10* (7),

2956–2964.

(175) Nakago, T.; Oki, Y.; Nousou, T.; Ogawa, T.; Shiraishi, K. Preparation of Zwitterionic Random and Block Poly(N-α-Acrylamide-L-Lysine-Co-2-Methacryloyloxyethyl Phosphorylcholine) Copolymers and Their Effect on Fibrinolytic Activity. *Mater. Adv.* **2024**, *5* (11), 4818–4831.

(176) Verbraeken, B.; Monnery, B. D.; Lava, K.; Hoogenboom, R. The Chemistry of Poly(2-Oxazoline)S. *Eur. Polym. J.* **2017**, *88*, 451–469.

(177) Kim, K.; Chen, W. C. W.; Heo, Y.; Wang, Y. Polycations and Their Biomedical Applications. *Prog. Polym. Sci.* **2016**, *60*, 18–50.

(178) Chen, J.; Hessler, J. A.; Putchakayala, K.; Panama, B. K.; Khan, D. P.; Hong, S.; Mullen, D. G.; DiMaggio, S. C.; Som, A.; Tew, G. N.; Lopatin, A. N.; Baker, J. R.; Holl, M. M. B.; Orr, B. G. Cationic Nanoparticles Induce Nanoscale Disruption in Living Cell Plasma Membranes. *J. Phys. Chem. B* **2009**, *113* (32), 11179–11185.

(179) Godbey, W. T.; Wu, K. K.; Mikos, A. G. Size Matters: Molecular Weight Affects the Efficiency of Poly(Ethylenimine) as a Gene Delivery Vehicle. *J. Biomed. Mater. Res.* **1999**, *45* (3), 268–275.

(180) Vaidyanathan, S.; Orr, B. G.; Banaszak Holl, M. M. Role of Cell Membrane–Vector Interactions in Successful Gene Delivery. *Acc. Chem. Res.* **2016**, *49* (8), 1486–1493.

(181) Seddon, A. M.; Casey, D.; Law, R. V.; Gee, A.; Templer, R. H.; Ces, O. Drug Interactions with Lipid Membranes. *Chem. Soc. Rev.* **2009**, *38* (9), 2509–2519.

(182) Karabaliev, M.; Kochev, V. Voltammetric Study of Levomepromazine Induced Ionic Permeability in a Model Lipid Membrane System. *Electrochem. commun.* **2001**, *3* (12), 742–745.

(183) Monnery, B. D.; Wright, M.; Cavill, R.; Hoogenboom, R.; Shaunak, S.; Steinke, J. H. G.; Thanou, M. Cytotoxicity of Polycations: Relationship of Molecular Weight and the Hydrolytic Theory of the Mechanism of Toxicity. *Int. J. Pharm.* **2017**, *521* (1–2), 249–258.

(184) Ballarín-González, B.; Howard, K. A. Polycation-Based Nanoparticle Delivery of RNAi Therapeutics: Adverse Effects and Solutions. *Adv. Drug Deliv. Rev.* **2012**, *64* (15), 1717–1729.

(185) Kwolek, U.; Jamróz, D.; Janiczek, M.; Nowakowska, M.; Wydro, P.; Kepczynski, M. Interactions of Polyethylenimines with Zwitterionic and Anionic Lipid Membranes. *Langmuir* **2016**, *32* (19), 5004–5018.

(186) Kopec, W.; Zak, A.; Jamroz, D.; Nakahata, R.; Yusa, S. I.; Gapsys, V.; Kepczynski, M. Polycation–Anionic Lipid Membrane Interactions. *Langmuir* **2020**, *36* (42), 12435–12450.

(187) Lächelt, U.; Wagner, E. Nucleic Acid Therapeutics Using Polyplexes: A Journey of 50 Years (and Beyond). *Chem. Rev.* **2015**, *115* (19), 11043–11078.

(188) Behr, J.-P. The Proton Sponge: A Trick to Enter Cells the Viruses Did Not Exploit. *Chimia (Aarau).* **1997**, *51* (1–2), 34.

(189) Haensler, J.; Szoka, F. C. Polyamidoamine Cascade Polymers Mediate Efficient Transfection of Cells in Culture. *Bioconjugate Chem* **1993**, *4*, 372–379.

(190) Van De Wetering, P.; Moret, E. E.; Schuurmans-Nieuwenbroek, N. M. E.; Van Steenbergen, M. J.; Hennink, W. E. Structure−Activity Relationships of Water-Soluble Cationic Methacrylate/Methacrylamide Polymers for Nonviral Gene Delivery. *Bioconjug. Chem.* **1999**, *10* (4), 589–597.

(191) Vermeulen, L. M. P.; Brans, T.; Samal, S. K.; Dubruel, P.; Demeester, J.; De Smedt, S. C.; Remaut, K.; Braeckmans, K. Endosomal Size and Membrane Leakiness Influence Proton Sponge-Based Rupture of Endosomal Vesicles. *ACS Nano* **2018**, *12* (3), 2332–2345.

(192) Yang, S.; May, S. Release of Cationic Polymer-DNA Complexes from the Endosome: A Theoretical Investigation of the Proton Sponge Hypothesis. *J. Chem. Phys.* **2008**, *129* (18).

(193) Won, Y. Y.; Sharma, R.; Konieczny, S. F. Missing Pieces in Understanding the Intracellular Trafficking of Polycation/DNA Complexes. *J. Control. Release* **2009**, *139* (2), 88–93.

(194) Bieber, T.; Meissner, W.; Kostin, S.; Niemann, A.; Elsasser, H. P. Intracellular Route and Transcriptional Competence of Polyethylenimine–DNA Complexes. *J. Control. Release* **2002**, *82* (2–3), 441–454.

(195) Trützschler, A. K.; Bus, T.; Reifarth, M.; Brendel, J. C.; Hoeppener, S.; Traeger, A.; Schubert, U. S. Beyond Gene Transfection with Methacrylate-Based Polyplexes—The Influence of the Amino Substitution Pattern. *Bioconjug. Chem.* **2018**, *29* (7), 2181–2194.

(196) Rehman, Z. U.; Hoekstra, D.; Zuhorn, I. S. Mechanism of Polyplex- and Lipoplex-Mediated Delivery of Nucleic Acids: Real-Time Visualization of Transient Membrane Destabilization without Endosomal Lysis. *ACS Nano* **2013**, *7* (5), 3767–3777.

(197) Bus, T.; Traeger, A.; Schubert, U. S. The Great Escape: How Cationic Polyplexes Overcome the Endosomal Barrier. *J. Mater. Chem. B* **2018**, *6* (43), 6904–6918.

(198) Moret, I.; Esteban Peris, J.; Guillem, V. M.; Benet, M.; Revert, F.; Dasí, F.; Crespo, A.; Alio, S. F. Stability of PEI–DNA and DOTAP–DNA Complexes: Effect of Alkaline PH, Heparin and Serum. *J. Control. Release* **2001**, *76* (1–2), 169–181.

(199) Lukacs, G. L.; Haggie, P.; Seksek, O.; Lechardeur, D.; Freedman, N.; Verkman, A. S. Size-Dependent DNA Mobility in Cytoplasm and Nucleus. *J. Biol. Chem.* **2000**, *275* (3), 1625–1629.

(200) Dauty, E.; Verkman, A. S. Actin Cytoskeleton as the Principal Determinant of Size-Dependent DNA Mobility in Cytoplasm. *J. Biol. Chem.* **2005**, *280* (9), 7823–7828.

(201) Karlsson, J.; Rhodes, K. R.; Green, J. J.; Tzeng, S. Y. Poly(Beta-Amino Ester)s as Gene Delivery Vehicles: Challenges and Opportunities. *Expert Opin. Drug Deliv.* **2020**.

(202) Sunshine, J. C.; Peng, D. Y.; Green, J. J. Uptake and Transfection with Polymeric Nanoparticles Are Dependent on Polymer End-Group Structure, but Largely Independent of Nanoparticle

Physical and Chemical Properties. *Mol. Pharm.* **2012**, *9* (11), 3375–3383.

(203) Karlsson, J.; Vaughan, H. J.; Green, J. J. Biodegradable Polymeric Nanoparticles for Therapeutic Cancer Treatments. *Annu. Rev. Chem. Biomol. Eng.* **2018**, *9*, 105–127.

(204) Klemm, P.; Solomun, J. I.; Rodewald, M.; Kuchenbrod, M. T.; Hänsch, V. G.; Richter, F.; Rgen Popp, J.; Hertweck, C.; Hoeppener, S.; Bonduelle, C.; Lecommandoux, S.; Traeger, A.; Schubert, S. Efficient Gene Delivery of Tailored Amphiphilic Polypeptides by Polyplex Surfing. **2022**, *23*, 4733.

(205) Wang, S. PH-Responsive Amphiphilic Carboxylate Polymers: Design and Potential for Endosomal Escape. *Front. Chem.* **2021**, *9*, 1–8.

(206) Kauffman, W. B.; Fuselier, T.; He, J.; Wimley, W. C. Mechanism Matters: A Taxonomy of Cell Penetrating Peptides. *Trends Biochem. Sci.* **2015**, *40* (12), 749–764.

(207) Ladavière, C.; Toustou, M.; Gulik-Krzywicki, T.; Tribet, C. Slow Reorganization of Small Phosphatidylcholine Vesicles upon Adsorption of Amphiphilic Polymers. *J. Colloid Interface Sci.* **2001**, *241* (1), 178–187.

(208) Yessine, M. Membrane-Destabilizing Polyanions: Interaction with Lipid Bilayers and Endosomal Escape of Biomacromolecules. *Adv. Drug Deliv. Rev.* **2004**, *56* (7), 999–1021.

(209) Polozova, A.; Winnik, F. M. Contribution of Hydrogen Bonding to the Association of Liposomes and an Anionic Hydrophobically Modified Poly(N-Isopropylacrylamide)†. *Langmuir* **1999**, *15* (12), 4222–4229.

(210) Chen, R.; Eccleston, M. E.; Yue, Z.; Slater, N. K. H. Synthesis and PH-Responsive Properties of Pseudo-Peptides Containing Hydrophobic Amino Acid Grafts. *J. Mater. Chem.* **2009**, *19* (24), 4217–4224.

(211) Chen, S.; Wang, S.; Kopytynski, M.; Bachelet, M.; Chen, R. Membrane-Anchoring, Comb-Like Pseudopeptides for Efficient, PH-Mediated Membrane Destabilization and Intracellular Delivery. *ACS Appl. Mater. Interfaces* **2017**, *9* (9), 8021–8029.

(212) Nelson, D. L.; Cox, M. M. Lehninger Principles of Biochemistry, Second Edition. *W H Free.* **2008**, 1158.

(213) Ciferri, A.; Kudaibergenov, S. Natural and Synthetic Polyampholytes, 1a Theory and Basic Structures. *Macromol. Rapid Commun.* **2007**, *28* (20), 1953–1968.

(214) Patrickios, C. S. Polypeptide Amino Acid Composition and Isoelectric Point: 1. A Closed-Form Approximation. *J. Colloid Interface Sci.* **1995**, *175* (1), 256–260.

(215) Williams, R. *PKa Data Compiled* ; 2022.

(216) Weers, J. G.; Rathman, J. F.; Axe, F. U.; Crichlow, C. A.; Poland, L. D.; Scheuing, D. R.; Wiersema, R. J.; Zielske, A. G. Effect of the Intramolecular Charge Separation Distance on the Solution Properties of Betaines and Sulfobetaines. *Langmuir* **1991**, *7*, 854–867.

(217) Hall, H. K. Correlation of the Base Strengths of Amines 1. *J. Am. Chem. Soc.* **1957**, *79* (20), 5441–5444.

(218) Bates, R. G.; Pinching, G. D. Acidic Dissociation Constant and Related Thermodynamic Quantities for Monoethanolammonium Ion in Water From 0° to 50 °C. *J. Res. Natl. Bur. Stand. .* **1951**, *46* (5), 349-352.

(219) Luis Bourdelande, J.; Gallardo, I.; Guirado, G. Inductive vs Solvation Effects in Primary Alkyl Amines: Determination of the Standard Potentials. *J. Am. Chem. Soc.* **2007**, 129, 2817-2821

(220) Raczyńska, E. D.; Gal, J. F.; Maria, P. C. Enhanced Basicity of Push–Pull Nitrogen Bases in the Gas Phase. *Chem. Rev.* **2016**, *116* (22), 13454–13511.

(221) Effenberger, F.; Fischer, P.; Schoeller, W. W.; Stohrer, W. D. The Donor Strength of Dialkylamino Functions—A Systematic Study of Δh/Hmo π-Electron Density Correlations in Aminobenzenes. *Tetrahedron* **1978**, *34* (15), 2409–2417.

(222) Burgers, J.; Hoefnagel, M. A.; Verkade, P. E.; Visser, H.; Wepster, B. M. Steric Effects on Mesomerism. XVII. Some Properties of Aromatic Nitro-, Amino-, and Acylamino Compounds with Bulky Ortho-Substituents. *Recl. des Trav. Chim. des Pays-Bas* **1958**, *77* (6), 491–530.

(223) Morozova, S.; Hu, G.; Emrick, T.; Muthukumar, M. Influence of Dipole Orientation on Solution Properties of Polyzwitterions. ACS Macro Lett. **2016**, 5, 118−122.

(224) Sarker, P.; Lu, T.; Liu, D.; Wu, G.; Chen, H.; Jahan Sajib, M. S.; Jiang, S.; Chen, Z.; Wei, T. Hydration Behaviors of Nonfouling Zwitterionic Materials. *Chem. Sci.* **2023**, *14* (27), 7500–7511.

(225) Erfani, A.; Seaberg, J.; Aichele, C. P.; Ramsey, J. D. Interactions between Biomolecules and Zwitterionic Moieties: A Review. *Biomacromolecules* **2020**, *21* (7), 2557–2573.

(226) Sedlák, M. Domain Structure of Polyelectrolyte Solutions: Is It Real? *Macromolecules* **1993**, *26*, 1158–1162.

(227) Paleg, L. G.; Stewart, G. R.; Bradbeer, J. W. Proline and Glycine Betaine Influence Protein Solvation. *Plant Physiol.* **1984**, *75* (4), 974–978.

(228) Arakawa, T.; Timasheff, S. N. Preferential Interactions of Proteins with Solvent Components in Aqueous Amino Acid Solutions. *Arch. Biochem. Biophys.* **1983**, *224* (1), 169–177.

(229) Ladd, J.; Zhang, Z.; Chen, S.; Hower, J. C.; Jiang, S. Zwitterionic Polymers Exhibiting High Resistance to Nonspecific Protein Adsorption from Human Serum and Plasma. *Biomacromolecules* **2008**, *9* (5), 1357–1361.

(230) Viklund, C.; Irgum, K. Synthesis of Porous Zwitterionic Sulfobetaine Monoliths and Characterization of Their Interaction with Proteins. Macromolecules **2000**, 33, 2539-2544

(231) Schlenoff, J. B. Zwitteration: Coating Surfaces with Zwitterionic Functionality to Reduce Nonspecific Adsorption. Langmuir **2014**, 30, 9625−9636

(232) Chen, S.; Li, L.; Zhao, C.; Zheng, J. Surface Hydration: Principles and Applications toward Low-Fouling/Nonfouling Biomaterials. *Polymer (Guildf).* **2010**, *51* (23), 5283–5293.

(233) He, M.; Gao, K.; Zhou, L.; Jiao, Z.; Wu, M.; Cao, J.; You, X.; Cai, Z.; Su, Y.; Jiang, Z. Zwitterionic Materials for Antifouling Membrane Surface Construction. *Acta Biomater.* **2016**, *40*, 142–152.

(234) Bernstein, R.; Belfer, S.; Freger, V. Bacterial Attachment to RO Membranes Surface-Modified by Concentration-Polarization-Enhanced Graft Polymerization. *Environ. Sci. Technol.* **2011**, *45* (14), 5973–5980.

(235) Theodorou, I.; Anilkumar, P.; Lelandais, B.; Clarisse, D.; Doerflinger, A.; Gravel, E.; Ducongé, F.; Doris, E. Stable and Compact Zwitterionic Polydiacetylene Micelles with Tumor-Targeting Properties. *Chem. Commun.* **2015**, *51* (80), 14937–14940. https://doi.org/10.1039/c5cc05333a.

(236) Takano, S.; Sakurai, K.; Fujii, S. Internalization into Cancer Cells of Zwitterionic Amino Acid Polymers via Amino Acid Transporter Recognition. *Polym. Chem.* **2021**, *12* (42), 6083–6087.

(237) Zhang, Z.; Chen, S.; Jiang, S. Dual-Functional Biomimetic Materials: Nonfouling Poly(Carboxybetaine) with Active Functional Groups for Protein Immobilization. *Biomacromolecules* **2006**, *7* (12), 3311–3315.

(238) Yang, H.; Wang, Y.; Yao, L.; Wang, J.; Chen, H. Antifouling Polymer Coatings for Bioactive Surfaces. *Langmuir* **2025**, *41* (10), 6471–6496.

(239) Erathodiyil, N.; Chan, H. M.; Wu, H.; Ying, J. Y. Zwitterionic Polymers and Hydrogels for Antibiofouling Applications in Implantable Devices. *Mater. Today* **2020**, *38*, 84–98.

(240) Zhang, Z.; Chen, S.; Chang, Y.; Jiang, S. Surface Grafted Sulfobetaine Polymers via Atom Transfer Radical Polymerization as Superlow Fouling Coatings. *J. Phys. Chem. B* **2006**, *110* (22), 10799–10804.

(241) Jiang, S.; Cao, Z. Ultralow-Fouling, Functionalizable, and Hydrolyzable Zwitterionic Materials and Their Derivatives for Biological Applications. *Adv. Mater.* **2010**, *22* (9), 920–932.

(242) Zhang, Z.; Shen, C.; Zhang, P.; Xu, S.; Kong, L.; Liang, X.; Li, C.; Qiu, X.; Huang, J.; Cui, X. Fundamental, Mechanism and Development of Hydration Lubrication: From Bio-Inspiration to Artificial Manufacturing. *Adv. Colloid Interface Sci.* **2024**, *327*, 103145.

(243) Milner, P. E.; Parkes, M.; Puetzer, J. L.; Chapman, R.; Stevens, M. M.; Cann, P.; Jeffers, J. R. T. A Low Friction, Biphasic and Boundary Lubricating Hydrogel for Cartilage Replacement. *Acta Biomater.* **2018**, *65*, 102–111.

(244) Gao, Y.; Liu, S.; Huang, J.; Guo, W.; Chen, J.; Zhang, L.; Zhao, B.; Peng, J.; Wang, A.; Wang, Y.; Xu, W.; Lu, S.; Yuan, M.; Guo, Q. The ECM-Cell Interaction of Cartilage Extracellular Matrix on Chondrocytes. *Biomed Res. Int.* **2014**, *2014*.

(245) Roughley, P. J. Articular Cartilage and Changes in Arthritis: Noncollagenous Proteins and Proteoglycans in the Extracellular Matrix of Cartilage. *Arthritis Res. Ther. 2001 36* **2001**, *3* (6),

342

(246) Jay, G. D.; Torres, J. R.; Warman, M. L.; Laderer, M. C.; Breuer, K. S. The Role of Lubricin in the Mechanical Behavior of Synovial Fluid. *Proc. Natl. Acad. Sci. U. S. A.* **2007**, *104* (15), 6194–6199.

(247) Liu, G.; Feng, Y.; Gao, X.; Chen, Z.; Zhao, N.; Zhou, F.; Liu, W. Synovial Fluid-Inspired Biomimetic Lubricating Microspheres: Zwitterionic Polyelectrolyte Brushes-Grafted Microgels. *Frict. 2022 116* **2022**, *11* (6), 938–948.

(248) Asadikorayem, M.; Surman, F.; Weber, P.; Weber, D.; Zenobi-Wong, M. Zwitterionic Granular Hydrogel for Cartilage Tissue Engineering. *Adv. Healthc. Mater.* **2024**, *13* (25), 2301831.

(249) Yuan, L.; Gao, Y.; Wang, Q.; Zhu, K.; Ren, L.; Yuan, X. Construction of Small-Diameter Vascular Grafts by Electrospun Zwitterionic Diselenide-Containing Poly(Ester Urethane)Urea with Enhanced Endothelialization. *Acta Biomater.* **2025** (early view).

(250) Li, S.; Zhao, F.; Tang, Y.; Zhang, Y.; Rong, H.; Liu, L.; Gao, R.; Liu, X.; Huangfu, Y.; Bai, Y.; Feng, Z.; Guo, Z.; Dong, A.; Wang, W.; Kong, D.; Huang, P. Bioinspired, Anticoagulative, 19F MRI-Visualizable Bilayer Hydrogel Tubes as High Patency Small-Diameter Vascular Grafts. *Small* **2023**, *19* (42), 2302621.

(251) Zhu, Y.; Zhang, C.; Liang, Y.; Shi, J.; Yu, Q.; Liu, S.; Yu, D.; Liu, H. Advanced Postoperative Tissue Antiadhesive Membranes Enabled with Electrospun Nanofibers. *Biomater. Sci.* **2024**, *12* (7), 1643–1661.

(252) Cao, X.; Lu, M.; Wang, J.; Wang, Y.; Zhao, Y. Verteporfin-Integrated Conductive Zwitterionic Hydrogels for Scarless Wound Management. *Nano Today* **2025**, *61*, 102659.

(253) Wei, M.; Wang, H.; Wu, J.; Yang, D.; Li, K.; Liu, X.; Wang, M.; Lin, B.; Wang, Z. Multihydrogen Bond Modulated Polyzwitterionic Removable Adhesive Hydrogel with Antibacterial and Hemostatic Function for Wound Healing. *ACS Appl. Mater. Interfaces* **2024**, *16* (17), 21472–21485.

(254) Li, L.; Yue, M.; Peng, Q.; Pu, X.; Li, Z. Metabolic Response Modulations by Zwitterionic Hydrogels for Achieving Promoted Bone Regeneration. *Adv. Funct. Mater.* **2024**, *34* (11), 2309594.

(255) Zhang, L.; Cao, Z.; Bai, T.; Carr, L.; Ella-Menye, J. R.; Irvin, C.; Ratner, B. D.; Jiang, S. Zwitterionic Hydrogels Implanted in Mice Resist the Foreign-Body Reaction. *Nat. Biotechnol. 2013 316* **2013**, *31* (6), 553–556.

(256) Bui, H. L.; Su, Y. H.; Yang, C. J.; Huang, C. J.; Lai, J. Y. Mucoadhesive, Antioxidant, and Lubricant Catechol-Functionalized Poly(Phosphobetaine) as Biomaterial Nanotherapeutics for Treating Ocular Dryness. *J. Nanobiotechnology 2024 221* **2024**, *22* (1), 160

(257) Ishihara, K.; Nomura, H.; Mihara, T.; Kurita, K.; Iwasaki, Y.; Nakabayashi, N. Why Do Phospholipid Polymers Reduce Protein Adsorption? *J Biomed Mater Res* **1998**, *39*, 323–330.

(258) Lewis, A. L. Phosphorylcholine-Based Polymers and Their Use in the Prevention of Biofouling. *Colloids Surfaces B Biointerfaces* **2000**, *18* (3–4), 261–275.

(259) Ng, S. C.; Shi, H. Y.; Hamidi, N.; Underwood, F. E.; Tang, W.; Benchimol, E. I.; Panaccione, R.; Ghosh, S.; Wu, J. C. Y.; Chan, F. K. L.; Sung, J. J. Y.; Kaplan, G. G. Worldwide Incidence and Prevalence of Inflammatory Bowel Disease in the 21st Century: A Systematic Review of Population-Based Studies. *Lancet* **2017**, *390* (10114), 2769–2778.

(260) Weng, M. T.; Hsiung, C. Y.; Wei, S. C.; Chen, Y. Nanotechnology for Targeted Inflammatory Bowel Disease Therapy: Challenges and Opportunities. *Wiley Interdiscip. Rev. Nanomedicine Nanobiotechnology* **2024**, *16* (5), e1999.

(261) Li, Y. F.; Udayakumar, V.; Sathuvan, M.; Liu, Y.; Liu, X.; Zhang, Y. Q.; Ma, W. Y.; Zhang, W.; Tang, S.; Cheong, K. L. Effects of Laminarin Zwitterionic Carboxylate and Sulfonate on the Intestinal Barrier Function and Gut Microbiota. *Carbohydr. Polym.* **2022**, *278*, 118898.

(262) Wang, R.; Hu, Q.; Huang, S.; Fang, Y.; Kong, X.; Kaur, P.; Zhang, J.; Wang, Y.; Liu, D.; Wu, H.; Li, Y.; Ji, J.; Yang, X.; Ye, L.; Zhai, G. Zwitterionic Injectable Hydrogel-Combined Chemo- and Immunotherapy Medicated by Monomolecular Micelles to Effectively Prevent the Recurrence of Tumor Post Operation. *ACS Appl. Mater. Interfaces* **2024**, *16* (3), 4071–4088.

(263) Wang, X.; Sun, X.; Lei, J.; Li, L.; Zhu, N.; Yu, Y.; Zeng, Y.; Kang, K.; Yi, Q. Y.; Wu, Y. Bioinspired Zwitterionic Lysine Glycopolymers: Enhancing Wound Repair through Microenvironment Modulation for Bacterial Elimination and Optimal Immunoregulation. *Nano Today* **2024**, *57*, 102354.

(264) Rivnay, J.; Raman, R.; Robinson, J. T.; Schreib, C.; Cohen-Karni, T.; Galloway, K. E.; Veiseh, O. Integrating Bioelectronics with Cell-Based Synthetic Biology. *Nat. Rev. Bioeng. 2025 34* **2025**, *3* (4), 317–332.

(265) Xie, X.; Doloff, J. C.; Yesilyurt, V.; Sadraei, A.; McGarrigle, J. J.; Omami, M.; Veiseh, O.; Farah, S.; Isa, D.; Ghani, S.; Joshi, I.; Vegas, A.; Li, J.; Wang, W.; Bader, A.; Tam, H. H.; Tao, J.; Chen, H. J.; Yang, B.; Williamson, K. A.; Oberholzer, J.; Langer, R.; Anderson, D. G. Reduction of Measurement Noise in a Continuous Glucose Monitor by Coating the Sensor with a Zwitterionic Polymer. *Nat. Biomed. Eng. 2018 212* **2018**, *2* (12), 894–906.

(266) Liang, B.; Zhang, G.; Zhong, Z.; Huang, Y.; Su, Z. Superhydrophilic Anti-Icing Coatings Based on Polyzwitterion Brushes. *Langmuir* **2018**, *35* (5), 1294–1301.

(267) Lv, Y.; Lin, Z.; Svec, F. Hypercrosslinked Large Surface Area Porous Polymer Monoliths for Hydrophilic Interaction Liquid Chromatography of Small Molecules Featuring Zwitterionic Functionalities Attached to Gold Nanoparticles Held in Layered Structure. *Anal. Chem.* **2012**, *84* (20), 8457–8460.

(268) Muttenthaler, M.; King, G. F.; Adams, D. J.; Alewood, P. F. Trends in Peptide Drug Discovery. *Nat. Rev. Drug Discov. 2021 204* **2021**, *20* (4), 309–325.

(269) Manzari, M. T.; Shamay, Y.; Kiguchi, H.; Rosen, N.; Scaltriti, M.; Heller, D. A. Targeted Drug Delivery Strategies for Precision Medicines. *Nat. Rev. Mater. 2021 64* **2021**, *6* (4), 351–370.

(270) Li, Y.; Zhang, R.; Lu, Z.; Ma, G.; Chen, L.; Tang, Q.; Zhang, X. Microenvironment-Responsive Three-Pronged Approach Breaking Traditional Chemotherapy to Target Cancer Stem Cells for Synergistic Inoperable Large Tumor Therapy. **2016**.

(271) Zhang, R.; Li, Y.; Hu, B.; Lu, Z.; Zhang, J.; Zhang, X. Traceable Nanoparticle Delivery of Small Interfering Rna and Retinoic Acid with Temporally Release Ability to Control Neural Stem Cell Differentiation for Alzheimer's Disease Therapy. *Adv. Mater.* **2016**, *28* (30), 6345–6352.

(272) Aryal, S.; Grailer, J. J.; Pilla, S.; Steeber, D. A.; Gong, S. Doxorubicin Conjugated Gold Nanoparticles as Water-Soluble and PH-Responsive Anticancer Drug Nanocarriers. *J. Mater. Chem.* **2009**, *19* (42), 7879–7884.

(273) Kita, K.; Dittrich, C. Drug Delivery Vehicles with Improved Encapsulation Efficiency: Taking Advantage of Specific Drug-Carrier Interactions. *Expert Opin. Drug Deliv.* **2011**, *8* (3), 329–342.

(274) Sun, Q.; Radosz, M.; Shen, Y. Challenges in Design of Translational Nanocarriers. *J. Control. Release* **2012**, *164* (2), 156–169.

(275) Ou, H.; Cheng, T.; Zhang, Y.; Liu, J.; Ding, Y.; Zhen, J.; Shen, W.; Xu, Y.; Yang, W.; Niu, P.; Liu, J.; An, Y.; Liu, Y.; Shi, L. Surface-Adaptive Zwitterionic Nanoparticles for Prolonged Blood Circulation Time and Enhanced Cellular Uptake in Tumor Cells. *Acta Biomater.* **2018**, *65*, 339–348.

(276) Lin, W.; Ma, G.; Ji, F.; Zhang, J.; Wang, L.; Sun, H.; Chen, S. Biocompatible Long-Circulating Star Carboxybetaine Polymers. *J. Mater. Chem. B* **2014**, *3* (3), 440–448.

(277) Izquierdo-Barba, I.; Colilla, M.; Vallet-Regí, M. Zwitterionic Ceramics for Biomedical Applications. *Acta Biomater.* **2016**, *40*, 201–211.

(278) Wang, Z.; Ma, G.; Zhang, J.; Lin, W.; Ji, F.; Bernards, M. T.; Chen, S. Development of Zwitterionic Polymer-Based Doxorubicin Conjugates: Tuning the Surface Charge To Prolong the Circulation and Reduce Toxicity. *Langmuir* **2014**, *30* (13), 3764–3774.

(279) Kusonwiriyawong, C.; Van De Wetering, P.; Hubbell, J. A.; Merkle, H. P.; Walter, E. Evaluation of PH-Dependent Membrane-Disruptive Properties of Poly(Acrylic Acid) Derived Polymers. *Eur. J. Pharm. Biopharm.* **2003**, *56* (2), 237–246.

(280) Park, S. Bin; Sung, M. H.; Uyama, H.; Han, D. K. Poly(Glutamic Acid): Production, Composites, and Medical Applications of the next-Generation Biopolymer. *Prog. Polym. Sci.* **2021**, *113*, 101341.

(281) Colley, H. E.; Hearnden, V.; Avila-Olias, M.; Cecchin, D.; Canton, I.; Madsen, J.; Macneil, S.; Warren, N.; Hu, K.; McKeating, J. A.; Armes, S. P.; Murdoch, C.; Thornhill, M. H.; Battaglia, G. Polymersome-Mediated Delivery of Combination Anticancer Therapy to Head and Neck Cancer Cells: 2D and 3D in Vitro Evaluation. *Mol. Pharm.* **2014**, *11* (4), 1176–1188.

(282) Govrin, R.; Tcherner, S.; Obstbaum, T.; Sivan, U. Zwitterionic Osmolytes Resurrect Electrostatic Interactions Screened by Salt. *J. Am. Chem. Soc.* **2018**, *140* (43), 14206–14210.

(283) Licciardi, M.; Craparo, E. F.; Giammona, G.; Armes, S. P.; Tang, Y.; Lewis, A. L. In Vitro Biological Evaluation of Folate-Functionalized Block Copolymer Micelles for Selective Anti-Cancer Drug Delivery. *Macromol. Biosci.* **2008**, *8* (7), 615–626.

(284) Qian, H.; Wang, K.; Lv, M.; Zhao, C.; Wang, H.; Wen, S.; Huang, D.; Chen, W.; Zhong, Y. Recent Advances on next Generation of Polyzwitterion-Based Nano-Vectors for Targeted Drug Delivery. *J. Control. Release* **2022**, *343*, 492–505.

(285) Keefe, A. J.; Jiang, S. Poly(Zwitterionic)Protein Conjugates Offer Increased Stability without Sacrificing Binding Affinity or Bioactivity. *Nat. Chem. 2011 41* **2011**, *4* (1), 59–63.

(286) Konno, T.; Watanabe, J.; Ishihara, K. Enhanced Solubility of Paclitaxel Using Water-Soluble and Biocompatible 2-Methacryloyloxyethyl Phosphorylcholine Polymers. *J. Biomed. Mater. Res. - Part A* **2003**, *65* (2), 209–214.

(287) Mitragotri, S.; Burke, P. A.; Langer, R. Overcoming the Challenges in Administering Biopharmaceuticals: Formulation and Delivery Strategies. *Nat. Rev. Drug Discov.* **2014**, *13* (9), 655–672.

(288) Zhong, Y.; Meng, F.; Deng, C.; Zhong, Z. Ligand-Directed Active Tumor-Targeting Polymeric Nanoparticles for Cancer Chemotherapy. *Biomacromolecules* **2014**, *15* (6), 1955–1969.

(289) Zununi Vahed, S.; Fathi, N.; Samiei, M.; Maleki Dizaj, S.; Sharifi, S. Targeted Cancer Drug Delivery with Aptamer-Functionalized Polymeric Nanoparticles. *J. Drug Target.* **2019**, *27* (3), 292–299.

(290) Miura, Y.; Hoshino, Y.; Seto, H. Glycopolymer Nanobiotechnology. *Chem. Rev.* **2015**, *116* (4), 1673–1692.

(291) Figueroa-Soto, C. G.; Valenzuela-Soto, E. M. Glycine Betaine Rather than Acting Only as an Osmolyte Also Plays a Role as Regulator in Cellular Metabolism. *Biochimie* **2018**, *147*, 89–97.

(292) Kempson, S. A.; Zhou, Y.; Danbolt, N. C. The Betaine/GABA Transporter and Betaine: Roles in Brain, Kidney, and Liver. *Front. Physiol.* **2014**, 81573.

(293) Wang, R.; Yang, S.; Xiao, P.; Sun, Y.; Li, J.; Jiang, X.; Wu, W. Fluorination and Betaine Modification Augment the Blood–Brain Barrier-Crossing Ability of Cylindrical Polymer Brushes. *Angew. Chemie* **2022**, *134* (19), e202201390.

(294) Han, X.; Lu, Y.; Xie, J.; Zhang, E.; Zhu, H.; Du, H.; Wang, K.; Song, B.; Yang, C.; Shi, Y.; Cao, Z. Zwitterionic Micelles Efficiently Deliver Oral Insulin without Opening Tight Junctions. *Nat. Nanotechnol.* **2020**, *15* (7), 605–614.

(295) Bröer, S. Amino Acid Transporters as Targets for Cancer Therapy: Why, Where, When, and How. *Int. J. Mol. Sci.* **2020**, *21* (17), 1–20.

(296) Yanagida, O.; Kanai, Y.; Chairoungdua, A.; Kim, D. K.; Segawa, H.; Nii, T.; Cha, S. H.; Matsuo, H.; Fukushima, J. ichi; Fukasawa, Y.; Tani, Y.; Taketani, Y.; Uchino, H.; Kim, J. Y.; Inatomi, J.; Okayasu, I.; Miyamoto, K. ichi; Takeda, E.; Goya, T.; Endou, H. Human L-Type Amino Acid Transporter 1 (LAT1): Characterization of Function and Expression in Tumor Cell Lines. *Biochim. Biophys. Acta - Biomembr.* **2001**, *1514* (2), 291–302.

(297) Fuchs, B. C.; Bode, B. P. Amino Acid Transporters ASCT2 and LAT1 in Cancer: Partners in Crime? *Semin. Cancer Biol.* **2005**, *15* (4), 254–266.

(298) Yamada, N.; Honda, Y.; Takemoto, H.; Nomoto, T.; Matsui, M.; Tomoda, K.; Konno, M.; Ishii, H.; Mori, M.; Nishiyama, N. Engineering Tumour Cell-Binding Synthetic Polymers with Sensing Dense Transporters Associated with Aberrant Glutamine Metabolism. *Sci. Rep.* **2017**, *7* (1), 6077.

(299) Leiske, M. N.; Mazrad, Z. A. I.; Zelcak, A.; Wahi, K.; Davis, T. P.; McCarroll, J. A.; Holst, J.; Kempe, K. Zwitterionic Amino Acid-Derived Polyacrylates as Smart Materials Exhibiting Cellular Specificity and Therapeutic Activity. *Biomacromolecules* **2022**, *23* (6), 2374–2387.

(300) Grewer, C.; Grabsch, E. New Inhibitors for the Neutral Amino Acid Transporter ASCT2 Reveal Its Na+ -Dependent Anion Leak. *J. Physiol.* **2004**, *557* (3), 747–759.

(301) Fujii, S.; Sakurai, K. Zwitterionic Amino Acid Polymer-Grafted Core-Crosslinked Particle toward Tumor Delivery. *Biomacromolecules* **2022**, *23* (9), 3968–3977.

(302) Qin, Z.; Chen, T.; Teng, W.; Jin, Q.; Ji, J. Mixed-Charged Zwitterionic Polymeric Micelles for Tumor Acidic Environment Responsive Intracellular Drug Delivery. *Langmuir* **2019**, *35* (5), 1242–1248.

(303) Cai, M.; Cao, J.; Wu, Z.; Cheng, F.; Chen, Y.; Luo, X. In Vitro and in Vivo Anti-Tumor Efficiency Comparison of Phosphorylcholine Micelles with PEG Micelles. *Colloids Surfaces B Biointerfaces* **2017**, *157*, 268–279.

(304) Monnery, B. D. Polycation-Mediated Transfection: Mechanisms of Internalization and Intracellular Trafficking. *Biomacromolecules* **2021**, *22* (10), 4060–4083.

(305) Deng, X.; Wang, Y.; Zhang, F.; Yin, Z.; Hu, Q.; Xiao, X.; Zhou, Z.; Wu, Y.; Sheng, W.; Zeng, Y. Acidic PH-Induced Charge-Reversal Nanoparticles for Accelerated Endosomal Escape and Enhanced MicroRNA Modulation in Cancer Cells. *Chem. Commun.* **2016**, *52* (15), 3243–3246.

2 Objective

Intracellular delivery remains a major challenge in the development of biotherapeutics.[1,2] To date, most clinically successful biologics still target extracellular receptors. This is based on a selectively permeable lipid–protein architecture of the cellular plasma membrane, which, effectively prevents the free passage of proteins, peptides, and nucleic acids.[3] As a result, these biomacromolecules typically enter cells via endocytosis, becoming entrapped within endosomal compartments rather than reaching their intended intracellular targets. Once internalized, most cargos are subjected to the endosomal maturation pathway: early endosomes acidify to pH 6.8–6.1 as adenosine triphosphate-driven proton pumps become active. During acidification, the cargos inside the endosomes are sorted and some are recycled back.[4] Non-recycled cargos progress to late endosomes, which acidify further to pH 6.0–4.8 before ultimately fusing with lysosomes, where degradation occurs at pH ~4.5. This maturation process represents a major barrier for intracellular delivery, as therapeutics that do not escape before lysosomal fusion are rapidly degraded.[5]

The pH gradient along the endocytic pathway offers an attractive opportunity to trigger structural changes in materials that could facilitate endosomal escape. In this context, the overarching objective of this dissertation is to design **pH-responsive polyelectrolytes** which could have the potential to target active internalization such as transporter-mediated uptake or endocytosis combined with improved cell internalization properties of future polymer-drug conjugates. This is mainly pursued through the design and synthesis of **amino-acid-derived polyelectrolytes**, which offer versatile opportunities for tuning physiochemical properties relevant to intracellular delivery. The latter is especially important in therapeutics *f.e.* cancer therapy

Furthermore, effective cancer therapy critically depends on **cellular specificity** *i.e.*, therapeutic agents must preferentially interact with and accumulate in cancer cells while leaving healthy cells unaffected. The polyelectrolytes will be designed to achieve such selective interactions without relying on the laborious and costly incorporation of external targeting moieties, such as antibodies or peptides, which complicate synthesis, reproducibility and scale-up. Instead, the focus lies on developing materials whose responsiveness and selectivity arise directly from their molecular composition and tunable structural features *i.e.* pH-responsivity, enabling straightforward preparation and flexible adjustment for future therapeutic applications. A simple way to implement pH-responsivity and, therefore, cellular targeting polyelectrolytes is the use of **amino acids** or amino-acid-like building blocks. The synthesis strategies and novel zwitterionic and anionic polymers shown in this work build upon performed work of my supervisor on polyzwitterions. There, structure-property relationships which were studied by alterations in the macromolecular structure (*e.g.* study of different polymer backbones) of and compromise detailed information on hydrophobicity and cell-polymer interactions.

Betain-like polyzwitterions

Amino-acid-derived polyzwitterions and **PBs** are two promising alternatives to non-ionic polymers, for example, to increase tumor permeability. PBs, one of the most studied categories of polyzwitterions, have emerged as promising alternative to traditional non-ionic polymers in tumor therapy. PBs are

characterized by the presence of both an anionic and permanently charged cationic group within the same repeat unit. Owing to their internal charge balance, they can resist non-specific protein adsorption or cell adhesion while at the same time being able to penetrate deeply into tumor tissue. Amino-acid-derived polyzwitterions, on the other hand, introduce a stereocenter due to their amino acid precursor. While the stereocenter offers unique opportunities towards molecular interactions, the primary amine functionality renders highly sensitive polymers towards pH changes. This high sensitivity makes it challenging to establish clear structure-property relationships.

The *first* part of this dissertation therefore aims to bridge the advantages of both classes by developing a synthetic strategy for **chiral, amino-acid-derived PBs**. Thereby, a strategy is developed to quaternize the amine in the functional group of the side-chain of the polyzwitterion. In more detail, a monomer resembling the targeted polymer structure will be synthesized. Subsequently, this monomer will be polymerized *via* RAFT for which a kinetic study will be performed. This will give the opportunity to directly obtain the chiral, amino-acid-derived PB with different X_n. Subsequently, the role of chirality and permanent positive charge is explored by comparing the quaternized and non-quaternized zwitterionic analogues obtained *via* PPM. Physical characterization, such as aggregation behavior at different pH values will be measured by dynamic light scattering (DLS) and will provide insight into the impact of quaternization. Circular dichroism (CD) spectroscopy aims to clarify the stereochemistry of the polymers. Initial biological evaluation will include protein fouling via DLS and, in cooperation with the chair for process biotechnology of Prof Dr Freitag, University of Bayreuth, cytocompatibility via 3-(4,5-di methyl thiazol-2-yl)-2,5-diphenyltetrazolium bromide) (MTT) assays will be performed by me.

Post-polymerization modification of pH-responsive polyanions

The *second* part of this dissertation focusses on **amino-acid-derived polyanions with different alkyl side-chains**. Unlike cationic polymers, polyanions do not destructively penetrate the negatively charged cell membrane due to repulsive interactions and therefore may serve as safer alternative for intracellular delivery. Their pH-responsiveness can be relevant in the late endosomes, where the pH decreases from 6.0 to 4.8 and structural transitions may facilitate endosomal escape.

To explore a systematic library of such materials, the PPM method of activated ester polymers with amino acids is used. By applying the same prepolymer, we can study the sole effect on the alterations of alkyl side-chain. The activated ester prepolymers, in this case activated ester PPFPA, will be synthesized by RAFT which will be done, in cooperation, by Michael Ringleb at the laboratory of organic and macromolecular chemistry of Prof Dr Schubert, Friedrich Schiller University Jena. Subsequently, the prepolymer will be modified with different amino acids through PPM to obtain fast and quantitative formation of amino-acid-derived polyanions. These will be used to investigate the alkyl side-chain (length and branching) influence on hydrophobicity, pH-response and other physicochemical properties.

Before testing the polymers in biological systems, protein fouling by DLS measurements will be performed. Afterward, interaction studies of the amino-acid-derived polyanions with cells were conducted to investigate the correlation between physicochemical and biological properties. The study will include an MTT assay, a hemocompatibility assay, an erythrocyte aggregation assay, time- and temperature-dependent cell association assay and imaging via confocal laser scanning microscopy.

These experiments will be conducted, in cooperation, by Michael Streiber at the Jena center of soft matter of Prof Dr Schubert, Friedrich Schiller university Jena.

Comparing Zwitterions and Polyanions Through Tailored Amino-Acid Functionality

Building upon the outcomes of the previous sections, the *third* part investigates direct structure-property relationship between amino-acid-based polyanions and zwitterionic counterparts. Therefore, zwitterionic (methylated) lysine and phenylaniline-functionalized polymers will be synthesized additionally to structurally analogous polyanions via PPM of an activated ester prepolymer. This design allows impact influence of aromaticity, charge, and hydrophobicity which be evaluated independently. The influence of those functional groups on hydrophobicity, pH-response and other physicochemical properties will be investigated, similarly to the *second* part.

Biological assays such as MTT assay, and cell association studies with different cell lines with and without the addition of specific amino acid transporter inhibition and competitive uptake assays will be performed at the chair for process biotechnology of Prof Dr Freitag, University of Bayreuth, by me. Additionally, confocal laser scanning microscopy (CLSM) measurements will be performed, in cooperation, by Jonas P Debbeler at the Jena center of soft matter of Prof Dr Schubert, Friedrich Schiller University Jena.

Together, these parts aim to establish comprehensive structure–property relationships for amino-acid-based polyelectrolytes with varying charge states, hydrophobicity, and stereochemical features. By combining synthetic design, detailed physicochemical characterization, and extensive biological evaluation, this dissertation seeks to contribute to the development of next-generation pH-responsive materials for intracellular delivery, with particular emphasis on selective cancer-targeting polymer systems.

[1] Stewart, M.P., Langer, R., and Jensen, K.F. Intracellular Delivery by Membrane Disruption: Mechanisms, Strategies, and Concepts. Chem. Rev., 2018, 118 (16), 7409–7531.

[2] van Haasteren, J., Li, J., Scheideler, O.J., Murthy, N., and Schaffer, D. V. The delivery challenge: fulfilling the promise of therapeutic genome editing. Nat. Biotechnol. 2020 387, 2020, 38 (7), 845–855.

[3] Pei, D., and Buyanova, M. Overcoming Endosomal Entrapment in Drug Delivery. Bioconjug. Chem., 2018, 30 (2), 273–283.

[4] Barysch, S. V., Aggarwal, S., Jahn, R., and Rizzoli, S.O. Sorting in early endosomes reveals connections to docking- and fusion-associated factors. Proc. Natl. Acad. Sci. U. S. A., 2009, 106 (24), 9697–9702.

[5] Huotari, J., and Helenius, A. Endosome maturation. EMBO J. 2011 3017, 2011, 30 (17), 3481–3500.

3 Synopsis

3.1 Overview of the Thesis

The general aim of this dissertation is to develop and systematically investigate amino-acid derived, pH-responsive polyelectrolytes as next-generation materials for intracellular delivery with particular emphasis on selective cancer-targeting polymer systems. The central idea is that precise control over charge, hydrophobicity, and side-chain architecture in amino-acid-derived polymers enables control over protein interactions, cell association and potential endosomal escape, without relying on external targeting ligands such as peptides or antibodies.

Amino-acid-derived polymers, considered as biomacromolecular cargo in the context of intracellular delivery, typically enter cells via energy dependent or endocytosis and encounter the progressively acidifying endosomal pathway. Exploiting the associated pH gradient, going from pH ≈ 6 in the early endosomes to pH ≈ 4.5 in the lysosomes, requires polymers that can respond in a controlled manner, *f.e.* by changing charge state or hydrophobicity. Thereby these polymers could initiate membrane interactions upon change in pH. pH-responsive polyelectrolytes (*i.e.* polyanions, polycations, and polyzwitterions) are particularly attractive candidates because their ionizable groups can be engineered to respond in this physiologically relevant pH range. Herein, amino acids form an interesting and versatile platform for the development of functional polyelectrolytes. Their intrinsic stereochemistry introduces chirality into polyelectrolytes which can influence molecular recognition and biological interactions. Additionally, the chemical versatility of amino acids, both synthetically and in nature, enables tuning of material properties, such as hydrophobicity. Moreover, amino acids contain ionizable groups that can be modified to remain permanently charged or to respond dynamically to pH changes which are required to exploit the acidification during the endosomal pathway. Finally, their biomimetic character contributes to reduced nonspecific fouling while enabling opportunities for selective interactions with cellular membranes or proteins.

The thesis therefore focuses on amino-acid-derived polyacrylamides, in which amino acids or amino-acid-like moieties are introduced as side-chains either directly via monomer design or via PPM of activated ester prepolymer. Across all three main studies, RAFT polymerization is used as a central tool to obtain well-defined precursors with narrow Đ and controlled X_n. An overview of the thesis is shown in Figure 7. The central theme of this thesis is the synthetic development to create a systematic library which gives insight to comparative fundamental structure–property relationships and biological screening. The resulting insights provide guidelines for the future design in amino-acid derived, pH-responsive polyelectrolytes as intracellular delivery agents.

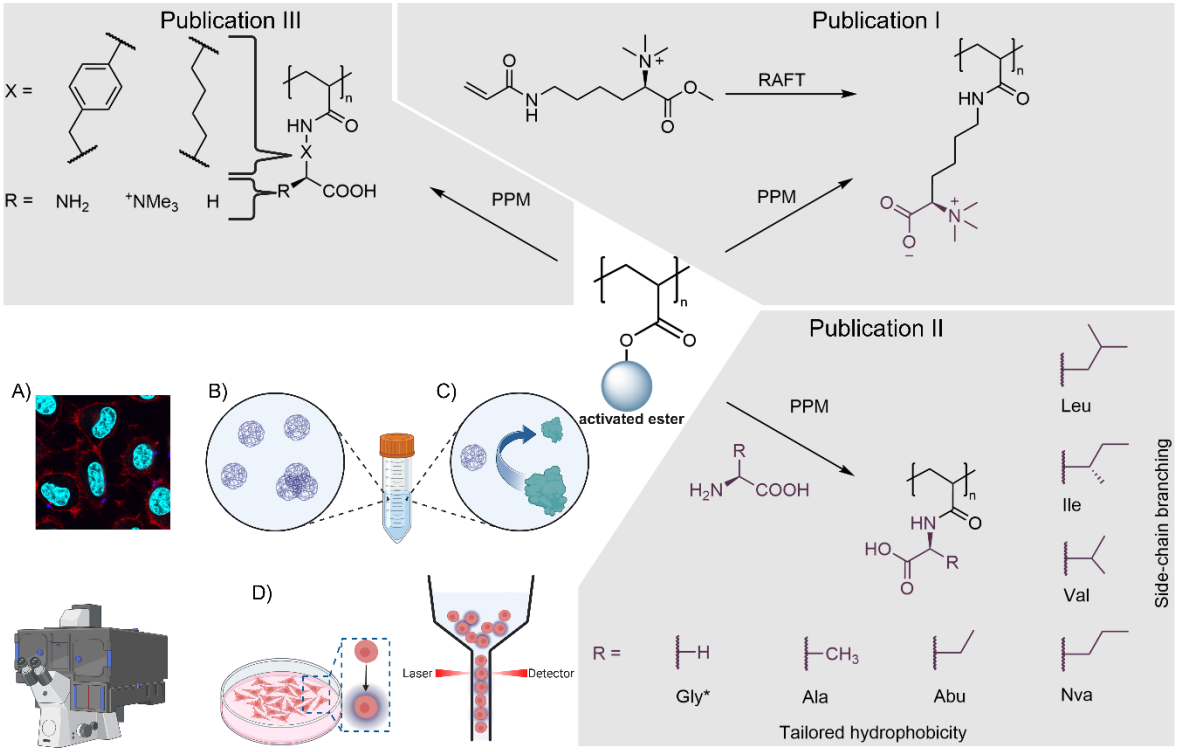


Figure 7: Overview of this thesis with an activated ester prepolymer standing central as it is used in the PPM routes in each publication. The first part introduces a robust methylation strategy to generate lysine-based betaine-like monomers and polymers. The second part extends the reach of this search as amino-acid-derived anionic polyacrylamides are created. The third part unifies these concepts by investigating both zwitterions and their anionic analogues. It further highlights the characterization methods used to derive structure-property relationships and its influence on biological environmental. A) confocal scanning laser microscopy, B,C) aggregation study of the polymers using differential light scattering in solutions at different pH (B) or in combination with model proteins (C). D) cell association studies with various cells using flow cytometry.

The main results of this thesis have been structured around three main manuscripts, two of which are published in peer-reviewed journals, and one is to be submitted.

The first part deals with the development of a synthetic toolbox for chiral, amino-acid-derived polybetaines, combining the advantages of polybetaines and amino-acid-derived polyzwitterions. It introduces a robust methylation strategy to generate lysine-based betaine-like monomers and polymers with a permanent cationic center and a carboxylate in the same side-chain and compares monomer-polymerization and PPM routes. The work establishes how a permanent positive charge affects pH-response, hydrophobicity, protein fouling, and cytocompatibility. In the second part, extends the reach of this search as in this part amino-acid-derived anionic polyacrylamides with systematically varied hydrophobicity and branching are created. Therefore, a library of polyanions is synthesized by PPM from one activated ester prepolymer with different α-amino acids, enabling the comparison of how side-chain hydrophobicity influences pK_a, hydrophobicity, protein interactions, and cell association without changing the polymer backbone, X_n or Đ. The last part unifies these concepts by investigating a library of amino-acid-derived polyelectrolytes, being zwitterions and their anionic analogues, with either aliphatic or aromatic spacers, obtained from one activated ester precursor via PPM. This study directly relates charge state (zwitterionic *vs* anionic), hydrophobicity (alkyl vs aromatic) and the nature of the

positive charge (permanent vs pH-dependent) to cell association, active vs passive uptake, and intracellular localization.

3.2 Zwitterionic Amino-Acid-Derived Polyacrylamides with a Betaine Twist

The first part deals with the development of a synthetic route for chiral, amino-acid-derived polybetaines, combining the advantages of polybetaines and amino-acid-derived polyzwitterions, which are both promising alternatives to non-ionic polymers such as PEG. Zwitterionic polymers as alternative for PEG try to combine low fouling with improved tumor permeability and deeper tissue penetration. Although, amino-acid-derived polyzwitterions have already shown low fouling properties, they often carry a primary amine which makes them highly pH-sensitive and complicates the interpretation of their structure–property relationships. Polybetaines, on the other hand, have a permanently charged quaternary ammonium, but lack the stereocenter and biomimetic structure of amino-acid-derived polymers. Therefore, a robust methylation strategy was developed to obtain lysine-based betaine-like monomers and polymers with a permanent cationic center and a carboxylate in the same side-chain, so the advantages of both classes are merged into one polymer (Fig 8). Lysine-based betaine-like monomers are developed to give the opportunity to directly obtain chiral, amino-acid-derived PB with different X_ns.

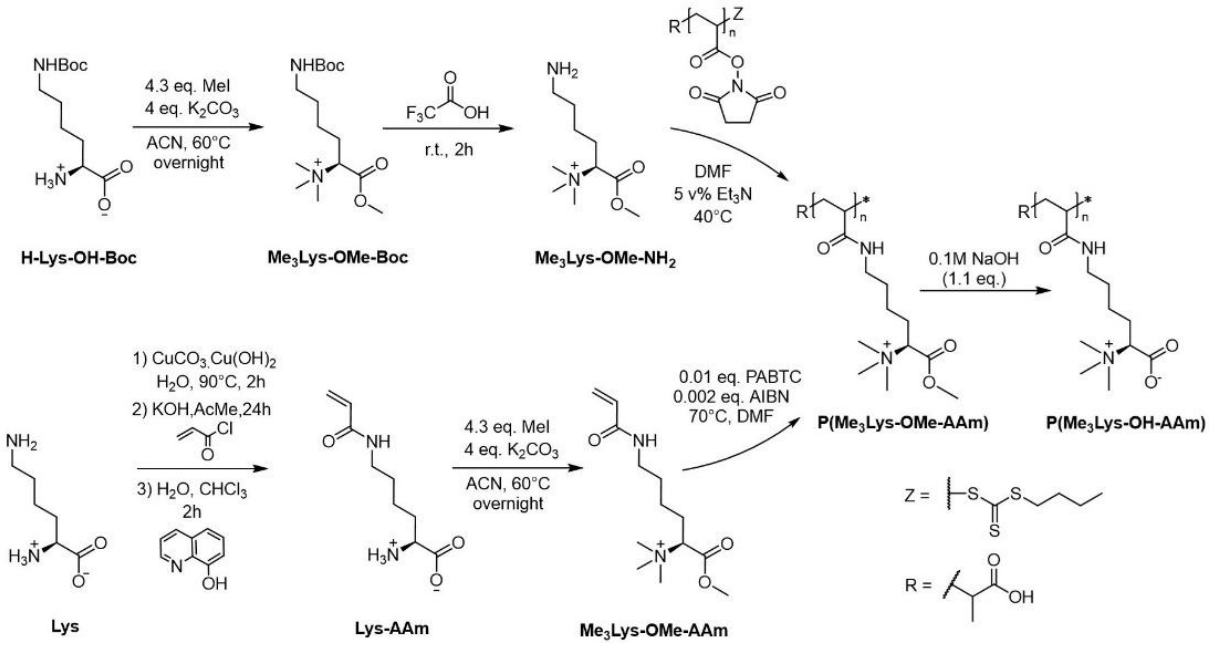


Figure 8: Synthesis of P(Me_3Lys-OH-AAm) from monomer resembling structure and via PPM. Used from Ref. 1 under a Creative Commons CC – BY license. Copyright Wiley 2024

As a proof of concept, L-alanine (Ala) was first used as model compound to find ideal reaction conditions for the methylation of the primary amine towards a quaternary amine. The ideal conditions resulted in simultaneous quaternary amine and ester formation. The ester formation brings advantages for later solubilization of the amino-acid-derived betaines in organic solvents, which is advantageous for controlled radical polymerization as well as the PPM of amine-reactive polymeric precursors. One particular challenge that this approach brings is the needed subsequent hydrolysis to yield the carboxylic acid functionality in the final polymer structure.

[1] De Breuck, J.; Jérôme, V.; Freitag. R, Leiske, M.; *Zwitterionic Amino-Acid-Derived Polyacrylamides with a Betaine Twist – Synthesis and Characterization,* Macromolecular Rapid Communications, 2025, 46, 2400623

This must happen without inducing the undesired Hofmann-elimination at the quaternary ammonium center. It was found that the amine and carboxylic acid group of alanine were methylated in non-protic hydrophilic solvent (acetonitrile) using excessive methyl iodide in the presence of potassium carbonate to obtain the methylated alanine (Me_3Ala-OMe). Formation of the quaternary amine and ester was shown by ^{1}H-NMR (Fig 9) as new peaks appeared at chemical shift (δ) = 3.25 ppm and δ = 3.86 ppm, corresponding to both new functional groups, respectively. Further confirmation was found by ^{13}C-NMR and Fourier transform infrared spectroscopy (FTIR).

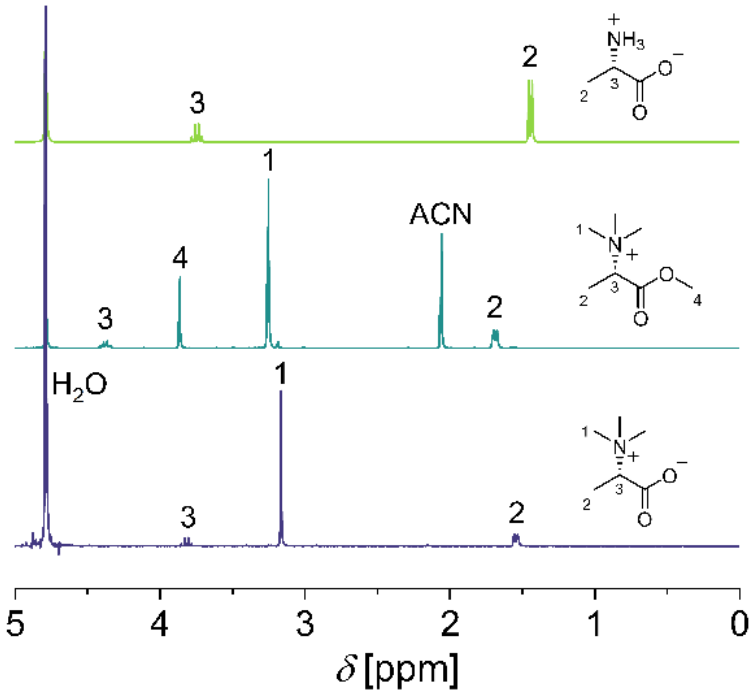


Figure 9: ^{1}H-NMR (300 MHz, D_2O) of Ala (top, green), Me_3Ala-OMe (middle, cyan), and Me_3Ala-OH (bottom, purple). Used from Ref. 1 under a Creative Commons CC – BY license. Copyright Wiley 2024

After Me_3Ala-OMe was obtained, it was used to find suitable conditions to hydrolyze the ester group while avoiding the Hoffmann-elimination of the quaternary amine. It was found that acid ester hydrolysis could only give us a degree of deprotection of 92%. Under mild basic conditions, on the other hand, full deprotection was obtained in absence of Hoffmann-elimination yielding Me_3Lys-OH. This was shown by the disappearance of the methoxy peak at δ = 3.86 ppm by ^{1}H-NMR measurement (Fig. 9). Also, ^{13}C-NMR and FTIR confirmed the successful hydrolysis of Me_3Ala-OMe.

Guided by this model system, L-lysine (Lys) was then transformed into a vinylic betaine-like monomer, Me_3Lys-OMe-AAm, in our first synthetic route. This was done by the methylation of lysine acrylamide (Lys-AAm) following the same procedure as for Ala. Lys-AAm was firstly synthesized after a previously published method using cupper complexation.[2] The methylated lysine product, Me_3Lys-OMe-AAm, showed the same new peaks at δ = 3.25 ppm and δ = 3.86 ppm in ^{1}H-NMR, corresponding to both new functional groups (Fig 9). Additionally, a shift from δ = 3.6 ppm to δ =4.2 ppm was observed for the α-CH group (Fig 10).

[2] Dinda, P.; Anas, M.; Banerjee, P.; Mandal, T. K. *Dual Thermoresponsive Boc-Lysine-Based Acryl Polymer: RAFT Kinetics and Anti-Protein-Fouling of Its Zwitterionic Form*. *Macromolecules* **2022**, *55* (10), 4011–4024.

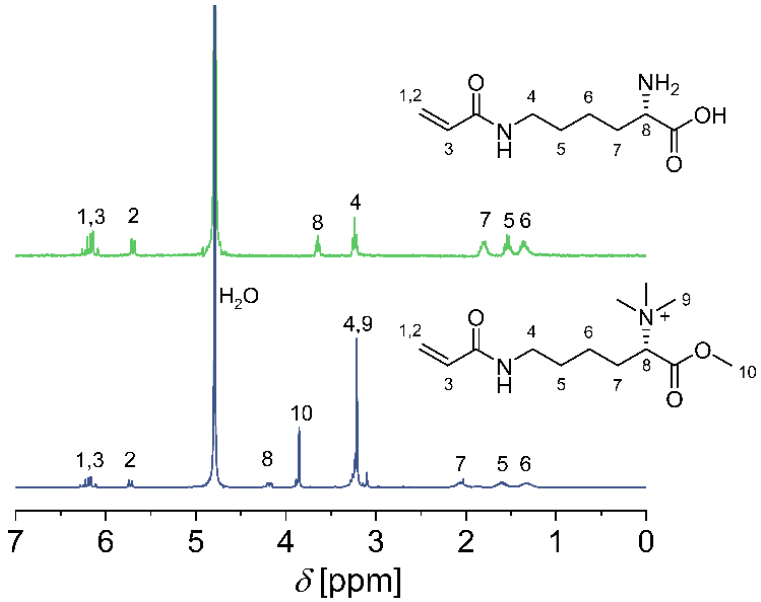


Figure 10: ^{1}H-NMR (300 MHz) of Lys-AAm (top, green, D_2O) and Me_3Lys-OMe-AAm (bottom, blue, D_2O). Used from Ref. 1 under a Creative Commons CC – BY license. Copyright Wiley 2024

The ^{13}C-NMR confirmed the formation of Me_3Lys-OMe-AAm by the new peaks corresponding to the quaternary amine and the methyl ester. FTIR measurements complementary showed the characteristic C═O and C─O absorption bands for an ester functional group appeared at ῡ = 1743, 1250 and 1167 cm−1 and a new C─N stretch absorption band corresponding to the quaternary amine appeared at ῡ = 1200 cm^{-1} compared to the FTIR spectrum of Lys-AAm. In addition, matrix-assisted laser-desorption/ionization time of flight mass spectrometry showed a peak with the highest intensity at the expected m/z of 257 Da which corresponds with the theoretical molar mass of the monomer.

Me_3Lys-OMe-AAm was subsequently polymerized *via* RAFT using 2-[[(butylsulfanyl)-carbonothioyl]sulfanyl] propanoic acid as CTA, yielding P(Me_3Lys-OMe-AAm) with monomodal molar-mass distributions and narrow Đ. The polymerizability of this monomer was investigated by a kinetic study that was analyzed *via* ^{1}H-NMR. The kinetics showed a typical trend for that is generally observed in RAFT-polymerization. The synthesis of the Me_3Lys-OMe-AAm monomer and the kinetic study of its polymerization capability gives the opportunity to this chiral, amino-acid-derived PB with different X_n in a direct way.

Although direct polymerization of monomer-resembling structures is often the method of choice, the role of chirality and permanent positive charge is explored by comparing the quaternized and non-quaternized zwitterionic analogues *via* another route, namely PPM. Therefore, Me_3Lys-OMe-NH_2 and the commercially available Boc-Lysine-OH (Boc-Lys-OH) were used for PPM with PNAS which acted as reactive prepolymer due its activated ester group in the side-chain. Both P(Me_3Lys-OMe-AAm) and P(Boc-Lys-OH-AAm) were obtained as monomodal distributed polymers according to aqueous SEC measurement. The polymers, P(Me_3Lys-OH-AAm) and P(Lys-OH-AAm), that will be compared are obtained by acidic deprotection of P(Boc-Lys-AAm) and by hydrolysis of P(Me_3Lys-OMe-AAm) under mildly basic conditions, respectively. Successful deprotection of P(Boc-Lys-AAm) was verified via ^{1}H-NMR as the Boc group signal at δ =1.4 ppm disappeared. Hydrolysis of the methyl ester of P(Me_3Lys-OMe-AAm) was confirmed by ^{1}H-NMR by the disappearance of the methoxy peak at δ = 4.0 ppm.

As our study aimed to obtain chiral PBs from amino acids, CD spectroscopy was used to verify the chirality by specific conformation of the polymers in solution. Reliable assignment of CD signals for chiral synthetic polymers is challenging as, unlike natural proteins, most synthetic chiral polymers adopt disordered conformations in solution, even when their main chains are highly stereoregular. Consequently, CD spectroscopy in this study is solely employed to verify that the polymers retain their chirality after synthesis. This was confirmed throughout both synthetic routes, indicating that neither the methylation nor the hydrolysis steps compromised the stereocenter. This is crucial for future work exploiting chiral recognition or stereoselective interactions.

pH titration and ζ-potential measurements revealed that P(Lys-OH-AAm) exhibited an p_I around pH ≈ 4.3, corresponding to a zwitterionic point where overall charge is balanced (Fig 11). The rather low p_I corresponds well to the acidic microenvironment of tumorous tissue. Therefore, it is expected that P(Lys-OH-AAm) can be applied for cellular targeting in future biological experiments. P(Me_3Lys-OH-AAm), differently, maintained a negative ζ-potential across the measured pH range above the carboxylate pK_a, indicating that the polymer remains zwitterionic over a broader pH range (Fig 11). Meaning that the permanent cationic centre stabilizes the zwitterionic state. This result emphasized the possible application of P(Me_3Lys-OH-AAm) as a zwitterionic-to-cationic charge-shifting polymer. In the zwitterionic state, it might be resistant to non-specific protein adsorption in blood but may also switch to a positive charged polymer to enhance cellular internalization at target sites.

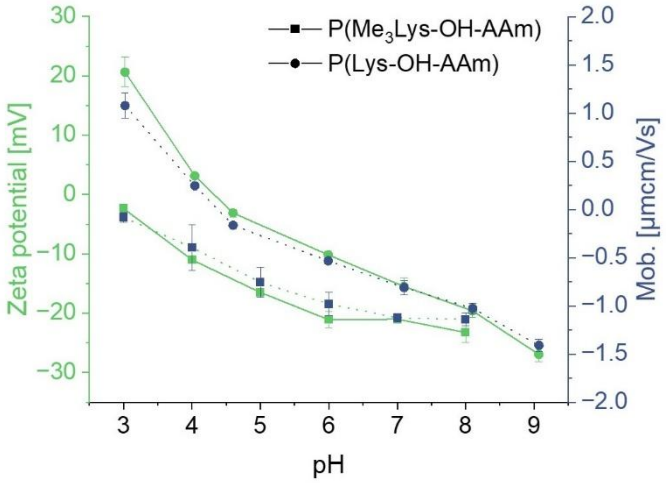


Figure 11: The ζ-potential (green) and electrophoretic mobility (blue) of 2 mg mL^{-1} aqueous solutions of P(Me_3Lys-OH-AAm) (squares) and P(Lys-OH-AAm) (circles) at indicated pH values. Used from Ref. 1 under a Creative Commons CC – BY license. Copyright Wiley 2024

Hydrophobicity was evaluated by comparing the high-performance liquid chromatography (HPLC) polymeric retention times (t_{ret}) and partition coefficients. Methylation increased hydrophobicity slightly following HPLC measurement, while partition coefficient measurements were inconclusive due incomplete phase separation of the organic and watery phase after mixing.

To gain information about the protein fouling, the interactions of P(Lys-OH-AAm) and P(Me_3Lys-OH-AAm) were studied with two representative proteins: bovine serum albumin (BSA) and lysozyme, where BSA was chosen as a negative and lysozyme a positively charged model protein. The fouling properties with these proteins were investigated by measuring the possible formation of aggregates in Dubelcco's

phosphate buffer solution (DPBS) (pH ≈ 7.4) over time using DLS. After 24h, only minor aggregates were observed for P(Lys-OH-AAm) or P(Me_3Lys-OH-AAm) in combination with BSA (Fig 12A, B). P(Me_3Lys-OH-AAm) forms nanoparticles in combination with Lysozyme with a hydrodynamic diameter (d_h) ≈ 30 nm after 24 hours, however these are also observed without the addition of any protein in DPBS (Fig 12D). In comparison, the interaction between lysozyme and P(Lys-OH-AAm) (Fig 12C) seems to be lower, as the formed aggregates are significantly smaller (d_h <10 nm). Nevertheless, both polymers retained low fouling behavior and remained well dispersed under physiologically relevant conditions.

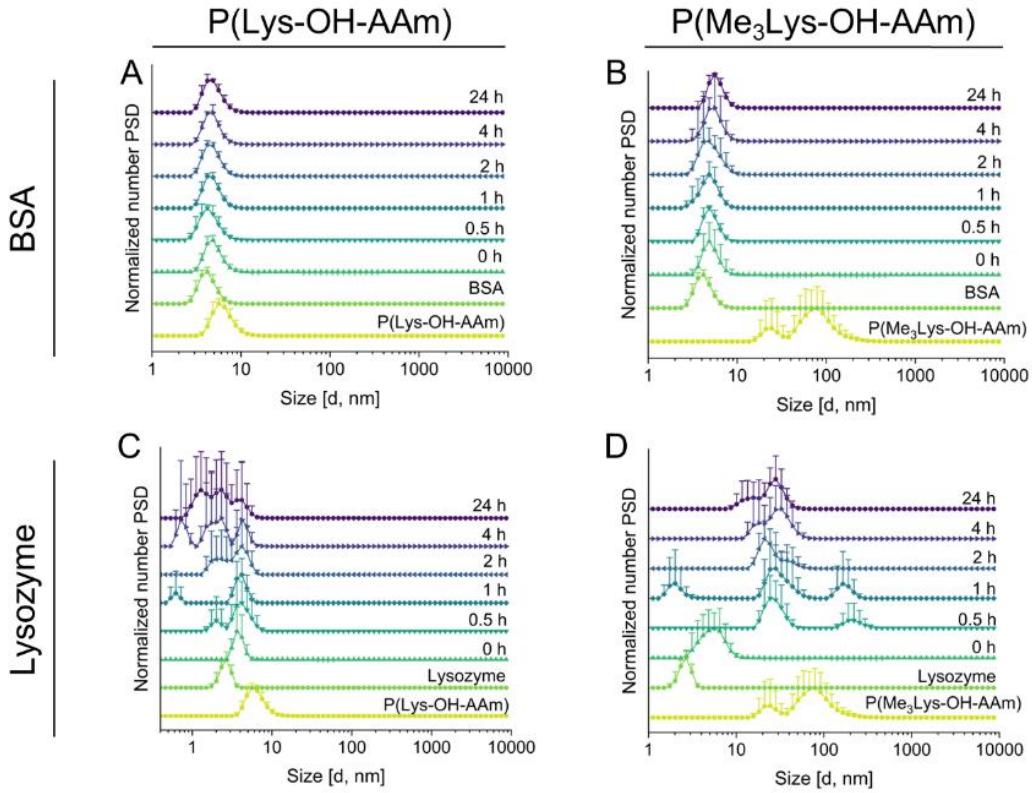


Figure 12: Number size distributions of polymer-protein-mixtures. The concentration of polymers and proteins was 0.5 mg mL^{-1} each in DPBS. Sizes were analyzed by DLS measurements at 37 °C. Values (scatter) represent the mean and SD of five measurements with three runs each. Dashed lines do not represent measured values. A and C: P(Lys-OH-AAm) with BSA and lysozyme, respectively. B and D: P(Me_3Lys-OH-AAm) with BSA and lysozyme, respectively. Used from Ref. 1 under a Creative Commons CC – BY license. Copyright Wiley 2024

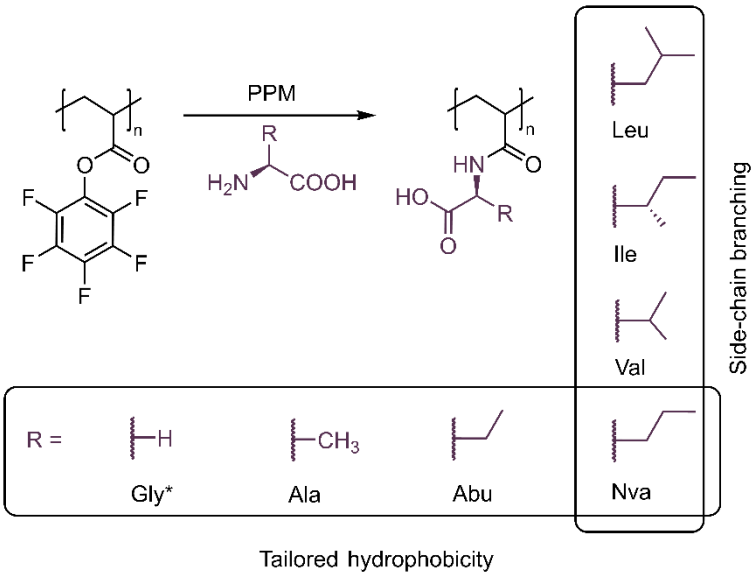
Eventually, cytocompatibility testing demonstrated that both P(Lys-OH-AAm) and P(Me_3Lys-OH-AAm) were well tolerated by MDA-MB-231 breast cancer cells up to concentrations of 1 mg mL^{-1}, indicating that the introduction of a permanent cationic center did not introduce appreciable cytotoxicity in the tested range.

In conclusion, a synthetic methylation strategy is developed to obtain chiral amino-acid-derived PBs via two synthetic strategies, either RAFT polymerization of a betaine like monomer or PPM of a prepolymer with an activated ester side-chain (Fig 8). It was further shown, by both pH titration and ζ -potential measurement, that the positive charge broadens the pH window of zwitterionic behavior. The permanent positive charge has small effect on the retention time during HPLC measurement just as it has a minimal effect on the protein interactions. For the last, it was observed that both polymers retained low fouling behavior at physiological conditions. The synthetic strategy together with the low fouling behavior and

cytocompatibility testing forms the foundation for the later studies (§3.4), where hydrophobicity and charge state are systematically varied in larger libraries and directly correlated with cell association and uptake.

.

3.3 Amino-Acid-Derived Anionic Polyacrylamides with Tailored Hydrophobicity



Scheme 7: Schematic representation of the synthesis of carboxylated polyacrylamides with tailored hydrophobicity via PPM of PPFPA with indicated amino acids, yielding anionic polymers with varying alkyl substituents. Used from Ref. 3 under a Creative Commons CC – BY license. Copyright American Chemical Society 2024.

The *second publication* focuses on polyanions, a promising class of pH-responsive polymers for intracellular delivery. Polycarboxylates are negatively charged at physiological pH and thus internalize into cells via membrane engulfment, referred to as endocytosis, without any cell disruption and therefore interesting for biomedical applications. During endosomal maturation, however, the pH decreases from approximately 6 in early endosomes to around 4.5 in lysosomes. In this acidic environment, pH-responsive polyanions get protonation, leading to loss or reduction of their anionic character. The protonation can increase membrane interaction of polyanions by a decreased ionic repulsion between polymers and the cell membrane. The resulting increase in membrane affinity can promote endosomal destabilization and facilitate endosomal escape. Importantly, this process is further influenced by an increase in polymer hydrophobicity for which a balance must be achieved while sufficient hydrophobicity supports the membrane interaction and excessive hydrophobicity risks inducing cytotoxicity.

We aim in this study to design a library of amino-acid-derived anionic polyacrylamides P(AA−OH-AAm) with systematically varied alkyl side-chain (length and branching) and to correlate it to their physicochemical properties being, pK_a, hydrophobicity and pH-responsiveness. Additionally, we aim to correlate physiochemical properties with protein fouling, cell association and preliminary uptake behavior. The central question was to what extent side-chain hydrophobicity alone, at fixed backbone and X_n, can influence cellular interactions and get an initial understanding of their potential applications in a biological environment.

---

[3] De Breuck, J.; Streiber, M.; Ringleb, M.; Schröder, D.; Herzog, N.; Schubert, U.; Zechel, S.; Traeger, A.; Leiske, L.; *Amino-Acid-Derived Anionic Polyacrylamides with Tailored Hydrophobicity–Physicochemical Properties and Cellular Interactions*. ACS Polymers Au, 2024, 4, 3, 222-234

To ensure high comparability with a fixed backbone and X_n, all P(AA−OH-AAm) were synthesized *via* a PPM approach from the same side-chain functionalized activated ester prepolymer, namely, PPFPA. The reactive prepolymer was obtained in a controlled manner by RAFT polymerization with narrow dispersity (Đ ≈ 1.32). The screened P(AA−OH-AAm) were derived from neutral α-amino acids with different alkyl substituents in α position, namely, glycine (Gly), Ala, aminobutyric acid (Abu), norvaline (Nva), valine, iso-leucine, and leucine, which were all used in their L-stereospecific form. This library allowed for a comparison of the effect of increasing hydrophobicity (Gly < Ala < Abu < Nva) as well as the effect of side-chain branching (Scheme 7)

A particular challenge in the PPM approach was the poor solubility of amino acids in organic solvents. Eventually, dimethylformamide was chosen as it was believed to at least partially solubilize the amino acids at elevated temperatures. Successful and quantitative conversion of the activated ester was achieved after heating at 40°C for 72 hours and was confirmed *via* ^{1}H, ^{19}F-NMR and FTIR spectroscopy. Generally, ^{1}H-NMR showed the appearance of the C-H adjacent to the newly formed amide bond while at the same time no peaks could be observed in the ^{19}F-NMR spectra of each P(AA−OH-AAm). Additionally, the FTIR spectra shows the conversion of functional groups by a shift in absorption band from a carbonyl adjacent to PFPP at $\tilde{\nu}$ = 1780 cm^{-1} to a carbonyl group in an amide bond at $\tilde{\nu}$ = 1550 cm^{-1}. As an example, the FTIR spectra of PPFPA and P(Nva-OH-AAm) are shown (Fig. 13).

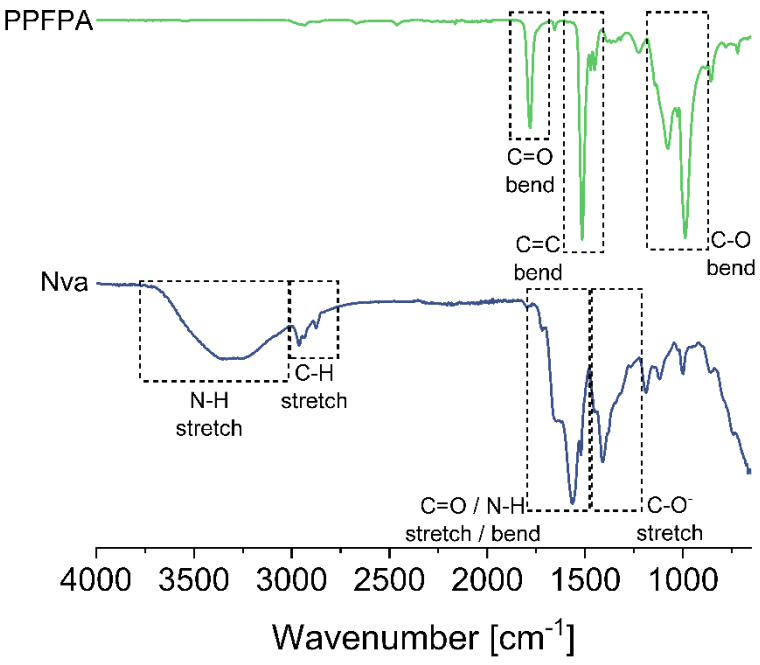


Figure 13: FTIR spectra of poly(pentafluorophenyl acrylate) (green) and P(Nva-OHAAm) (blue). Used from Ref. 3 under a Creative Commons CC – BY license. Copyright American Chemical Society 2024.

SEC measurements in 0.07 M aqueous Na_2HPO_4 as eluent revealed shorter elution times for P(AA−OH-AAm) with increasing alkyl side-chains as could be expected due increased molar mass and higher hydrodynamic volume. Interestingly, terminal short chain branching and branching feature later elution times due to their decreased sterical hindrance and more compact polymer alignment.

Hydrophobicity was evaluated via partition coefficient measurements and HPLC retention times, while pH-dependent ionization was quantified by titration and ζ-potential analysis. HPLC measurements of all 6-aminofluorescein-labeled P(AA−OH-AAm) on a reversed-phase column revealed in increase in retention time upon increase in number of carbons in the α-substituted amino acid. However, side-chain alkyl branching did not affect the retention time and, therefore, hydrophobicity. This was confirmed by partition coefficient measurements at pH = 7. Remarkably, titration of all P(AA-OH-AAm) revealed pK_a values between 4.8 and 5.5 attributed to the carboxylic acid in the side-chain and similar to poly(acrylic acid) (pKa ≈ 4.5), despite clear differences in hydrophobicity and side-chain structure. This suggests that the α-substituted amino acid moieties can be used to modulate hydrophobicity largely independently of the acid dissociation equilibrium. Additionally, ζ-potential measurements of P(AA−OH-AAm) in DPBS verified the expected negative surface charge at the physiological pH of the bloodstream. DLS measurements at polymer concentrations of 2 mg mL^{-1} in DPBS excluded possible formation of aggregates, which could lead to an altered uptake profile.

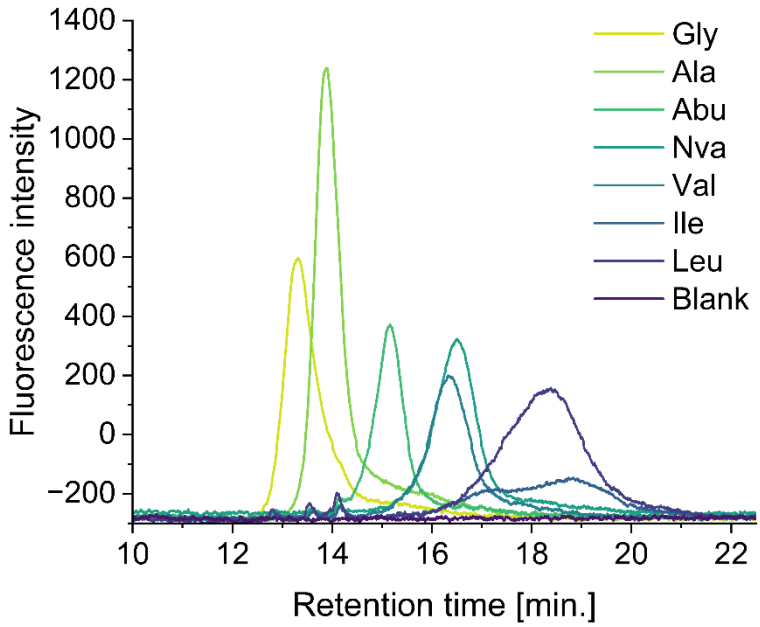


Figure 14: HPLC chromatograms (acetonitrile/water gradient, 0.1V% TFA) of P(AA-OH-AAm). Spectra show the absolute fluorescence intensity of eluting 6AF-labeled polymers (λ_{ex} = 480 nm; λ_{em} = 520 nm). Used from Ref. 3 under a Creative Commons CC – BY license. Copyright American Chemical Society 2024

Similar to the *first publication*, protein fouling was studied using DLS to measure the formation of possible aggregates of P(AA-OH-AAm) over time in mixtures with model proteins. Therefore, the interaction of two representatives, being the more hydrophilic, P(Gly-OH-AAm), and the more hydrophobic, P(Nva-OH-AAm), with two representative proteins: BSA and lysozyme were measured. Mixtures of P(Nva-OH-AAm) and lysozyme formed large nanoparticles (d_h ≈ 700 nm) while P(Gly-OH-AAm) formed smaller aggregates (d_h ≈ 150 nm) which were both expected due the stronger interaction between polyanions and cationic proteins. As expected, mixtures of BSA and P(Nva-OH-AAm) only revealed a minor formation of aggregates, while surprisingly aggregation of P(Gly-OH-AAm) with BSA was observed. This might be explained by increased exposure of the hydrophobic polymer backbone.

Before studying cell association, cytocompatibility was evaluated by MTT assay with L929 mouse fibroblasts, showing that all P(AA-OH-AAm) were well tolerated up to 0.1 mg mL^{-1}. Hemolysis and

erythrocyte aggregation assays confirmed the absence of membrane disruption at pH 7.4 and 6, indicating a favorable balance between anionic character and hydrophobicity.

Cell association was then investigated by flow cytometry using 6-aminofluorescein-labeled polymers. For all seven polyanions, both the fraction of 6AF-positive cells and the mean fluorescence intensity (MFI) increased over time. Here, polymers with more hydrophobic amino acids (*i.e.*, Nva, valine, isoleucine, and leucine) exhibited rapid and higher cell association, reaching ≥70% 6-aminofluorescein-positive cells after 1 h, whereas more hydrophilic polymers (Gly, Ala and Abu) associated more slowly and followed an inverse trend relative to their hydrophobicity (Gly > Ala > Abu). The last can in combination with the protein-fouling experiments be related to some hydrophobic character of the polymer backbone.

As the P(AA-OH-AAm)s are polyanions and therefore negatively charged at physiological pH, as shown by, ζ-potential measurements, they are expected to enter cells predominantly through membrane engulfment processes, such as endocytosis, without causing membrane disruption. Typically, polymer association or uptake via active pathways, including endocytosis or macropinocytosis, can be suppressed when the incubation temperature is reduced from 37 to 4 °C. Surprisingly, however, neither the number of 6AF-positive cells nor the MFI decreased substantially under low-temperature conditions (Fig 15), indicating that the polymers do not rely on an active uptake mechanism.

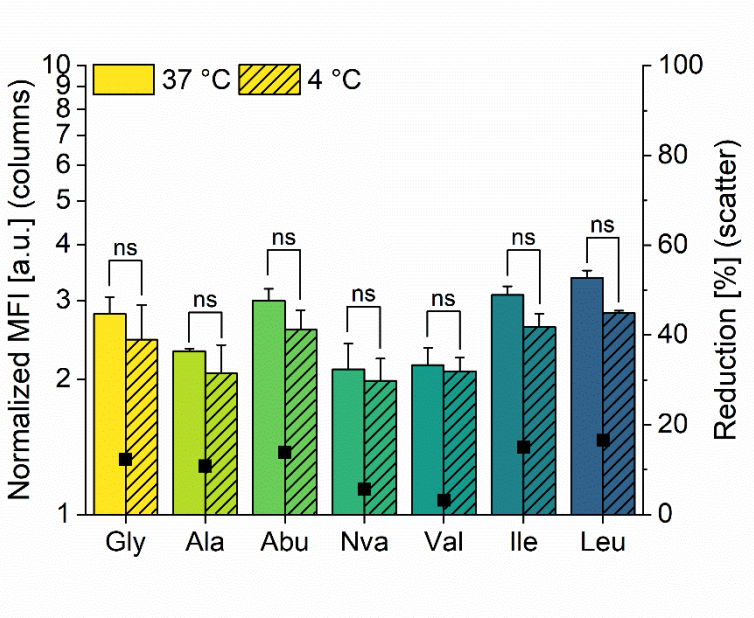


Figure 15: Cellular association of different 6AF-labeled P(AA−OH-AAm) determined via flow cytometry measurements. Polymer concentration: 1 mMRU, 50,000 cells seeded in 250 µL in a 48 well plate. incubation at 37 or 4 °C in DMEM supplemented with 10% FBS for 4 h. Statistical analysis (one-way ANOVA with Tukey test) was performed for 4 h incubation time. Used from Ref. 3 under a Creative Commons CC – BY license. Copyright American Chemical Society 2024

To further investigate the interaction between P(AA−OHAAm) with cells, imaging *via* CLSM was performed. After 4 h of incubation, a strong colocalization of 6AF-labeled P(Nva-OH-AAm) with the cell membrane was observed and no intracellular 6-aminofluorescein signal was detectable (Fig. 16). This provides further clarification on the temperature study as polymer association to the cell membrane happens in a passive way. Further incubation for 24 h showed intracellular spot-like 6AF signals

indicating a vesicular localization and, consequently, active albeit very slow polymer internalization (Fig. 16).

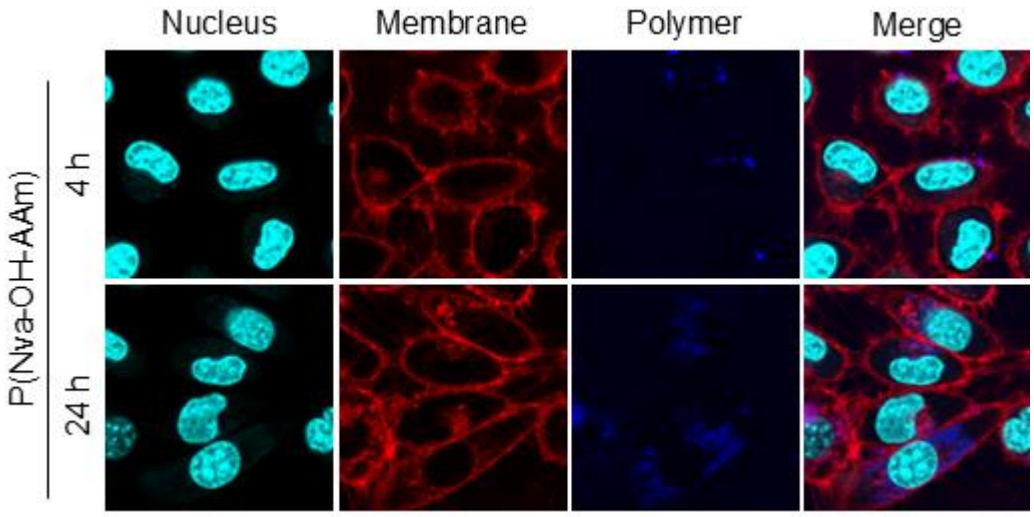


Figure 16: Cellular uptake of 6AF-labeled P(Nva-OH-AAm) into L929 mouse fibroblasts visualized by CLSM. Cells were incubated with polymers at 37 °C for indicated times. Cyan: Hoechst 33342/nucleus. Red: CellMask Plasma Membrane Stain/membrane. Blue: 6AF/polymer. Used from Ref. 3 under a Creative Commons CC – BY license. Copyright American Chemical Society 2024

Beyond establishing a clear relationship between side-chain hydrophobicity, t_{ret} and protein interactions, the *second publication* also provides important insights into how P(AA-OH-AAm) interact with cells over time. Compared with previous reports on polymer uptake, the kinetics observed here are noticeably slower, however lead to a pronounced internalization of the more hydrophobic anionic polymers. Such a combination of slow uptake but strong membrane association of anionic polymers appears to be relatively uncommon in literature and therefore particularly noteworthy in the context of designing intracellular delivery systems.

These observations can be understood by the specific balance of anionic charge and hydrophobic character as on the one hand, non-ionic hydrophobic polymers are typically known to strongly interact with cell membranes. At the other, anionic polymers generally show very low interaction due to electrostatic repulsion from the negatively charged membrane. In the present system, increasing the alkyl chain length simultaneously increased hydrophobicity and decreased the charge density of the polymer, thereby reducing repulsion and enabling association with the membrane. This trend is shown by HPLC measurements, while the protein fouling and cell association experiments show that more hydrophobic, less densely charged polyanions interact more strongly with proteins and cell surfaces, but still without inducing acute cytotoxicity or hemolysis under the tested conditions. These results highlight the existence of an optimum window where hydrophobicity and charge density are balanced as sufficient hydrophobicity is required to promote membrane interaction. The amino-acid-derived nature of the side-chains, likely further contributes to the observed behavior by facilitating interactions with the cell surface compared to purely synthetic moieties.

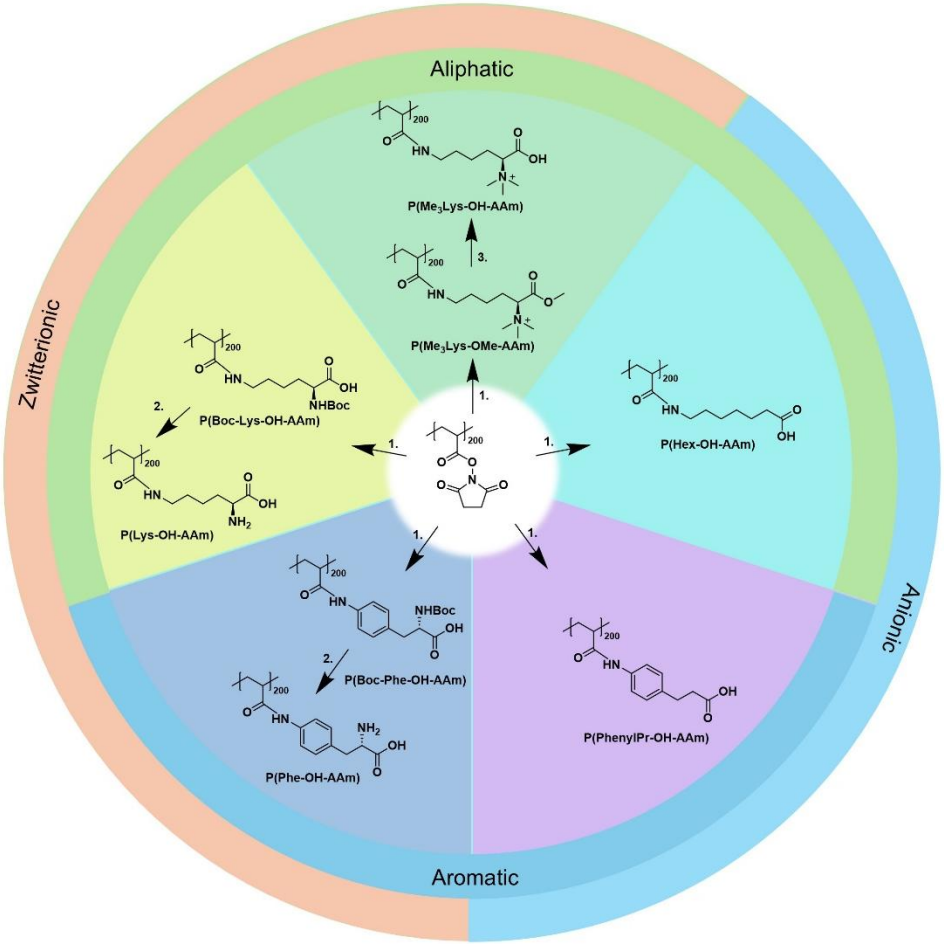
In the broader context of the thesis, these findings strongly motivate the studies in §3.4. The unusual combination of slow but strong membrane accumulation in the polyanion library raised the question of

how general this behavior can be exploited and to what extent it depends on overall charge state (anionic vs zwitterionic).

3.4 Impact of the Polymer Side-Chain Chemistry on Interactions of Amino-Acid-Derived Polyelectrolytes with Cells

The *third publication* represents the integrative part of this thesis and, therefore, builds directly on the structure–property relationships uncovered in publication II, extending them to a mixed library of zwitterionic and anionic polymers with both aliphatic and aromatic side-chains. By doing so, it aims to study the mechanistic understanding of how **hydrophobicity, charge distribution, and biomimetic design** determine protein fouling, cell association, and intracellular uptake across this entire class of amino-acid-derived polyelectrolytes. This was of particular interest as polyelectrolytes can be designed to control (i) intermolecular interactions such as polymer-protein interactions (*i.e.* reduce aggregation with proteins), (ii) self-assembly to form higher-level structures for stable drug transport in the biological environment, and (iii) responsiveness to external stimuli to facilitate cellular uptake into the targeted cells.

Therefore, a small but defined library of five polymers, where different amino acid or amino acid-like structures are substituted in the side-chain to obtain zwitterionic or anionic analogue amino acid-derived polyelectrolytes. This was designed in a way, only the side-chain motif is changed while the polymer backbone, X_n, and Đ are kept as constant as possible by relying on the PPM method (Scheme 8). The five polymers study the influence of the side-chain motifs: (i) aliphatic vs aromatic side-chains, (ii) permanent vs non-permanent charge, and (iii) zwitterionic vs anionic patterns. The influence of both the charge character and aromaticity on the hydrophilicity of the polyelectrolytes was measured by HPLC, while aggregation under influence of the full pH range for complete material characterization. Additional experiments in the presence of proteins or more complex protein mixtures were measured by DLS. Together with cell association with different cancer and non-cancer cell lines, these studies are performed to provide information regarding structural driving forces for the association efficiency.



Scheme 8: Synthetic overvies of P(Boc-Lys-OH-AAm), P(Me_3Lys-OMe-AAm), P(Hex-OH-AAm), P(Boc-Phe-OH-AAm) and P(PhenylPr-OH-AAm) via PPM. (1) Et_3N, DMF and Boc-Lys-OH, Me_3Lys-OMe-NH_2, 6-aminohexanoic acid, Boc-4-aminophenylalanine and 3-(4-aminophenyl)propanoic acid, respectively. 24 h at room temperatures (2) 50:50 [TFA/H_2O], overnight at room temperature (3) 0.1 M NaOH, 24 h at room temperature.

For comparability, also here, the polyelectrolytes were obtained *via* PPM of PNAS, which was obtained from RAFT polymerization and subsequently reacted with different amino acids to design three different polyzwitterions as well as two corresponding polyanions. Consequently, the PPM of PNAS with five different reagents was conducted: (i) Me_3Lys-OMe-NH_2, (ii) Boc-Lys-OH, (iii) Boc-4-aminophenylalanine, (iv) 6-aminohexanoic acid, and (v) 3-(4-aminophenyl)propanoic acid. The successful PPM was verified *via* ^{1}H NMR measurements, showing the disappearance of the characteristic peak of NAS at δ = 2.8 ppm after the reaction, indicating full conversion. This is exemplary shown for the PPM with Boc-Lys-OH (Fig 17). Further deprotection of the Boc-protected intermediates and hydrolysis of the methyl ester group yielded the targeted polymers. In addition, the Cy5-labeled polymers, which are needed for cell association experiments, were synthesized *via* sequential PPM with Cy5-amine and the respective amino acids.

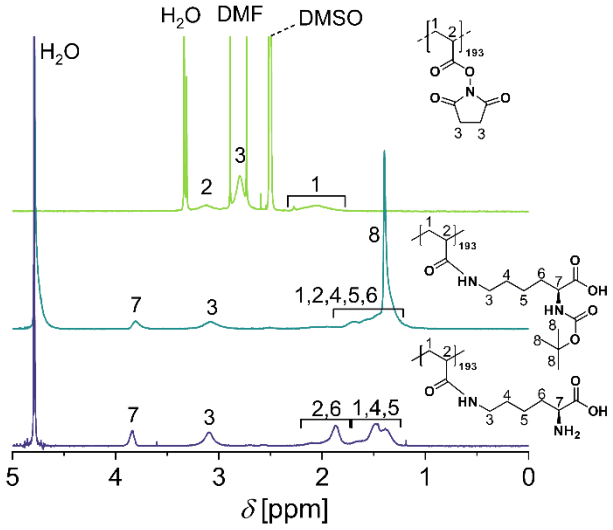


Figure 17: ^{1}H NMR spectra (300 MHz) of poly(N-acryloyl succinimide) (green, DMSO), P(BocLys-OH-AAm) (cyan, D_2O) and P(Lys-OH-AAm) (blue, D_2O)

The physiochemical properties of the synthesized polyelectrolytes were determined by combining HPLC, DLS, and electrophoretic light scattering. The Cy5-labeled polymers were analyzed by their t_{ret} after reversed-phase HPLC at pH ≈ 2 to determine their relative hydrophobicity. The anionic polymers P(PhenylPr-OH-AAm)-Cy5 (t_{ret} ≈ 16 min) and P(Hex-OH-AAm)-Cy5 (t_{ret} ≈ 15 min) showed the longest retention times, indicating the highest hydrophobicity within the library (Table 1). This increased hydrophobicity is attributed to protonation of the carboxylic acids at pH 2 and, in the case of P(PhenylPr-OH-AAm), to the enhanced polarizability and London dispersion interactions of the aromatic spacer relative to the purely aliphatic hexyl spacer. In contrast, the polyzwitterions P(Lys-OH-AAm)-Cy5, P(Me_3Lys-OH-AAm)-Cy5, and P(Phe-OH-AAm)-Cy5 all exhibited similar retention times (~12 min), suggesting that neither aromaticity nor a permanent positive charge significantly alters their hydrophobicity under these conditions. These HPLC results extend and refine the trends observed in *the second publication* as hydrophobicity could already be tuned via α-substituted amino acids. The present study shows that aromatic spacers can further amplify hydrophobicity in anionic systems, while zwitterionic systems remain comparatively hydrophilic even upon introduction of aromatic groups.

Table 1: Polymer characteristics

Polymer	M[a] [Da]	$X_{n,theo}$[b]	$M_{n,theo}$[b] [kDa]	$M_{n,app}$[c] [kDa]	Đ[c]	t_{ret}[d] [min.]
P(Lys-OH-AAm)	200.24	193	38.5	1.9	3.27	11.80
P(Me_3Lys-OH-AAm)	243.33	188	46.5	10.7[e]	1.96[e]	11.75
P(Hex-OH-AAm)	185.22	193	35.6	16.5	2.30	14.49
P(Phe-OH-AAm)	234.25	193	45.0	13.0	2.14	11.97
P(PhenylPr-OH-AAm)	219.24	193	42.1	11.0	2.71	15.94

[a]Molar mass (M) of repeating unit RU after deprotection. [b] $X_{n,theo}$ and $M_{n,theo}$ was calculated from ^{1}H-NMR. [c] $M_{n,app}$ and Đ was determined by aqueous SEC measurements (0.07M Na_2HPO_4) on a Suprema column set (PMA standard). [d] t_{ret} obtained from HPLC using a reversed phase column with a water/acetonitrile mixture + 0.1 vol% trifluoroacetic acid as eluent. [e]determined by aqueous SEC measurements (80/20 V% [H_2O/ACN] + 0.1M NaCl + 0.3% TFA) on a Novema column set (P2VP standard).

pH-dependent DLS measurements provided complementary information on self-assembly and aggregation. For the polyanions, large d_h (>1000 nm) were observed around and below their pK_a values (pH 3–5), in agreement with partial or full protonation of the carboxylic acid side-chains and consequent loss of electrostatic repulsion. At higher pH, both polyanions formed significantly smaller particles (d_h ≈ 1–10 nm) (Fig 18A). These observations are consistent with the known pK_a values of hexanoic acid and 3-phenylpropanoic acid and illustrate how slight differences in side-chain structure determine aggregation behavior at biologically relevant pH values. For the polyzwitterions, P(Lys-OH-AAm) remained mostly dissolved (d_h ≈ 10 nm) across the entire pH range from 3 to 11, whereas P(Phe-OH-AAm) and P(Me_3Lys-OH-AAm) showed the formation of small aggregates (D_h ≈ 20–160 nm) around pH 6–7, close to their PI (Fig 18B). Such aggregation at mildly acidic pH resembles behavior previously associated with enhanced tumor retention, as the extracellular pH in solid tumors often lies between 6.5 and 6.8. This suggests that the polyzwitterions may also be tuned for pH-triggered changes in solubility and aggregation in the tumor microenvironment.

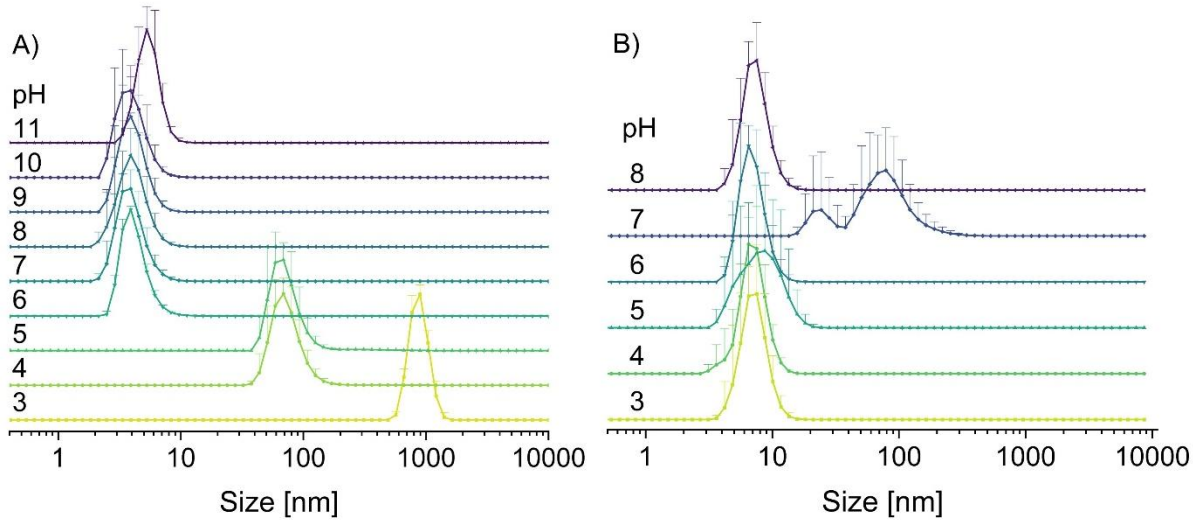


Figure 18: pH dependent number size distribution of A: P(Hex-OH-AAm). B: P(Me3Lys-OH-Aam). in water (2 mg mL^{-1}) determined by DLS measurements. Values (scatter) represent the mean and SD

Protein fouling was investigated using lysozyme (positively charged model protein) and BSA (negatively charged protein) in DPBS at pH 7.4. DLS measurements revealed no significant aggregation for the polyzwitterions with either lysozyme or BSA, again confirming the low-fouling character of polyzwitterions. By contrast, the anionic polymers displayed markedly different behavior as P(Hex-OH-AAm) remained stable in the presence of lysozyme over 24 h, whereas P(PhenylPr-OH-AAm) immediately formed large aggregates upon mixing, leading to visible sedimentation and strongly reduced scattering signals at later time points (Fig 19). Additionally, no aggregation was observed for either polyanion in mixtures with BSA. This difference between non-aggregating aliphatic and immediately aggregating aromatic polyanions can be rationalized by looking at the HPLC data obtained here and in *the second publication*. In the polyanion series, the more hydrophilic P(Gly-OH-AAm) (t_{ret} ≈ 13.2 min) formed small, stable aggregates with lysozyme (D_h ≈ 150 nm), whereas the more hydrophobic P(Nva-OH-AAm) (t_{ret} ≈ 16.3 min) formed substantially larger complexes (D_h ≈ 700 nm). In the present study, P(PhenylPr-OH-AAm) (t_{ret} ≈ 15.9 min) exhibits a retention time comparable to P(Nva-OH-AAm) and shows immediate aggregation with lysozyme, while P(Hex-OH-AAm) (t_{ret} ≈ 14.5 min) falls between

P(Gly-OH-AAm) and P(Nva-OH-AAm) and does not aggregate. Building on these findings, further fouling experiments were conducted in PBS containing 10 V% FBS to evaluate potential polymer aggregation under biologically relevant conditions. This experiment showed no aggregation with each individual polymer over a period of 5 h.

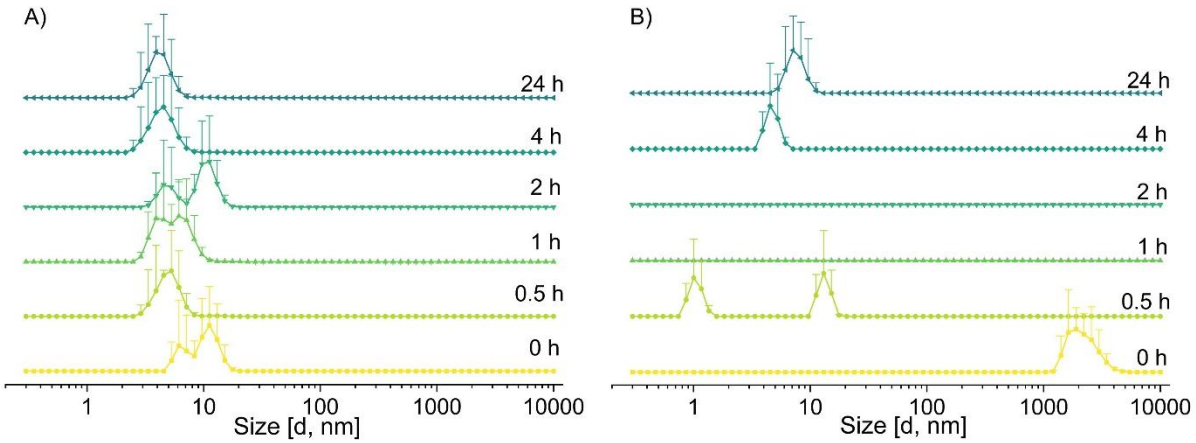


Figure 19: Number size distribution of A: P(Hex-OH-AAm). B: P(PhenylPr-OH-AAm). in Lysozyme-mixtures. The concentration of polymers and proteins was 0.5 mg mL^{-1} each in DPBS. Sizes were analyzed by DLS measurements at 37 °C. Values (scatter) represent the mean and SD of five measurements with three runs each. Lines do not represent measured values.

With the physicochemical profile established, the cellular interactions of all five Cy5-labeled polymers were investigated by MTT assays, flow cytometry, and CLSM. MTT assays with MDA-MB-231 breast cancer cells confirmed that all polymers were well tolerated up to 1 mg mL^{-1}, after 24 h of incubation, a concentration an order of magnitude higher than used in association experiments, and in agreement with earlier findings on amino-acid-derived polyanions.

Cell association was first quantified by flow cytometry in four cell lines: two human cancer cell lines (MDA-MB-231, HCC-78), murine NIH 3T3 fibroblasts, and non-tumorigenic human mammary epithelial cells (MCF10A). Non-ionic PNAM-Cy5 served as standard, as non-ionic polymers showed unspecific association, and as a result all MFIs were normalized accordingly (Fig 20). Generally, the interaction of P(Me_3Lys-OH-AAm)-Cy5 with MDA-MB-231 was higher compared to HCC-78 cells in flow cytometer measurement. However, the fluorescence images showed a similar uptake compared to P(Lys-OH-AAm)-Cy5, which indicates that the negative membrane charge of HCC-78 cells is less pronounced and the interactions between MDA-MB 231 and P(Me_3Lys-OH-AAm)-Cy5 are increased. When comparing these association results to the polymer association with NIH 3T3 fibroblasts, it was observed that the overall polymer association was significantly lower compared to cancer cell lines - except for P(Me_3Lys-OH-AAm)-Cy5, which showed the highest association to the fibroblasts. An explanation for these results may be found in the extracellular matrix of fibroblasts, which is composed of a higher quantity of hyaluronic acid and thus repel anionic charged polymers. For the non-tumorigenic human breast cells (MCF10A), the interaction between the permanently, positively charged P(Me_3Lys-OH-AAm)-Cy5 is statistically significant lower ($p < 0.05$) since the cell membrane charge is less negative compared to both investigated cancer cell lines. Consequently, the permanently charged P(Me_3Lys-OH-AAm)

exhibits the highest potential for further investigations of specific interaction with cancer cells without affecting healthy human cells – albeit these association studies provide no direct information about this context.

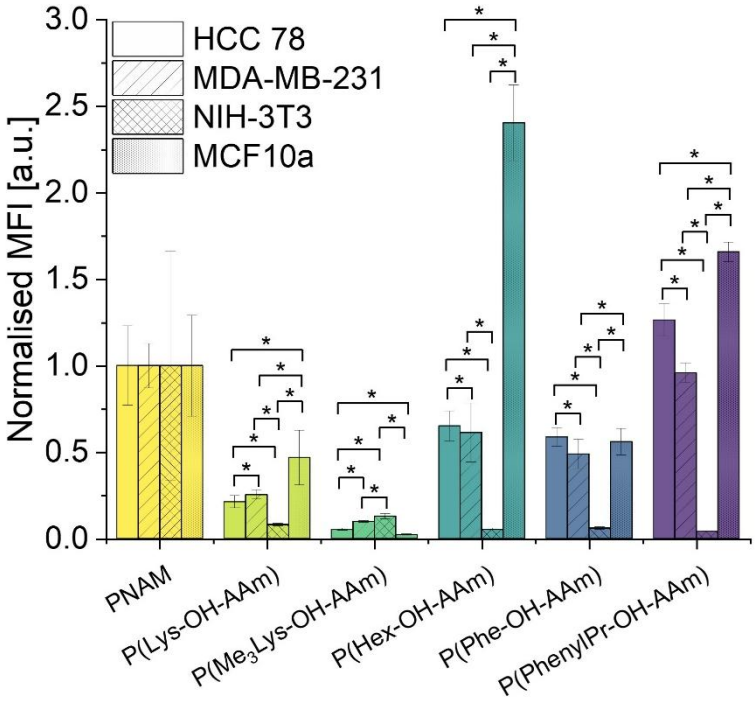


Figure 20: Cellular association of Cy5-labelled polymers with HCC-78, MDA-MB-231, NIH 3T3, and MCF10a as determined by flow cytometry. The cells were seeded in 24-well plates (50,000 cells/well) and incubated with 2.5 µM polymer solutions (500 µL of FBS-containing cell culture media) at indicated temperatures for 4 h. Values represent mean and SD (n = 4). *Indicates a significance of $p < 0.05$

CLSM with MDA-MB-231 cells provided spatial insight into polymer localization. After 1 h incubation, the intracellular fluorescence signal was comparatively weak for the polyzwitterions, whereas both polyanions exhibited strong intracellular signals and clear colocalization within the cytoplasm (Fig 21). Interestingly, P(Phe-OH-AAm)-Cy5 displayed a slower uptake behavior: its intracellular signal was lower after 1 h but increased noticeably after 4 h, pointing to a delayed internalization relative to its aliphatic counterparts. These observations align with the hydrophobicity and protein-fouling trends: hydrophobic, especially aromatic, anionic polymers associate more rapidly with cells and are internalized more efficiently, while polyzwitterions are more stealth-like and slower to enter cells.

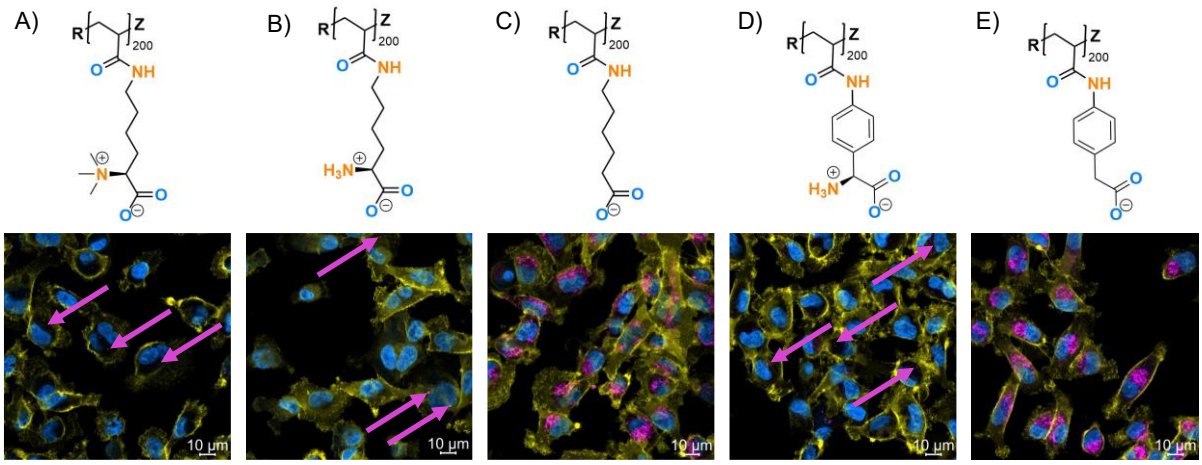


Figure 21: MDA-MB-231 cancer cells visualised by CLSM 1 h after treatment with polymers. Blue: Hoechst 33342/nucleus. Yellow: Cell membrane (CellMaskTM Green Plasma Membrane stain). Magenta: Cy5/polymer channel. Cells were treated with Cy5 modified polymers A: P(Lys-OH-AAm)-Cy5. B: P(Me_3Lys-OH-AAm)-Cy5. C: P(Hex-OH-AAm)-Cy5. D: P(Phe-OH-AAm)-Cy5 E: P(PhenylPr-OH-AAm)-Cy5

To elucidate the uptake mechanism, T-dependent cell association was studied. Here, approximately 60–80% in MFI at 4 °C compared with 37 °C was observed for all polymers, indicating that uptake is predominantly active and energy dependent. Therefore, a panel of competitive inhibitors targeting AATs overexpressed in MDA-MB-231 cells (sodium-coupled Neutral Amino Acid Transporter 1/2, ASCT1/2, LAT1/2, cystein/glutamate-antiporter, monocarboxylate transporter 4) was applied, alongside competitive free amino acids (leucine, phenylalanine, Glu). Surprisingly, no strong, transporter-specific inhibition was observed. These data suggest that AATs are not the dominant uptake pathway for the studied polyelectrolytes and that other, more general endocytic mechanisms are likely responsible.

Conclusively, the cellular experiments reveal a clear correlation between hydrophobicity, which is characterized by HPLC (t_{ret}) and consequently its protein fouling. It is shown that hydrophobicity is a key determinant of both the extent and speed of cell association and internalization, especially for anionic systems. Generally, *the third publication* reaches over the topics of this thesis by integrating and extending the structure–property relationships established in *the first and second publication* into a unified, side-chain-focused framework. It has shown that hydrophobicity, determined by HPLC, is a crucial parameter giving a strong indication in not only protein fouling but also cell association. The charge (zwitterionic vs anionic) has its influence on stealth and interacting properties as polyzwitterions remain low-fouling with a slower uptake consequently. Polyanions, on the other hand, engage more strongly with cells and proteins, especially when they are more hydrophobic. This higher hydrophobicity can be achieved by incorporating an aromatic group in the side-chain. In combination with the synthetic toolbox for chiral polybetaines developed in *the first publication* and the hydrophobicity gradient established for anionic polyacrylamides in *the second publication*, *the third publication* completes a comprehensive structure–property–function map for amino-acid-derived, pH-responsive polyelectrolytes.

4 Publications

4.1 Individual contributions to joint publications

All publications included in this thesis are the result of close collaborative work of several researchers across multiple disciplines. The individual contributions of each author and coauthor are given in this section.

Publication I: Zwitterionic Amino-Acid-Derived Polyacrylamides with a Betaine Twist – Synthesis and Characterization

Jonas De Breuck, Valérie Jérôme, Ruth Freitag, Meike N. Leiske
Macromol. Rapid Commun. 2025, 46, 2400623, DOI: 10.1002/marc.202400623

The first publication focusses on the development of a synthetic toolbox for chiral, amino-acid-derived polybetaines. It introduces a robust methylation strategy to generate lysine-based betaine-like monomers and polymers using both direct polymerization and PPM routes. I conducted all the synthetic work. Characterization such as NMR was conducted by me. FTIR measurements were performed by me in the lab of Prof Brendel. HPLC measurements were performed by me in the labs of Prof Scheibel. DLS and ELS measurements were also performed by me in the labs of Prof Dr Papastavrou. matrix-assisted laser-desorption/ionization time of flight mass spectrometry was performed by Roman Schneller in the labs of Prof Dr Brendel. pH-titration was performed by me under the assistance of Marius Alexander Methfessel. Rika performed SEC measurements of the obtained polymers at the chair of Prof Dr Greiner. Preliminary biocompatibility assessment was conducted under the assistance of Jana Ulmann and supervision of Dr Jérôme in the labs of Prof Dr Freitag. Prof Dr Leiske, Prof Freitag and Dr Jérôme were involved in scientific discussions during the project, in the interpretation of the results and in the outline of the manuscript. I prepared the figures and wrote the initial draft of the manuscript. All authors were involved in finalizing the manuscript and in the revision of the manuscript.

Publication II: Amino-Acid-Derived Anionic Polyacrylamides with Tailored Hydrophobicity–Physicochemical Properties and Cellular Interactions

Jonas De Breuck, Michael Streiber, Michael Ringleb, Dennis Schröder, Natascha Herzog, Ulrich S. Schubert, Stefan Zechel, Anja Traeger, Meike N. Leiske
ACS Polym. Au 2024, 4, 3, 222–234. DOI: 10.1021/acspolymersau.3c00048

The second publication focusses on amino-acid-derived anionic polyacrylamides with systematically varied hydrophobicity and branching are created. Michael Ringleb performed the PPFPA synthesis under supervision of Dr Stefan Zechel. I conducted all the PPM synthesis with support from Natascha Herzog. Characterization such as ^{1}H NMR and ^{13}C NMR was conducted by me while ^{19}F NMR was conducted by Dennis Schröder. FTIR measurements were performed by me in the lab of Prof Dr Brendel. HPLC measurements were performed by me in the labs of Prof Dr Scheibel. DLS and ELS measurements were also performed by me in the labs of Prof Dr Papastavrou. pH-titration and measurement of the partition coefficient was performed by me. Rika performed SEC measurements of the obtained polymers at the chair of Prof Dr Greiner, except for PPFPA which was measured in Jena. Biological assessments were conducted in Jena by Michael Streiber under the supervision of Dr Traeger in the labs of Prof Dr Schubert. Jonas De Breuck, Michael Streiber, Michael Ringleb, Dr Zechel, Prof Dr Traeger and Prof Dr Leiske were involved in scientific discussions during the project, in the interpretation of the results and in the outline of the manuscript. I prepared the figures and wrote the initial draft of the manuscript. All authors were involved in finalizing the manuscript and in the revision of the manuscript.

Publication III: Impact of the polymer side-chain chemistry on interactions of amino-acid-derived polyelectrolytes with cells

Jonas De Breuck, Theresa M. Lutz, Christian Jahns, Jonas Debbeler, Valérie Jérôme, Ruth Freitag, Anja Traeger, Meike N. Leiske

Submitted to Journal of Material Chemistry B, currently under peer-review

The third publication focusses on the investigating of a library of amino-acid-derived polyelectrolytes, being zwitterions and their anionic analogues, with either aliphatic or aromatic spacers, obtained from one activated ester precursor via PPM. I conducted all the synthetic work with the assistance of Christian Jahns. Characterization such as NMR was conducted by me. HPLC measurements were performed by me in the labs of Prof Dr Scheibel. DLS and ELS measurements were also performed by me in the labs of Prof Dr Brendel. Robert Bätz and Sebastian Städter performed SEC measurements of the obtained prepolymers at the chair of Prof Dr Brendel. All post modified polymers were measured on an aqueous SEC system in our lab. Biocompatibility assessment and cell association/uptake experiments were conducted by me with the assistance of Dr Lutz under supervision of Dr Jérôme in the labs of Prof Dr Freitag. CLSM measurements were performed by Jonas Debbeler und supervision of Dr Traeger. Jonas De Breuck, Dr Lutz, Jonas Debbeler, Dr Traeger, Prof Dr Leiske, Prof Dr Freitag and Dr Jérôme were involved in scientific discussions during the project, in the interpretation of the results and in the outline of the manuscript. I prepared the figures and wrote the initial draft of the manuscript. All authors were involved in finalizing the manuscript and in the revision of the manuscript.

4.2 Zwitterionic Amino-Acid-Derived Polyacrylamides with a Betaine Twist – Synthesis and Characterization

RESEARCH ARTICLE

Macromolecular Rapid Communications
www.mrc-journal.de

Zwitterionic Amino-Acid-Derived Polyacrylamides with a Betaine Twist – Synthesis and Characterization

*Jonas De Breuck, Valérie Jérôme, Ruth Freitag, and Meike N. Leiske**

Amino-acid-derived polyzwitterions and polybetaines (PBs) are two promising alternatives to non-ionic polymers, for example, to increase tumor permeability. In this study, amino-acid-derived polyzwitterions are synthesized and a strategy to quarternize the amine in the side chain functional group is developed to combine the advantages of both types. The functional monomer is polymerized via reversible addition–fragmentation chain-transfer polymerization for which a kinetic study is performed. Further, the impact of the permanent positive charge on amino-acid-derived polyzwitterions is studied based on two zwitterionic polymers obtained via post-polymerization modification (PPM) of Poly(*N*-acryloxysuccinimide) to allow good comparison between methylated and non-methylated polymers. Circular dichroism shows that the stereocenter remains intact during PPM. pH titration and ζ-potential measurements show that the methylated polymer has a negative ζ-potential over the measured pH range and, therefore, the polymer remains zwitterionic over a broader pH range than its non-methylated equivalent. Both polymers are well tolerated by mammalian cells up to concentrations of 1 mg mL^{-1}. The study introduces a path to a new polymer class that combines the advantages of both PBs and amino-acid-derived polyzwitterions and highlights the impact a permanent charge has on the physiochemical properties.

J. De Breuck, M. N. Leiske
Macromolecular Chemistry
University of Bayreuth
Universitätsstraße 30, 95447 Bayreuth, Germany
E-mail: meike.leiske@uni-bayreuth.de
V. Jérôme, R. Freitag
Process Biotechnology
University of Bayreuth
Universitätsstraße 30, 95447 Bayreuth, Germany
R. Freitag
Bayreuth Center for Molecular Biosciences (BZMB)
University of Bayreuth
Universitätsstraße 30, 95447 Bayreuth, Germany
M. N. Leiske
Bavarian Polymer Institute
Universitätsstraße 30, 95447 Bayreuth, Germany

© 2024 The Author(s). Macromolecular Rapid Communications published by Wiley-VCH GmbH. This is an open access article under the terms of the Creative Commons Attribution License, which permits use, distribution and reproduction in any medium, provided the original work is properly cited.

DOI: 10.1002/marc.202400623

1. Introduction

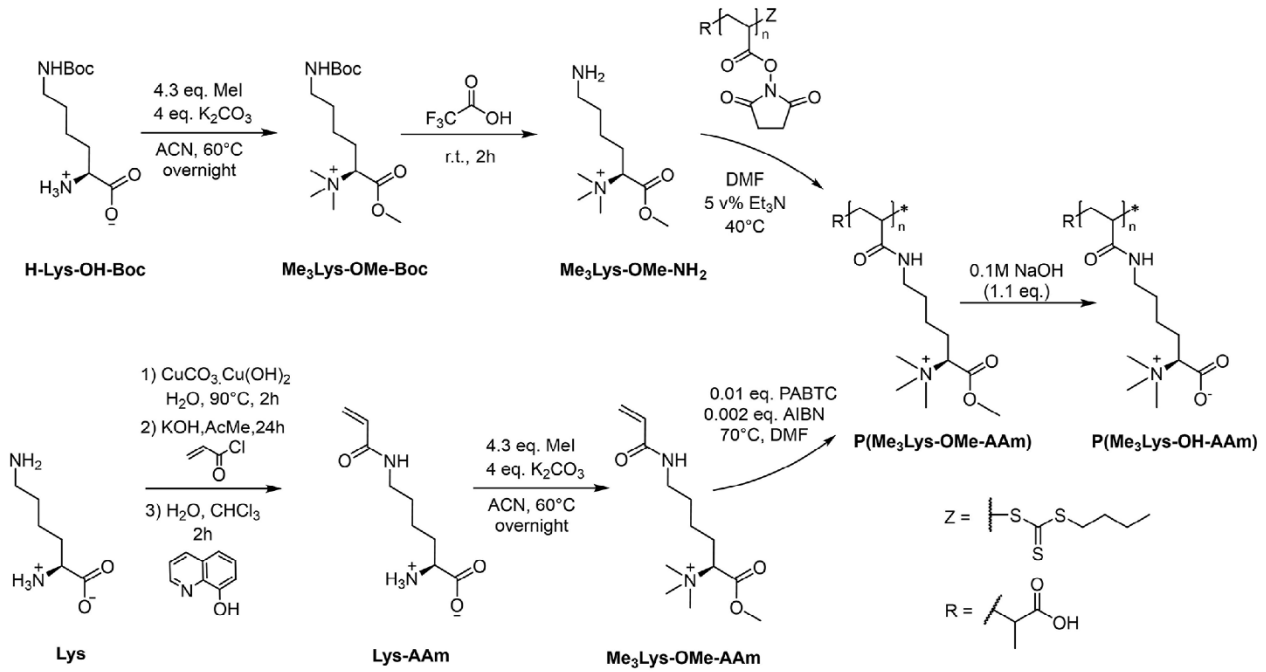
One major challenge in nanomedicine, especially for cancer-related treatments, is site-specificity. Non-ionic, biocompatible polymers having antifouling or so-called "stealth" properties are indispensable as carriers to increase the blood retention time of disease-treating therapeutics, that are often unstable or immiscible in the biological environment and lack tissue specificity.[1] Conventional non-ionic polymers such as poly(ethylene glycol) (PEG) are designed to prevent any interaction with biological matter (e.g., proteins or cells). However, these properties also prevent the much wanted interactions with target sites, for example, tumor cells.[2,3] While long-circulating polymers such as PEG may easily access tumorous tissue through the enhanced permeation retention (EPR) effect,[4,5] they often lack deep penetration into the tissue.[6] Polyzwitterions are one promising alternative to non-ionic polymers for this purpose as they combine low-fouling properties with increased tumor permeability and better uptake by cancer cells.[7–10] Like polyampholytes, polyzwitterions contain both, cationic and anionic groups along the main chain or the side chains.[11] In contrast to polyampholytes, polyzwitterions are characterized by positive and negative charges at non-adjacent positions on the same pendant groups.[12] Due to their ionic nature, they are often able to switch properties with changing environments.[11] The different possible ionic functionalities of polyzwitterions lead to structural versatility.

Polybetaines (PBs) are one heavily researched category of polyzwitterions. They can be subdivided into three main categories: (i) poly(carboxybetaine)s (PCBs), (ii) poly(sulfobetaine)s (PSBs), and (iii) poly(phosphobetaine)s (PPBs).

PBs can be polymerized from their corresponding zwitterionic monomers using various polymerization techniques such as step-growth polymerization, anionic polymerizations,[11,13] and radical polymerization.[14–16] Limitations of this approach refer to the limited solubility of monomers[17] or incompatibility of the ionic functionality with the opted polymerization technique. The synthesis of neutral or protected polymeric precursors and subsequent deprotection and/or post-polymerization modification (PPM) has revealed itself useful to circumvent these issues.[18–21] One prominent example in the area of radical polymerization techniques is the PPM of poly(2-(dimethylamino)ethyl methacrylate) (PDMAEMA) via ring opening of sultones,

ADVANCED SCIENCE NEWS
www.advancedsciencenews.com

Macromolecular Rapid Communications
www.mrc-journal.de



Scheme 1. Synthesis of P(Me_3Lys-OH-AAm) from monomer resembling structure and via PPM.

2-*oxo*-dioxaphopholanes, and strained lactones to form the corresponding PSB, PPB, and PCB.[11] From these, PCBs have shown to be highly resistant to non-specific protein adsorption or cell adhesion.[22] This makes the material promising for applications in medical diagnostics, biomaterials/tissue engineering, and drug delivery.[23] Previous studies have shown that all PBs can penetrate deeply into tumor tissue, with particularly PCBs showing efficient cellular uptake into cancer cells.[6]

Recently, amino-acid-derived polyzwitterions were synthesized from different amino acids such as serine, [24–26] lysine[24,27] glutamine,[28,29] and glutamic acid.[9,10,30] Unlike PBs, they feature an amino-acid-derived stereocenter, however, the primary amine functionality renders them highly responsive to changes in the pH value, which results in characterization difficulties and complicates the interpretation of structure-property-relationships even further. Inspired by the advantages that both classes, PBs, and amino-acid-derived polyzwitterions, offer, we were keen to develop an approach for the synthesis of chiral, amino-acid-derived PBs. Chirality plays a crucial role in further applications, particularly in the development of metal ion absorbents,[31] drug delivery systems,[32,33] and biocompatible materials.[34] This approach will create a new class of non-biological molecules with biomimetic structures and properties. A straightforward and scalable synthesis was a specific goal. To the best of our knowledge, only chiral small molecule betaines have been synthesized from amino acids before,[35] however, chiral PBs from amino acids have not been reported and will therefore be presented in this study for the first time.

In our approach, it was attempted to synthesize polymers resembling amino-acid-derived betaine structures via two approaches: (i) polymerization of monomer resembling structures and (ii) PPM of activated polymeric precursors (**Scheme 1**). As a result, the obtained polymers, showing stereoselectivity, underwent a preliminary biocompatibility assessment.

2. Results and Discussion

2.1. Synthesis and Characterization of Me_3Ala-OH as Proof-of-Concept Compound

The polymerization of betaine-derived monomers is often hampered by their challenging solubility behavior.[17] To enable adequate solubilization of amino-acid-derived betaines in organic solvents, which is advantageous for controlled radical polymerization techniques as well as the PPM of amine-reactive polymeric precursors, we attempted a quantitative quarternization of the amine as well as a methylation of the carboxylic acid yielding a methoxy group. One particular challenge of this approach is the subsequent basic hydrolysis required to yield the carboxylic acid functionality in the final polymer structure as Hofmann-elimination might occur as an unwanted side reaction.[36,37] In order to find a suitable procedure to quarternize the amino acid and hydrolyze a methoxy group in the vicinity of a quaternary amine, L-alanine (Ala) was used as a model compound for screening suitable procedures. The amine and carboxylic acid group of Ala were methylated in non-protic hydrophilic solvent (acetonitrile) using excessive methyl iodide (MeI) in the presence of potassium carbonate to obtain the methylated Ala (Me_3Ala-OMe), according to an established protocol for the methylation of *tert*-butyl (2-aminoethyl)carbamate.[38] After purification, Me_3Ala-OMe was analyzed via Fourier-transform infrared spectroscopy (FT-IR), as well as proton (^{1}H-) and carbon nuclear resonance spectroscopy (^{13}C-NMR). In the ^{1}H-NMR (**Figure 1**) new signals appeared at δ = 3.25 ppm attributed to the methyl groups bound to the

 © 2024 The Author(s). Macromolecular Rapid Communications published by Wiley-VCH GmbH

15213927, 0, Downloaded from https://onlinelibrary.wiley.com/doi/10.1002/marc.202400623 by Media N. Leiske - Staats- Und Universitätsbibliothek Dresde , Wiley Online Library on [01/10/2024]. See the Terms and Conditions (https://onlinelibrary.wiley.com/terms-and-conditions) on Wiley Online Library for rules of use; OA articles are governed by the applicable Creative Commons License

ADVANCED SCIENCE NEWS
www.advancedsciencenews.com

Macromolecular Rapid Communications
www.mrc-journal.de

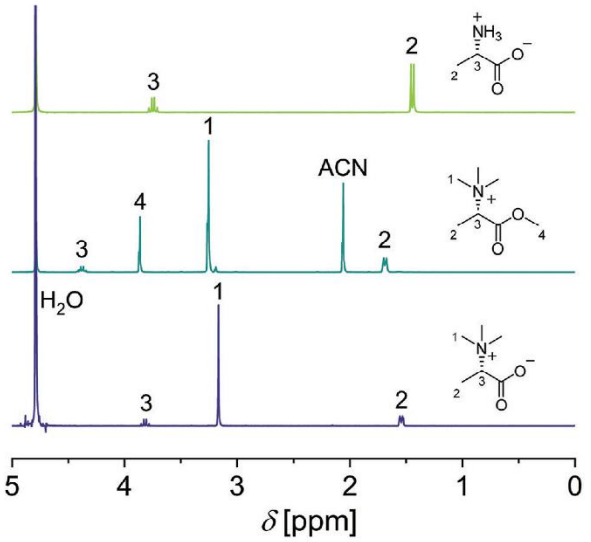


Figure 1. ^{1}H-NMR (300 MHz, D_2O) of Ala (top, green), Me_3Ala-OMe (middle, cyan), and Me_3Ala-OH (bottom, purple).

nitrogen (H1) and δ = 3.86 ppm corresponding to the newly formed methyl ester group (H4). Additionally, a shift of the signal of the α-CH-group (H3) from δ = 3.7 ppm to δ = 4.4 ppm was observed, suggesting successful product formation. The ^{13}C-NMR (Figure S1A, Supporting Information) confirmed these results by the newly appearing signals at δ = 52.0 ppm (C1) and δ = 53.8 ppm (C5). In addition, the ^{13}C-NMR spectrum revealed a second set of peaks, which referred to a product with hydrolyzed methoxy groups or incomplete methylation of the carboxylic acid, respectively. While in ^{1}H-NMR the presence of the hydrolyzed product was not obvious, ^{13}C-NMR measurements of the final product Me_3Ala-OH showed the same distinct chemical shifts. FT-IR measurements (Figure S2, Supporting Information) further revealed a shift of the characteristic band of the C=O stretch at $\tilde{\nu}$ = 1747 cm^{-1}, corresponding to the formation of an ester group as well as the disappearance of the NH_3^+-stretch at $\tilde{\nu}$ = 2710 to 3100 cm^{-1}.

Next, Me_3Ala-OMe was used to establish suitable conditions to hydrolyze the ester group, while avoiding the Hoffmann-elimination of the quaternary amine, to obtain Me_3Ala-OH. Due to the expected sensitivity toward the base, we first attempted an acidic ester hydrolysis at room temperature and elevated temperatures as these were previously applied for the deprotection of dehydroalanine-derived polymers.[39] Unfortunately, the maximum degree of deprotection was 92% conversion (data not shown). For this reason, it was decided to use mild basic conditions at room temperature, which were found to obtain full conversion and consequently complete hydrolysis in the absence of Hoffmann elimination. This is shown in the ^{1}H-NMR spectrum (Figure 1)[35] and in the ^{13}C-NMR spectrum (Figure S1B, Supporting Information) where the methoxy peak at δ = 3.9 ppm (H4) and δ = 53.8 ppm (C5) respectively disappeared. Complementary, FT-IR analysis (Figures S2 and S4, Supporting Information) confirmed the hydrolysis by a shift from a C=O stretch toward $\tilde{\nu}$ = 1615 cm^{-1} corresponding to a C=O stretch of a carboxylic acid.

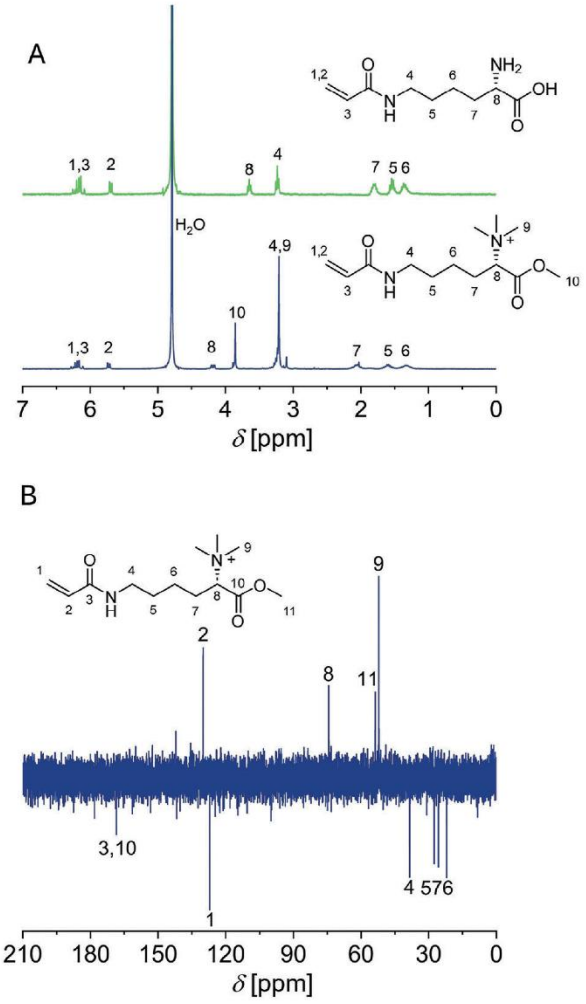


Figure 2. A) ^{1}H-NMR (300 MHz) of Lys-AAm (top, green, D_2O) and Me_3Lys-OMe-AAm (bottom, blue, D_2O) and B) ^{13}C-NMR (75 MHz) of Me_3Lys-OMe-AAm (D_2O).

2.2. Synthesis of P(Me_3Lys-OMe-AAm) via Reversible Addition-Fragmentation Chain-Transfer (RAFT)-Polymerization of the Monomer Resembling Structure

The successful proof of concept prompted us to develop a synthetic route to obtain chiral PBs from L-lysine (Lys, Scheme 1). In the first route, L-lysinyl acrylamide (Lys-AAm) was synthesized using a cupric complexation step, according to a procedure described by *Mandal* et al.[27] While in the previous publication, Lys-AAm was used toward *tert*-butyloxycabonyl protection, here Lys-AAm was methylated with MeI applying the procedure optimized for the model compound to yield a vinylic betaine-like Lys-AAm monomer (Me_3Lys-OMe-AAm).

In alignment with the synthesis of Me_3Ala-OMe, this product caused the appearance of the same new signals in the ^{1}H-NMR spectrum (**Figure 2**A) at δ = 3.25 and δ = 3.86 ppm (H9 and H10). A shift from δ = 3.6 ppm to δ = 4.2 ppm was further observed for the α-CH-group (H8). The ^{13}C-NMR (Figure 2B) confirmed the

 © 2024 The Author(s). Macromolecular Rapid Communications published by Wiley-VCH GmbH

15213927, 0, Downloaded from https://onlinelibrary.wiley.com/doi/10.1002/marc.202400623 by Media N. Lesiko - Staats- Und Universitätsbibliothek Dresde , Wiley Online Library on [01/10/2024]. See the Terms and Conditions (https://onlinelibrary.wiley.com/terms-and-conditions) on Wiley Online Library for rules of use; OA articles are governed by the applicable Creative Commons License

ADVANCED SCIENCE NEWS
www.advancedsciencenews.com

Macromolecular Rapid Communications
www.mrc-journal.de

formation of Me_3Lys-OMe-AAm by the appearance of two signals attributed to the methyl groups bound to the quartered amine (δ = 52 ppm, C9) and the methyl ester (δ = 54 ppm, C11).

FT-IR measurements then corroborated the formation of Me_3Lys-OMe-AAm (Figures S5 and S6, Supporting Information) as the characteristic C═O and C—O absorption bands for an ester functional group appeared at $\tilde{\nu}$ = 1743, 1250 and 1167 cm^{-1} and a new C—N stretch absorption band corresponding to the quaternary amine appeared at $\tilde{\nu}$ = 1200 cm^{-1} compared to the FT-IR spectrum of Lys-AAm. In addition, matrix-assisted laser-desorption/ionization time of flight mass spectrometry (MALDI-ToF MS, Figure S7, Supporting Information) showed a peak with the highest intensity at the expected m/z of 257 which corresponds with the theoretical molar mass of the monomer.

Me_3Lys-OMe-AAm was subsequently polymerized in the presence of 2-[[(butylsulfanyl)-carbonothioyl]sulfanyl] propanoic acid (PABTC) as chain-transfer agent (CTA) to obtain P(Me_3Lys-OMe-AAm). To gain information about the polymerizability of this monomer, a kinetic study was performed and analyzed via ^{1}H-NMR (Figure S8, Supporting Information). The kinetic plots of this polymerization follow a typical trend that is generally observed in RAFT-polymerization, where a plateau is reached after 8 h at a conversion of 87.5%.[40] The polymerization also revealed a linear increase in molar mass with conversion and a narrow dispersity (Figure S9, Supporting Information).

2.3. Synthesis of P(Me_3Lys-OMe-AAm) via Post-Polymerization Modification (PPM)

While direct polymerization of monomer-resembling structures is often the method of choice, the preparation of functional polymers via PPM also offers advantages. These particularly address the need for comparable polymer structures with variations in the side chain, fluorescent labeling, or copolymerization with monomers of opposing solubility. For this reason, we also investigated the potential to prepare P(Me_3-Lys-OMe-AAm) via PPM (Scheme 1). In the first step, Me_3Lys-OMe-NH_2 was synthesized by methylation of commercially available H-Lys-OH-Boc using the procedure described above. ^{1}H-NMR (Figure S10, Supporting Information) confirmed the formation of a methyl ester by the appearance of a peak at δ = 3.9 ppm (H7) and the formation of a quaternary amine at δ = 3.2 ppm (H6). Subsequent acidic deprotection of the *tert*-butyloxycarbonyl (Boc) group yielded Me_3Lys-OMe-NH_2. Successful deprotection was shown by the disappearance of the Boc peak at δ = 1.4 ppm (H1) and at δ = 27 ppm (C1) in the ^{1}H- and ^{13}C-NMR spectrum, respectively (Figures S10 and S11, Supporting Information). P(Me_3Lys-OMe-AAm) was obtained by PPM of poly(*N*-acryloxysuccinimide) (PNAS) as a reactive precursor. PNAS was post-modified using the synthesized Me_3Lys-OMe-NH_2 to retrieve P(Me_3Lys-OMe-AAm) (Scheme 1). ^{1}H-NMR (**Figure 3**) showed a peak shift from δ = 3.0 ppm to δ = 3.3 ppm, indicating a change in environment for the CH_2 adjacent to the ϵ-amine (H3), now positioned adjacent to the amide of P(Me_3Lys-OMe-AAm). Additionally, the characteristic peak of the NAS at δ = 2.8 ppm[41] disappeared after the reaction, indicating full conversion. According to the synthesis of Me_3Ala-OMe, in Figure 3 some hydrolysis could already be observed before the deprotection step. In particular, the peak at δ = 3.8 ppm could be

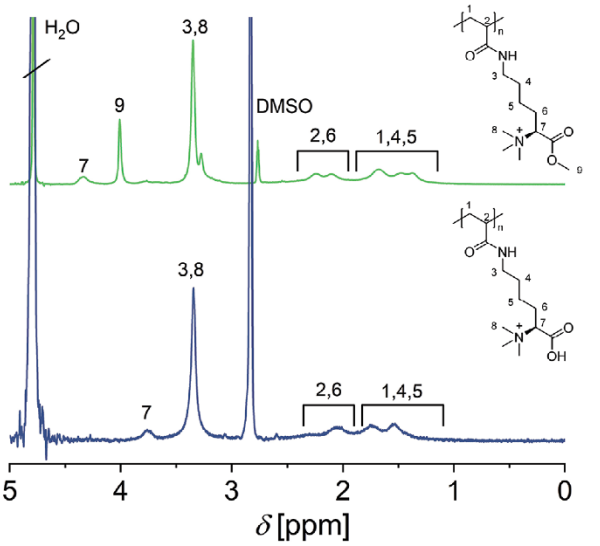


Figure 3. ^{1}H NMR (300 MHz) of P(Me_3Lys-OMe-AAm) (top, green, 1:1 v [D_2O/DMSO-d6]) and P(Me_3Lys-OH-AAm) (bottom, blue, 1:1 v [D_2O/DMSO-d6]).

assigned to the hydrolyzed product. P(Me_3Lys-OMe-AAm) possessed a monomodal molar mass distribution determined by aqueous size-exclusion chromatography (SEC, Figure S12, Supporting Information) indicating the absence of unwanted chain coupling during the reaction. The theoretical molar mass $M_{n,theo}$ was estimated from the conversion of NAS during the RAFT-polymerization (Figure S13, Supporting Information) and determined to be 49.1 kDa.

2.4. Effect of Methylation on the Characteristics of Chiral, Amino-Acid-Derived Polyzwitterions

As a second part of this study, we investigated the impact of the permanent positive charge on the physico-chemical properties of amino-acid-derived polyzwitterions. For comparison, P(Boc-Lys-OH-AAm) was synthesized by PPM of PNAS with commercially available Boc-Lysine-OH (Boc-Lys-OH). Similarly to the PPM of PNAS with Me_3Lys-OMe-NH_2, this reaction yielded polymers with monomodal molar mass distribution according to aqueous SEC measurements (Figure S14, Supporting Information). The theoretical molar mass $M_{n,theo}$ was estimated from the conversion of NAS during the RAFT-polymerization (Figure S15, Supporting Information) and determined to be 55.1 kDa. From these two modified polymers, P(Lys-OH-AAm) and P(Me_3Lys-OH-AAm) were obtained by acidic deprotection of P(Boc-Lys-AAm) and by hydrolysis of P(Me_3Lys-OMe-AAm) under mildly basic conditions, respectively. Successful deprotection of P(Boc-Lys-AAm) was verified via ^{1}H-NMR as the Boc group signal at δ = 1.4 ppm disappeared (H8, Figure S16, Supporting Information). Hydrolysis of the methyl ester of P(Me_3Lys-OMe-AAm) was confirmed by ^{1}H-:NMR by the disappearance of the methoxy peak at δ = 4.0 ppm (H9, Figure 3). Furthermore, a shift from δ = 4.3 ppm to δ = 3.7 ppm was observed for the α-CH-group (H7).

© 2024 The Author(s). Macromolecular Rapid Communications published by Wiley-VCH GmbH

15213927, 0, Downloaded from https://onlinelibrary.wiley.com/doi/10.1002/marc.202400623 by Meike N. Leiske - Staats- Und Universitätsbibliothek Dresde , Wiley Online Library on [01/10/2024]. See the Terms and Conditions (https://onlinelibrary.wiley.com/terms-and-conditions) on Wiley Online Library for rules of use; OA articles are governed by the applicable Creative Commons License

ADVANCED SCIENCE NEWS
www.advancedsciencenews.com

Macromolecular Rapid Communications
www.mrc-journal.de

Table 1. Properties of P(Lys-OH-AAm) and P(Me_3Lys-OH-AAm).

Polymer name	M[a] [Da]	DP_{theo}[b]	$M_{n,theo}$[b] [kDa]	pK_a[d]	pI[e] [pH]	Ret. time[f] [min.]
P(Lys-OH-AAm)	200.24	193	38.9 (55.1)[c]	2.4 (COOH) 5.8 (NH_2)	4.3	13.1
P(Me_3Lys-OH-AAm)	243.33	188	46.5 (49.1)[c]	2.8 (COOH)	<3.0	14.1

[a] Molar mass of repeating unit (RU) after deprotection; [b] calculated from ^{1}H-NMR; [c] $M_{n,theo}$ of modified polymer before deprotection; [d] Titration of a 5 mg mL^{-1} polymer solution with 0.1 M NaOH; [e] ELS measurements in water (2.0 mg mL^{-1}) at varying pH. See Figure S20 (Supporting Information) for values; [f] HPLC using a reversed phase column with a water/acetonitrile mixture + 0.1 V% trifluoroacetic acid (TFA) as eluent.

The PPM approach allowed for a good comparison between the methylated and non-methylated polymers. The characteristics obtained by SEC, high-performance liquid chromatography (HPLC) as well as ζ-potential and pH titration of the polymers of the polymers are summarized in **Table 1**.

Since most naturally occurring proteins are optically active and show characteristic functionalities in living systems, our study aimed to obtain chiral PBs from amino acids. Herein, circular dichroism (CD) spectroscopy can verify chirality by specific conformation of the polymers in solution. Reliable assignment of the CD signals of chiral synthetic polymer seems to be difficult because unlike natural proteins most synthetic chiral polymers have a disordered conformation in solution even if the polymers possess highly stereoregular structures in the main chain.[42] Consequently, CD measurements are not used to elucidate the polymeric conformation out of the CD signals in this study as the required comparison of spectra of known structures is not possible, but rather to confirm that chirality is maintained in the polymer. The CD spectrum of both polymers, P(BocLys-OH-AAm) and P(Me_3Lys-OMe-AAm), obtained by RAFT-polymerization of its monomer resembling structure was measured in aqueous solution (pH 6, 0.5 wt%) (Figure S17, Supporting Information). Similar CD spectrums are obtained for the deprotected polymers, P(Lys-OH-AAm) and P(Me_3Lys-OH-AAm), obtained by PPM measured in aqueous solution (pH 7, 0.5 wt%) as better spectra were obtained at neutral pH after their deprotection (Figure S18, Supporting Information). The fact that all spectra contained peaks indicated that both the methylated and non-methylated polymer has an overall one-handed helical preference and, consequently, chiral repeating units, independent from their preparation method. The spectra of the polymers with a similar structure, but different synthetic approach, showed the same trend. Consequently, their secondary structures do not depend on its synthetic approach. The spectra of P(BocLys-OH-AAm) are also in line with previous studies by *Mandal* and coworkers.[27]

To investigate the pH-responsive properties of the polymers in water, an acid-base titration was conducted to determine the logaritmic acidic dissociation constant (pK_a) values. P(Me_3Lys-OH-AAm) showed a pK_a of 2.8, attributed to the (—COOH) functional group in its side chain (Figure S19A, Supporting Information). The titration curve of P(Lys-OH-AAm) revealed pK_a values of 2.9 and 5.8, corresponding to the (—COOH) and (—NH_2) functional groups in the side chain, respectively (Figure S19B, Supporting Information). To investigate the effect of the pH on conductivity and self-assembly, ζ-potential and dynamic light scattering (DLS) as well as electrophoretic light scattering (ELS) measurements were performed at different pH values. The ζ-potential of the P(Lys-OH-AAm) solution varied from −27 to 21 mV upon decreasing the pH value from 9 to 3 with the isoelectric point (pI) at pH 4.3 (Figure S20, Supporting Information), which is in line with what is expected from the pK_a values derived from the titration curve and other previously reported amino-acid-derived polyzwitterions.[9,25] Furthermore, the rather low pI corresponds well to the acidic microenvironment of tumorous tissue. Therefore, it is expected that P(Lys-OH-AAm) can be applied for cellular targeting in future biological experiments, just as previous polyzwitterions with similar pH responsiveness.[10,29] In contrast, measurements of P(Me_3Lys-OH-AAm) show a ζ-potential value from −23 to −2 mV upon decreasing the pH value from pH 8 to 3 indicating free carboxylic groups of the polymer are located at the surface over this pH range. The ζ-potential decreased with increasing pH as more carboxylate groups were deprotonated. The ζ-potential over this pH range was negative as the pK_a of the carboxylate group was below the measured pH range. These results are in agreement with other betaine studies where a negative ζ-potential was obtained below the pK_a of the anionic group.[43,44] This result emphasized the possible application of P(Me_3Lys-OH-AAm) as a zwitterionic-to-cationic charge-shifting polymer. In the zwitterionic state, it might be resistant to non-specific protein adsorption in blood but may also switch to a positive charge to enhance cellular internalization at target sites. This would be suited for cancer therapy as tumor cells have a lower pH compared to blood and normal tissue.[45] Analysis of the DLS measurement of both polymers at different pH values showed that the changes in the diameter are negligible. Solely P(Me_3Lys-OH-AAm) formed assemblies with a hydrodynamic diameter (d_H) of ≈160 nm at a pH 7 (Figure S21, Supporting Information), indicating aggregation of this polymer. It has already been shown that aggregation to a larger size at acidic extracellular tumor pH (pH ≈ 6.6)[46] might be beneficial for retention in tumor tissues as long as they exhibit a small hydrodynamic diameter at physiochemical conditions.[47] The last is tested by protein fouling tests.

In addition to pH response, it was aimed to gain information about the effect of quarternization on the hydrophobicity of the resulting polymers. It is generally known that polyzwitterions possess their highest hydrophobicity in the zwitterionic state.[11] For this reason, HPLC measurements of the Cyanine-5 (Cy5)-labeled polymers P(Lys-OH-AAm)-Cy5 and P(Me_3Lys-OH-AAm)-Cy5 were conducted to gain information about the hydrophobicity of the polymers at relevant conditions HPLC measurements using a gradient from water (0.1 V% TFA, pH 2)

 © 2024 The Author(s). Macromolecular Rapid Communications published by Wiley-VCH GmbH

15213927, 0, Downloaded from https://onlinelibrary.wiley.com/doi/10.1002/marc.202400623 by Maike N. Leiske - Staats- Und Universitätsbibliothek Dresde , Wiley Online Library on [01/10/2024]. See the Terms and Conditions (https://onlinelibrary.wiley.com/terms-and-conditions) on Wiley Online Library for rules of use; OA articles are governed by the applicable Creative Commons License

ADVANCED SCIENCE NEWS
www.advancedsciencenews.com

Macromolecular Rapid Communications
www.mrc-journal.de

15213927, 0, Downloaded from https://onlinelibrary.wiley.com/doi/10.1002/marc.202400623 by Maike N. Lesiak - Staats- Und Universitätsbibliothek Dresde , Wiley Online Library on [01/10/2024]. See the Terms and Conditions (https://onlinelibrary.wiley.com/terms-and-conditions) on Wiley Online Library for rules of use; OA articles are governed by the applicable Creative Commons License

to acetonitrile on a reversed phase column confirmed these results by the later retention time of P(Me_3Lys-OH-AAm)-Cy5 compared to P(Lys-OH-AAm)-Cy5 (Figure S22, Supporting Information; Table 1). To confirm these results, it was attempted to perform partition coefficient (PC) measurements in water at pH 4 and 7, and in Dulbecco's PBS (DPBS) (pH 7.4) Unfortunately, the fluorescence measurements were not meaningful due to an observed increase in fluorescence intensity after sample mixing with organic solvent, as compared to before mixing (data not shown). We propose that this phenomenon was attributed to incomplete phase separation. While two very different pH values were tested, the ζ-potential and titration results have indicated that P(Me_3Lys-OH-AAm) remains zwitterionic over a very broad pH range, while P(Lys-OH-AAm) possesses a pI around pH 4 and is, consequently, in cationic or anionic state at most conditions. This shift toward one side of charge consequently improves the hydrophilicity of the polymer.

2.5. Effect of Methylation on the Cytocompatibility and Protein-Fouling of Polyzwitterions

Different polyzwitterions have shown great promise for applications at the biointerface.[7,8,22] For this reason, we performed preliminary experiments to investigate the impact of the permanent positive charge on cell viability and aggregation in the presence of proteins. To gain information about the aggregation properties, the interactions of P(Lys-OH-AAm) and P(Me_3Lys-OH-AAm) were studied with two representative proteins: bovine serum albumin (BSA) and lysozyme, where BSA was chosen as a negative and lysozyme a positively charged model protein.[48] The fouling was analyzed in DPBS solution via DLS (Figure S23, Supporting Information) and provided information about the formation of aggregates over time as this would induce an increase in diameter in the solution over time. It was already shown that zwitterionic polymers can reduce interaction with various proteins due to both their hydration ability and the neutrality of the zwitterionic groups in the PBS buffer solution.[49] It was observed that BSA does only forms very minor aggregates in the presence of P(Lys-OH-AAm) or P(Me_3Lys-OH-AAm) after 24 h (Figure S23A–D, Supporting Information), which is in line with previous literature reports for P(Lys-OH-AAm).[27] However, mixtures of P(Me_3Lys-OH-AAm) and lysozyme indicated the formation of large nanoparticles ($d \approx 30$ nm and 220 nm) after 30 min, which remained with $d \approx 30$ nm even after 24 h incubation time (Figure S23E–F, Supporting Information). This can be related toward the size of nanoparticles, P(Me_3Lys-OH-AAm), forms without any protein added. In comparison, the interaction between lysozyme and P(Lys-OH-AAm) seems to be slightly reduced, as the formed aggregates are significantly smaller ($d <$ 10 nm), however, neither polymer revealed strong protein fouling. The reduced interaction of the synthesized polyzwitterions compared to polyanions in our previous study might be attributed to the positive charges of the amino groups which can influence protein-fouling as well as protein-repellent properties.[50] This in combination with the higher hydrophilicity of P(Lys-OH-AAm) compared to P(Me_3Lys-OH-AAm) can contribute to smaller aggregates. Therefore, it can be assumed that free, pH-responsive amino groups provide some benefits for polymer hydration and, consequently, the low-fouling properties of polyzwitterions. Eventually, the cell viability of MDA-MB-231 breast cancer cells in the presence of both polymers, which were obtained via PPM, was studied by an 3-(4,5-dimethylthiazol-2-yl)-2,5-diphenyltetrazolium bromide (MTT) assay (Figure S24, Supporting Information), which showed that both P(Lys-OH-AAm) and P(Me_3Lys-OH-AAm) were well tolerated by MDA-MB-231 breast cancer cells at concentrations up to 1.0 mg mL^{-1} (for 24 h). These results confirmed that the methylation of chiral, amino-acid-derived polymers and their subsequent change in properties does not impact the tolerance by cells, thus, rendering both materials suitable for applications in the life-science area. Future studies will evaluate the differences in cell interactions caused by quarternization to further understand these systems in more detail.

3. Conclusions and Outlook

This study reports for the first time the synthesis and properties of chiral, amino-acid-derived betaine-like polyzwitterions. Mildly basic conditions were found to yield complete hydrolysis of the model compound Me_3Ala-OMe, in the absence of Hoffmann-elimination. By transferring these conditions, Me_3Lys-OMe-AAm was successfully synthesized by methylation of Lys-AAm and, subsequently, polymerized via RAFT to obtain P(Me_3Lys-OMe-AAm). In the future, this method can be used to obtain P(Me_3Lys-OH-AAm) in the most direct way. This study further highlights the potential of PPM, which yields highly comparable polymers with varying side chains. A kinetic study of polymerization was successfully performed. To investigate the impact of the permanent positive charge on amino-acid-derived polyzwitterions, P(Lys-OH-AAm) and P(Me_3Lys-OH-AAm) were synthesized via PPM of an amine-reactive polymeric precursor to allow an adequate comparison between the methylated and non-methylated compound. CD confirmed that a stereocenter was maintained via both approaches which will allow us to study the impact of chirality in these polymers in future in vitro experiments. The combination of pH titration and ζ-potential measurements showed that P(Lys-OH-AAm) possessed a pI $\approx$ 4.3 as compared to P(Me_3Lys-OH-AAm), which is expected to be present in its zwitterionic state at all pH-values above the pK_a value of its (—COOH) group. Having this zwitterionic character over a broader pH range can have advantages for cellular targetability. We found that the methylation increased the hydrophobicity and the protein fouling of P(Me_3Lys-OH-AAm) compared to P(Lys-OH-AAm), which is useful to combine them in the future with nanoparticles for cancer chemotherapy to improve their retention time in blood and subsequent tumor accumulation. Both polymers were well tolerated by cells up to concentrations of 1 mg mL^{-1}. Further studies will focus on further comparing the interactions of both polymers with cells.

Supporting Information

Supporting Information is available from the Wiley Online Library or from the author.

 © 2024 The Author(s). Macromolecular Rapid Communications published by Wiley-VCH GmbH

ADVANCED SCIENCE NEWS
www.advancedsciencenews.com

Macromolecular Rapid Communications
www.mrc-journal.de

Acknowledgements

The authors would like to acknowledge Prof Andreas Greiner, Prof Johannes C. Brendel, Prof Thomas Scheibel, and Prof Georg Papastavrou for providing access to their laboratories and equipment. The authors thank Dr Martin Humenik for his help with high-performance liquid chromatography measurements. The authors would like to thank Rika Schneider for conducting size-exclusion chromatography measurements, Martina Fried and Marius Alexander Methfessel for assistance with syntheses, and Jana Ullmann for assistance with the cytocompatibility assays. This project was generously supported by the German Research Foundation (DFG; project number 535904448). M.N.L. further acknowledges financial support from the "Fonds der Chemischen Industrie im Verband der Chemischen Industrie."

Open access funding enabled and organized by Projekt DEAL.

Conflict of Interest

The authors declare no conflict of interest.

Data Availability Statement

The data that support the findings of this study are available from the corresponding author upon reasonable request.

Keywords

amino acid, betaine, chirality, post-polymerization modification, RAFT-polymerization, zwitterionic polymers

Received: July 31, 2024
Revised: September 2, 2024
Published online:

[1] G. Villaverde, A. Baeza, *Beilstein J. Nanotechnol.* **2019**, *10*, 168.
[2] M. Barz, R. Luxenhofer, R. Zentel, M. J. Vicent, *Polym. Chem.* **2011**, *2*, 1900.
[3] K. Knop, R. Hoogenboom, D. Fischer, U. S. Schubert, *Angew. Chemie – Int. Ed.* **2010**, *49*, 6288.
[4] R. Haag, F. Kratz, *Angew. Chem., Int. Ed.* **2006**, *45*, 1198.
[5] R. Duncan, M. J. Vicent, *Adv. Drug Delivery Rev.* **2013**, *65*, 60.
[6] S. Fujii, S. Takano, K. Nakazawa, K. Sakurai, *Biomacromolecules* **2022**, *23*, 2846.
[7] Z. G. Estephan, P. S. Schlenoff, J. B. Schlenoff, *Langmuir* **2011**, *27*, 6794.
[8] S. Jiang, Z. Cao, *Adv. Mater.* **2010**, *22*, 920.
[9] M. N. Leiske, B. G. De Geest, R. Hoogenboom, *Bioact. Mater.* **2023**, *24*, 524.
[10] M. N. Leiske, Z. A. I. Mazrad, A. Zelcak, K. Wahi, T. P. Davis, J. A. McCarroll, J. Holst, K. Kempe, *Biomacromolecules* **2022**, *23*, 2374.
[11] L. D. Blackman, P. A. Gunatillake, P. Cass, K. E. S. Locock, *Chem. Soc. Rev.* **2019**, *48*, 757.
[12] A. Laschewsky, *Polymers* **2014**, *6*, 1544.
[13] A. B. Lowe, C. L. McCormick, *Chem. Rev.* **2002**, *102*, 4177.
[14] Y.-Z. You, C.-Y. Hong, C.-Y. Pan, *Nanotechnology* **2006**, *17*, 2350.
[15] J. Yuan, X. Huang, P. Li, L. Li, J. Shen, *Polym. Chem.* **2013**, *4*, 5074.
[16] G. Huang, Z. Xiong, H. Qin, J. Zhu, Z. Sun, Y. Zhang, X. Peng, J. Ou, H. Zou, *Anal. Chim. Acta* **2014**, *809*, 61.
[17] A. Laschewsky, I. Zerbe, *Polymer* **1991**, *32*, 2070.
[18] J. Bohrisch, U. Wendler, W. Jaeger, *Macromol. Rapid Commun.* **1997**, *18*, 975.
[19] V. A. Izumrudov, A. N. Zelikin, M. V. Zhiryakova, W. Jaeger, J. Bohrisch, *J. Phys. Chem. B* **2003**, *107*, 7982.
[20] P. Ferruti, A. Bettelli, A. Feré, *Polymer* **1972**, *13*, 462.
[21] M. Eberhardt, R. Mruk, R. Zentel, P. Théato, *Eur. Polym. J.* **2005**, *41*, 1569.
[22] D. W. Grainger, *Nat. Biotechnol.* **2013**, *31*, 507.
[23] Z. Zhang, S. Chen, S. Jiang, *Biomacromolecules* **2006**, *7*, 3311.
[24] S. Takano, K. Sakurai, S. Fujii, *Polym. Chem.* **2021**, *12*, 6083.
[25] T. Maji, S. Banerjee, Y. Biswas, T. K. Mandal, *Macromolecules* **2015**, *48*, 4957.
[26] Y. Sun, J. Liu, Z. Li, J. Wang, Y. Huang, *ACS Appl. Mater. Interfaces* **2021**, *13*, 18454.
[27] P. Dinda, M. Anas, P. Banerjee, T. K. Mandal, *Macromolecules* **2022**, *55*, 4011.
[28] N. Yamada, Y. Honda, H. Takemoto, T. Nomoto, M. Matsui, K. Tomoda, M. Konno, H. Ishii, M. Mori, N. Nishiyama, *Sci. Rep.* **2017**, *7*, 6077.
[29] S. Fujii, K. Sakurai, *Biomacromolecules* **2022**, *23*, 3968.
[30] M. N. Leiske, C. Kuenneth, J. De Breuck, B. G. De Geest, R. Hoogenboom, *Macromol. Chem. Phys.* **2023**, *224*, 1.
[31] A. Lekchiri, J. Morcellet, M. Morcellet, *Macromolecules* **1987**, *20*, 49.
[32] M. Casolaro, R. Barbucci, *Int. J. Artif. Organs* **1991**, *14*, 732.
[33] R. Barbucci, M. Casolaro, A. Magnani, *J. Controlled Release* **1991**, *17*, 79.
[34] A. Bentolila, I. Vlodavsky, R. Ishai-Michaeli, O. Kovalchuk, C. Haloun, A. J. Domb, *J. Med. Chem.* **2000**, *43*, 2591.
[35] Y. Goldberg, E. Ābele, G. Bremanis, P. Trapenciers, A. Gaukhman, J. Popelis, A. Gomtsyan, I. Kalviņš, M. Shymanska, E. Lukevics, *Tetrahedron* **1990**, *46*, 1911.
[36] A. C. Cope, A. S. Mehta, *J. Am. Chem. Soc.* **1963**, *85*, 1949.
[37] K. Banert, M. Hagedorn, M. Heck, R. Hertel, A. Ihle, I. Müller, T. Pester, T. Shoker, P. R. Rablen, *J. Org. Chem.* **2020**, *85*, 13630.
[38] A. Saha, S. Panda, S. Paul, D. Manna, *Chem. Commun.* **2016**, *52*, 9438.
[39] M. Billing, G. Festag, P. Bellstedt, F. H. Schacher, *Polym. Chem.* **2017**, *8*, 936.
[40] G. Moad, C. Barner-Kowollik, *Handb. RAFT Polym.* **2008**, 51.
[41] T. J. Paul, A. K. Strzelczyk, M. I. Feldhof, S. Schmidt, *Biomacromolecules* **2020**, *21*, 2913.
[42] Y. Okamoto, E. Yashima, in *Circular Dichroism: Principles and Applications*, (Eds: N. Berova, K. Nakanishi, R. W. Woody), John Wiley and Sons, Hoboken, NJ **2000**.
[43] W. Wang, W. Zhang, H. Sun, X. Li, Q. Du, C. Wei, X. Ge, C. Li, *J. Mol. Liq.* **2019**, *291*, 111312.
[44] M. Billing, J. K. Elter, F. H. Schacher, *Polymer* **2016**, *104*, 40.
[45] E. S. Lee, Z. Gao, Y. H. Bae, *J. Controlled Release* **2008**, *132*, 164.
[46] R. van Sluis, Z. M. Bhujwalla, N. Raghunand, P. Ballesteros, J. Alvarez, S. Cerdn, J.-P. Galons, R. J. Gillies, *Magn. Reson. Med.* **1999**, *41*, 743.
[47] Z. Qin, T. Chen, W. Teng, Q. Jin, J. Ji, *Langmuir* **2019**, *35*, 1242.
[48] J. Jasinski, M. V. Wilde, M. Voelkl, V. Jérôme, T. Fröhlich, R. Freitag, T. Scheibel, *ACS Appl. Mater. Interfaces* **2022**, *14*, 47277.
[49] Y. N. Chou, M. Z. Ou, *ACS Appl. Polym. Mater.* **2023**, *5*, 5411.
[50] J. De Breuck, M. Streiber, M. Ringleb, D. Schröder, N. Herzog, U. S. Schubert, S. Zechel, A. Traeger, M. N. Leiske, *ACS Polym. Au* **2024**, *4*, 222.

 © 2024 The Author(s). Macromolecular Rapid Communications published by Wiley-VCH GmbH

15213927, 0, Downloaded from https://onlinelibrary.wiley.com/doi/10.1002/marc.202400623 by Maike N. Leiske - Staats- Und Universitätsbibliothek Dresde , Wiley Online Library on [01/10/2024]. See the Terms and Conditions (https://onlinelibrary.wiley.com/terms-and-conditions) on Wiley Online Library for rules of use; OA articles are governed by the applicable Creative Commons License

Macromolecular Rapid Communications

Supporting Information

for *Macromol. Rapid Commun.*, DOI 10.1002/marc.202400623

Zwitterionic Amino-Acid-Derived Polyacrylamides with a Betaine Twist – Synthesis and Characterization

*Jonas De Breuck, Valérie Jérôme, Ruth Freitag and Meike N. Leiske**

WILEY-VCH

Supporting information

Zwitterionic amino-acid-derived polyacrylamides with a betaine twist – Synthesis and characterization

Jonas De Breuck,[a] Valérie Jérôme,[b] Ruth Freitag,[b,c] Meike N. Leiske[a,d,*]

[a] Macromolecular Chemistry, University of Bayreuth, Universitätsstraße 30, 95447 Bayreuth, Germany

[b] Process Biotechnology, University of Bayreuth, Universitätsstraße 30, 95447 Bayreuth, Germany

[c] Bayreuth Center for Molecular Biosciences (BZMB), University of Bayreuth, Universitätsstraße 30, 95447 Bayreuth, Germany

[d] Bavarian Polymer Institute, Universitätsstraße 30, 95447 Bayreuth, Germany

*correspondence to: meike.leiske@uni-bayreuth.de

1. Experimental Part

1.1. Materials and instrumentation

1.1.1. Materials

Acetonitrile (99.9%), diethyl ether (99.5%), dimethylformamide (99.5%), methanol (99.9%), sodium hydrogen carbonate (>99.7%) and methyl iodide (99.0%) were purchased from FisherScientific. Chloroform (99.8%), dichloromethane (99.8%), isopropanol (99.9%), sodium hydroxide (99.5%), potassium hydroxide (99.5%), Hydrochloric acid (32%), Dulbecco's Modified Eagle Medium (DMEM) Low Glucose, Fetal Bovine Serum Advanced, Penicillin/Streptomycin (Pen/Strep), Dulbecco's PBS, Bovine serum albumin (BSA) and lysozyme, from which the last two obtained as lyophilized powders, were purchased from VWR Chemicals. Triethylamine (99.5%), potassium carbonate (99.0%), 8-hydroxyquinoline (for synthesis) and Anisole (99.0%) were purchased from Sigma Aldrich. Thiazolyl blue tetrazolium bromide (MTT) was purchased from TCI Chemicals. Cyanin5-amine (95.0%) was purchased from Lumiprobe. H-Lys(Boc)-OH (97.0%) and *N*-hydroxysuccinimide (98.0%) were purchased from BLD Pharmatech ltd. Trifluoroacetic acid (99.0%) was purchased from abcr. Acryloyl chloride (96%) was purchased from ThermoScientific. Cupric (II) carbonate basic was purchased from Honeywell. Boc-Lys-OH (98%) and L-lysine hydrochloride (98%) were purchased from Carbolution.

Azobis(isobutyronitril) (AIBN) (Fluka or Sigma Aldrich, 98.0%) was recrystallized from methanol before use. *N*-Acryloxysuccinimide (NAS)[37] and 2-{[(butylsulfanyl)-carbonothiosyl]sulfanyl}propanoic acid (PABTC)[44] were synthesized and characterized following known procedures in literature.

1.1.2. Proton nuclear resonance (^{1}H-NMR) and carbon nuclear resonance (^{13}C-NMR) spectroscopy

^{1}H- and ^{13}C-NMR spectra of all compounds were recorded on a Bruker Avance 300 (300 MHz) spectrometer equipped with a BACS-120 autosampler and a ^{1}H, ^{13}C, ^{19}F and ^{31}P-BBO probe at room temperature.

1.1.3. Size-exclusion chromatography (SEC)

Aqueous SEC measurements of P(Me_3Lys-OMe-AAm) and P(Me_3Lys-OMe-AAm)-Cy5 were performed on an instrument consisting of a column set with a NOVEMA Max precolumn (particle size = 10 µm) and three NOVEMA Max main columns (particle size = 10 µm, 1 × 100 Å; 2 × 3000 Å) with separation range from 100 to 3 000 000 Da (PSS, Mainz, Germany) together with a variable wavelength detector (1200 Series, Agilent Technologies). As solvent 80:20 Water/ACN mixture + 0.1 M NaCl + 0.1 V% TFA was used (for dissolving polymer and as eluting solvent) with a flow rate of 0.5 mL/min and the columns were maintained at room temperature. As internal standard ethylene glycol (HPLC grade) was used. The calibration was done with narrowly distributed Poly(2-vinylpyridine) (narrowly distributed P2VP homo-polymers, PSS calibration kit). An injection volume of 60 µL was used for the measurements. The samples were dissolved with a concentration of 2 mg mL^{-1} and filtered through a 0.22 µm PTFE Nylon filter before analysis. The UV-detector was set to λ = 600 nm for measurements of Cy5-labeled polymers.

Aqueous SEC measurements of P(BocLys-OH-AAm) and P(BocLys-OH-AAm)-Cy5 were performed on an instrument consisting of a column set with a SUPREMA precolumn (particle size = 5 µm), one SUPREMA (particle size = 5 µm, 30 Å) and two NOVEMA Max main columns (particle size = 5 µm, 2 × 1000 Å) with separation range from 100 to 1 000 000 Da (PSS, Mainz, Germany) together with a variable wavelength detector (1200 Series, Agilent Technologies). As solvent 65:35 Water/ACN mixture + 50 mM LiBr + 0.1 M $NaHCO_3$ was used (for dissolving polymer and as eluting solvent) with a flow rate of 0.8 mL min^{-1} and the columns were maintained at room temperature. As internal standard ethylene glycol (HPLC grade) was used. The calibration was done with narrowly distributed poly(ethylene glycol) (narrowly distributed PEG homo-polymers, PSS calibration kit). An injection volume of 60 µL was used for the measurements. The samples were dissolved with a concentration of 2 mg mL^{-1} and filtered through a 0.22 µm PTFE Nylon filter before analysis. The UV-detector was set to λ = 600 nm for measurements of Cy5-labeled polymers.

DMF SEC measurements of PNAS was performed on an instrument consisting of a GRAM precolumn (particle size = 10 µm) and two GRAM main columns (Particle size= 10 µm, 1 × 100 A, 1 × 3000 A) with separation range from 100 to 5 000 000 Da (PSS, Mainz, Germany) together with a diode array and refractive index detector (1260 Infinity, Agilent Technologies). As solvent DMF (HPLC grade) with lithium bromide was used (for dissolving polymer and as eluting solvent) with a flow rate of 0.5 mL/min and the columns were maintained at room temperature. As internal

standard Toluene (HPLC grade) was used. The calibration was done with narrowly distributed polystyrene homo-polymers (PSS calibration kit). An injection volume of 20 µL was used for the measurements. The samples were dissolved with a concentration of 2 mg mL^{-1} and filter through a 0.22 µm PTFE Nylon filter before analysis.

1.1.4. High-performance liquid chromatography (HPLC)

HPLC measurements were conducted with a Jupiter 5 µm C18 300 Å LC column (250 × 4.6 mm). The run time was 35 min. A mixture of 0.1 v/v% TFA in water and acetonitrile served as eluent (**Table S1**). The fluorescence detected was set to λ_{ex} = 640 nm and λ_{em} = 680 nm with 1× gain. The ELSD detector was set to λ = 215 nm.

Table S1. Composition of HPLC eluent at indicated time points.

Time [min]	Fraction of 0.1v% aqueous TFA [%]	Fraction of acetonitrile [%]
0	98.0	2.0
5	50.0	50.0
10	0.0	100.0
17	0.0	100.0
25	98.0	2.0
35	98.0	2.0

1.1.5. Dynamic light scattering (DLS)

DLS was measured on a Zetasizer Nano-ZS Malvern apparatus (Malvern Instruments Ltd) using disposable cuvettes. The excitation light source was a He–Ne laser at 633 nm and the intensity of the scattered light was measured at an angle of 173°. This method measures the rate of intensity fluctuation, and the size of the particles is determined through the Stokes–Einstein equation. The concentration of the polymer solution was 2 mg mL^{-1} in all cases.

1.1.6. Electrophoretic light scattering (ELS)

ELS was used to measure the zeta potential (ζ). The measurement was also performed on a Zetasizer Nano ZS by applying laser Doppler velocimetry. For each measurement, 20 runs were carried out using the slow-field reversal and the fast-field reversal mode at 150 V. Each experiment was performed in triplicates at 25 °C. The ζ-potential was calculated from the electrophoretic

mobility (μ) according to the Henry equation. Henry coefficient f(ka) was calculated according to Ohshima.[45] The concentration of the polymer solution was 2 mg mL^{-1} in all cases.

1.1.7. Fourier-Transform Infrared Spectroscopy (FT-IR)

IR spectra were recorded from solids on a Perkin Elmer Spectrum 100 FT-IR spectrometer in attenuated total reflection (ATR) mode.

1.1.8. Matrix-assisted laser desorption/ionization time-of-flight mass spectroscopy (MALDI-ToF MS)

measurements were performed using a Bruker AutoFlex Max mass spectrometer equipped with a Smart-beam II laser. The analyte was embedded in the matrix/salt combination of 2,3-Dihydroxybenzoic acid (DHB)/ Pottasium trifluoroacetate (KTFA) in the matrix:analyte:salt mass ratio 20:3:1.

1.2. Synthesis and characterization

1.2.1. Synthesis of PNAS

In a 2 mL reaction vessel (Biotage), 507 mg NAS (3 mmol, 200 equiv.), 0.082 mg AIBN (5×10^{-7} mol, 0.1 equiv.), 1.19 mg PABTC (5×10^{-6} mol, 1 equiv.) were dissolved in 1 mL DMF and sealed with a rubber septum. A sample was taken (t = 0 h) for ^{1}H-NMR spectroscopy in DMSO-d6 or $CDCl_3$ as indicated to determine the conversion by comparing the sample with a sample at the end of the reaction. The reaction mixture was deoxygenated with Ar for 30 min and subsequently placed in a preheated sand bath and stirred at 70 °C for 24 h. The reaction was terminated by cooling to RT and purging air in. A sample was taken (t = 24 h) and analyzed *via* ^{1}H-NMR spectroscopy in DMSO-d6. The crude polymer was precipitated in ice-cold diethyl ether twice. After centrifugation (5000 rpm, 6 min), the supernatant was discarded, and the polymer was dried under reduced pressure overnight to obtain the product as a yellow viscous oil. The key properties are summarized in Table S2.

Table S2. Properties of PNAS used for the synthesis of different amino-acid-functionalized polymers.

	^{1}H-NMR[a]			SEC[c]	
PNAS for PPM towards:	Conv. [%]	DP_{theo}[b]	$M_{n,theo}$[b] [KDa]	$M_{n,app}$ [kDa]	Đ
P(Lys-OH-AAm)	96.4	193	32.8	18.4	1.52
P(Me_3Lys-OH-AAm)	94.2	188	32.0	16.5	1.53

[a] ^{1}H NMR (300 MHz). [b]calculated from monomer conversion. [c]SEC in DMF (PS calibration).

1.2.2. Post-polymerization modification of PNAS with Boc-Lys-OH

In a 25 mL round bottom flask, PNAS (200 mg, 6.8×10^{-6} mol, 1.00 equiv.) was dissolved in anhydrous DMF (9.5 mL). 500 µL triethylamine were added. After that, Boc-Lys-OH (297 mg, 1.21 mmol, 205 equiv. per polymer) was added, the reaction vial was closed with a septum and the suspension was stirred at 40 °C for 24 h. Then, the solid was filtered off and the remaining solution was dialyzed (RC, MWCO 3.5 kDa, SpectraPor) against 1 L deionized water for three days with daily water changes. Upon lyophilization, the product was yielded as an off-white powder.

SEC (PEG-cal.): $M_{n,app}$ = 37,100 g mol^{-1}; Đ = 1.50.

1.2.3. Post-polymerization modification of PNAS with Me_3Lys-OMe-NH_2

In a 25 mL round bottom flask, PNAS (300 mg, 9.36×10^{-6} mol, 1.00 equiv.) was dissolved in anhydrous DMF (4.75 mL). 250 µL triethylamine were added. After that, Me_3Lys-OMe-NH_2 (395 mg, 1.94 mmol, 205 equiv. per polymer) was added, the reaction vial was closed with a septum and the suspension was stirred at 40 °C for 24 h. Then, the solid was filtered off and the remaining solution was dialyzed (RC, MWCO 3.5 kDa, SpectraPor) against 1 L deionized water for three days with daily water changes. Upon lyophilization, the product was yielded as a yellowish powder. The success of the reaction was verified *via* ^{1}H-NMR and FTIR.

SEC (P2VP-cal.): $M_{n,app}$ = 10,100 g mol^{-1}; Đ = 1.96.

1.2.4. Post-polymerization modification of PNAS with Cy5-amine and BocLys-OH or Me_3Lys-OMe-NH_2

The labeling process is exemplarily described for PNAS yielding P(Me_3Lys-OMe-AAm)-Cy5. In a small reaction vessel, 45 mg of PNAS (1.39×10^{-6} mol, 1.0 equiv.) and 1 µL of Et_3N (7.0×10^{-6} mol, 5 equiv. per polymer) were dissolved in anhydrous 1 mL DMF and stirred at RT in the dark for 24 h. Subsequently, a 10 mg mL^{-1} solution of Cy5-amine (1.0 mg, 1.7×10^{-6} mol, 1.2 equiv. per polymer) in anhydrous DMF was added. The reaction was stirred at RT in the dark overnight. Then, 62 mg of Me_3Lys-OMe-NH_2 (3.05×10^{-4}, 220 equiv. per polymer) and 55 µL of Et_3N (3.95×10^{-4}, 284 equiv. per polymer) were added to the reaction mixtures which was stirred at RT in the dark for an additional 24 h. After that, the solid was filtered off and the remaining solution was dialyzed (RC, MWCO 3.5 kDa, SpectraPor) against 1 L deionized water for four days (until water outside membrane was colourless) with daily water changes in the dark. Upon lyophilization, the product was yielded as a blue powder.

P(Me_3Lys-OMe-AAm)-Cy5: Aqueous (SEC) (P2VP-cal.): $M_{n,app}$ = 7,600 g mol^{-1}; Đ = 2.53

P(BocLys-OH-AAm)-Cy5: Aqueous (SEC) (PEG-cal.): $M_{n,app}$ = 3,700 g mol^{-1}; Đ = 1.32

1.2.5. Acidic deprotection of P(Boc-Lys-AAm) yielding P(Lys-OH-AAm)

In a reaction vessel, 250 mg of polymer were dissolved in 1 mL trifluoroacetic acid, and the reaction was stirred at room temperature for 2 h. Dye-labelled polymers were stirred in the dark in a 50/50 V% [TFA:water] mixture. Subsequently, the reaction mixture was diluted with 1 mL EtOH and the polymer was precipitated in 40 mL ice-cold diethyl ether. Then, the suspension was centrifuged (5000 rpm, 6 min) and the supernatant was discarded. The polymer was re-dissolved in H_2O and freeze-dried to obtain the product as a white powder.

The success of the deprotection of the polymer was analyzed by ^{1}H-NMR in D_2O, showing the disappearance of the BOC, signal at δ = 1.4 ppm.

1.2.6. Basic deprotection of P(Me_3Lys-OMe-AAm) yielding P(Me_3Lys-OH-AAm)

In a reaction vessel, 100 mg of P(Me_3Lys-OMe-AAm) (2.15×10^{-6} mol, 1.0 equiv.) were dissolved in 5 mL of 0.1 N NaOH solution (5×10^{-4} mol, 230 equiv. per polymer). The reaction mixture was stirred at room temperature for 24 h. Dye-labeled polymers were stirred in the dark. Subsequently, the solution was dialyzed (RC, MWCO 3.5 kDa, SpectraPor) against 1 L deionized water for four days with daily water exchanges (Cy5-labeled polymers were dialyzed in the dark). Upon

lyophilization, the product was recovered as a white to yellowish powder (blue powder for the Cy5-labeled polymers).

1.2.7. pH response

The response of the different polymers to the pH value was investigated by titration. A 5 mg mL^{-1} solution of the polymer in deionized water was prepared and 20 µL 1.0 M aq. HCl were added to obtain a starting pH value < 3. Subsequently, the solution was titrated with 0.1 M aq. NaOH until a pH value > 9 was reached. Measurements were done with a Mettler Toledo digital pH meter.

1.3. Biological testing

1.3.1. Protein fouling

Fouling of P(Me_3Lys-OH-AAm) and P(Lys-OH-AAm) by proteins (BSA and lysozyme) was analyzed by DLS measurements.

Stock solutions of the polymers and the proteins were prepared separately in DPBS (1 mg mL^{-1}) and mixed in a ratio of 1:1, resulting in final concentrations of c = 0.5 mg mL^{-1}. The samples were analyzed immediately after mixing (t = 0 h) and at indicated time points (0.5 h, 1 h, 2 h, 4 h, 24 h) thereafter. In between measurements the samples were incubated at 37 °C whilst being shaken at 100 rpm. Measurements were conducted at 37 °C with five measurements and three runs each. After the measurement, samples were placed back into the incubator immediately.

1.3.2. Cell culture

MDA-MB-231 cells (HTB-26, ATCC) were maintained in DMEM cell culture medium supplemented with 10% fetal calf serum (FCS), 100 mg mL^{-1} streptomycin, 100 U mL^{-1} penicillin, and 4 mM glutamine. Cells were cultivated at 37 °C in a humidified 5% CO_2 atmosphere.

1.3.3. Cell viability

The cytotoxicity of P(Me_3Lys-OH-AAm) and P(Lys-OH-AAm)), which were obtained *via* PPM approach, were tested using MDA-MB-231 breast cancer cells. The polymers stock solutions were prepared at concentrations ≤ 20 mg mL^{-1}. The polymers were tested in a concentration range from 0 to 1.0 mg mL^{-1}. The cells (10^4 cells per well) were seeded in culture medium (100 µL per well)

in 96-well plates and allowed to adhere overnight. No cells were seeded in the outer wells, these were just filled with water. The medium was subsequently removed and replaced by fresh polymer-containing media. Then, the cells were incubated for an additional 24 h. After that, the medium was removed, the cells were washed with 100 µL Dulbecco's PBS (DPBS) and fresh culture medium containing thiazolyl blue tetrazolium bromide (MTT) (concentration: 1 mg mL^{-1}) was added (100 µL per well). Note: MTT (50 mg) was dissolved in 10 mL of sterile DPBS and 1 to 5 diluted in culture medium prior to use in this assay. After incubation for 3 h at 37 °C, the medium was removed and 100 µL of isopropanol (^{i}PrOH) was added to each well. Then, the plates were gently shaken in the dark for 15 minutes to dissolve the formazan crystals. Quantification was done by measuring the absorbance at λ = 580 nm using a microplate reader (Genios Pro, Tecan). Untreated cells on the same plate served as negative control (100% viability), cells treated with 20% DMSO as positive control (0% viability), and wells without cells as background. For data evaluation, Excel was used. For each dilution step, 6 wells were measured and performed in triplicate. The cell viability was calculated according to equation (2).

$$\%\ Cell\ viability = \frac{(Abs.sample - Abs.background)}{(Abs.negative\ control - Abs.background)} \times 100 \qquad (2)$$

2. Results

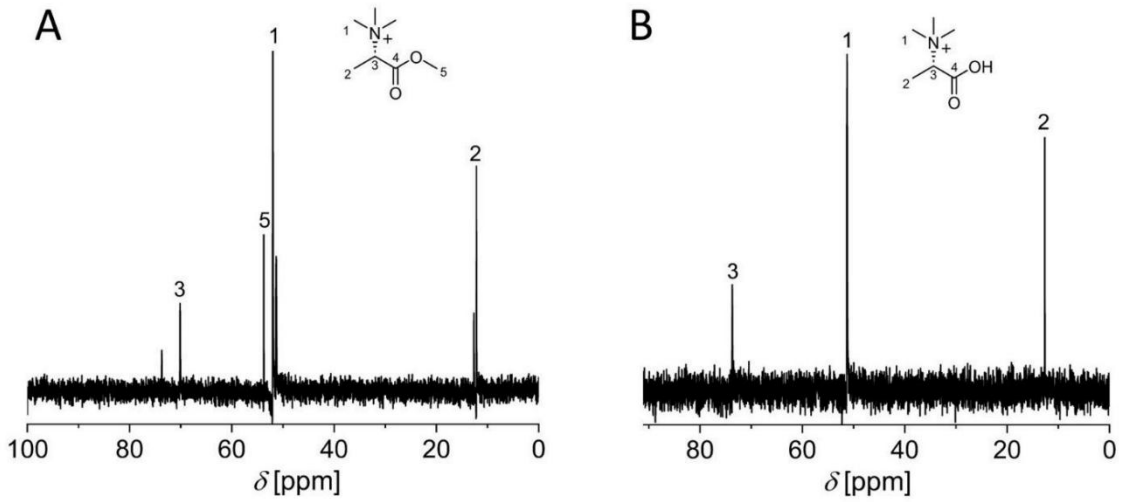


Figure S1. ^{13}C-NMR (75 MHz, D_2O) of A: Me_3Ala-OMe and B: Me_3Ala-OH.

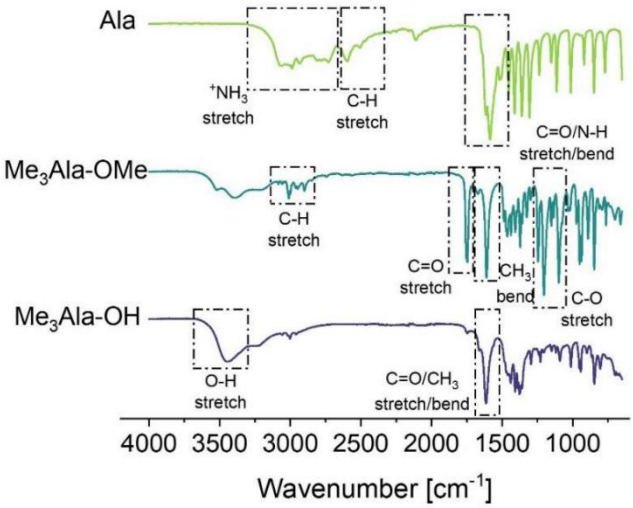


Figure S2. FT-IR spectra of Ala (top, green), Me_3Ala-OMe (middle, cyan) and Me_3Ala-OH (bottom, purple).

WILEY-VCH

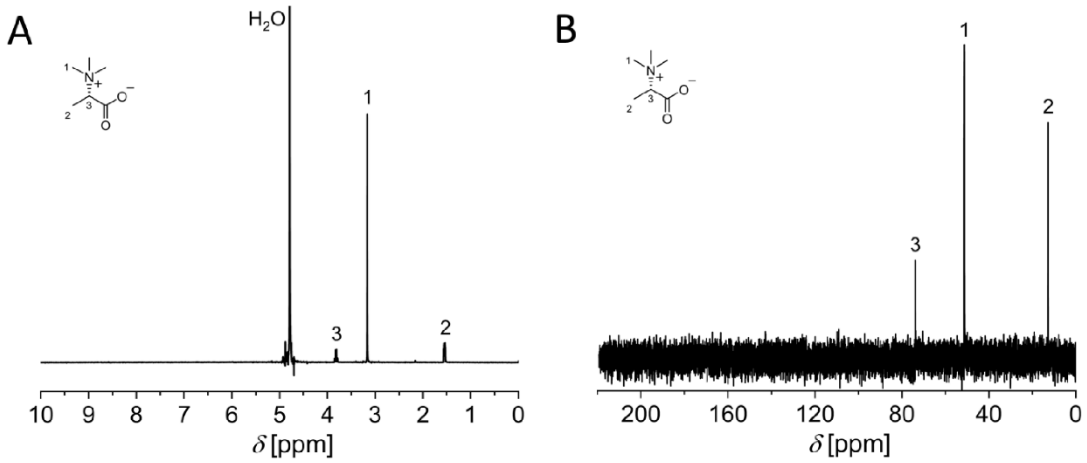


Figure S3. *A: ^{1}H-NMR (300 MHz, D_2O) Me_3Ala-OH and B: ^{13}C-NMR (75 MHz, D_2O).*

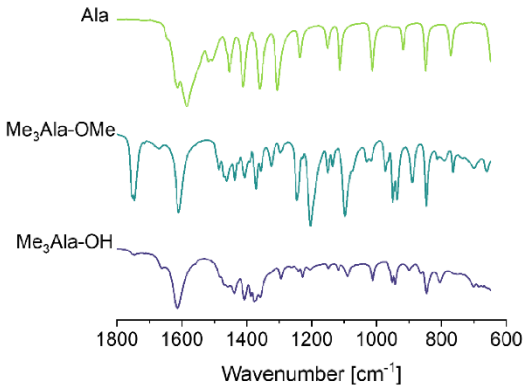


Figure S4. 1800-600 cm^{-1} region of FT-IR spectra of Ala (top, green), Me_3Ala-OMe (middle, cyan) and Me_3Ala-OH (bottom, purple).

WILEY-VCH

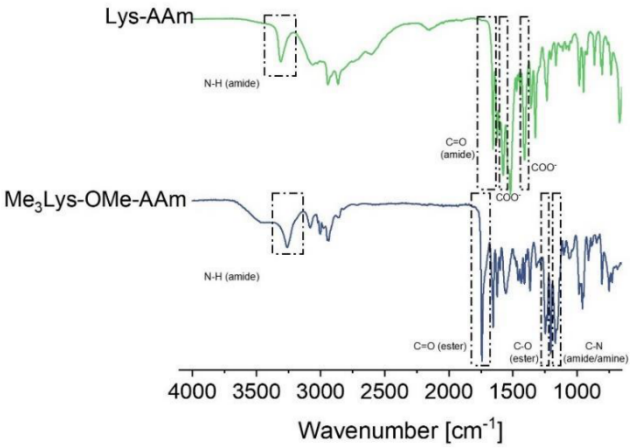


Figure S5. FT-IR spectra of Lys-AAm (top, green) and Me_3Lys-OMe-AAm (bottom, blue).

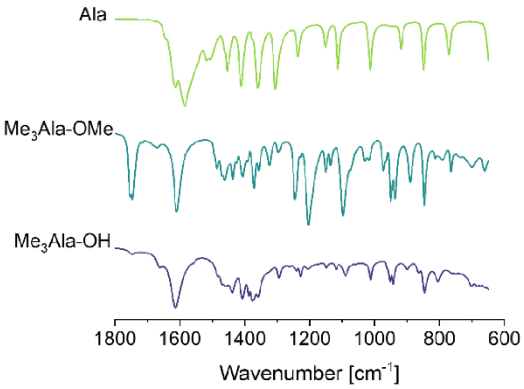


Figure S6. 1800-600 cm^{-1} region of Lys-AAm (top, green) and Me_3Lys-OMe-AAm (bottom, blue).

WILEY-VCH

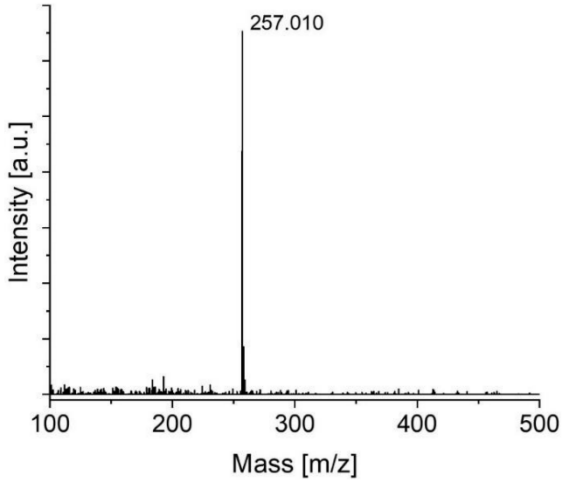


Figure S7. MALDI-ToF mass spectrum of Me_3Lys-OMe-AAm.

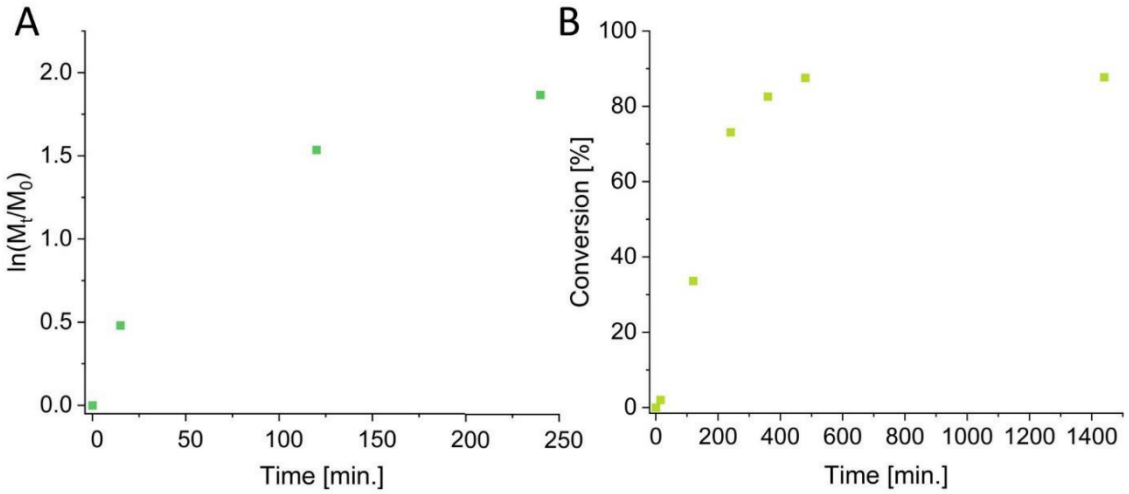


Figure S8. Time-dependent polymerization kinetics on the RAFT-polymerization of Me_3Lys-OMe-AAm using PABTC as CTA ([M]/[CTA]/[I] = 100:1:0.2). Polymerizations were conducted in DMF at 70°C using AIBN as initiator. The monomer conversion was calculated by ^{1}H-NMR, using trioxane as an internal standard. A: logarithmic plot of the polymerization kinetics until 240 min. (linear region). B: monomer conversion over time.

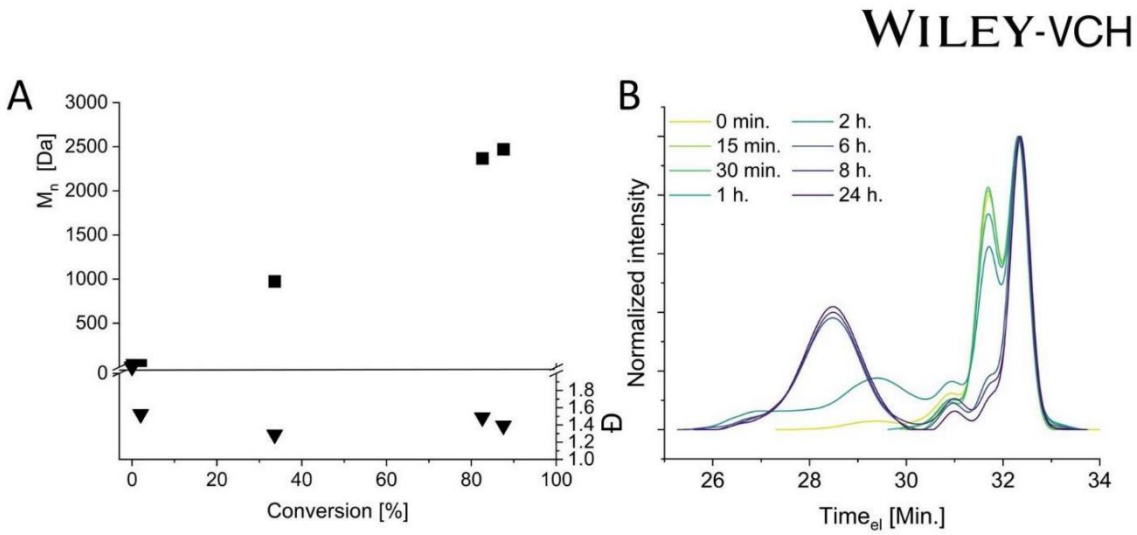


Figure S9. A: development of apparent molecular weight and polydispersity index (PDI) of P(Me_3Lys-OMe-AAm) on conversion B: Aqueous SEC traces of kinetic studies of Me_3Lys-OMe-AAm in 80:20 V% [H_2O/ACN] + 0.1M NaCl + 0.3v% TFA (standard: P2VP).

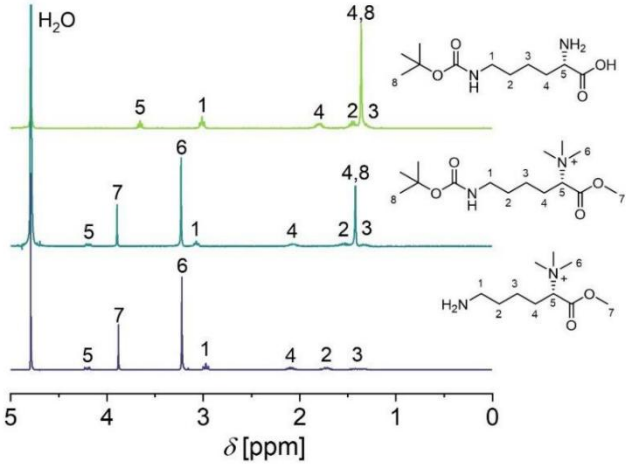


Figure S10. ^{1}H-NMR (300 MHz, D_2O) of H-Lys-OH-Boc (top, green), Me_3Lys-OMe-Boc (middle, cyan) and Me_3Lys-OMe-NH_2 (bottom, purple).

WILEY-VCH

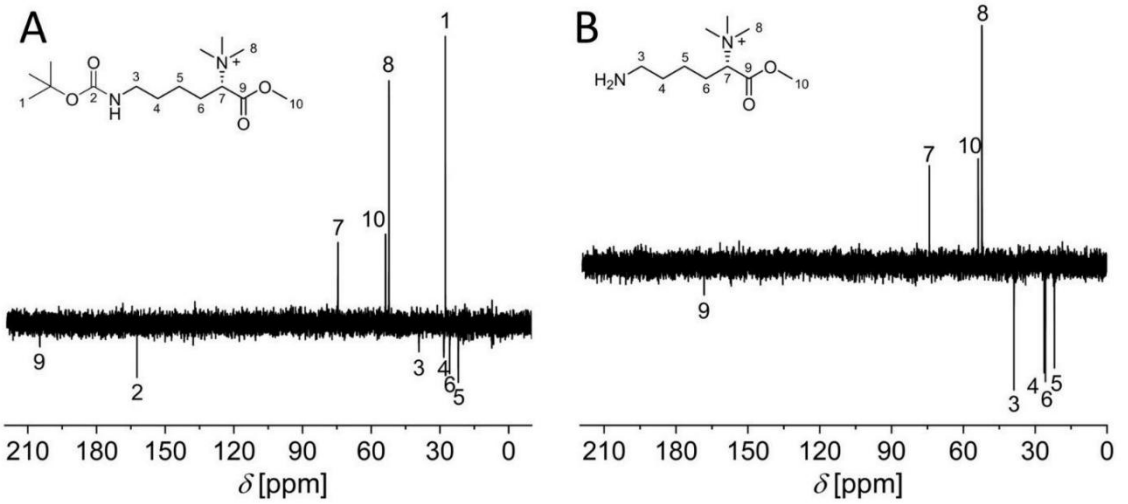


Figure S11. ^{13}C-NMR (75 MHz, D_2O) of A: Me_3Lys-OMe-Boc and B: Me_3Lys-OMe-NH_2.

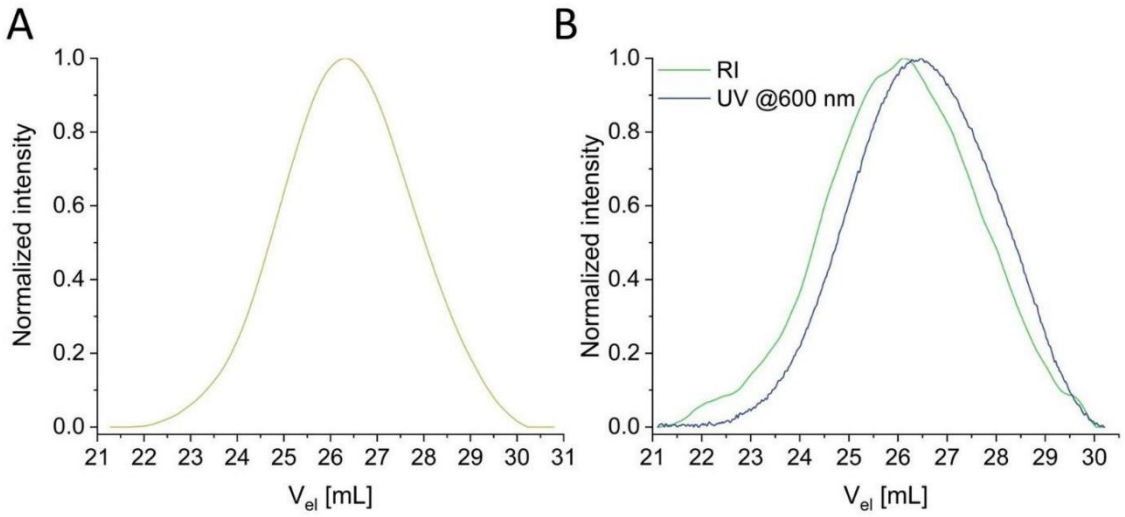


Figure S12. Aqueous SEC elugram of A: P(Me_3Lys-OMe-AAm) and B: P(Me_3Lys-OMe-AAm)-Cy5 in 80:20 V% [H_2O/ACN] + 0.1M NaCl + 0.3v% TFA (standard: P2VP).

WILEY-VCH

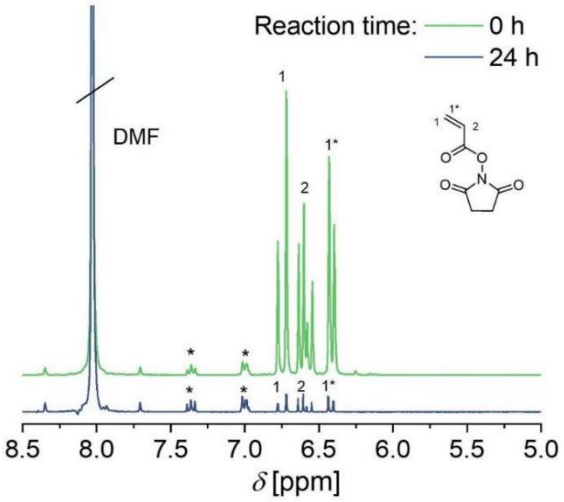


Figure S13. ^{1}H-NMR (300 MHz, DMSO-d6) of reaction mixtures during RAFT synthesis of PNAS at t = 0 h (top, green) and t = 24 h (bottom, blue) using anisole as internal standard to follow conversion (indicated by *). PNAS was used in PPM to obtain P(Me_3Lys-OMe-AAm).

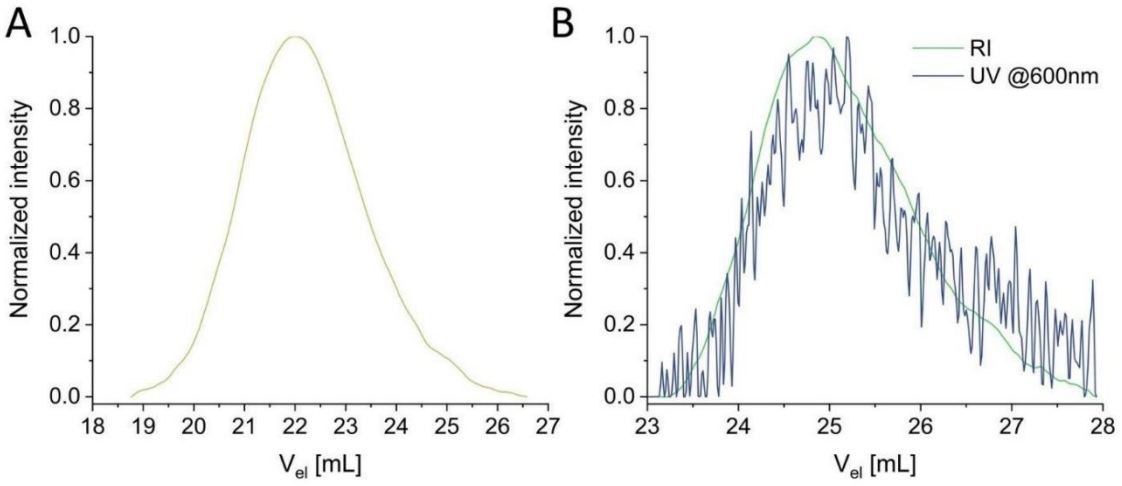


Figure S14. Aqueous SEC elugram of A: P(BocLys-OH-AAm) and B: P(BocLys-OH-AAm)-Cy5 in 65:35 [H_2O/ACN] mixture + 50 mM LiBr + 0.1 M $NaHCO_3$ (Standard: PEG).

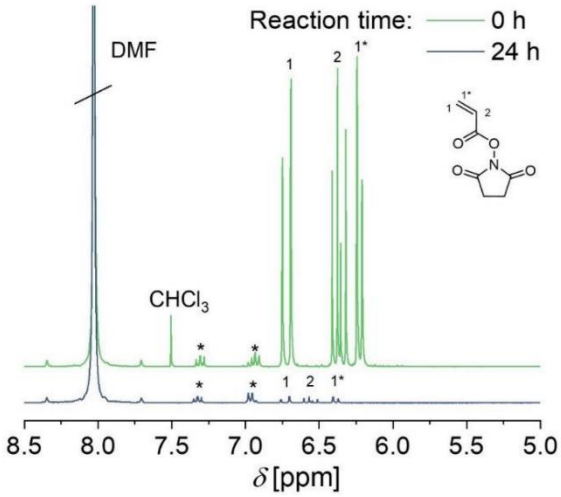


Figure S15. ^{1}H-NMR (300 MHz) of reaction mixtures during RAFT synthesis of PNAS at t = 0 h (top, green, $CDCl_3$) and t = 24 h (bottom, blue, DMSO-d6) using anisole as internal standard to follow conversion (indicated by *). PNAS was used in PPM to obtain P(Boc-Lys-OH-AAm).

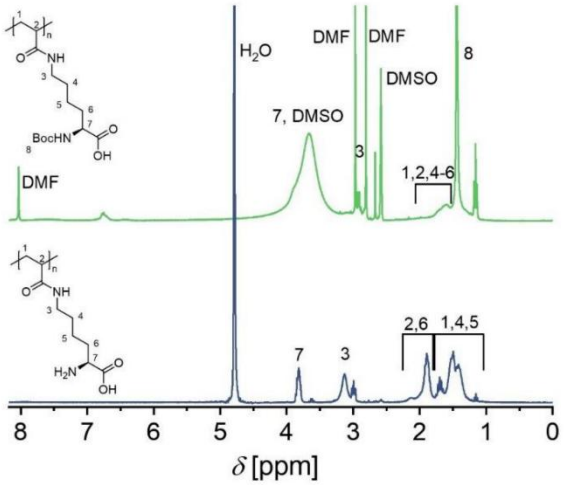


Figure S16. ^{1}H-NMR (300 MHz, D_2O) of P(Boc-Lys-OH-AAm) (top, green) and P(Lys-OH-AAm) (bottom, blue).

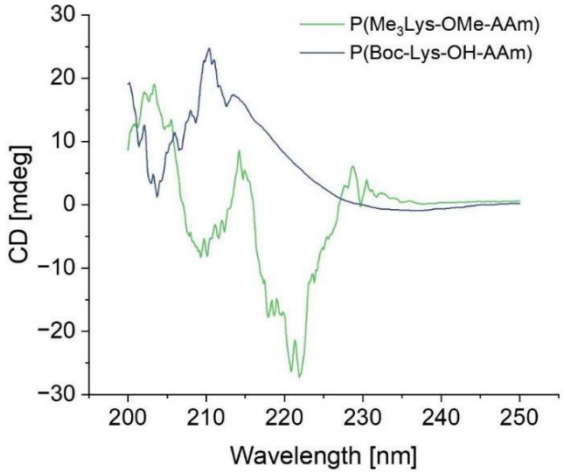


Figure S17. CD spectrum of P(Boc-Lys-OH-AAm) (blue) and P(Me_3Lys-OMe-AAm) (green), obtained by RAFT of monomer resembling structure, in water at pH 6.

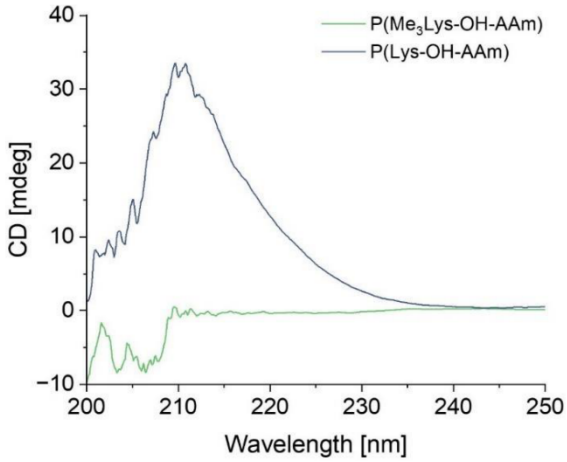


Figure S18. CD spectrum of P(Lys-OH-AAm) (blue) and P(Me_3Lys-OH-AAm) (green), obtained by PPM approach, in water at pH 7.

WILEY-VCH

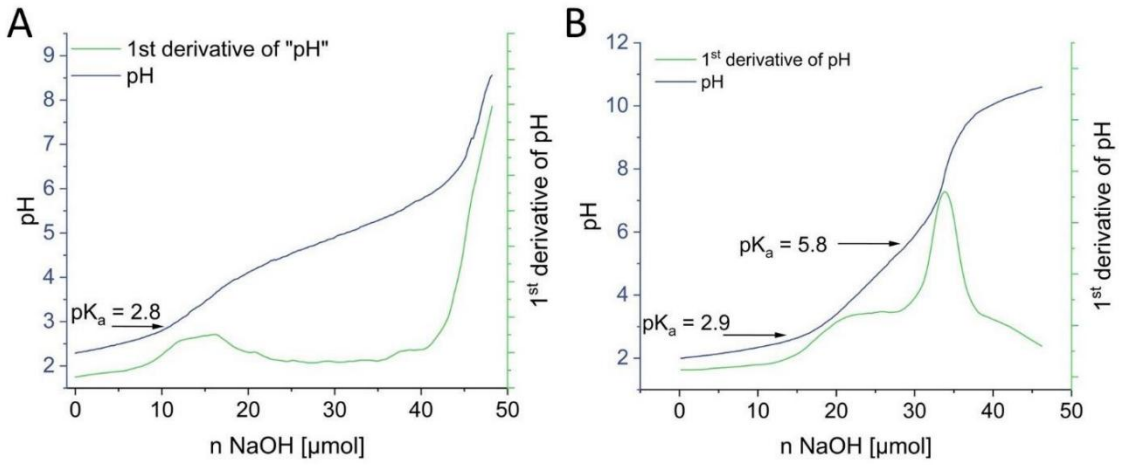


Figure S19. Titration curve and the first derivative of (A) P(Me3Lys-OH-AAm) and (B) P(Lys-OH-AAm) (5 mg mL^{-1} in H_2O) with NaOH (0.1 M in H_2O).

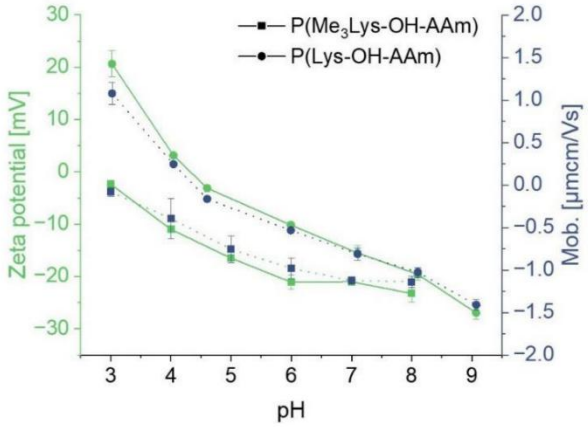


Figure S20. The ζ-potential (green) and electrophoretic mobility (blue) of 2 mg mL^{-1} aqueous solutions of P(Me_3Lys-OH-AAm) (squares) and P(Lys-OH-AAm) (circles) at indicated pH values.

WILEY-VCH

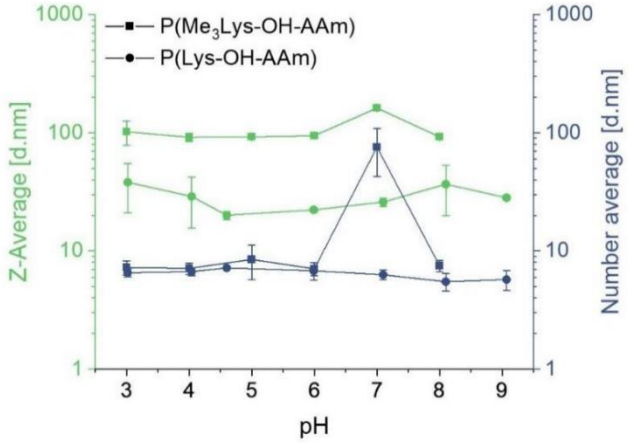


Figure S21. Intensity weighted (green) and number mean (blue) sizes of 2 mg mL^{-1} aqueous solutions of P(Me_3Lys-OH-AAm) and P(Lys-OH-AAm) at indicated pH values.

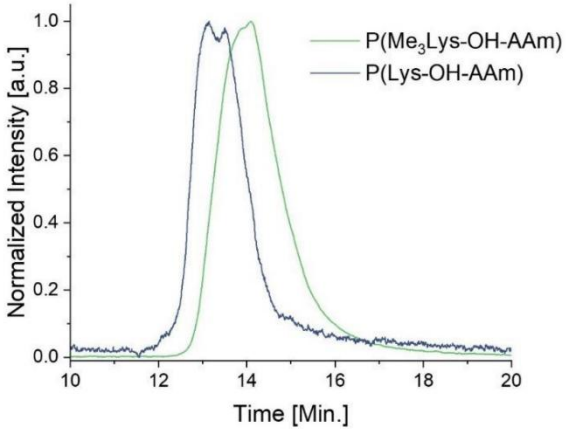


Figure 22. HPLC chromatograms (acetonitrile/water gradient, 0.1v% TFA). Spectra shows the normalized fluorescence intensity of eluting Cy5-labeled polymers (λ_{ex} = 640 nm; λ_{em} = 680 nm).

WILEY-VCH

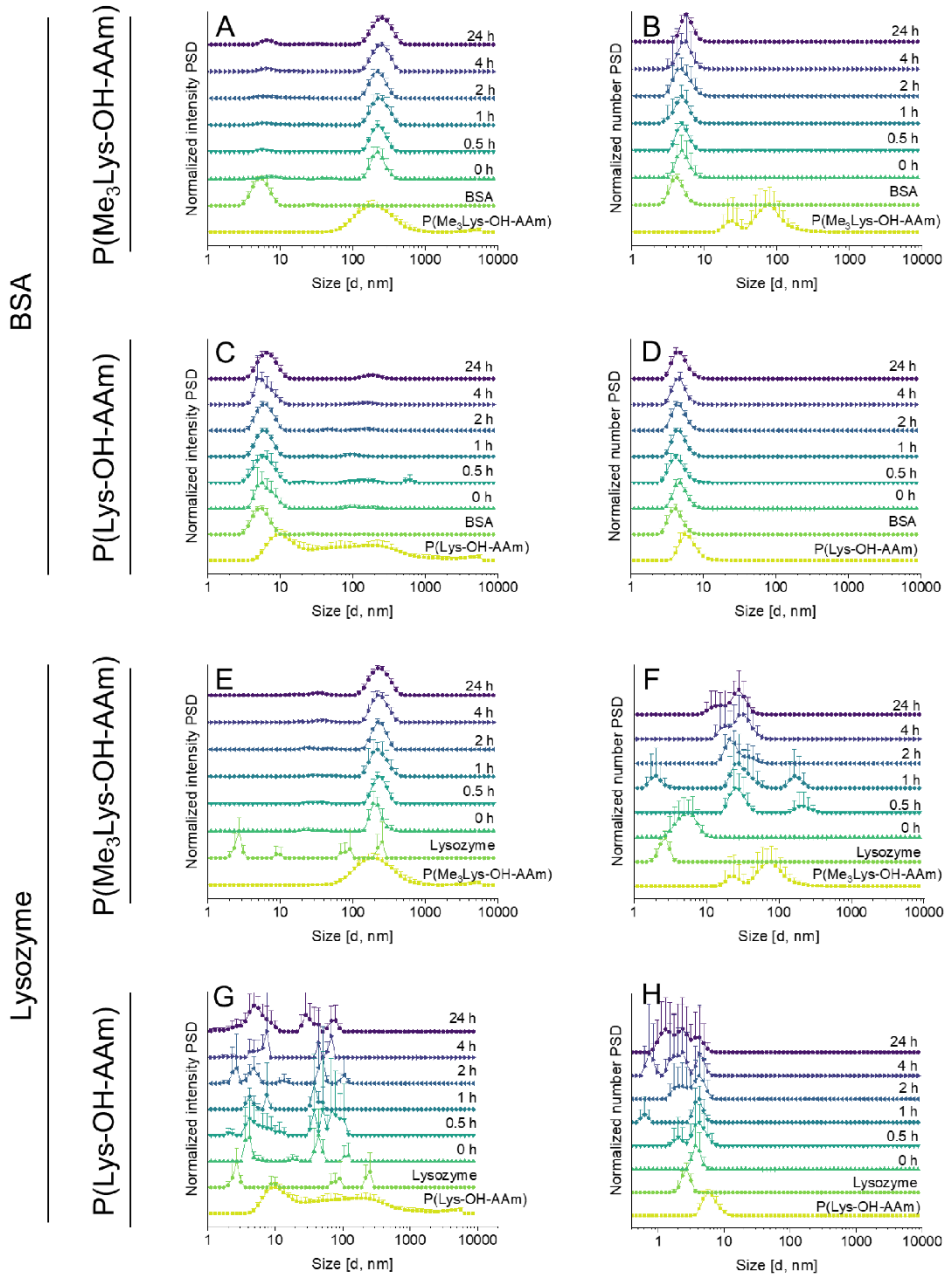


Figure S23. Intensity and number size distributions of polymer-protein-mixtures. The concentration of polymers and proteins was 0.5 mg mL^{-1} each in DPBS. Sizes were analyzed by DLS measurements at 37 °C. Values (scatter) represent the mean and SD of five measurements with three runs each. Dashed lines do not represent measured values. A and B: P(Me_3Lys-OH-AAm) and BSA. C and D: P(Lys-OH-AAm) and BSA. E and F: P(Me_3Lys -OH-AAm) and lysozyme. G and H: P(Lys-OH-AAm) and lysozyme.

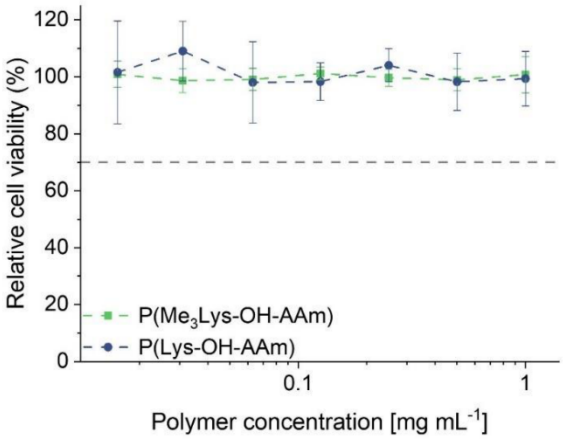


Figure S24. Cell viability of MDA-MB-231 breast cancer cells after incubation with P(Me_3Lys-OH-AAm) and P(Lys-OH-AAm), which were obtained *via* PPM, for 24 h. Cell viability was determined by MTT assay. Cells without polymer treatment served as negative control (NC, 100% cell viability). Values shown are relative to the NC. Cells treated with 20% DMSO served as positive control (PC, 0% cell viability, data not shown).

4.3 Amino-Acid-Derived Anionic Polyacrylamides with Tailored Hydrophobicity–Physicochemical Properties and Cellular

ACS POLYMERS Au
AN OPEN ACCESS JOURNAL OF THE AMERICAN CHEMICAL SOCIETY

Open Access
This article is licensed under CC-BY-NC-ND 4.0

pubs.acs.org/polymerau
Article

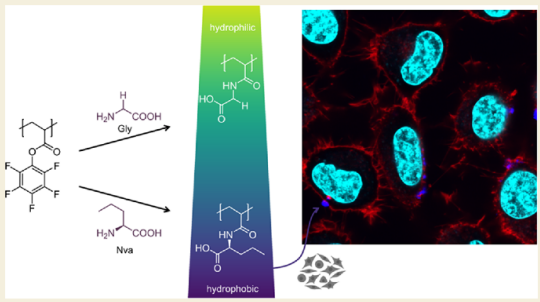
Amino-Acid-Derived Anionic Polyacrylamides with Tailored Hydrophobicity−Physicochemical Properties and Cellular Interactions

Jonas De Breuck, Michael Streiber,[⊥] Michael Ringleb,[⊥] Dennis Schröder, Natascha Herzog, Ulrich S. Schubert, Stefan Zechel, Anja Traeger, and Meike N. Leiske*

Cite This: ACS Polym. Au 2024, 4, 222−234
Read Online

ACCESS | Metrics & More | Article Recommendations | Supporting Information

ABSTRACT: Polyanions can internalize into cells via endocytosis without any cell disruption and are therefore interesting materials for biomedical applications. In this study, amino-acid-derived polyanions with different alkyl side-chains are synthesized via postpolymerization modification of poly(pentafluorophenyl acrylate), which is synthesized via reversible addition−fragmentation chain-transfer (RAFT) polymerization, to obtain polyanions with tailored hydrophobicity and alkyl branching. The success of the reaction is verified by size-exclusion chromatography, NMR spectroscopy, and infrared spectroscopy. The hydrophobicity, surface charge, and pH dependence are investigated in detail by titrations, high-performance liquid chromatography, and partition coefficient measurements. Remarkably, the determined pK_a-values for all synthesized polyanions are very similar to those of poly(acrylic acid) (pK_a = 4.5), despite detectable differences in hydrophobicity. Interactions between amino-acid-derived polyanions with L929 fibroblasts reveal very slow cell association as well as accumulation of polymers in the cell membrane. Notably, the more hydrophobic amino-acid-derived polyanions show higher cell association. Our results emphasize the importance of macromolecular engineering toward ideal charge and hydrophobicity for polymer association with cell membranes and internalization. This study further highlights the potential of amino-acid-derived polymers and the diversity they provide for tailoring properties toward drug delivery applications.



KEYWORDS: *polycarboxylate, amino-acid-derived polymer, polyanion, polyelectrolyte, biomimicking polymer, postpolymerization modification, cell association*

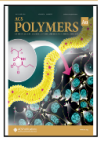
Downloaded via UNIV BAYREUTH on December 5, 2025 at 14:18:33 (UTC).
See https://pubs.acs.org/sharingguidelines for options on how to legitimately share published articles.

1. INTRODUCTION

During the last decades, the application of (polymeric) nanocarriers became an essential asset for drug delivery, therapeutic, and diagnostic systems.[1] To increase the therapeutic efficiency, it is important not only to repress undesired interactions with cells and tissue but also to induce a targetability to specific cells.[2] Recently, significant effort was made to incorporate tissue-targeting motifs into polymeric nanocarriers to increase their specificity.[3−6] Their performance was shown to highly depend on several physiochemical properties of the nanocarriers, such as its shape, size, charge, and hydrophobicity.[7]

The intracellular delivery of therapeutic biomacromolecules such as nucleic acids or peptides is of critical importance for their therapeutic efficiency. Owing to their size, charge, and inherent instability, biomacromolecules often need to be encapsulated for more stability and enhanced cellular uptake via endocytic pathways for intracellular delivery of drugs as they are impermeable to the cell membrane. After membrane engulfment, referred to as endocytosis, a rapid release of the therapeutics (i.e., endosomal escape) is required to minimize degradation and maximize therapeutic efficiency.[8] Over the years, various pH-responsive materials have been investigated regarding their endosomal escape property. pH-responsive polymers are protonated during endosomal maturation, as the pH value of the extracellular physiological environment (bloodstream: pH = 7.4) differs from the endosomal pH value (5.0−6.8). Biocompatible, biodegradable, and amphiphilic polypeptides have shown a pH-dependent membrane-permeabilizing capability due to their pH-responsive amines or carboxylic acid groups.[9] Besides, synthetic alternatives, which

Received: November 29, 2023
Revised: February 7, 2024
Accepted: February 8, 2024
Published: March 12, 2024



ACS Publications
© 2024 The Authors. Published by American Chemical Society

https://doi.org/10.1021/acspolymersau.3c00048
ACS Polym. Au 2024, 4, 222−234

Interactions

are often more cost-effective compared with peptides, have attracted attention in the past.[10−12] pH-responsive polymers are polyelectrolytes and can carry anionic (polyanions) or cationic (polycation) dissociable groups. Polycations (i.e., poly(ethylene imine)s) are known for their buffer capacity and protonation inside endosomal compartments, which is linked to its potential to cross these after acidification resulting in osmotic swelling, also discussed as the proton sponge effect.[13] Furthermore, strong interactions with the endolysosomal membrane have been described to facilitate the release of therapeutics by pore formation.[14] Here, a slightly acidic pK_a-value of the polymeric amine is desirable in order to promote endosomal membrane interaction under acidic conditions, but at the same time to minimize interactions with the cytoplasmic membrane to improve the compatibility of the polycations.[10] This high membrane interaction further renders them suitable for applications as antimicrobial polymers.[15,16]

In contrast, polyanions are often formed of polycarboxylates, that are negatively charged at the physiological pH value of blood (pH = 7.4) and, consequently, do not penetrate negatively charged cell membranes due to repulsive interactions.[8] However, their pH-induced protonation and loss/reduction of anionic character can cause endosomal membrane disruption. To this end, the pH response of polyanions (i.e., the pK_a-value) often takes place at physiologically relevant pH values (i.e., pH = 4−6),[8] making them an attractive alternative to polycations, which often feature a higher pK_a-value outside the physiological range (i.e., pH = 7−9).[17] Below the pK_a, the increased membrane interaction of polyanions is attributed to less ionic repulsion between polymers and the cell membrane, which is also facilitated by their increased hydrophobicity in the nonionic state. Consequently, the pH-dependent endosomolytic activity of polyanions is generally considered less harmful, as they are unlikely to be internalized into cells via translocation of the synthetic bilayer, which often causes cell disruption.[18] When lipid membranes are faced with polyelectrolytes, which also contain hydrophobic groups, these are often incorporated into the bilayer instead of self-association.[12] Here, the additional hydrophobic forces were shown to be critical to enable the binding of anionic polymer to neutral and even negatively charged lipid bilayers.[19] Conversely, it was previously shown that excessive polymer hydrophobicity can lead to cell toxicity at a neutral pH value.[20] This is probably caused by the globule configuration adopted by the polymer in the solution. While polyanions seem to be promising materials for intracellular drug delivery, little is known about the potential to manipulate these polymers and they need to be evaluated more carefully.

It was already shown that polyelectrolytes with different polymer backbones (e.g., acrylate, methacrylate, acrylamide, methacrylamide) incorporating large hydrophobic moieties as well as using branched structures increased the interaction with lipid membranes.[21−23] However, to optimize the performance of polyanions and particularly polycarboxylates, their physicochemical properties should be molecularly engineered by the development of tailored, functional polymers with an optimal hydrophilic−lipophilic balance (HLB). Investigations regarding protonation and hydrophobicity of polyanions with tailored structures are needed for the identification of structure−property relationships.

Functional polymers are often prepared from the respective monomers.[24−26] However, if the synthesis of a target polymer to a certain molar mass with narrow dispersity is hampered and/or its corresponding monomer is difficult if not impossible to synthesize, postpolymerization modification (PPM) of reactive prepolymers is the method of choice.[27,28] Some examples are radical thiol−ene,[29] nucleophilic thiol−ene modification,[30] and aminolysis modification with functional polymers.[31,32]

In this context, polymers with activated ester side chains, such as *N*-acryloxysuccinimide (NAS) and pentafluorophenyl acrylate (PFPA), are widely used. Reports have shown that activated ester polymers such as poly(*N*-acryloxysuccinimide) (PNAS) and poly(pentafluorophenyl) acrylate (PPFPA) react fast and quantitively with primary or secondary amines resulting in the corresponding poly(acrylamide) (P(AAm)) derivatives.[33,34] While among activated ester monomers, NAS is the oldest and the most regularly employed one,[35,36] polymers derived from PFPA commonly feature a higher hydrolytic stability and enhanced solubility in a wider range of organic solvents.[34] Previously, PNAS and PPFPA were already employed to synthesize various polymer architectures, such as activated polymer brushes[32,37] and nano(hydro)gels.[38] The modification of activated ester polymers with cross-linking bisamines,[39] amino-modified chromophores,[40,41] amino-sugars,[31] and alkylated amines[42] has been shown. They have further been modified with small peptides.[43−46] However, the modification with amino acids is less explored.

Instead, vinylic polymers with amino acids in the side chains were often retrieved by radical polymerization.[47] Side-chain amino-acid-functionalized poly(meth)acrylates (P(M)A) or poly(meth)acrylamides (P(M)AAm) were obtained from esterified amino acids. The esterification was performed by the Steglich esterification reaction of 2-hydroxyethyl (meth)acrylates or (meth)acrylamides, respectively, with the carboxylic acid moiety of the α-amine-protected amino acid, yielding cationic or zwitterionic polymers.[17,21,48−50] Alternatively, side-chain amino-acid-functionalized P(M)A or P(M)AAm was previously synthesized from the amino-acid-derived vinyl monomers. In general, the monomers were synthesized by the reaction of the carboxylic acid or the amine group of the (protected) amino acid with an activated vinyl compound (e.g., (meth)acryloyl chloride).[3,51,52]

The aim of this study was to synthesize various amino-acid-derived anionic polyacrylamides (P(AA−OH-AAm)) with carboxylic acids in the side chain and tailored hydrophilicity. These polyanions were obtained by the modification of the same PPFPA precursor to obtain fast and quantitative formation of P(AA−OH-AAm). Modification with different amino acids was performed to investigate the correlation between the alkyl side-chain (length and branching) and the physicochemical properties of the polymer. Additionally, we expected the synthesized polyanions to show low-fouling properties due to their peptide-like moieties, enabling applications in the field of protein interactions and delivery materials. Therefore, an investigation was conducted to assess whether different physicochemical properties of the synthesized P(AA−OH-AAm) influence their interactions with proteins and cells to get an initial understanding of their potential applications in a biological environment.

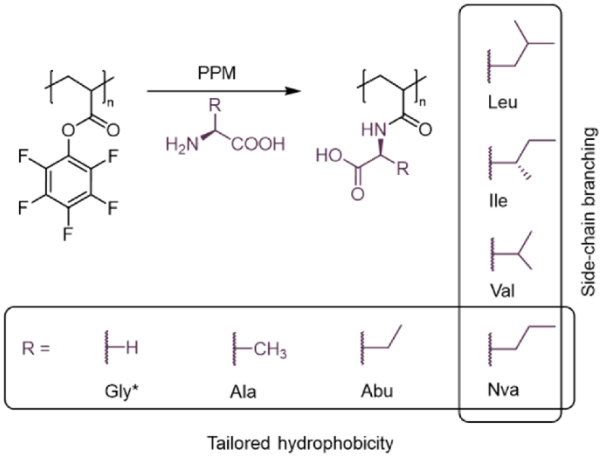
https://doi.org/10.1021/acspolymersau.3c00048
ACS Polym. Au 2024, 4, 222−234

2. RESULTS AND DISCUSSION

2.1. Synthesis and Characterization of Amino-Acid-Derived Polyanions

Neutral α-amino acids with different alkyl substituents in α-position served as starting material for the development of P(AA−OH-AAm) with tailored hydrophilicity. The screened P(AA−OH-AAm) were derived from glycine (Gly), alanine (Ala), aminobutyric acid (Abu), norvaline (Nva), valine (Val), *iso*-leucine (Ile), and leucine (Leu), which were all used in their L-stereospecific form. This library allowed for a comparison of the effect of increasing hydrophobicity (Gly < Ala < Abu < Nva) as well as the effect of side-chain branching (Scheme 1). To ensure high comparability of these polymers and eliminate effects caused by polymer length and dispersity, it was chosen to prepare them via a PPM approach.

Scheme 1. Schematic Representation of the Synthesis of Carboxylated Polyacrylamides with Tailored Hydrophobicity via PPM of PPFPA with Indicated Amino Acids, Yielding Anionic Polymers with Varying Alkyl Substituents[a]



[a]Please note that Gly does not feature a stereo center.

P(AA−OH-AAm) were synthesized by the active ester approach employing the polymerization of PFPA according to Zerdan et al.[53] Reversible addition−fragmentation chain-transfer (RAFT) polymerization proceeded in a controlled manner using a monomer to chain-transfer agent (CTA) ratio of 257 yielding PPFPA ($M_{n,app(PPFPA)}$ = 33,900 g mol^{-1}) with a narrow dispersity ($Đ$ = 1.32) according to size-exclusion chromatography (SEC) measurements (Table 1 and Figure S1). The proton nuclear magnetic resonance (^{1}H NMR) spectrum of PPFPA showed characteristic signals from the backbone protons around δ = 2.0 and 3.0 ppm (Figure 1B).

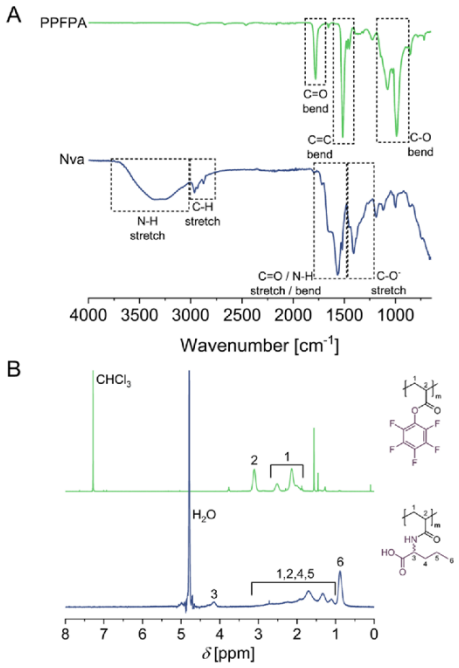


Figure 1. (A) FTIR spectra and (B) ^{1}H NMR spectra (300 MHz) of poly(pentafluorophenyl acrylate) (green, $CDCl_3$) and P(Nva-OH-AAm) (blue, d-DPBS).

Complementary ^{19}F NMR analysis (Figure S2A) showed the expected three signals at δ = −153, − 157, and −163 ppm, which were attributed to the PFP group. The absence of hydrolytic poly(acrylic acid) (PAA) byproducts was confirmed by ^{13}C NMR spectroscopy (Figure S2B). Here, only one type of carbonyl signal was present at δ = 170 ppm, suggesting the absence of hydrolyzed PAA groups in the polymer, which would generally reveal a second carbonyl signal around δ = 180 ppm. In addition, FTIR spectroscopy (Figure S5B) did not show the characteristic PAA band at $\tilde{\nu}$ = 1738 cm^{-1}.[54]

Table 1. Properties of PPFPA and Different Amino-Acid-Functionalized Polymers

polymer name	M[a] [g mol^{-1}]	rel. 6-AF by emission[b]	$M_{n,app}$[c] [g mol^{-1}]	$Đ$[c]	pK_a[d]	ZP[e] [mV]
PPFPA	238.11	n.a.	33,900[f]	1.32[f]	n.a.	n.a.
P(Gly-OH-AAm)	129.12	1.00	11,800	1.73	5.0	−26.6 ± 1.9
P(Ala-OH-AAm)	143.14	1.94	16,300	1.79	5.5	−41.9 ± 1.0
P(Abu−OH-AAm)	157.17	1.06	22,200	1.54	5.1	−37.8 ± 2.3
P(Nva-OH-AAm)	171.2	2.39	13,800	2.77	5.0	−31.1 ± 3.3
P(Val-OH-AAm)	171.2	1.94	22,800	1.43	4.8	−38.4 ± 2.2
P(Ile-OH-AAm)	185.22	1.28	24,900	1.75	5.0	−31.6 ± 1.9
P(Leu-OH-AAm)	185.22	1.23	19,600	1.48	5.1	−37.1 ± 2.2

[a]Molar mass of repeating unit (RU). [b]Fluorescence measurements (λ_{ex} = 450 nm, λ_{em} = 517 nm) in DPBS (1.0 mg mL^{-1}). Values correspond to 6AF-labeled polymers. [c]SEC in 0.07 M aq. Na_2HPO_4 (standard: PMA Na salt). [d]Titration of a 5 mg mL^{-1} polymer solution with 0.1 M HCl. pK_a-value refers to carboxylic acid function. [e]ELS measurements in DPBS (2.0 mg mL^{-1}). [f]SEC in DMAc + 0.21 w% LiCl (standard: PMMA). n.a. not applicable.

https://doi.org/10.1021/acspolymersau.3c00048
ACS Polym. Au 2024, 4, 222−234

PPM of PPFPA was performed by aminolysis with different amino acids comprising varying alkyl substituents in R-position (Scheme 1). A particular challenge was the poor solubility of amino acids in organic solvents.[55,56] Eventually, dimethylformamide (DMF) was chosen as it is regularly employed for PPM of PPFPA,[34] and was found to suspend all amino acids used in this study well. It was further assumed that DMF slightly dissolves amino acids at elevated temperatures.[57] The reaction was performed at 40 °C for 72 h to allow adequate solvation and consumption of the suspended amino acids, leading to a continuous reaction. Hence, PPM of homopolymers with Gly, Ala, Abu, Nva, Val, Ile, and Leu proceeded with the quantitative conversion of the activated ester functional groups yielding the corresponding polyacrylamides P(Gly-OH-AAm), P(Ala-OH-AAm), P(Abu−OH-AAm), P(Nva-OH-AAm), P(Val-OH-AAm), P(Ile-OH-AAm), and P(Leu-OH-AAm), respectively. The success of each synthetic step was verified *via* ^{1}H-, ^{19}F-NMR, and FTIR spectroscopy.

^{1}H NMR spectra of all amino-acid-modified polymers (Figure S3), and exemplarily P(Nva-OH-AAm) in Figure 1B, showed the appearance of a new signal at δ = 4.0 ppm attributed to the C−H adjacent to the newly formed amide bond. Moreover, predominant peaks of CH_3-groups appeared in the spectra ($\delta \approx$ 0.0−2.0 ppm) of amino-acid-derived polymers with long linear alkyl substituents (i.e., Nva) or branched alkyl substituents (i.e., Val, Ile, and Leu). The absence of any peak in ^{19}F NMR spectra (Figure S4) of the AA-side-chain polymer indicated a full conversion of active esters in all PPM reactions.

Additionally, as an example, the FTIR spectra of PPFPA and (P(Nva-OH-AAm) are shown in Figure 1A while the other FTIR spectra are depicted in Figure S5A. Here, the conversion of functional groups is also shown by a shift in absorption band from a carbonyl adjacent to PFPP at $\tilde{\nu}$ = 1780 cm^{-1} to a carbonyl group in an amide bond at $\tilde{\nu}$ = 1550 cm^{-1}.[58] The presence of the carboxylic acid functional group in the polyanions can also be distinguished by its C═O symmetric stretch at $\tilde{\nu}$ = 1410 cm^{-1}. The absence of PAA groups, which may occur as a hydrolytic byproduct, was further suggested by the absence of the characteristic band at $\tilde{\nu}$ = 1738 cm^{-1} (Figure S5B).[54]

SEC measurements (Figure 2 and Table 1) in 0.07 M aqueous Na_2HPO_4 as eluent were performed to verify the integrity of the polymers during the PPM process.

The results revealed an increased $Đ$ (Table 1), potentially related to the more polar eluent and high density of charged groups in the polymers which can cause hydrogen bonding and ionic interactions with the stationary phase leading to broader peaks and longer retention times.[59] Furthermore, the slight high-molar mass shoulder was visible in some polymers, indicating minor chain coupling, which may occur during aminolysis. It was observed that P(AA−OH-AAm) with increasing alkyl chain show shorter elution times (Figure 2A) as can be expected due to the higher molar mass and hydrodynamic volume. Interestingly, branching and the position of branching points also influenced the elution time due to altered sterical hindrance. Figure 2B shows that Val-functionalized polymers (branched alkyl substituent) feature a later elution time, meaning smaller size, compared with Nva-functionalized polymers (linear alkyl substituent). We attribute this apparent smaller size of P(Val-OH-AAm) to their decreased sterical hindrance and more compact alignment of polymers with short-chain branching. A similar trend was observed for polymers modified with P(Ile-OH-AAm) (long-chain branching) and P(Leu-OH-AAm) (terminal short-chain branching) as shown in Figure 2C.

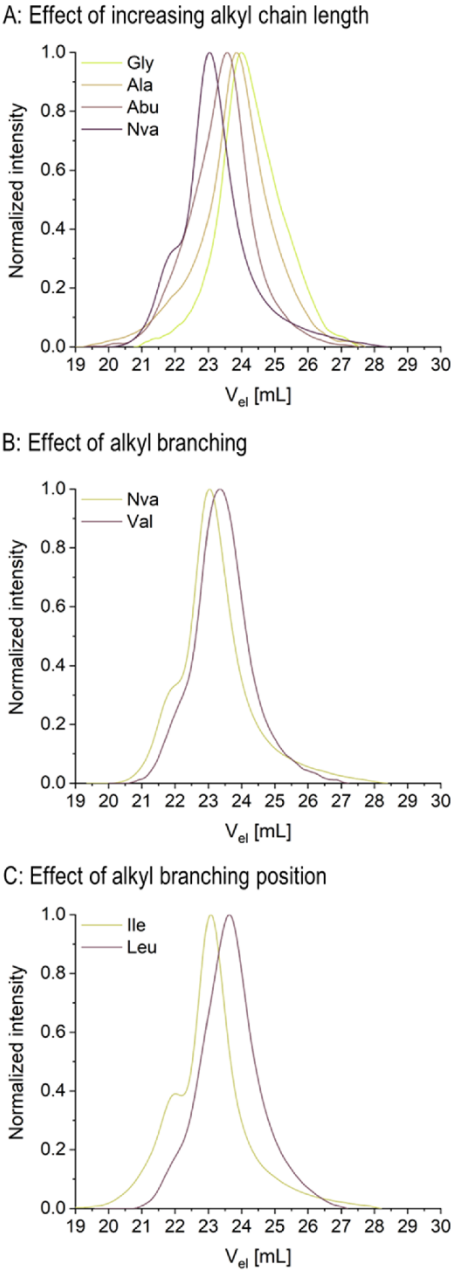


Figure 2. Size-exclusion chromatograms (0.07 M aq. Na_2HPO_4) of P(AA−OH-Aam). (A) Effect of increasing alkyl chain length. (B) Effect of alkyl branching. (C) Effect of alkyl branching position.

To allow for more in-depth materials characterization as well as biological evaluation, fluorescently labeled P(AA−OH-AAm) were further prepared. Here, a controlled number of fluorescent dye molecules, namely, 6-aminofluorescein (6-AF), was incorporated into the PPFPA prepolymer side chain prior to PPM with amino acids. This method allowed to achieve a similar labeling efficiency of the polymers as was determined by fluorescence spectroscopy measurements (Table 1). The resulting fluorescently labeled P(AA−OH-AAm) will further

https://doi.org/10.1021/acspolymersau.3c00048
ACS Polym. Au 2024, 4, 222−234

be referred to as P(AA−OH-AAm)-6AF. The successful dye labeling was verified by the overlay of SEC traces obtained by the RI and the UV detector (λ = 490 nm; Figure S9). The absence of other signals of the UV trace indicated the absence of unbound dye.

2.2. pH-Responsiveness and Hydrophobicity

Next, the physiochemical properties and *in vitro* properties of the homopolymers were characterized to investigate the influence of the length and branching of alkyl groups in the side chain of polycarboxylates. Acid−base titration was utilized to gain information about the pK_a-values of P(AA−OH-AAm) polymers (Figures S6 and S7). It was found that all P(AA−OH-AAm) possessed pK_a-values between pH = 4.8 and 5.5 attributed to the carboxylic acid in the side chain while some also showed less pronounced pK_a-value around pH ≈ 8, which might be caused by intramolecular interactions with the amide function. The pK_a-values of the carboxylic acids are similar to the pK_a-value of poly(acrylic acid) (pK_a = 4.5).[60] An effect of the alkyl substituent was not observed. ζ Potential measurements of P(AA−OH-AAm) in DPBS (pH = 7.4) verified the presence of a negative surface charge at the physiological pH of the bloodstream (Figure S8A and Table S2). Dynamic light scattering (DLS) measurements in DPBS were performed to exclude aggregation, which could lead to an altered uptake profile. At a polymer concentration of 2 mg mL^{-1}, all P(AA−OH-AAm) revealed a number size distribution of around 10 nm diameter (Figure S8B and Table S1), indicating the absence of larger polymer aggregates in buffered systems.

To assess the extent of influence of the alkyl substituent on the hydrophilicity of P(AA−OH-AAm), high-performance liquid chromatography (HPLC) measurements of all P(AA−OH-AAm)-6AF were performed on a reversed-phase column with an acetonitrile/water gradient. The aqueous phase was acidified with 0.1v% trifluoroacetic acid (TFA) to ensure protonation of the carboxylic acid groups. The polymers showed different retention times related to the hydrophobicity of the alkyl substituent in the side chain (Figure 3A). It was observed that with increasing linear alkyl substituent (Gly < Ala < Abu < Nva), the retention time increased due to the stronger interaction with the column confirming increased hydrophobicity. However, it was also observed that side-chain alkyl branching (i.e., Nva and Val, Ile and Leu) did not affect the hydrophobicity of P(AA−OH-Aam).

These results were further supported by partition coefficient (PC) measurements of P(AA−OH-AAm)-6AF at pH = 7 (Figure 3B), where the decrease of fluorescence of an aqueous polymer solution upon treatment with a hydrophobic $CHCl_3$ phase was quantified by fluorescence spectroscopy measurements. Here, the fluorescence reduction followed the same increasing trend with increasing alkyl chain while revealing similar values for structural isomers. Additionally, the PC of P(AA−OH-AAm) was determined at pH = 4 to gain information about the increase in hydrophobicity at lower pH values. The results in Figure 3B confirmed the expected increased hydrophobicity of carboxylated polymers at pH = 4 compared with pH = 7. In addition, the increase was found to be more drastic for polymers that contained more hydrophobic amino acids in the side chain.

2.3. Protein Fouling of Amino-Acid-Derived Polyanions

To gain important information about the protein fouling of P(AA−OH-AAm), we studied the interaction of two representatives, namely, P(Gly-OH-AAm) and P(Nva-OH-AAm), with bovine serum albumin (BSA) and lysozyme. Here, BSA was chosen as a negatively charged model protein, while lysozyme represented a positively charged model protein.[61] Fouling was analyzed by DLS measurements (Figures 4 and S14 and Table S3), which provided information about the

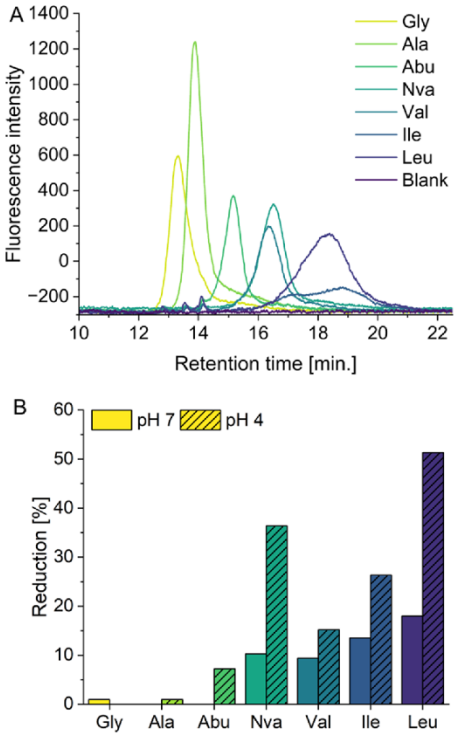


Figure 3. Hydrophilicity of P(AA−OH-AAm). (A) HPLC chromatograms (acetonitrile/water gradient, 0.1v% TFA). Spectra show the absolute fluorescence intensity of eluting 6AF-labeled polymers (λ_{ex} = 480 nm; λ_{em} = 520 nm). (B) pH-dependent relative hydrophilicity of 6AF-labeled polymers. Columns show the reduction of fluorescence of a 0.1 mg mL^{-1} aqueous solution at the indicated pH value after treatment with $CHCl_3$ compared with the fluorescence of the sample prior to treatment with $CHCl_3$. For normalized fluorescence graphs, please refer to Figures S12 and S13.

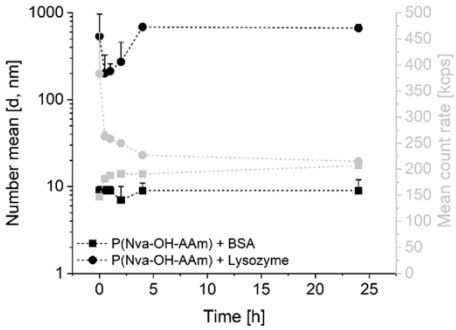


Figure 4. Interaction of P(Nva-OH-AAm) with BSA and Lysozyme. P(Nva-OH-AAm) (c = 0.5 mg mL^{-1}) and indicated proteins (c = 0.5 mg mL^{-1}) were incubated in DPBS at 37 °C for indicated durations. Number mean diameter (black) and mean count rate (gray) were analyzed by DLS measurements at 37 °C. Values (scatter) represent the mean and SD of five measurements with three runs each. Dashed lines do not represent measured values.

https://doi.org/10.1021/acspolymersau.3c00048
ACS Polym. Au 2024, 4, 222−234

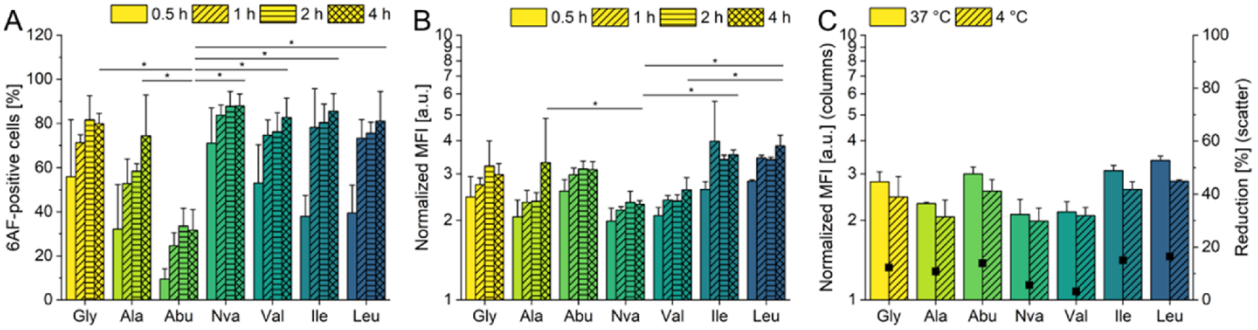


Figure 5. Cellular association of different P(AA−OH-AAm)-6AF determined via flow cytometry measurements. Polymer concentration: 1 mM_{RU}, 50,000 cells seeded in 250 μL in a 48 well plate. Normalized MFI was calculated by eq 3. (A, B) Association of polymers with L929 mouse fibroblasts in DMEM supplemented with 10% FBS. Incubation for indicated time points at 37 °C. (C) Incubation at 37 or 4 °C in DMEM supplemented with 10% FBS for 4 h. Reduction was calculated by eq 4. Statistical analysis (one-way ANOVA with Tukey test) was performed for 4 h incubation time (A, B) to compare the association efficiency of the different P(AA−OH-AAm)-6AF. For temperature-dependent experiments (C), the statistical analysis compared the association at 37 °C versus 4 °C per polymer type. *Indicates a significance of $p < 0.5$. All other comparisons were not statistically significant at $p < 0.5$.

formation of aggregates over time. Owing to the negative charge of P(AA−OH-AAm), a stronger interaction with lysozyme than with BSA was expected. Indeed, mixtures of BSA and P(Nva-OH-AAm) only revealed a minor formation of aggregates, as could be concluded from stable particle diameters and count rates (Figure 4). The aggregation of P(Gly-OH-AAm) with BSA appeared to be slightly increased, which might be caused by increased exposure of the hydrophobic polymer backbone. However, mixtures of P(Nva-OH-AAm) and lysozyme indicated the formation of large nanoparticles ($d \approx 700$ nm) over the course of 4 h, which remained stable up to 24 h. The formation of aggregates was further suggested by a decrease of the mean count rate over time. Lysozyme interacts as well with P(Gly-OH-AAm), leading to, however, smaller aggregates ($d \approx 150$ nm). Thus, the interaction with proteins depends on both, the protein and polymer characteristics, showing stronger interactions with cationic proteins. However, polyanions, in particular sulfated and carboxylated polysaccharides, are known for their good modulation of blood coagulation.[62]

2.4. Interaction of Amino-Acid-Derived Polyanions with Cells

Following the in-depth examination of the obtained polymers, they were tested for their properties in biological systems. As such, the first test should provide information about their cytocompatibility. The cytocompatibility of all P(AA−OH-AAm) was studied by an MTT assay (Figure S15), showing that all polymers were well tolerated by L929 mouse fibroblasts at concentrations up to 0.1 mg mL^{-1} (for 24 h). Additionally, no hemolytic activity at pH 7.4 or 6 and no erythrocyte aggregation were detected at concentrations per repeating unit (c_{RU}) = 1 mM (Figures S16 and S19).

Previously, Duvall and co-workers have screened a library of copolymers with acrylic acid moieties and different hydrophobic alkyl acrylamide units of varying ratios aiming to find an ideal ionic−hydrophobic balance for the modification of cell membranes.[63] Their copolymers further showed some pH-dependent activity. In contrast, the amino-acid-derived anionic polymers of the current study did not reveal any hemolytic activity or erythrocyte aggregation (Figures S16 and S19), emphasizing a favorable balance between anionic character and hydrophobicity. These results further indicated that no membrane disruption and, consequently, no harm to the cells were expected for subsequent cell association experiments.

In previous studies, carboxylated polymers have already shown unique cell association properties. For example, Kempe and co-workers as well as Thayumanavan and colleagues reported the passive diffusion of Cy5-labeled anionic polymers into cells, resulting in mitochondrial colocalization.[7,64] These previous studies also highlighted the importance of the dye for the phenomenon. To avoid passive diffusion, 6AF-labeled polymers were used in the current study. In a preliminary experiment (Figure S20), different concentrations were investigated, in which c_{RU} = 1 mM ($c_{polymer}$ = 4 μM) was determined to be the optimal concentration for subsequent more detailed investigations.

Next, the time-dependent association of polymers with L929 mouse fibroblasts was studied by flow cytometry. It was found that for all seven P(AA−OH-AAm)-6AF, both the mean fluorescence intensity (MFI) and the number of 6AF-positive cells increased over time (Figure 5A,B). Here, polymers with more hydrophobic amino acids (i.e., Nva, Val, Ile, and Leu) showed high cell association with ≥70% 6AF-positive cells after 1 h of incubation. Polymers with more hydrophilic amino acids (i.e., Gly, Ala, and Abu) associated slower to L929 mouse fibroblasts while following an association trend, which is opposite to their hydrophobicity (Gly > Ala > Abu). Based on the results of the protein fouling, one can assume that P(Gly-OH-AAm) revealed some hydrophobic character due to the accessibility of the hydrophobic polymer backbone. Consequently, the polymers follow different association pathways.

Several studies have shown that polymer association or uptake which follows an active pathway, such as endocytosis or macropinocytosis, can be suppressed by lowering the incubation temperature from 37 to 4 °C. Surprisingly, neither the number of 6AF-positive cells nor the MFI dropped significantly when the cells were incubated at a lower temperature (Figure 5C), suggesting the absence of active polymer uptake.

To further investigate the interaction between P(AA−OH-AAm) with cells, L929 fibroblasts were incubated with P(Nva-OH-AAm)-6AF and imaged via confocal laser scanning microscopy (CLSM). We specifically chose this polymer based on its hydrophilic−lipophilic balance (HLB) of 10.05,

https://doi.org/10.1021/acspolymersau.3c00048
ACS Polym. Au 2024, 4, 222−234

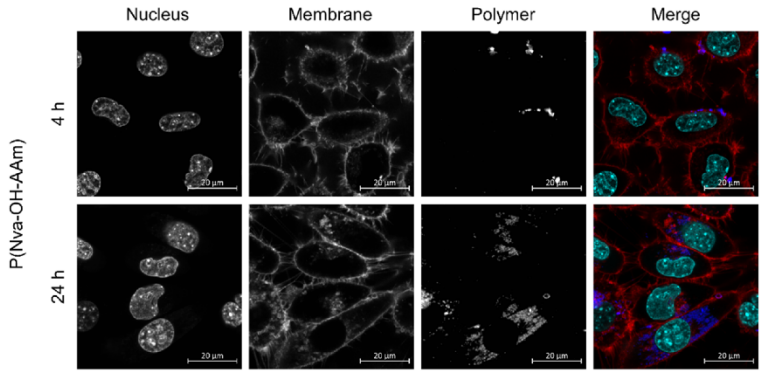


Figure 6. Cellular uptake of P(Nva-OH-AAm)-6AF into L929 mouse fibroblasts visualized by CLSM. Cells were incubated with polymers at 37 °C for indicated times. Cyan: Hoechst 33342/nucleus. Red: CellMask Plasma Membrane Stain/membrane. Blue: 6AF/polymer.

which was calculated after Griffin.[65] In contrast, P(Gly-OH-AAm) possessed an HLB value of 12.83 and could consequently be considered a detergent. A previous study has found that a series of Triton X, commonly applied membrane-permeabilizing agents, possessed altered membrane-disrupting activity depending on their HLB value, which revealed a maximum at an HLB of 12−13 (Triton X-100), while at an HLB of 10, the activity was negligibly low.[66] Other earlier studies have further described the potential to remove phospholipids from cell membranes by anionic detergents such as Triton X-100 or sodium dodecyl sulfate.[67] In particular, the solubilization process relies on the formation of mixed micelles of the detergent and the phospholipids.[68,69] These properties were further suggested after testing the emulsifying properties of P(AA−OH-AAm) with linear alkyl substituents (see the SI for further information).

After 4 h of incubation, a strong colocalization of P(Nva-OH-AAm)-6AF with the cell membrane was observed and no intracellular 6AF signal was detectable (Figure 6). These imaging results provided further clarification on the temperature study as polymer association to cell membranes is mostly a passive process.

To further verify the compatibility and uptake mechanism, L929 mouse fibroblasts were incubated with P(Nva-OH-AAm)-6AF for 24 h. Subsequently, intracellular spot-like fluorescence signals of 6AF were visible, indicating a vesicular localization and, consequently, active albeit very slow polymer internalization. Acute cell death was not observed. Previous studies showed an intracellular mitochondrial colocalization of carboxylated Cy5-labeled polymers after 4 h (passive diffusion).[7] In addition, our previous reports revealed a lysosomal colocalization of glutamic-acid-derived polymers after 4 h (active uptake).[49] However, in the current study, the polymer uptake appeared to be slower compared with these previous reports. In particular, the slow and strong accumulation of anionic polymers at the cell membrane appears to be a rare occurrence in literature. We assume that the combination of anionic and hydrophobic features in our polymers favors this accumulation.

L929 fibroblasts were used as a well-studied eukaryotic model cell line. As such, the cell membrane consists of a phospholipid bilayer, which is characterized by its lipophilic center and anionic outer lipid head groups. Hydrophobic, nonionic polymers are known to interact strongly with these membranes,[70] while anionic polymers generally show very low association.[8] It is assumed that the use of anionic, hydrophobic polymers which may possess both properties leads to the phenomenon of slow membrane integration. In addition, the increasing alkyl chain length inversely correlates with the charge density and, thus, electrostatic repulsion further influencing its accessibility. Therefore, it is important to tune the length of the alkyl chain to find an optimum between hydrophobicity and charge density. Furthermore, we assume that the biomimicking motifs in our amino-acid-derived polymers contributed to the incorporation into the cell membrane. Future studies will focus on a detailed understanding of the cell association of anionic, amino-acid-derived polymers as well as their exploitation for cell-membrane modifications.

3. CONCLUSIONS

P(AA−OH-AAm) with different alkyl substituents were successfully synthesized via PPM of PPFPA which was verified via ^{1}H-, ^{19}F-NMR, and FTIR spectroscopy. Characterization of the physicochemical properties revealed that the alkyl chain did not show any relation between the side chain and the pK_a-value of the carboxylic acid as all were in a similar range of poly(acrylic acid). This emphasizes the complicated nature of the relationship between hydrophobicity and protonation of polyelectrolytes and shows that there are no simple correlations in this complex interplay. ζ-Potential and DLS measurements in DPBS confirmed that the surface charge and no self-assembly occurred. HPLC measurements confirmed the hypothesis that the alkyl chain can tailor the side chain hydrophobicity resulting in increased hydrophobicity for longer alkyl chains. Interestingly, branching in the alkyl chain did not affect the hydrophobicity of P(AA−OH-AAm). The results were supported by PC measurements at pH = 7. Additionally, PC measurement at pH = 4 confirmed the expected increase in hydrophobicity where it was found more drastic for the more hydrophobic P(AA−OH-AAm). All P(AA−OH-AAm) were tolerated by cells up to concentrations of 0.1 mg mL^{-1}. Time-dependent association with L929 fibroblast revealed higher association of more hydrophobic P(AA−OH-AAm), namely, P(Nva-OH-AAm), P(Val-OH-AAm), P(Ile-OH-AAm), and P(Leu-OH-AAm). CLSM measurements revealed that P(Nva-OH-AAm) accumulated at the membrane and was internalized very slowly. Further studies will aim for a more detailed understanding of the cell association of anionic P(AA−OH-AAm) and their molecular engineering to tailor the pH response and membrane interactions further.

https://doi.org/10.1021/acspolymersau.3c00048
ACS Polym. Au 2024, 4, 222−234

4. EXPERIMENTAL PART

4.1. Materials and Instrumentation

4.1.1. Materials. Pentafluorophenyl acrylate (PFPA) was purchased from abcr with 95% purity. 2-(Dodecylthiocarbonothioylthio)-2-methylpropionic acid (DTCTTMPA) (98% purity), Triton X-100, and MEHQ inhibitor remover were purchased from Sigma-Aldrich. The initiator 2,2′-azobis(2,4-dimethylvaleronitril) (V65) was purchased from Wako Chemicals with 98% purity. Acetonitrile was purchased from Fisher Scientific as an extra dry solvent with a purity of 99.9%. THF (stabilized with 0.025% butylated hydroxytoluene) for dialysis was purchased from Fisher Scientific in analytical reagent grade. Dimethylformamide (DMF) was purchased from Fisher Scientific. Amino acids were purchased from Carbolution. 6-Aminofluoresceine (6-AF) was obtained from BLDPharm. Thiazolyl blue tetrazolium bromide (MTT) was obtained from TCI Chemicals. Dulbecco's phosphate buffered saline (DPBS) was purchased from VWR. Dulbecco's Modified Eagle Medium (DMEM) Low Glucose, Fetal Bovine Serum Advanced, Penicillin/Streptomycin (Pen/Strep), and Dulbecco's PBS were purchased from Capricorn Scientific. Polyethylene imine, branched, M_w 10,000 (bPEI 10,000) was purchased from Polysciences Inc. Bovine serum albumin (BSA) and lysozyme were obtained as lyophilized powders from VWR.

4.1.2. Proton Nuclear Resonance (^{1}H NMR) and Fluorine Nuclear Resonance (^{19}F-NMR) Spectroscopy. ^{1}H- and ^{19}F-NMR spectra of PPFPA were recorded on a Bruker Avance Neo Nanobay (300 MHz) spectrometer equipped with a ^{1}H, ^{13}C, ^{19}F, and ^{31}P-BBO probe at room temperature. ^{13}C-NMR spectra of PPFPA were recorded on a Bruker Avance IV (NEO) (500 MHz) spectrometer equipped with a ^{1}H, ^{13}C, and ^{19}F probe at room temperature. Chemical shifts are given in parts per million (ppm or δ-scale) relative to deuterated chloroform or water as indicated in the spectra. Amino-acid-modified polymers were analyzed from deuterated DPBS (d-DPBS), which was prepared by lyophilization of commercial DPBS and subsequent addition of D_2O at an equal volume.

^{1}H- and ^{19}F-NMR spectra of amino-acid-derived polyacrylamides were recorded on a Bruker Avance 300 (300 MHz) spectrometer equipped with a BACS-120 autosampler and a ^{1}H, ^{13}C, ^{19}F, and ^{31}P-BBO probe at room temperature.

4.1.3. Size-Exclusion Chromatography (SEC). SEC measurements of PPFPA were performed on the following setup: Agilent 1200 series, PSS (degasser), G1310A (pump), G1329A (autosampler), Techlab (oven), G7162A (RI detector), G1315D (diode array detector), and PSS GRAM 30 Å guard column and PSS GRAM 1000 Å (10 μm particle size) (column set), dimethylacetamide (DMAc) with 0.21 w% of lithium chloride as additive as eluent at 1 mL min^{-1} at 40 °C, poly(methyl methacrylate) (PMMA) (standard).

Aqueous SEC measurement was performed on an instrument consisting of a column set with a Suprema precolumn (particle size = 5 μm) and three Suprema main columns (particle size = 5 μm, 1 Å × 30 Å; 2 Å × 1000 Å) with separation range from 100 to 1,000,000 Da (PSS, Mainz, Germany) together with a variable wavelength detector (1200 Series, Agilent Technologies). As solvent, 0.07 M aqueous Na_2HPO_4 was used (for dissolving polymer and as eluting solvent) with a flow rate of 0.8 mL min^{-1} and the columns were maintained at room temperature. As internal standard, ethylene glycol (HPLC grade) was used. The calibration was done with narrowly distributed poly(methacrylic acid) sodium salt homopolymers (PMA Na salt; PSS calibration kit). An injection volume of 60 μL was used for the measurements. The samples were dissolved with a concentration of 2 mg mL^{-1} and filtered through a 0.22 μm PTFE Nylon filter before analysis. The UV detector was set to λ = 490 nm for measurements of 6AF-labeled polymers.

Reported molar masses of polymers in this study are based on the indicated standards and denoted as $M_{n,app}$.

4.1.4. High-Performance Liquid Chromatography (HPLC). HPLC measurements were conducted with a Jupiter 5 μm C18 300 Å LC column (250 mm × 4.6 mm). The run time was 35 min. A mixture of 0.1 v/v% TFA in water and acetonitrile served as eluent (Table 2). The fluorescence detected was set to λ_{ex} = 480 nm and λ_{em} = 520 nm with 1× gain. The ELSD detector was set to λ = 215 nm.

Table 2. Composition of HPLC Eluent at Indicated Time Points

time [min]	fraction of 0.1 v/v% aqueous TFA [%]	fraction of acetonitrile [%]
0	98.0	2.0
5	50.0	50.0
10	0.0	100.0
17	0.0	100.0
25	98.0	2.0
35	98.0	2.0

4.1.5. UV-Vis Spectroscopy. Absorption measurements were performed on a Jasco Spectrometer V-670 in the range of 250−500 nm (scan speed 400 nm min^{-1}) at 25 °C using a quartz glass cuvette (D = 10 mm). Baseline correction was carried out by measuring a blank sample with deionized water before measurements.

4.1.6. Fluorescence Spectroscopy. Fluorescence emission (λ_{em} = 517 nm) curves were measured on a Shimadzu RF 5301 PC spectro-fluorophotometer at an excitation wavelength of 450 nm using a quartz glass cuvette (D = 10 mm). Baseline correction was carried out by a background measurement prior to the sample measurement.

4.1.7. Dynamic Light Scattering (DLS). DLS was measured on a Zetasizer Nano-ZS Malvern apparatus (Malvern Instruments Ltd.) using disposable cuvettes. The excitation light source was a He−Ne laser at 633 nm and the intensity of the scattered light was measured at an angle of 173°. This method measures the rate of intensity fluctuation, and the size of the particles is determined through the Stokes−Einstein equation. Results are based on the material's properties of polystyrene latexes through the settings of the instrument. The concentration of the polymer solution was 2 mg mL^{-1} (in DPBS) in all cases. Details regarding size results as well as count rates can be found in Table S1.

4.1.8. Electrophoretic Light Scattering (ELS). ELS was used to measure the zeta potential (ζ). The measurement was also performed on a Zetasizer Nano-ZS by applying laser Doppler velocimetry. For each measurement, 20 runs were carried out using the slow-field reversal and the fast-field reversal mode at 150 V. Each experiment was performed in triplicates at 25 °C. The zeta potential was calculated from the electrophoretic mobility (μ) according to the Henry equation. Henry coefficient f(ka) was calculated according to Ohshima.[71] The concentration of the polymer solution was 2 mg mL^{-1} (in DPBS) in all cases. Details regarding charge results as well as count rates can be found in Table S2.

4.1.9. Fourier-Transform Infrared Spectroscopy (FTIR). IR spectra were recorded from solids on a PerkinElmer Spectrum 100 FTIR spectrometer in attenuated total reflection (ATR) mode.

4.2. Synthesis and Characterization

4.2.1. Poly(pentafluorophenyl) Acrylate (PPFPA). Poly(pentafluorophenyl) acrylate was prepared utilizing a modified procedure originally described by Zerdan et al.[53]

Ten grams of pentafluorophenyl acrylate (PFPA) was transferred into a 10 mL vial and stirred with inhibitor remover for 49 min. Meanwhile, a 25 mL round-bottom flask equipped with a rare earth stirring bar was heated with a heat gun. The atmosphere inside the flask was converted into an argon atmosphere by three cycles of applying a vacuum and subsequently filling the flask with argon. Afterward,12 mL (9.4 g) of anhydrous acetonitrile was transferred to the flask. 55 mg (0.151 mmol) of the chain-transfer agent (CTA) 2-(dodecylthiocarbonothyolthio)-2-methylpropionic acid (DTCTTMPA) was added to the reaction flask and the solution was stirred until all DTCTTMPA was dissolved. Afterward, the monomer was separated from the inhibitor remover utilizing a needle with a smaller diameter than the diameter of the inhibitor remover

https://doi.org/10.1021/acspolymersau.3c00048
ACS Polym. Au 2024, 4, 222−234

beads. 9.21 g (38.69 mmol) of the monomer PFPA was added to the flask to achieve a ratio of monomer:CTA of 257:1. A solution of V65 in acetonitrile (c = 10 mg mL^{-1}) was then prepared and 937 μL (0.038 mmol) of the solution was added to the flask and it was sealed with a rubber septum. The final monomer:CTA:initiator ratio was 257:1:0.25. The mixture was stirred for 2 min to homogenize the solution before it was purged with argon for 15 min. The yellow mixture was then transferred into a preheated oil bath thermostated at 60 °C and stirred for 17 h. The mixture was subsequently transferred to a dialysis tubing (Spectrum Spectra/Por Cellulose Ester, MWCO: 8 kDa), and dialysis against THF was performed for 3 days with daily solvent change. Then, the solvent was removed under reduced pressure and the polymer was dried in a vacuum oven at 60 °C for 1 day. The product was obtained as a yellow solid. Yield: 1.97 g (21%).

The DP of the resulting polymer was calculated by end-group analysis, using the signal of the CTA's terminal CH_3 group at δ = 0.91 ppm and the CH group of the polymer backbone at δ = 3.12 ppm, suggesting a DP of 132.

SEC (DMAc + 0.21 w% LiCl; PMMA-standard): $M_{n,app}$ = 33,900 g mol^{-1}; $Đ$ = 1.32.

4.2.2. Postpolymerization Modification of PPFPA with Aliphatic Amino Acids. The postpolymerization modification of PPFPA is exemplarily described for reactions with Gly-yielding P(Gly-OH-AAm). Quantities and moles are given relative to the single repeating unit PFPA of the polymer and can be found in Table 3.

Table 3. Quantities of Amino Acids Used for PPM of PPFPA

amino acid	n [mmol]	m [mg]
Gly	1.26	95
Ala		112
Abu		130
Nva		148
Val		148
Ile		165
Leu		165

In a 5 mL reaction vessel (Biotage), PPFPA (100 mg, 0.42 mmol, 1.00 equiv) was dissolved in anhydrous DMF (5 mL). 250 μL of triethylamine was added. After that, Gly (95 mg, 1.26 mmol, 3 equiv) was added, the reaction vial was closed with a septum, and the suspension was stirred at 40 °C for 72 h. Then, the solid was filtered off and the remaining solution was dialyzed (RC, MWCO 3.5 kDa, SpectraPor) against 1 L of deionized water for 3 days with daily water change. Upon lyophilization, the product was yielded as an off-white to yellowish powder. Polymers were analyzed via ^{1}H NMR, ^{19}F-NMR, FTIR spectroscopy, and aqueous SEC. ^{1}H NMR showing C−H adjacent to an amide bond (δ = 4.0 ppm) and FTIR showing a shift in absorption from a carbonyl adjacent to PFP at $\tilde{\nu}$ = 1780 cm^{-1} toward a carbonyl group in an amide bond $\tilde{\nu}$ = 1550 cm^{-1} both confirmed the conversion of the reaction. NMR and FTIR spectra can be found in the Supporting Information. Molar mass and dispersity from SEC measurements can be found in Table 1.

4.2.3. Postpolymerization Modification of PPFPA with 6-AF and Aliphatic Amino Acids. The postpolymerization modification of PPFPA is exemplarily described for reactions with Gly-yielding P(Gly-OH-AAm)-6AF. Quantities and moles are given relative to the single repeating unit PFPA of the polymer and can be found in Table 3.

In a 5 mL reaction vessel (Biotage), PPFPA (100 mg, 0.42 mmol, 1.00 equiv) was dissolved in anhydrous DMF (5 mL). Twenty-five μL triethylamine was added. After that, 6-AF (1 mg, 0.004 mmol, 0.01 equiv) was added and the reaction vessel was closed with a septum. The reaction mixture was stirred in the dark at 40 °C for 24 h. Then, 225 μL of triethylamine and Gly (95 mg, 1.26 mmol, 3 equiv) were added, the reaction vial was closed with a septum, and the suspension was stirred at 40 °C for 72 h. Then, the solid was filtered off and the remaining solution was dialyzed (RC, MWCO 3.5 kDa, SpectraPor) against 1 L of deionized water for 3 days with daily water changes. Upon lyophilization, the product was yielded as a yellow to greenish powder. Yields were determined gravimetrically. The labeling efficiency (LE) was determined by UV−vis measurements in DPBS according to the calibration of pure 6-AF in DPBS (Figure S10).

Yields (% assuming quantitative amino acid modification) and LE:
P(Gly-OH-AAm)-6AF: 19 mg (35%); LE: 11%
P(Ala-OH-AAm)-6AF: 48 mg (80%); LE: 14%
P(Abu−OH-AAm)-6AF: 47 mg (71%); LE: 8%
P(Nva-OH-AAm)-6AF: 45 mg (63%); LE: 12%
P(Val-OH-AAm)-6AF: 45 mg (63%); LE: 13%
P(Ile-OH-AAm)-6AF: 48 mg (62%); LE: 10%
P(Leu-OH-AAm)-6AF: 52 mg (67%); LE 9%

Polymers were analyzed by aqueous SEC (0.07 M aq. Na_2HPO_4 (standard: PMA Na salt)). Elugrams can be found in Figure S9.
P(Gly-OH-AAm)-6AF: $M_{n,app}$ = 11,500 g mol^{-1}; $Đ$ = 1.84.
P(Ala-OH-AAm)-6AF: $M_{n,app}$ = 14,200 g mol^{-1}; $Đ$ = 1.70.
P(Abu−OH-AAm)-6AF: $M_{n,app}$ = 13,800 g mol^{-1}; $Đ$ = 1.70.
P(Nva-OH-AAm)-6AF: $M_{n,app}$ = 13,400 g mol^{-1}; $Đ$ = 1.62.
P(Val-OH-AAm)-6AF: $M_{n,app}$ = 14,200 g mol^{-1}; $Đ$ = 1.57.
P(Ile-OH-AAm)-6AF: $M_{n,app}$ = 16,300 g mol^{-1}; $Đ$ = 1.55.
P(Leu-OH-AAm)-6AF: $M_{n,app}$ = 10,500 g mol^{-1}; $Đ$ = 2.11.

4.2.4. pH Response. The pH response of the different polymers was investigated by acidic titration. A 5 mg mL^{-1} solution of the polymer in deionized water was prepared and 20 μL of 1.0 M aq. NaOH was added to obtain a starting pH value >11. Subsequently, the solution was titrated with 0.1 M aq. HCl until a pH value <3 was reached. Measurements were done with a Mettler Toledo digital pH meter. The pK_a was calculated from the first derivation of the titration curve according to our previous work.[72]

4.2.5. Hydrophilic/Hydrophobic Ratio. The procedure was modified from the literature.[21] A known concentration of amino-acid-functionalized polymers (1 or 0.1 mg mL^{-1} as indicated) was dissolved in deionized water (diH_2O) of indicated pH value or DPBS. To ensure precise pH values, 200 μL of a 10-fold stock solution of the respective polymer was diluted with diH_2O to a total volume of 1.5 mL. The pH value was adjusted by the addition of an aqueous 0.1 M HCl or NaOH solution. After the desired pH value was reached, diH_2O was added to reach a final volume of 2.0 mL. The fluorescence of this solution was measured. Then, an equal volume of chloroform was added, and the solution was vortexed for 1 min at maximum speed. The 0.1 mg mL^{-1} solution was allowed to stand for 15 min (or 24 h in the case of 1 mg mL^{-1} solutions) to separate the aqueous and the organic layer. A sample was carefully taken from each layer and analyzed via fluorescence measurements (λ_{ex} = 450 nm, λ_{em} = 517 nm). To obtain the relative fluorescence, the raw results were normalized by the peak maximum of the emission trace of the respective polymer observed before the addition of chloroform (eq 1). The results show the normalized fluorescence intensity.

$$\text{relative fluorescence emission} = \frac{\text{intensity after chloroform treatment}}{\text{intensity before chloroform treatment}} \quad (1)$$

The hydrophobic−lipophilic balance (HLB) of polymers was predicted with MarvinSketch 23.14 using the Griffin method.[65]

4.2.6. Protein Fouling. Protein fouling of P(Gly-OH-AAm) and P(Nva-OH-AAm) with BSA and lysozyme, respectively, was analyzed by DLS measurements.

Stock solutions of the polymers and the proteins in DPBS were prepared (c = 1 mg mL^{-1}) and mixed in a ratio of 1:1, yielding concentrations of c = 0.5 mg mL^{-1}. The samples were measured immediately after mixing (t = 0 h) and at indicated time points (i.e., 0.5, 1, 2, 4, and 24 h). The time points indicate the time interval in-between measurements at which the samples were incubated at 37 °C while shaking at 100 rpm. Measurements were conducted at 37 °C with five measurements and three runs each. After the measurement, samples were placed back into the incubator immediately.

4.2.7. Statistical Analysis. All data plotted with error bars were expressed as means with standard deviation. p-Values were generated

https://doi.org/10.1021/acspolymersau.3c00048
ACS Polym. Au 2024, 4, 222−234

by analyzing data with a one-way ANOVA and Turkey test using OriginLab.

4.3. Biological Evaluation

4.3.1. Cell Culture. L929 cells were cultured in low-glucose Dulbecco's Modified Eagle Medium (DMEM) supplemented with 10% fetal bovine serum, 100 U mL^{-1} penicillin, and 100 μg mL^{-1} streptomycin. The cells were incubated at 37 °C using 5% CO_2 in a humidified incubator.

4.3.2. Cell Viability Assay. The cell viability assay was slightly modified from our previous procedure.[2] Cells were cultured as described above. For the cell viability assay, cells (10^4 per well) were seeded in 96 well plates and allowed to adhere overnight. No cells were seeded in the outer wells. The media was subsequently removed and replaced by fresh polymer-containing media. Then, the cells were incubated at 37 °C for an additional 24 h. After that, the media was removed, the cells were washed with 100 μL of DPBS, and then fresh media containing thiazolyl blue tetrazolium bromide (MTT) (concentration: 1 mg mL^{-1}) was added (100 μL/well). Note: MTT (50 mg) was dissolved in 10 mL of sterile PBS, filtrated (membrane, 0.22 μm), and 1 to 5 diluted in culture medium prior to use in this assay. After incubation for 3 h at 37 °C, 100 μL of *i*-PrOH was added to each well and the plates were gently shaken in the dark for 15 min to dissolve the formazan crystals. Quantification was done by measuring the absorbance at λ = 580 nm using a microplate reader (Genios Pro, Tecan). Untreated cells on the same plate served as negative control (100% viability), cells treated with 20% DMSO as positive control (0% viability), and wells without cells as background. Experiments were formed in triplicates on three different plates. Relative cell viability was calculated by using eq 2.

$$\%\ \text{cell viability} = \frac{\text{Abs. sample} - \text{Abs. background}}{\text{Abs. negative control} - \text{Abs. background}} \times 100 \quad (2)$$

4.3.3. Cell Association via Flow Cytometry. *4.3.3.1. Cell Association Assay I: Concentration-Dependent Polymer Association with L929.* The cell association assay is adapted from Leiske et al.[21] The L929 cells were cultured at 37 °C in a humidified 5% (v/v) CO_2 atmosphere in DMEM Low Glucose (1 g L^{-1}). The media was supplemented with 10% (v/v) fetal bovine serum (FBS), 100 U mL^{-1} penicillin, and 100 μg mL^{-1} streptomycin (culture medium). For the experiments, 2×10^5 cells mL^{-1} were seeded in 250 μL of culture medium in a 48 well plate and cultivated for 24 h until treatment. One hour before the treatment, the medium was changed to 225 μL of fresh culture medium. The polymers were diluted in DPBS to a concentration of c_{RU} = 0.5, 1.0, 5.0, and 10 mM. Cells were treated with 25 μL of respective polymer to receive final concentrations of c_{RU} = 0.05, 0.10, 0.50, and 1.00 mM. Cells were additionally treated with 25 μL of DPBS as negative control (NC). After 4 h of incubation at 37 °C, 5% (v/v) CO_2, the supernatant was discarded. The cells were immediately detached with trypsin-EDTA, resuspended in PBS, and analyzed by flow cytometry (cytoFLEX (Beckman Coulter)). A minimum of 10,000 single cells were measured and analyzed by forward and sideward scatter (FSC/SSC). Fluorescence was measured at λ_{ex} = 488 nm with a 510/20 nm bandpass filter (GFP channel). Positive cells were identified by gating against NC. A detailed gating strategy is provided in Figure S17.

The normalized MFI was calculated using eq 3.

$$\text{normalized MFI[a. u.]} = \frac{\text{MFI}_{\text{sample}}}{\text{MFI}_{\text{NC}}} \times \frac{1}{r\ \text{fluorescence}_{\text{sample}}} \quad (3)$$

4.3.3.2. Cell Association Assay II: Time- and Temperature-Dependent Polymer Association with L929. L929 cells were seeded as described before and cultivated for 24 h until treatment. One hour before the treatment, the medium got changed to 225 μL of fresh culture medium. The polymers were diluted in DPBS to a concentration of c_{RU} = 10 mM. Cells were treated with 25 μL of the respective polymer at different time points to achieve final incubation times of 0.5, 1.0, 2.0, and 4.0 h at 37 °C, 5% (v/v) CO_2 with c_{RU} = 1.0 mM. Cells were additionally treated with 25 μL of DPBS as NC. An additional 48 well plate was treated in parallel at 4 °C (refrigerator) for 4 h. After incubation, the cells were measured as described before. A detailed gating strategy is provided in Figure S18.

The normalized MFI was calculated using eq 3. The temperature-dependent reduction of cell association was calculated using eq 4.

$$\text{reduction[\%]} = 1 - \frac{\text{MFI}_{4°\text{C}}(\text{normalized})}{\text{MFI}_{37°\text{C}}(\text{normalized})} \times 100\% \quad (4)$$

4.3.4. Confocal Laser-Scanning Microscopy (CLSM). The assay is adapted from Richter et al.[73] For cell association studies, cells were seeded as described before in 500 μL of culture medium in 4 well glass-bottomed dishes (Greiner Bio-One, Cat# 627860) and cultivated for 24 h until treatment. One hour prior to treatment, the medium got changed to 450 μL of fresh culture medium. The polymers were diluted in DPBS to a concentration of 10 mM (RU). Cells were treated with 50 μL of the polymer to achieve a final concentration of 1.0 mM (RU) and incubated for 4 or 24 h at 37 °C in humidified 5% (v/v) CO_2. To stain nuclei, Hoechst 33342 (Invitrogen, Cat# H3570) was added (1:1000). To stain cellular membrane, CellMask Plasma Membrane Stain (Invitrogen, Cat# C10046) was added (1:1000). After further incubation of 10 min, the medium was replaced by 500 μL of fresh medium. Live cell imaging was performed using a LSM880, Elyra PS.1 system (Zeiss) applying laser for excitation at 405 nm (1.0%) (emission filter 410–484 nm, detection of Hoechst), 488 nm (2.0%) (emission filter 490–579 nm, detection of fluorescein), and 633 nm (1.5%) (emission filter 638–759 nm, detection of CellMask). To avoid cross-talk between the dyes, three different tracks were used. Images were acquired using the ZEN software, version 2.3 SP1 (Zeiss). The experiments were performed at least twice. All images were processed with ZEN software, version 3.7 (ZEN lite) (Zeiss). The same values were applied to all images.

4.3.5. Hemoglobin Release and Erythrocyte Aggregation. The erythrocyte aggregation and hemoglobin release assay were adapted from Richter et al.[73] The interaction of polymers with cellular membranes was detected by measuring the release of hemoglobin from erythrocytes due to potential membrane lysis. The blood, collected in tubes with citrate, was provided by the Department of Transfusion Medicine of the University Hospital, Jena. The experimental protocols used therein were approved by the ethics committee of the Jena University Hospital (2021–2058-Material). Blood from at least three different human donors was used. To isolate erythrocytes, the blood was centrifuged at 4500*g* for 5 min. The pellet was washed three times with DPBS. 500 μL of aliquots of erythrocytes were mixed with 500 μL of polymer solution in DPBS to receive a final concentration of c_{RU} = 1 mM (Test solution). To determine aggregation, 100 μL of the respective test solutions were transferred to a 96 well plate in three technical replicates. bPEI 10000 was used as a positive control (50 μg mL^{-1}) and only DPBS as NC. After incubation at 37 °C for 2 h, the absorbance was measured at λ = 645 nm. The aggregation rate was calculated by eq 5.

$$\text{aggregation rate} = \frac{\text{absorbance}_{\text{NC}}}{\text{absorbance}_{\text{sample}}} \quad (5)$$

Exemplary microscopy images of aggregation are provided in Figure S19.

In parallel, the remaining 700 μL of test solutions was incubated for 1 h at 37 °C. To determine hemoglobin release, the tubes were centrifuged at 2400*g* for 5 min and the supernatant was transferred to a 96 well plate in three technical replicates. To measure the hemolytic effect of the polymers, the absorbance was measured at λ = 544 with λ = 630 nm as reference bandwidth. As a positive control, 1% Triton X-100 (T-X) was used (100% hemolysis) and pure DPBS was used as NC. The hemolysis (%) was calculated using eq 6.

https://doi.org/10.1021/acspolymersau.3c00048
ACS Polym. Au 2024, 4, 222–234

$$\text{hemolysis}(\%) = \frac{\text{absorbance}_{\text{sample}}}{\text{absorbance}_{\text{T-X}}} \times 100 \quad (6)$$

Values below 2% hemolysis are classified as nonhemolytic, values between 2 and 5% are slightly hemolytic, and values above 5% are hemolytic.

■ ASSOCIATED CONTENT

Supporting Information

The Supporting Information is available free of charge at https://pubs.acs.org/doi/10.1021/acspolymersau.3c00048.

The Supporting Information is available free of charge and contains further analysis of the materials in this study, including ^{1}H and ^{19}F-NMR spectra, fluorescence spectra, FTIR spectra, SEC data, cell viability data, cell association, and uptake data (PDF)

■ AUTHOR INFORMATION

Corresponding Author

Meike N. Leiske − *Macromolecular Chemistry, University of Bayreuth, 95447 Bayreuth, Germany; Bavarian Polymer Institute, 95447 Bayreuth, Germany;* orcid.org/0000-0002-8525-2324; Email: meike.leiske@uni-bayreuth.de

Authors

Jonas De Breuck − *Macromolecular Chemistry, University of Bayreuth, 95447 Bayreuth, Germany*

Michael Streiber − *Laboratory of Organic and Macromolecular Chemistry (IOMC), Friedrich Schiller University Jena, 07743 Jena, Germany; Jena Center for Soft Matter (JCSM), Friedrich Schiller University Jena, 07743 Jena, Germany*

Michael Ringleb − *Laboratory of Organic and Macromolecular Chemistry (IOMC), Friedrich Schiller University Jena, 07743 Jena, Germany; Jena Center for Soft Matter (JCSM), Friedrich Schiller University Jena, 07743 Jena, Germany;* orcid.org/0000-0002-7320-8529

Dennis Schröder − *Macromolecular Chemistry, University of Bayreuth, 95447 Bayreuth, Germany; Bavarian Polymer Institute, 95447 Bayreuth, Germany*

Natascha Herzog − *Macromolecular Chemistry, University of Bayreuth, 95447 Bayreuth, Germany*

Ulrich S. Schubert − *Laboratory of Organic and Macromolecular Chemistry (IOMC), Friedrich Schiller University Jena, 07743 Jena, Germany; Jena Center for Soft Matter (JCSM), Friedrich Schiller University Jena, 07743 Jena, Germany;* orcid.org/0000-0003-4978-4670

Stefan Zechel − *Laboratory of Organic and Macromolecular Chemistry (IOMC), Friedrich Schiller University Jena, 07743 Jena, Germany; Jena Center for Soft Matter (JCSM), Friedrich Schiller University Jena, 07743 Jena, Germany*

Anja Traeger − *Laboratory of Organic and Macromolecular Chemistry (IOMC), Friedrich Schiller University Jena, 07743 Jena, Germany; Jena Center for Soft Matter (JCSM), Friedrich Schiller University Jena, 07743 Jena, Germany;* orcid.org/0000-0001-7734-2293

Complete contact information is available at: https://pubs.acs.org/10.1021/acspolymersau.3c00048

Author Contributions

[⊥]M.S. and M.R. contributed equally to this work. The primary data are available. CRediT: **Jonas De Breuck** data curation, formal analysis, methodology, writing-original draft; **Michael Streiber** data curation, formal analysis, methodology, writing-review & editing; **Michael Ringleb** data curation, formal analysis, methodology, writing-review & editing; **Dennis Schröder** data curation, formal analysis, writing-review & editing; **Natascha Herzog** data curation, formal analysis; **Ulrich S. Schubert** funding acquisition, supervision, writing-review & editing; **Stefan Zechel** project administration, supervision, writing-review & editing; **Anja Traeger** conceptualization, funding acquisition, project administration, supervision, writing-review & editing; **Meike N. Leiske** conceptualization, funding acquisition, supervision, writing-original draft.

Notes

The authors declare no competing financial interest.

■ ACKNOWLEDGMENTS

The authors would like to acknowledge Prof Ruth Freitag, Prof Andreas Greiner, Prof Hans-Werner Schmidt, Prof Thomas Scheibel, and Prof Georg Papastavrou for providing access to their laboratories and equipment. The authors thank Dr Martin Humenik for his help with high-performance liquid chromatography measurements. The authors would like to thank Rika Schneider for conducting size-exclusion chromatography measurements, Martina Fried for assistance with polymer titrations, and Carolin Kellner for support with hemolysis and erythrocyte aggregation assays. M.N.L. acknowledges the financial support from the "Fonds der Chemischen Industrie im Verband der Chemischen Industrie." The authors gratefully acknowledge the Bundesministerium für Bildung und Forschung (BMBF, Germany, #13XP5034A PolyBioMik), the DFG Projects PolyTarget (SFB 1278, project B01, C06, project ID: 316213987) as well as the "Thüringer Aufbaubank (TAB)" (2021 FGI 0005), and the "Europäischer Fond für regionale Entwicklung (EFRE)" (2018FGI0025) for funding of flow cytometry devices at the Jena Center for Soft Matter (JCSM). This work was performed within the Joint Lab for Polymers Jena-Bayreuth.

■ REFERENCES

(1) Duncan, R.; Gaspar, R. Nanomedicine(s) under the Microscope. *Mol. Pharmaceutics* **2011**, *8* (6), 2101−2141.

(2) Villaverde, G.; Baeza, A. Targeting Strategies for Improving the Efficacy of Nanomedicine in Oncology. *Beilstein J. Nanotechnol.* **2019**, *10*, 168−181.

(3) Takano, S.; Sakurai, K.; Fujii, S. Internalization into Cancer Cells of Zwitterionic Amino Acid Polymers via Amino Acid Transporter Recognition. *Polym. Chem.* **2021**, *12* (42), 6083−6087.

(4) Li, Y.; Yang, H. Y.; Thambi, T.; Park, J. H.; Lee, D. S. Charge-Convertible Polymers for Improved Tumor Targeting and Enhanced Therapy. *Biomaterials* **2019**, *217*, No. 119299, DOI: 10.1016/j.biomaterials.2019.119299.

(5) Choi, H. S.; Liu, W.; Liu, F.; Nasr, K.; Misra, P.; Bawendi, M. G.; Frangioni, J. V. Design Considerations for Tumour-Targeted Nanoparticles. *Nat. Nanotechnol.* **2010**, *5* (1), 42−47.

(6) Theodorou, I.; Anilkumar, P.; Lelandais, B.; Clarisse, D.; Doerflinger, A.; Gravel, E.; Ducongé, F.; Doris, E. Stable and Compact Zwitterionic Polydiacetylene Micelles with Tumor-Targeting Properties. *Chem. Commun.* **2015**, *51* (80), 14937−14940.

(7) Mahmoud, A. M.; de Jongh, P. A. J. M.; Briere, S.; Chen, M.; Nowell, C. J.; Johnston, A. P. R.; Davis, T. P.; Haddleton, D. M.; Kempe, K. Carboxylated Cy5-Labeled Comb Polymers Passively Diffuse the Cell Membrane and Target Mitochondria. *ACS Appl. Mater. Interfaces* **2019**, *11* (34), 31302−31310.

(8) Wang, S. PH-Responsive Amphiphilic Carboxylate Polymers: Design and Potential for Endosomal Escape. *Front. Chem.* **2021**, *9* (March), 1−8.
(9) Li, M.; Zhang, W.; Li, J.; Qi, Y.; Peng, C.; Wang, N.; Fan, H.; Li, Y. Zwitterionic Polymers: Addressing the Barriers for Drug Delivery. *Chin. Chem. Lett.* **2023**, *34* (11), No. 108177.
(10) Monnery, B. D. Polycation-Mediated Transfection: Mechanisms of Internalization and Intracellular Trafficking. *Biomacromolecules* **2021**, *22* (10), 4060−4083.
(11) Agarwal, S.; Zhang, Y.; Maji, S.; Greiner, A. PDMAEMA Based Gene Delivery Materials. *Mater. Today* **2012**, *15* (9), 388−393.
(12) Yessine, M. Membrane-Destabilizing Polyanions: Interaction with Lipid Bilayers and Endosomal Escape of Biomacromolecules. *Adv. Drug Delivery Rev.* **2004**, *56* (7), 999−1021.
(13) Behr, J.-P. The Proton Sponge: A Trick to Enter Cells the Viruses Did Not Exploit. *Chimia Aarau* **1997**, *51* (1−2), 34.
(14) Bus, T.; Traeger, A.; Schubert, U. S. The Great Escape: How Cationic Polyplexes Overcome the Endosomal Barrier. *J. Mater. Chem. B* **2018**, *6* (43), 6904−6918.
(15) Braksch, C. P.; Lehnen, A. C.; Bapolisi, A. M.; Gurke, J.; De Breuck, J.; Leiske, M. N.; Hartlieb, M. Staphylococcus Aureus Selective Antimicrobial Polymers Based on an Arginine-Derived Monomer. *J. Polym. Sci.* **2024**, *62* (1), 132−145.
(16) Lehnen, A. C.; Kogikoski, S.; Stensitzki, T.; AlSawaf, A.; Bapolisi, A. M.; Wolff, M.; De Breuck, J.; Müller-Werkmeister, H. M.; Chiantia, S.; Bald, I.; Leiske, M. N.; Hartlieb, M. Anisotropy in Antimicrobial Bottle Brush Copolymers and Its Influence on Biological Activity. *Adv. Funct. Mater.* **2023**, No. 2312651, DOI: 10.1002/adfm.202312651.
(17) Nayak, K.; Ghosh, P.; Khan, M. E. H.; De, P. Side-Chain Amino-Acid-Based Polymers: Self-Assembly and Bioapplications. *Polym. Int.* **2022**, *71* (4), 411−425.
(18) Kauffman, W. B.; Fuselier, T.; He, J.; Wimley, W. C. Mechanism Matters: A Taxonomy of Cell Penetrating Peptides. *Trends Biochem. Sci.* **2015**, *40* (12), 749−764.
(19) Ladavière, C.; Tousto, M.; Gulik-Krzywicki, T.; Tribet, C. Slow Reorganization of Small Phosphatidylcholine Vesicles upon Adsorption of Amphiphilic Polymers. *J. Colloid Interface Sci.* **2001**, *241* (1), 178−187.
(20) Yessine, M.-A.; Lafleur, M.; Meier, C.; Petereit, H.-U.; Leroux, J.-C. Characterization of the Membrane-Destabilizing Properties of Different PH-Sensitive Methacrylic Acid Copolymers. *Biochim. Biophys. Acta, Biomembr.* **2003**, *1613* (1−2), 28−38, DOI: 10.1016/S0005-2736(03)00137-8.
(21) Leiske, M. N.; De Geest, B. G.; Hoogenboom, R. Impact of the Polymer Backbone Chemistry on Interactions of Amino-Acid-Derived Zwitterionic Polymers with Cells. *Bioact. Mater.* **2023**, *24* (January), 524−534.
(22) Wang, S.; Chen, R. PH-Responsive, Lysine-Based, Hyperbranched Polymers Mimicking Endosomolytic Cell-Penetrating Peptides for Efficient Intracellular Delivery. *Chem. Mater.* **2017**, *29* (14), 5806−5815.
(23) Chen, S.; Wang, S.; Kopytynski, M.; Bachelet, M.; Chen, R. Membrane-Anchoring, Comb-Like Pseudopeptides for Efficient, PH-Mediated Membrane Destabilization and Intracellular Delivery. *ACS Appl. Mater. Interfaces* **2017**, *9* (9), 8021−8029.
(24) Lehnen, A.-C.; Gurke, J.; Bapolisi, A. M.; Reifarth, M.; Bekir, M.; Hartlieb, M. Xanthate-Supported Photo-Iniferter (XPI)-RAFT Polymerization: Facile and Rapid Access to Complex Macromolecules. *Chem. Sci.* **2023**, *14* (3), 593−603.
(25) Martin, L.; Gody, G.; Perrier, S. Preparation of Complex Multiblock Copolymers via Aqueous RAFT Polymerization at Room Temperature. *Polym. Chem.* **2015**, *6* (27), 4875−4886.
(26) Mori, H.; Endo, T. Amino-Acid-Based Block Copolymers by RAFT Polymerization. *Macromol. Rapid Commun.* **2012**, *33* (13), 1090−1107.
(27) Leiske, M. N.; Singha, R.; Jana, S.; De Geest, B. G.; Hoogenboom, R. Amidation of Methyl Ester-Functionalised Poly(2-Oxazoline)s as a Powerful Tool to Create Dual PH- and Temperature-Responsive Polymers as Potential Drug Delivery Systems. *Polym. Chem.* **2023**, *14* (17), 2034−2044.
(28) Das, A.; Theato, P. Activated Ester Containing Polymers: Opportunities and Challenges for the Design of Functional Macromolecules. *Chem. Rev.* **2016**, *116* (3), 1434−1495.
(29) Singha, N. K.; Gibson, M. I.; Koiry, B. P.; Danial, M.; Klok, H. A. Side-Chain Peptide-Synthetic Polymer Conjugates via Tandem "Ester-Amide/Thiol-Ene" Post-Polymerization Modification of Poly(Pentafluorophenyl Methacrylate) Obtained Using ATRP. *Biomacromolecules* **2011**, *12* (8), 2908−2913.
(30) Gok, O.; Kosif, I.; Dispinar, T.; Gevrek, T. N.; Sanyal, R.; Sanyal, A. Design and Synthesis of Water-Soluble Multifunctionalizable Thiol-Reactive Polymeric Supports for Cellular Targeting. *Bioconjugate Chem.* **2015**, *26* (8), 1550−1560.
(31) Boyer, C.; Davis, T. P. One- Pot Synthesis and Biofunctionalization of Glycopolymers via RAFT Polymerization and Thiol−Ene Reactions. *Chem. Commun.* **2009**, No. 40, 6029−6031.
(32) Murata, H.; Prucker, O.; Rühe, J. Synthesis of Functionalized Polymer Monolayers from Active Ester Brushes. *Macromolecules* **2007**, *40* (15), 5497−5503.
(33) Moog, K. E.; Barz, M.; Bartneck, M.; Beceren-Braun, F.; Mohr, N.; Wu, Z.; Braun, L.; Dernedde, J.; Liehn, E. A.; Tacke, F.; Lammers, T.; Kunz, H.; Zentel, R. Polymeric Selectin Ligands Mimicking Complex Carbohydrates: From Selectin Binders to Modifiers of Macrophage Migration. *Angew. Chemie - Int. Ed.* **2017**, *56* (5), 1416−1421.
(34) Eberhardt, M.; Mruk, R.; Zentel, R.; Théato, P. Synthesis of Pentafluorophenyl(Meth)Acrylate Polymers: New Precursor Polymers for the Synthesis of Multifunctional Materials. *Eur. Polym. J.* **2005**, *41* (7), 1569−1575.
(35) Batz, H. G.; Franzmann, G.; Ringsdorf, H. Pharmakologisch Aktive Polymere, 5. Modellreaktionen Zur Umsetzung von Pharmaka Und Enzymen Mit Monomeren Und Polymeren Reaktiven Estern. *Die Makromol. Chemie* **1973**, *172* (1), 27−47.
(36) Ferruti, P.; Bettelli, A.; Feré, A. High Polymers of Acrylic and Methacrylic Esters of N-Hydroxysuccinimide as Polyacrylamide and Polymethacrylamide Precursors. *Polymer Guildf* **1972**, *13* (10), 462−464.
(37) Choi, J.; Schattling, P.; Jochum, F. D.; Pyun, J.; Char, K.; Theato, P. Functionalization and Patterning of Reactive Polymer Brushes Based on Surface Reversible Addition and Fragmentation Chain Transfer Polymerization. *J. Polym. Sci., Part A: Polym. Chem.* **2012**, *50* (19), 4010−4018.
(38) Kockelmann, J.; Zentel, R.; Nuhn, L. Post-Polymerization Modifications to Prepare Biomedical Nanocarriers with Varying Internal Structures, Their Properties and Impact on Protein Corona Formation. *Macromol. Chem. Phys.* **2023**, *224*, No. 2300199, DOI: 10.1002/macp.202300199.
(39) De Coen, R.; Vanparijs, N.; Risseeuw, M. D. P.; Lybaert, L.; Louage, B.; De Koker, S.; Kumar, V.; Grooten, J.; Taylor, L.; Ayres, N.; Van Calenbergh, S.; Nuhn, L.; De Geest, B. G. PH-Degradable Mannosylated Nanogels for Dendritic Cell Targeting. *Biomacromolecules* **2016**, *17* (7), 2479−2488.
(40) Duret, D.; Haftek-Terreau, Z.; Carretier, M.; Ladavière, C.; Charreyre, M.-T.; Favier, A. Fluorescent RAFT Polymers Bearing a Nitrilotriacetic Acid (NTA) Ligand at the α-Chain-End for the Site-Specific Labeling of Histidine-Tagged Proteins. *Polym. Chem.* **2017**, *8* (10), 1611−1615.
(41) Cepraga, C.; Gallavardin, T.; Marotte, S.; Lanoë, P. H.; Mulatier, J. C.; Lerouge, F.; Parola, S.; Lindgren, M.; Baldeck, P. L.; Marvel, J.; Maury, O.; Monnereau, C.; Favier, A.; Andraud, C.; Leverrier, Y.; Charreyre, M. T. Biocompatible Well-Defined Chromophore-Polymer Conjugates for Photodynamic Therapy and Two-Photon Imaging. *Polym. Chem.* **2013**, *4* (1), 61−67.
(42) Engler, A. C.; Chan, J. M. W.; Coady, D. J.; O'Brien, J. M.; Sardon, H.; Nelson, A.; Sanders, D. P.; Yang, Y. Y.; Hedrick, J. L. Accessing New Materials through Polymerization and Modification of a Polycarbonate with a Pendant Activated Ester. *Macromolecules* **2013**, *46* (4), 1283−1290.

https://doi.org/10.1021/acspolymersau.3c00048
ACS Polym. Au 2024, 4, 222−234

(43) Smith, E.; Bai, J.; Oxenford, C.; Yang, J.; Somayaji, R.; Uludag, H. Conjugation of Arginine-Glycine-Aspartic Acid Peptides to Thermoreversible N-Isopropylacrylamide Polymers. *J. Polym. Sci., Part A: Polym. Chem.* **2003**, *41* (24), 3989−4000.
(44) Baessler, K. A.; Lee, Y.; Sampson, N. S. B1 Integrin Is an Adhesion Protein for Sperm Binding To Eggs. *ACS Chem. Biol.* **2009**, *4* (5), 357−366.
(45) Börner, H. G.; Sütterlin, R. I.; Theato, P.; Wiss, K. T. Topology-Dependent Swichability of Peptide Secondary Structures in Bioconjugates with Complex Architectures. *Macromol. Rapid Commun.* **2014**, *35* (2), 180−185.
(46) Nuhn, L.; Hartmann, S.; Palitzsch, B.; Gerlitzki, B.; Schmitt, E.; Zentel, R.; Kunz, H. Water-Soluble Polymers Coupled with Glycopeptide Antigens and T-Cell Epitopes as Potential Antitumor Vaccines. *Angew. Chem., Int. Ed.* **2013**, *52* (40), 10652−10656, DOI: 10.1002/anie.201304212.
(47) Leiske, M. N.; Kempe, K. A Guideline for the Synthesis of Amino-Acid-Functionalized Monomers and Their Polymerizations. *Macromol. Rapid Commun.* **2022**, *43* (2), 1−24.
(48) Maity, T.; Paul, S.; De, P. Side-Chain Amino Acid-Based Macromolecular Architectures. *J. Macromol. Sci. Part A* **2023**, *60* (1), 2−17.
(49) Leiske, M. N.; Mazrad, Z. A. I.; Zelcak, A.; Wahi, K.; Davis, T. P.; McCarroll, J. A.; Holst, J.; Kempe, K. Zwitterionic Amino Acid-Derived Polyacrylates as Smart Materials Exhibiting Cellular Specificity and Therapeutic Activity. *Biomacromolecules* **2022**, *23* (6), 2374−2387.
(50) Fujii, S.; Sakurai, K. Zwitterionic Amino Acid Polymer-Grafted Core-Crosslinked Particle toward Tumor Delivery. *Biomacromolecules* **2022**, *23* (9), 3968−3977.
(51) Koyama, E.; Sanda, F.; Endo, T. Syntheses and Radical Polymerizations of Methacrylamides Derived from Optically Active Amino Alcohols. *Macromol. Chem. Phys.* **1997**, *198* (11), 3699−3707.
(52) Yaşayan, G.; Redhead, M.; Magnusson, J. P.; Spain, S. G.; Allen, S.; Davies, M.; Alexander, C.; Fernández-Trillo, F. Well-Defined Polymeric Vesicles with High Stability and Modulation of Cell Uptake by a Simple Coating Protocol. *Polym. Chem.* **2012**, *3* (9), 2596−2604.
(53) Bou Zerdan, R.; Geng, Z.; Narupai, B.; Diaz, Y. J.; Bates, M. W.; Laitar, D. S.; Souvagya, B.; Van Dyk, A. K.; Hawker, C. J. Efficient Synthesis of Branched Poly(Acrylic Acid) Derivatives via Post-polymerization Modification. *J. Polym. Sci.* **2020**, *58* (14), 1989−1997.
(54) Hu, H.; Saniger, J.; Garcia-Alejandre, J.; Castaiio, V. M. Fourier Transform Infrared Spectroscopy Studies of the Reaction between Polyacrylic Acid and Metal Oxides. *Mater. Lett.* **1991**, *12*, 281−285, DOI: 10.1016/0167-577X(91)90014-W.
(55) Roy, S.; Mahali, K.; Mondal, S.; Dolui, B. K. Thermodynamics of DL-Alanine Solvation in Water-Dimethylsulfoxide Mixtures at 298.15 K. *Russ. J. Phys. Chem. A* **2015**, *89* (4), 654−662.
(56) Needham, T. E.; Paruta, A. N.; Gerraughty, R. J. Solubility of Amino Acids in Pure Solvent Systems. *J. Pharm. Sci.* **1971**, *60* (4), 565−567.
(57) Mahali, K.; Roy, S.; Dolui, B. K. Solubility and Solvation Thermodynamics of a Series of Homologous α-Amino Acids in Nonaqueous Binary Mixtures of Ethylene Glycol and Dimethyl Sulfoxide. *J. Chem. Eng. Data* **2015**, *60* (5), 1233−1241.
(58) Jochum, F. D.; Theato, P. Temperature- and Light-Responsive Polyacrylamides Prepared by a Double Polymer Analogous Reaction of Activated Ester Polymers. *Macromolecules* **2009**, *42* (16), 5941−5945.
(59) Chiantore, O. Polymer-Substrate Interactions in Size Exclusion Chromatography with Silica Gels and Pure Solvents. *J. Liq. Chromatogr.* **1984**, *7* (1), 1−11.
(60) Echeverria, C.; Peppas, N. A.; Mijangos, C. Novel Strategy for the Determination of UCST-like Microgels Network Structure: Effect on Swelling Behavior and Rheology. *Soft Matter* **2012**, *8* (2), 337−346.
(61) Jasinski, J.; Wilde, M. V.; Voelkl, M.; Jérôme, V.; Fröhlich, T.; Freitag, R.; Scheibel, T. Tailor-Made Protein Corona Formation on Polystyrene Microparticles and Its Effect on Epithelial Cell Uptake. *ACS Appl. Mater. Interfaces* **2022**, *14* (41), 47277−47287.
(62) Swieton, J.; Kaminski, K.; Miklosz, J.; Mogielnicki, A.; Kalaska, B. Anionic and Cationic Block Copolymers as Promising Modulators of Blood Coagulation. *Eur. Polym. J.* **2023**, *199*, No. 112452.
(63) Dailing, E. A.; Kilchrist, K. V.; Tierney, J. W.; Fletcher, R. B.; Evans, B. C.; Duvall, C. L. Modifying Cell Membranes with Anionic Polymer Amphiphiles Potentiates Intracellular Delivery of Cationic Peptides. *ACS Appl. Mater. Interfaces* **2020**, *12* (45), 50222−50235.
(64) Jiang, Z.; Liu, H.; He, H.; Yadava, N.; Chambers, J. J.; Thayumanavan, S. Anionic Polymers Promote Mitochondrial Targeting of Delocalized Lipophilic Cations. *Bioconjugate Chem.* **2020**, *31* (5), 1344−1353.
(65) Griffin, W. C. Classification of Surface-Active Agents by "HLB. *J. Cosmet. Sci.* **1949**, *1*, 311−326.
(66) Egan, R. W. Hydrophile-Lipophile Balance and Critical Micelle Concentration as Key Factors Influencing Surfactant Disruption of Mitochondrial Membranes. *J. Biol. Chem.* **1976**, *251* (14), 4442−4447.
(67) Rideal, E.; Taylor, F. H. On Haemolysis by Anionic Detergents. *Proc. R. Soc. London, Ser. B* **1957**, *146* (923), 225−241, DOI: 10.1098/rspb.1957.0007.
(68) Manaargadoo-Catin, M.; Ali-Cherif, A.; Pougnas, J.-L.; Perrin, C. Hemolysis by Surfactants—A Review. *Adv. Colloid Interface Sci.* **2016**, *228*, 1−16.
(69) Lichtenberg, D.; Robson, R. J.; Dennis, E. A. Solubilization of Phospholipids by Detergents Structural and Kinetic Aspects. *Biochim. Biophys. Acta, Rev. Biomembr.* **1983**, *737* (2), 285−304, DOI: 10.1016/0304-4157(83)90004-7.
(70) Bochicchio, D.; Panizon, E.; Monticelli, L.; Rossi, G. Interaction of Hydrophobic Polymers with Model Lipid Bilayers. *Sci. Rep.* **2017**, *7* (1), No. 6357, DOI: 10.1038/s41598-017-06668-0.
(71) Ohshima, H. A Simple Expression for Henry's Function for the Retardation Effect in Electrophoresis of Spherical Colloidal Particles. *J. Colloid Interface Sci.* **1994**, *168* (1), 269−271.
(72) Leiske, M. N.; Walker, J. A.; Zia, A.; Fletcher, N. L.; Thurecht, K. J.; Davis, T. P.; Kempe, K. Synthesis of Biscarboxylic Acid Functionalised EDTA Mimicking Polymers and Their Ability to Form Zr(Iv) Chelation Mediated Nanostructures. *Polym. Chem.* **2020**, *11* (16), 2799−2810.
(73) Richter, F.; Leer, K.; Martin, L.; Mapfumo, P.; Solomun, J. I.; Kuchenbrod, M. T.; Hoeppener, S.; Brendel, J. C.; Traeger, A. The Impact of Anionic Polymers on Gene Delivery: How Composition and Assembly Help Evading the Toxicity-Efficiency Dilemma. *J. Nanobiotechnol.* **2021**, *19* (1), 292.

https://doi.org/10.1021/acspolymersau.3c00048
ACS Polym. Au 2024, 4, 222−234

Supporting information

Amino-acid-derived anionic polyacrylamides with tailored hydrophobicity – physicochemical properties and cellular interactions

Jonas De Breuck,[a] Michael Streiber,[b,c] Michael Ringleb,[b,c] Dennis Schröder,[a,d] Natascha Herzog,[a] Ulrich S. Schubert,[b,c] Stefan Zechel,[b,c] Anja Traeger,[b,c] Meike N. Leiske[a,d,*]

[a]Macromolecular Chemistry, University of Bayreuth, Universitätsstraße 30, 95447 Bayreuth, Germany

[b]Laboratory of Organic and Macromolecular Chemistry (IOMC), Friedrich Schiller University Jena, Humboldtstrasse 10, 07743 Jena, Germany

[c]Jena Center for Soft Matter (JCSM), Friedrich Schiller University Jena, Philosophenweg 7, 07743 Jena, Germany

[d]Bavarian Polymer Institute, Universitätsstraße 30, 95447 Bayreuth, Germany

*correspondence to: meike.leiske@uni-bayreuth.de

Supplementary results

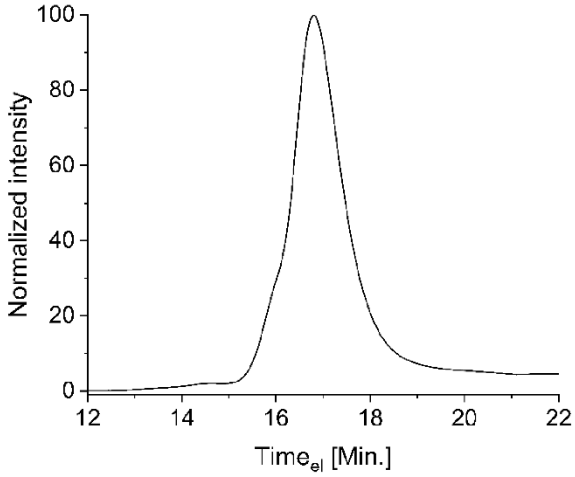


Figure S1. SEC (DMAc + 0.21 w% LiCl) elugram of PPFPA.

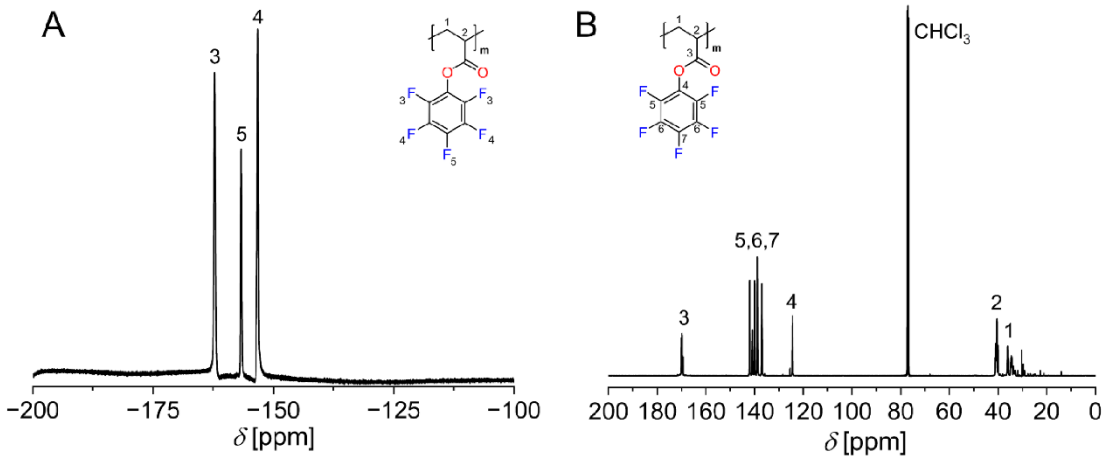


Figure S2. A: ^{19}F NMR ($CDCl_3$, 280 MHz) of PPFPA. B: ^{13}C NMR ($CDCl_3$, 125 MHz) of PPFPA

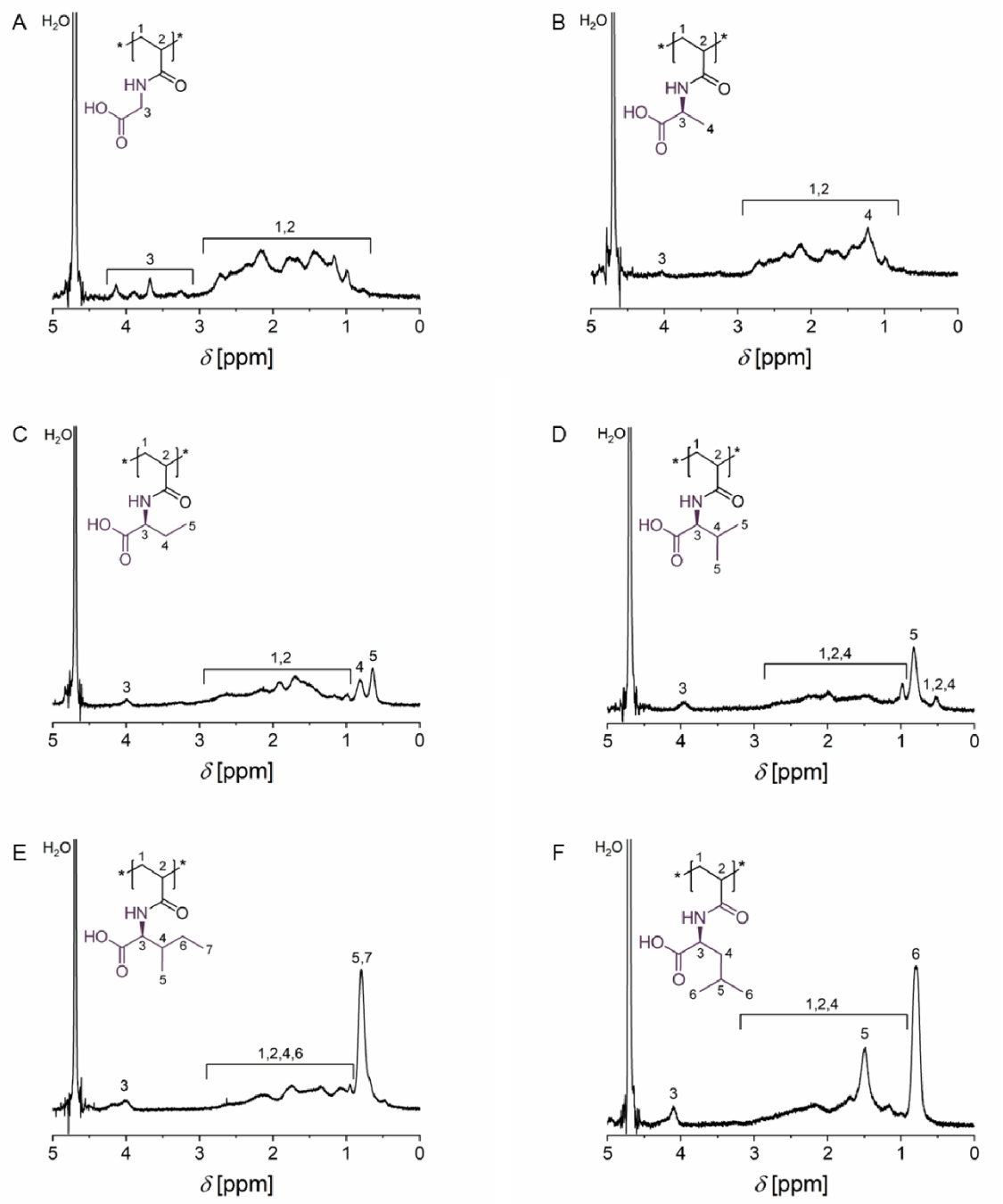


Figure S3. ^{1}H NMR (d-DPBS, 250 MHz) spectra of P(AA-OH-AAm). A: P(Gly-OH-AAm). B: P(Ala-OH-AAm). C: P(Abu-OH-AAm). D: P(Val-OH-AAm). E: P(Ile-OH-AAm). F: P(Leu-OH-AAm).

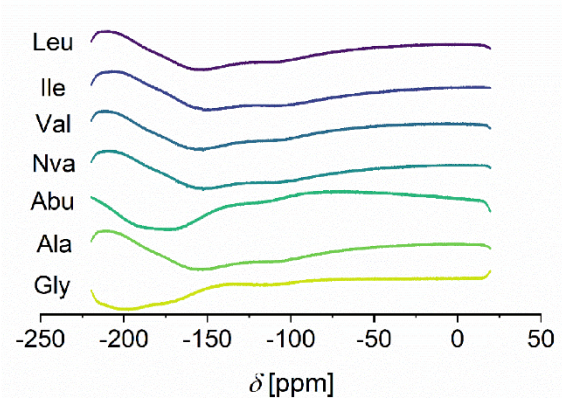


Figure S4. ^{19}F NMR (d-DPBS, 235 MHz) spectra of P(AA-OH-AAm).

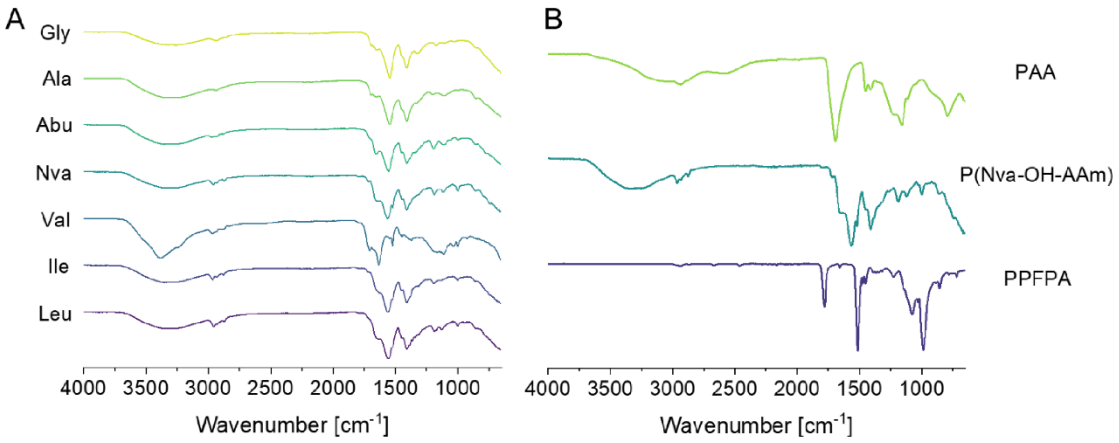


Figure S5. FTIR spectra of A: P(AA-OH-AAm). B: PAA, P(Nva-OH-Aam) and PPFPA (top to bottom)

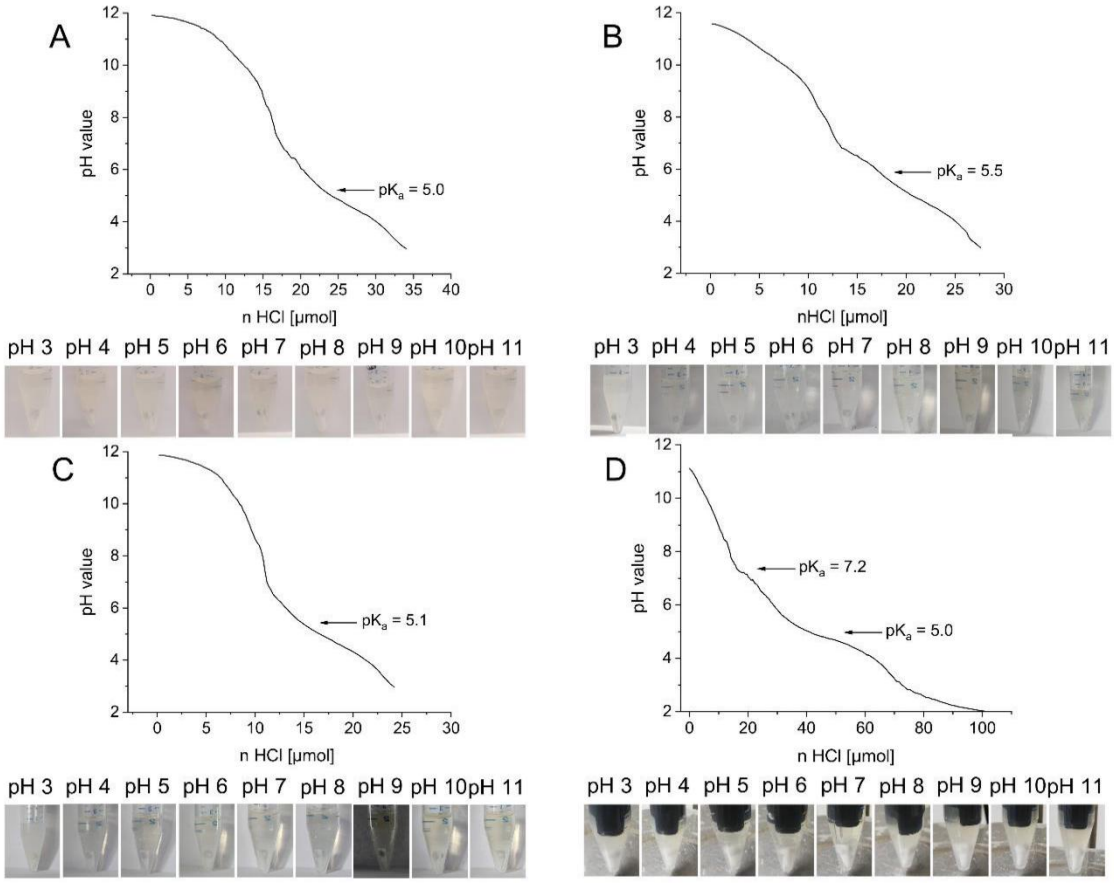


Figure S6. Titration of P(AA-OH-AAm) with linear alkyl substituents (5 mg mL^{-1} in H_2O) with HCl (0.1 M in H_2O). A: P(Gly-OH-AAm). B: P(Ala-OH-AAm). C: P(Abu-OH-AAm). D: P(Nva-OH-AAm).

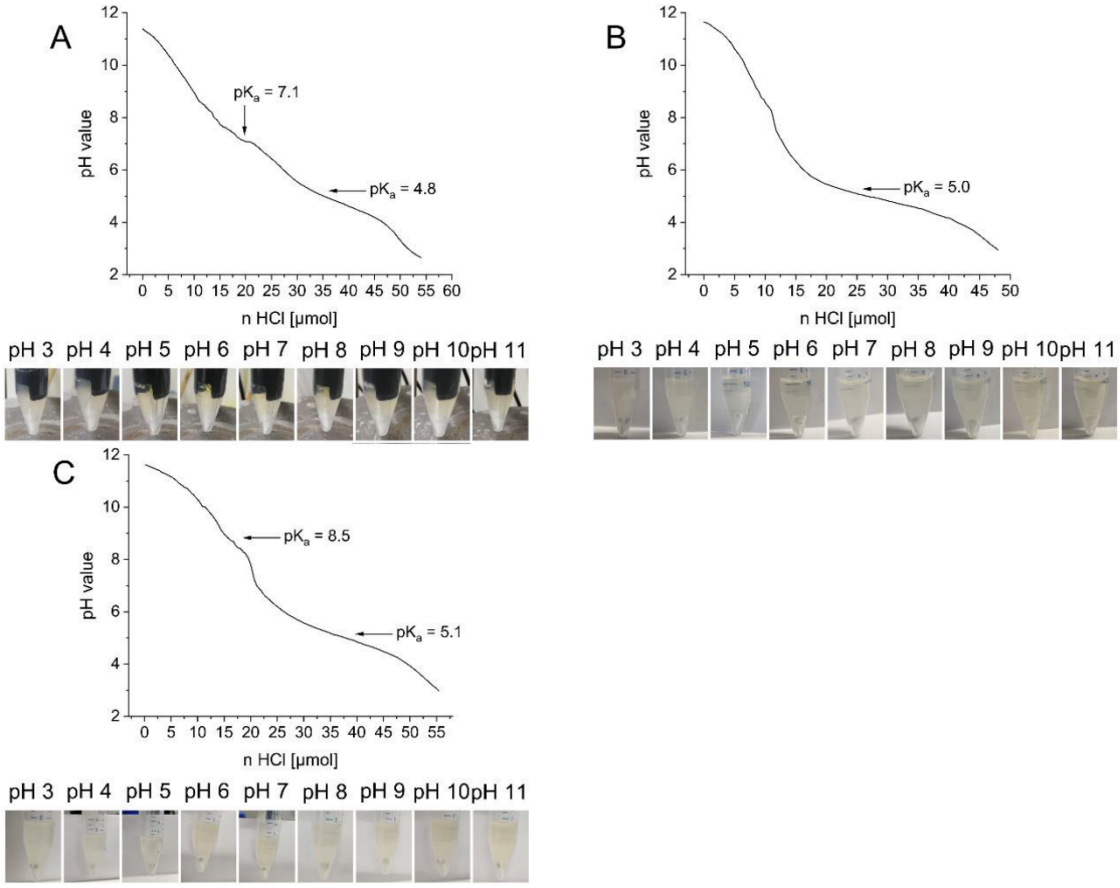


Figure S7. Titration of P(AA-OH-AAm) with branched alkyl substituents (5 mg mL^{-1} in H_2O) with HCl (0.1 M in H_2O). A: P(Val-OH-AAm) B: P(Ile-OH-AAm). C: P(Leu-OH-AAm).

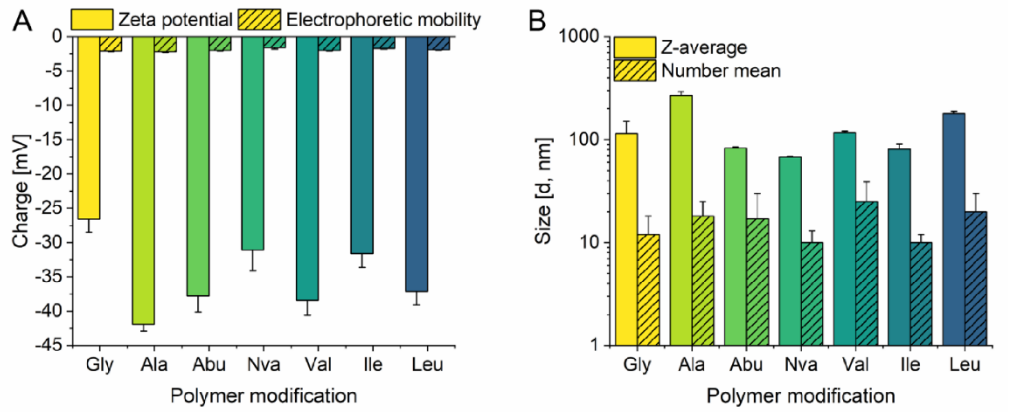


Figure S8. A: Charge and B: size of P(AA-OH-AAm) in DPBS (2 mg mL^{-1}) determined by ELS (A) and DLS (B) measurements.

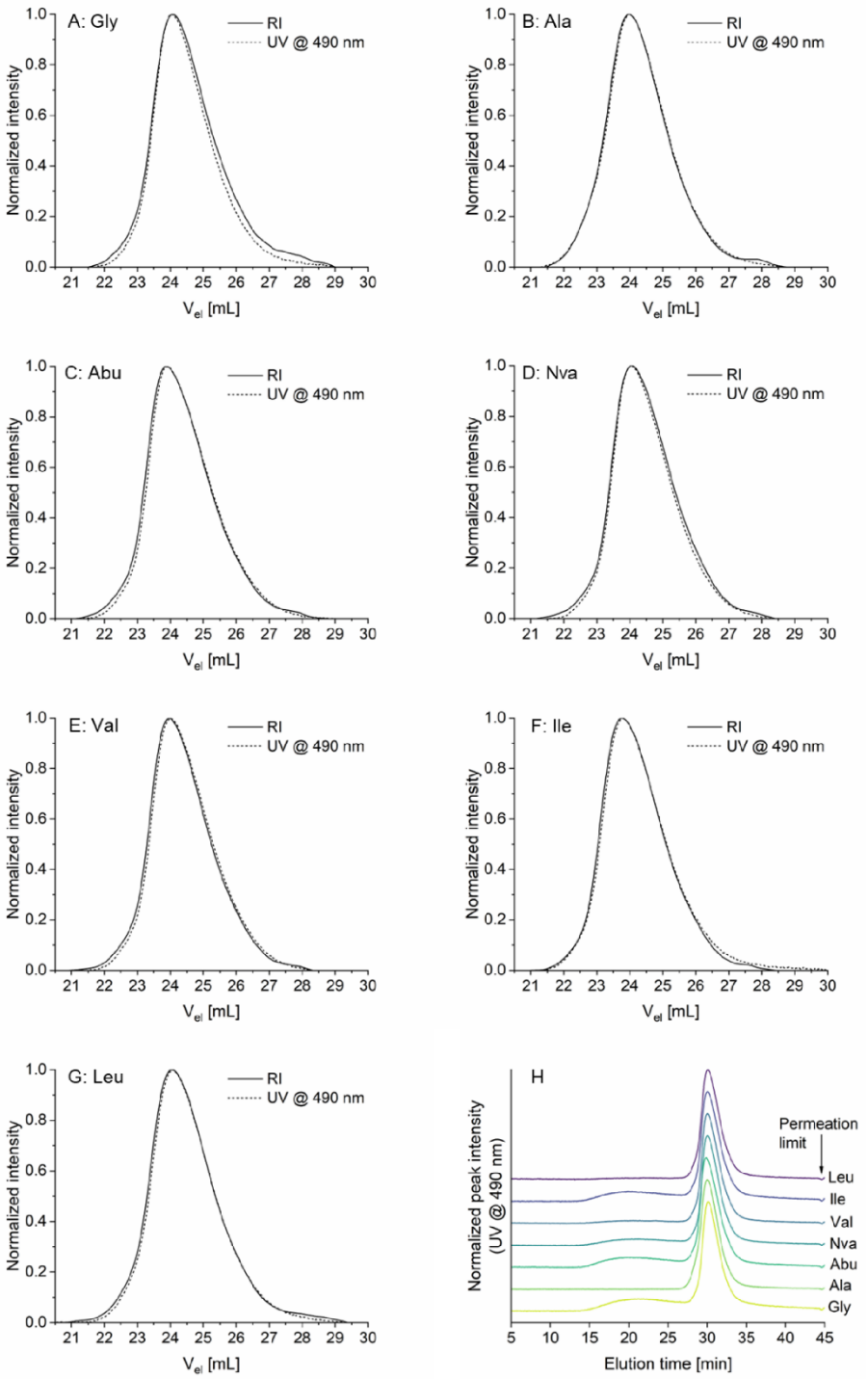


Figure S9. Size-exclusion chromatograms (0.07 M aq. Na_2HPO_4) of 6-aminofluorescein (6-AF) labeled P(AA-OH-AAm). A: P(Gly-OH-AAm)-6AF. B: P(Ala-OH-AAm)-6AF. C: P(Abu-OH-AAm)-6AF. D: P(Nva-OH-AAm)-6AF. E: P(Val-OH-AAm)-6AF. F: P(Ile-OH-AAm)-6AF. G: P(Leu-OH-AAm)-6AF. G: Raw elution time showing the absence of free dye.

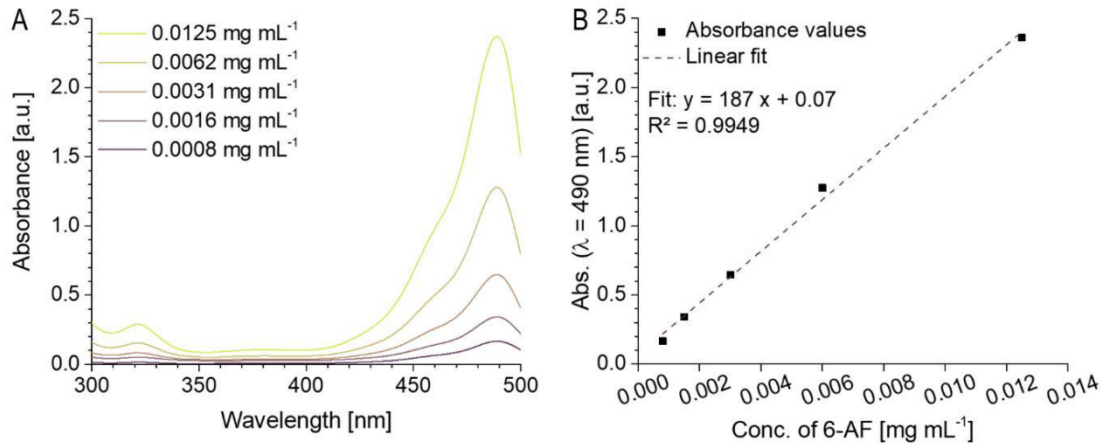


Figure S10. Absorbance and resulting calibration of 6-AF in DPBS at indicated concentrations measured by UV vis.

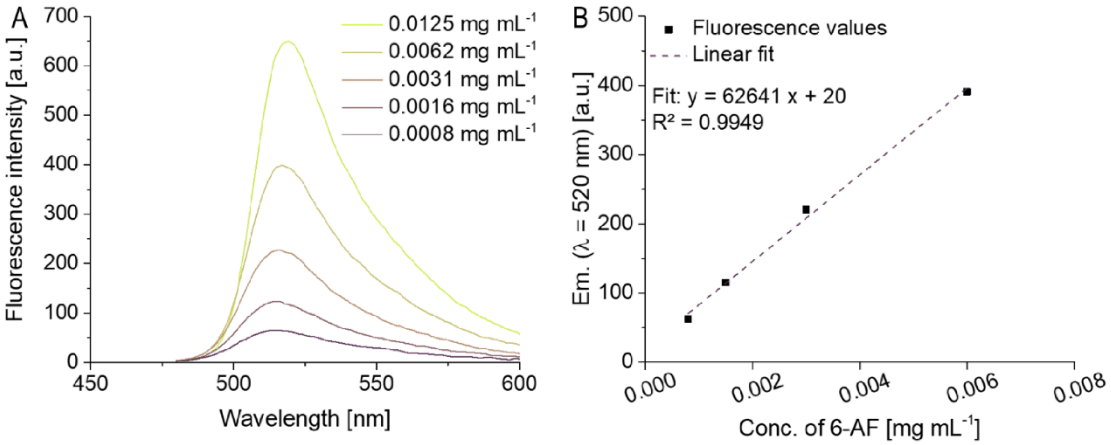


Figure S11. Fluorescence and resulting calibration of 6-AF in DPBS at indicated concentrations measured by fluorescence. λ_{ex} = 450 nm.

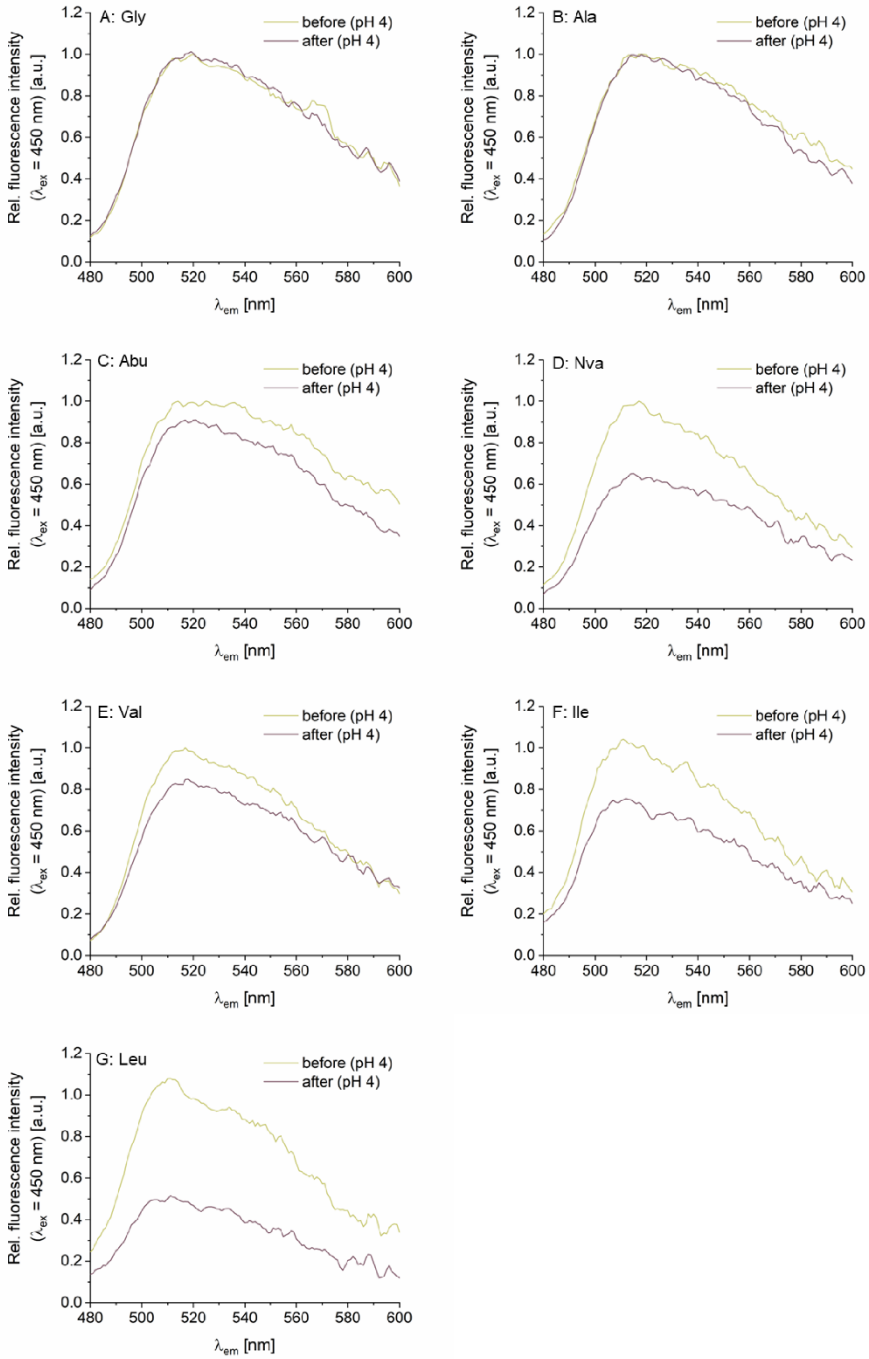


Figure S12. Fluorescence of polymer solutions. 6AF-labeled polymers with indicated amino acid substituent were dissolved in DI H_2O (c = 0.1 mg mL^{-1}). The final solution possessed a pH-value of 4. An equal volume of chloroform was added, and the solutions were vortexed for 20 seconds. The fluorescence of the aqueous phase was measured prior and after the mixing process. A: P(Gly-OH-AAm)-6AF. B: P(Ala-OH-AAm)-6AF. C: P(Abu-OH-AAm)-6AF. D: P(Nva-OH-AAm)-6AF. E: P(Val-OH-AAm)-6AF. F: P(Ile-OH-AAm)-6AF. G: P(Leu-OH-AAm)-6AF.

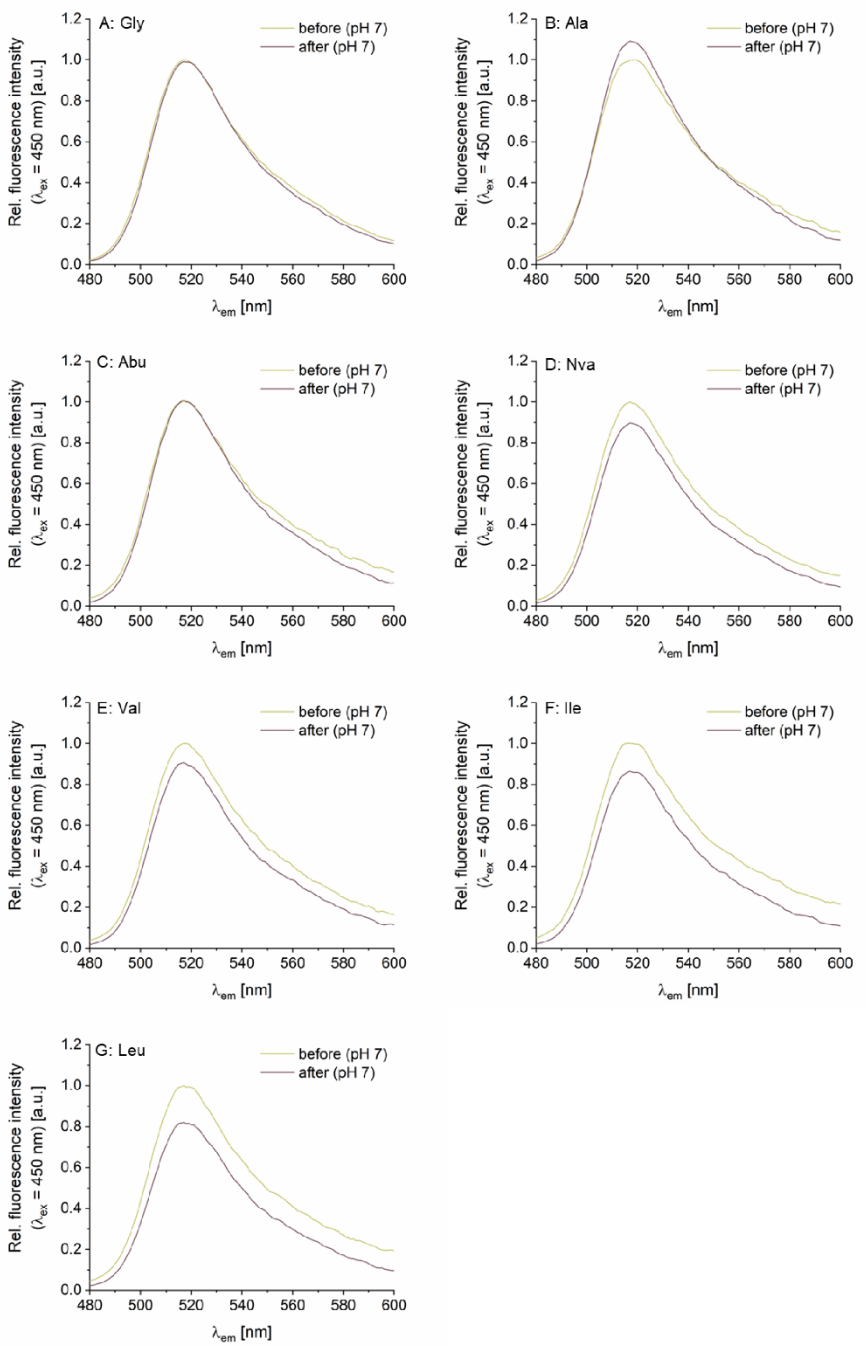


Figure S13. Fluorescence of polymer solutions. 6AF-labelled polymers with indicated amino acid substituent were dissolved in DI H_2O (c = 0.1 mg mL^{-1}). The final solution possessed a pH-value of 7. An equal volume of chloroform was added, and the solutions were vortexed for 20 seconds. The fluorescence of the aqueous phase was measured prior and after the mixing process. A: P(Gly-OH-AAm)-6AF. B: P(Ala-OH-AAm)-6AF. C: P(Abu-OH-AAm)-6AF. D: P(Nva-OH-AAm)-6AF. E: P(Val-OH-AAm)-6AF. F: P(Ile-OH-AAm)-6AF. G: P(Leu-OH-AAm)-6AF.

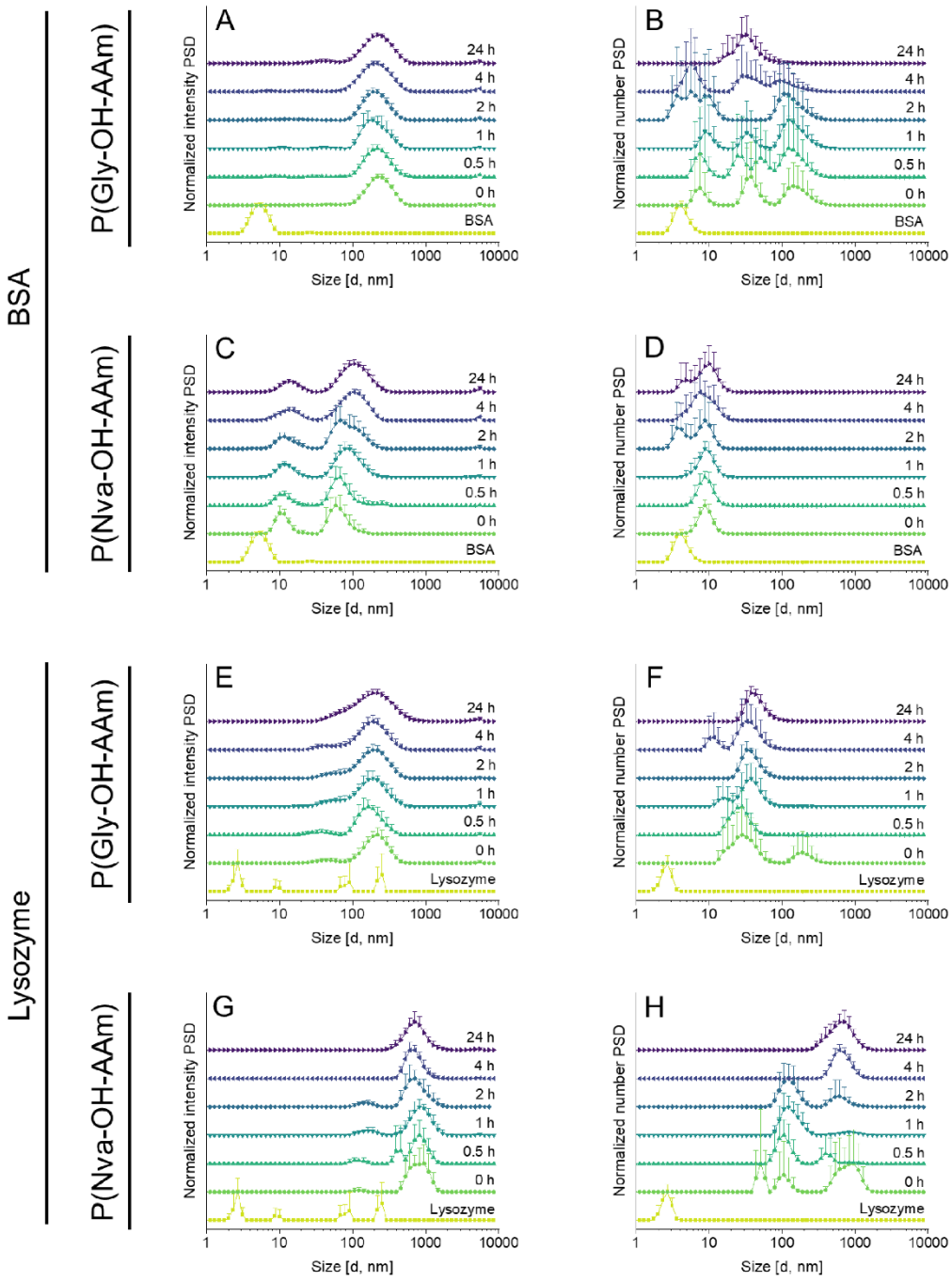


Figure S14. Intensity and number size distributions of polymer-protein-mixtures. Concentrations of polymers and proteins were 0.5 mg mL^{-1} each in DPBS. Sizes were analyzed by DLS measurements at 37 °C. Values (scatter) represent the mean and SD of five measurements with three runs each. Dashed lines do not represent measured values. A and B: P(Gly-OH-AAm) and BSA. C and D: P(Nva-OH-AAm) and BSA. E and F: P(Gly-OH-AAm) and lysozyme. G and H: P(Nva-OH-AAm) and lysozyme.

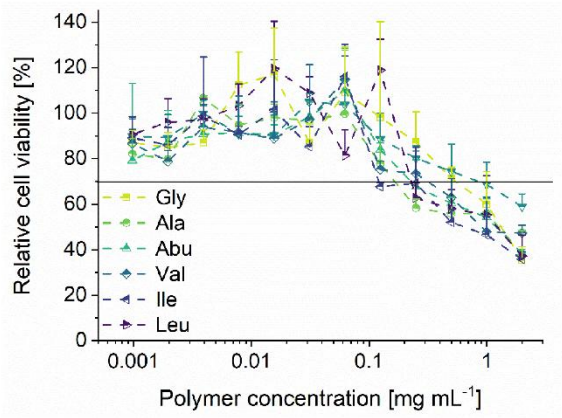


Figure S15. Cell viability of L929 mouse fibroblasts after incubation with different P(AA-OH-AAm) for 24 h. Cell viability was determined by MTT assay. Cells without polymer treatment served as negative control (NC, 100% cell viability). Values shown are relative to the NC. Cells treated with 20% DMSO served as positive control (PC, 0% cell viability, data not shown)

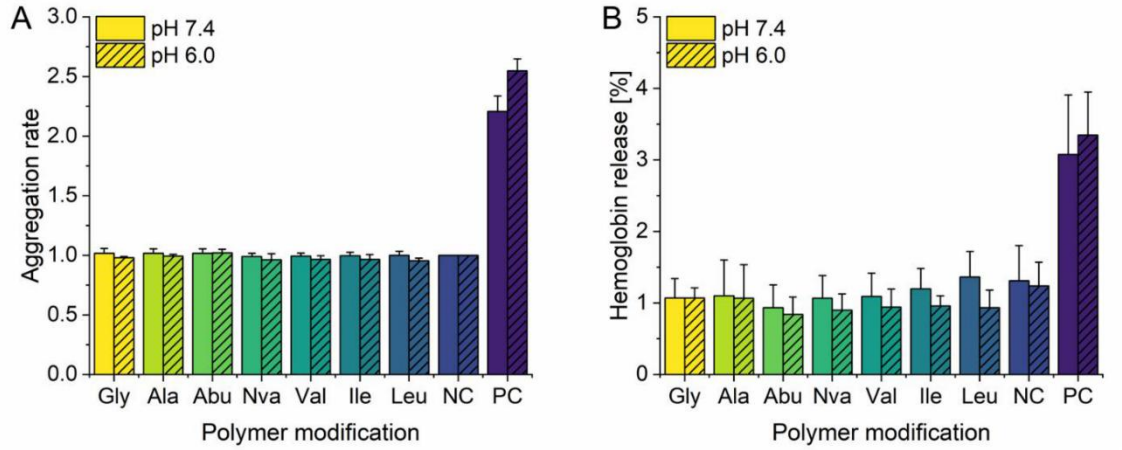


Figure S16. Hemocompatibility of P(AA-OH-AAm). A: Hemoglobin release assay of erythrocytes after incubation with different polymers (c = 1 mM_{RU}) for 1 h. A value less than 2% hemoglobin release is classified as non-hemolytic. B: Erythrocyte aggregation in the presence of different polymers. NC: DPBS. PC: bPEI.

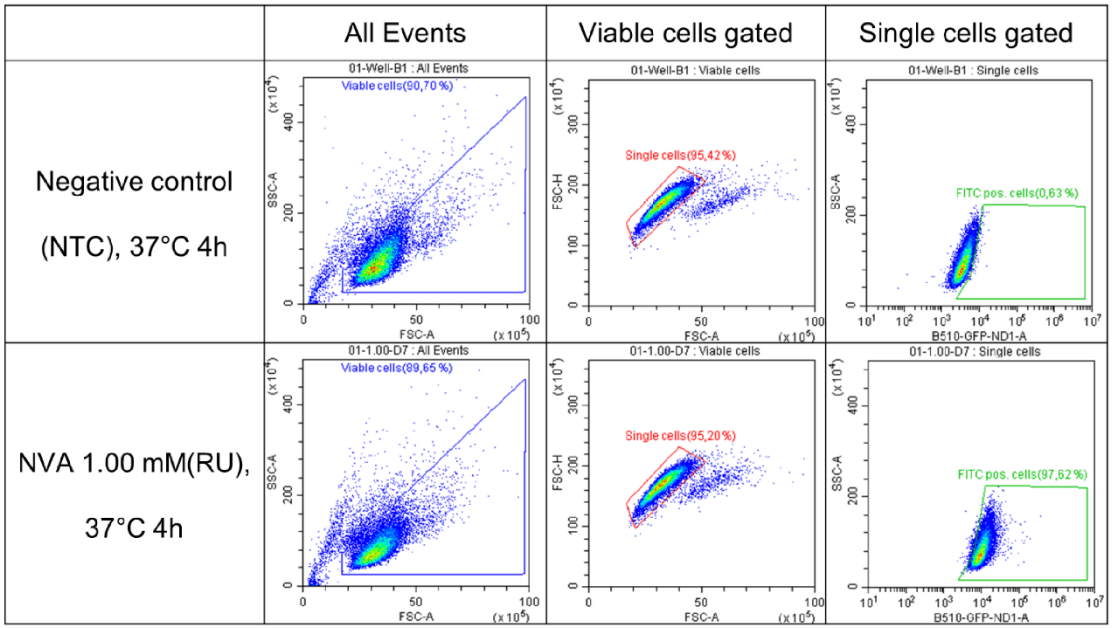


Figure S17. Gating strategy Cell association assay I. Viable cells were gated according to the FSC/SSC pattern. Subsequently the single cells were discriminated from doublets in the sample using the area of FSC signal plotted against the FSC height. 6-AF positive cells were identified by gating the single cells to the negative control.

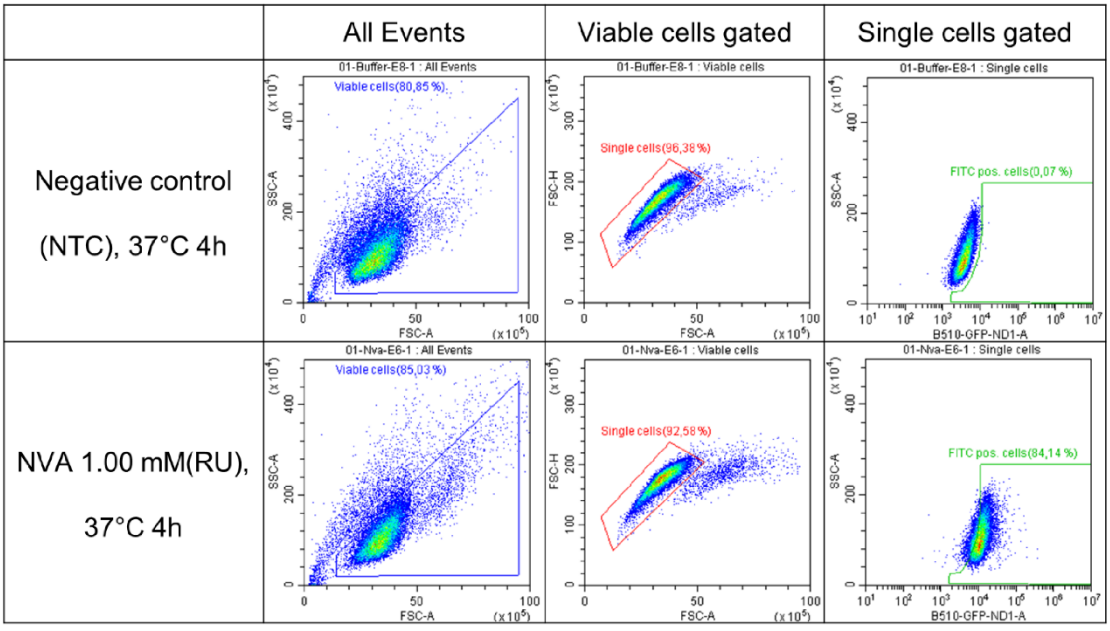


Figure S18. Gating strategy Cell association assay II. Viable cells were gated according to the FSC/SSC pattern. Subsequently the single cells were discriminated from doublets in the sample using the area of FSC signal plotted against the FSC height. 6-AF positive cells were identified by gating the single cells to the negative control.

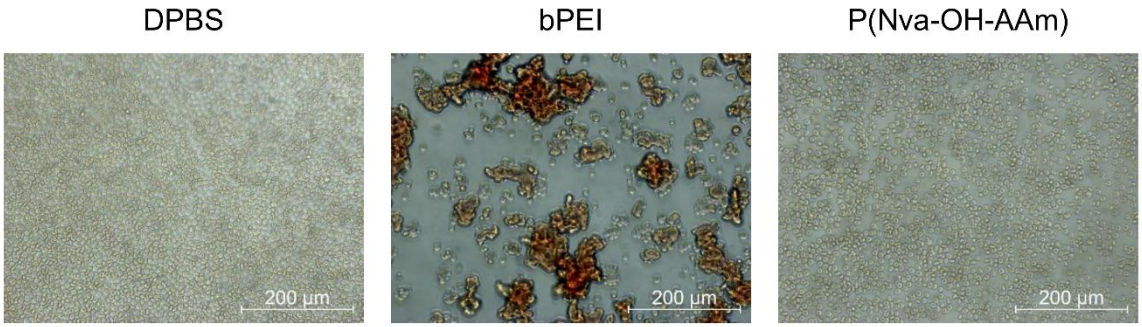


Figure S19. Microscopy images of erythrocyte aggregation upon incubation with indicated polymers. Images were obtained after aggregation assay (see Figure S15).

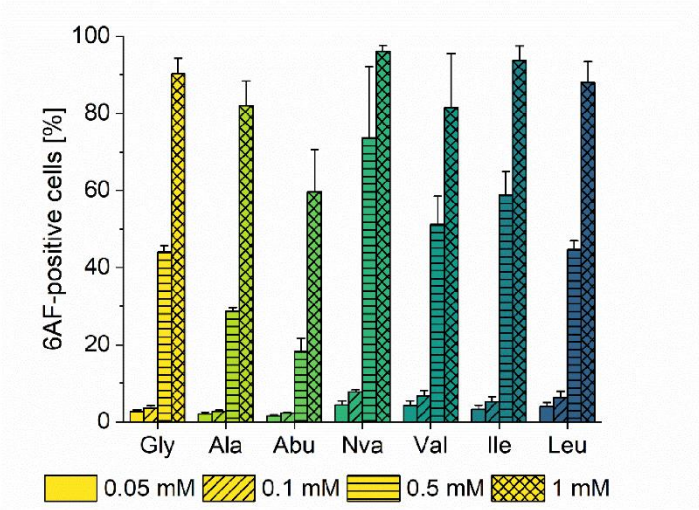


Figure S20. Concentration-dependent cell association of 6AF-labelled P(AA-OH-AAm) with L929 fibroblasts determined *via* flow cytometry measurements. Concentrations refer to repeating units. Incubation for 4 h at 37 °C. 20,000 cells per well in 250 µL medium (48-well plate).

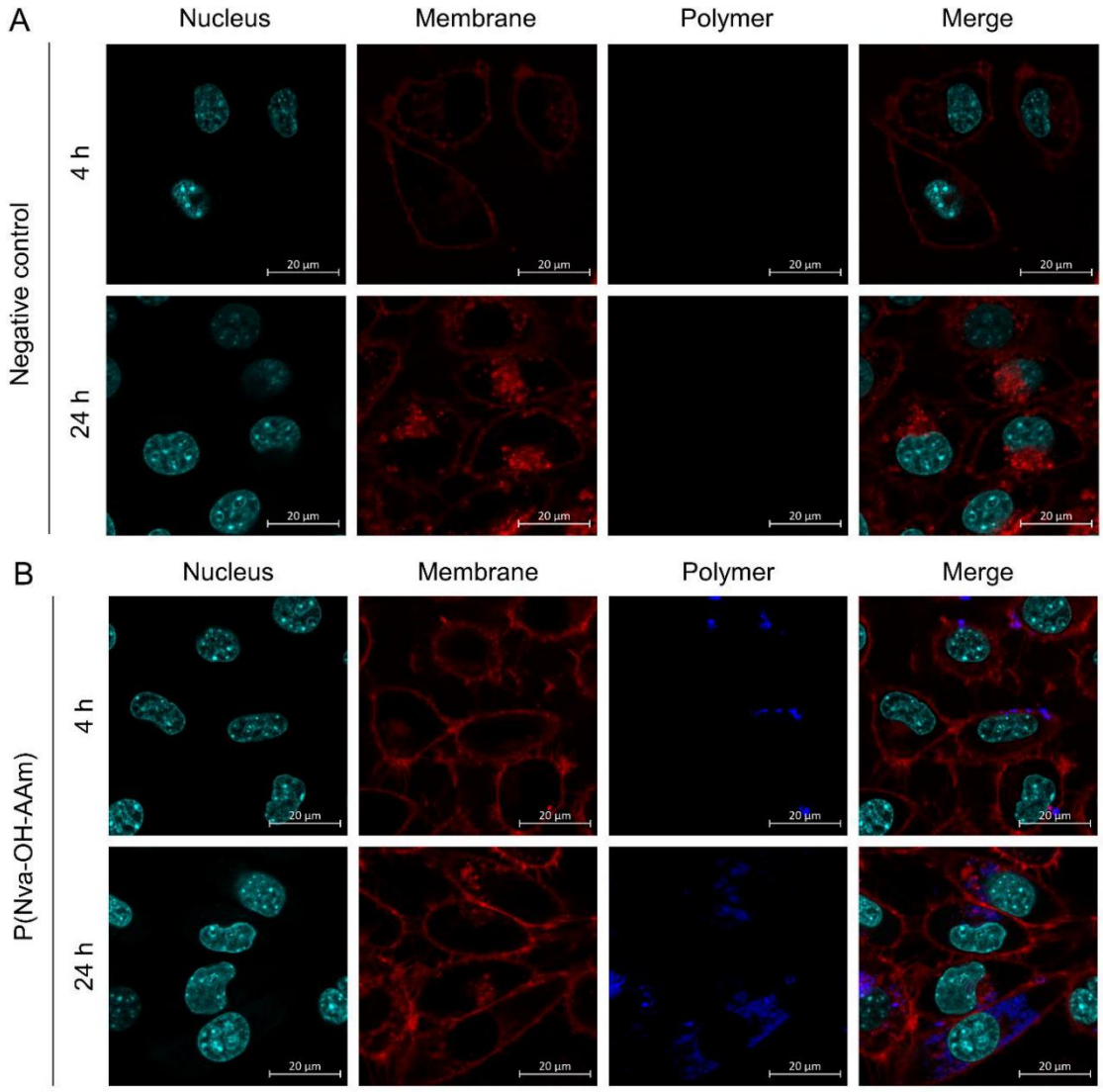


Figure S21. L929 fibroblasts visualized by CLSM. Cyan: Hoechst 33342/nucleus. Red: Membrane tracker deep red/cell membrane. Blue: 6AF/polymer channel. A: Cells were treated with PBS as control experiment for polymer treatment. B: Cells were treated with P(Nva-OH-AAm).



Figure S22. Visual appearance of polymeric dispersions. 6AF-labelled polymers with indicated amino acid substituent were dissolved in DPBS ($c_{polymer}$ = 1 mg mL^{-1}). An equal volume of chloroform was added, and the solutions were vortexed for 20 seconds. Photographs were taken after the mixing process. From left to right: P(Gly-OH-AAm)-6AF; P(Ala-OH-AAm)-6AF; P(Abu-OH-AAm)-6AF; P(Nva-OH-AAm)-6AF.

Table S1. Properties obtained by DLS measurements in DPBS (polymer concentration: 2 mg mL^{-1}). Values represent the mean and standard deviation of five measurements with three runs each.

Polymer	z-average [d, nm]	Number mean [d, nm]	PdI	Mean count rate	Intercept
P(Gly-OH-AAm)	115 ± 36	12 ± 6	0.62 ± 0.17	200 ± 12	0.92 ± 0.01
P(Ala-OH-AAm)	256 ± 34	24 ± 14	0.68 ± 0.12	135 ± 7	0.94 ± 0.04
P(Abu-OH-AAm)	83 ± 2	17 ± 13	0.48 ± 0.06	292 ± 9	0.93 ± 0.01
P(Nva-OH-AAm)	68 ± 1	13 ± 8	0.42 ± 0.05	256 ± 5	0.93 ± 0.01
P(Val-OH-AAm)	142 ± 56	27 ± 14	0.48 ± 0.11	147 ± 15	0.97 ± 0.00
P(Ile-OH-AAm)	81 ± 10	10 ± 2	0.49 ± 0.13	305 ± 19	0.92 ± 0.01
P(Leu-OH-AAm)	178 ± 8	27 ± 19	0.70 ± 0.09	473 ± 20	0.92 ± 0.01

Table S2. Properties obtained by ELS measurements in DPBS (polymer concentration: 2 mg mL^{-1}). Values represent the mean and standard deviation of three measurements with three runs each.

Polymer	Zeta potential [mV]	Electrophoretic mobility [µmcm/Vs]	Mean count rate
P(Gly-OH-AAm)	-26.6 ± 1.9	-2.1 ± 0.1	555 ± 298
P(Ala-OH-AAm)	-41.9 ± 1.0	-2.2 ± 0.1	360 ± 147
P(Abu-OH-AAm)	-37.8 ± 2.3	-2.0 ± 0.1	735 ± 596
P(Nva-OH-AAm)	-31.1 ± 3.3	-1.6 ± 0.2	102 ± 39
P(Val-OH-AAm)	-38.4 ± 2.2	-2.0 ± 0.1	286 ± 50
P(Ile-OH-AAm)	-31.6 ± 1.9	-1.7 ± 0.1	333 ± 115
P(Leu-OH-AAm)	-37.1 ± 2.2	-1.9 ± 0.1	380 ± 248

Table S3. Results of the protein fouling study obtained by DLS measurements in DPBS (polymer concentration: 0.5 mg mL^{-1}; protein concentration: 0.5 mg mL^{-1}). *Pure protein samples were measured at a concentration of 1 mg mL^{-1}. Measurements were carried out at 37 °C. In-between measurements, samples were incubated at 37 °C while

shaking at 100 rpm. Values represent the mean and standard deviation of five measurements with three runs each.

Sample	Incubation time [h]	z-average [d, nm]	Number mean [d, nm]	PdI	Mean count rate	Intercept
BSA*	0	199 ± 181	4 ± 0	0.31 ± 0.21	374 ± 27	0.93 ± 0.05
Lysozyme*	0	2628 ± 827	3 ± 0	1.00 ± 0.00	148 ± 4	1.38 ± 0.10
P(Gly-OH-AAm) + BSA	0	192 ± 16	88 ± 80	0.40 ± 0.04	240 ± 4	0.96 ± 0.00
	0.5	181 ± 16	82 ± 69	0.45 ± 0.07	195 ± 14	0.97 ± 0.01
	1	178 ± 15	103 ± 75	0.45 ± 0.02	196 ± 1	0.97 ± 0.01
	2	174 ± 15	61 ± 74	0.44 ± 0.04	194 ± 3	0.97 ± 0.01
	4	163 ± 4	47 ± 53	0.46 ± 0.04	193 ± 2	0.97 ± 0.00
	24	157 ± 7	37 ± 15	0.49 ± 0.04	193 ± 2	0.96 ± 0.00
P(Gly-OH-AAm) + Lysozyme	0	171 ± 9	31 ± 11	0.44 ± 0.02	38 ± 3	0.98 ± 0.0
	0.5	173 ± 19	27 ± 6	0.42 ± 0.05	296 ± 9	0.97 ± 0.01
	1	167 ± 13	37 ± 12	0.44 ± 0.09	301 ± 9	0.97 ± 0.01
	2	161 ± 9	40 ± 6	0.43 ± 0.04	299 ± 9	0.96 ± 0.00
	4	160 ± 7	34 ± 15	0.43 ± 0.02	122 ± 4	0.98 ± 0.01
	24	153 ± 11	47 ± 7	0.36 ± 0.04	131 ± 8	0.97 ± 0.00
P(Nva-OH-AAm) + BSA	0	126 ± 51	9 ± 1	0.33 ± 0.08	147 ± 1	1.02 ± 0.03
	0.5	140 ± 66	9 ± 1	0.42 ± 0.13	182 ± 4	1.01 ± 0.04
	1	58 ± 14	9 ± 1	0.51 ± 0.22	188 ± 4	0.97 ± 0.01
	2	68 ± 37	7 ± 3	0.58 ± 0.24	191 ± 4	0.97 ± 0.03
	4	55 ± 4	9 ± 2	0.57 ± 0.09	191 ± 3	0.96 ± 0.00
	24	58 ± 7	9 ± 3	0.59 ± 0.04	207 ± 4	0.96 ± 0.01
P(Nva-OH-AAm) + Lysozyme	0	1883 ± 1365	536 ± 431	0.76 ± 0.17	383 ± 79	1.06 ± 0.13
	0.5	1054 ± 163	200 ± 126	0.74 ± 0.12	263 ± 9	1.00 ± 0.03
	1	835 ± 56	213 ± 45	0.59 ± 0.12	258 ± 4	0.97 ± 0.00
	2	802 ± 53	273 ± 185	0.66 ± 0.07	250 ± 2	0.97 ± 0.02
	4	709 ± 32	686 ± 63	0.24 ± 0.05	227 ± 6	0.95 ± 0.01
	24	676 ± 47	665 ± 66	0.16 ± 0.11	215 ±	0.95 ± 0.01

4.4 Impact of the polymer side-chain chemistry on interactions of amino-acid-derived polyelectrolytes with cells

Impact of the polymer side-chain chemistry on interactions of amino-acid-derived polyelectrolytes with cells

Jonas De Breuck,[a] Theresa M. Lutz,[a] Christian Jahns,[a] Jonas Debbeler,[b,c] Valérie Jérôme,[d] Ruth Freitag,[d,e] Anja Traeger,[b,c,f] Meike N. Leiske[a,g,*]

[a] Macromolecular Chemistry, University of Bayreuth, Universitätsstraße 30, 95447 Bayreuth, Germany

[b] Laboratory of Organic and Macromolecular Chemistry (IOMC), Friedrich Schiller University Jena, Humboldtstr. 10, 07743 Jena, Germany

[c] Jena Center for Soft Matter (JCSM), Friedrich Schiller University Jena, Philosophenweg 7, 07743 Jena, Germany

[d] Process Biotechnology, University of Bayreuth, Universitätsstraße 30, 95447 Bayreuth, Germany

[e] Bayreuth Center for Molecular Biosciences (BZMB), University of Bayreuth, Universitätsstraße 30, 95447 Bayreuth, Germany

[f] Department of Pharmaceutical Chemistry, Institute of Pharmacy, Friedrich Schiller University, Philosophenweg 14, Jena, Germany

[g] Bavarian Polymer Institute, Universitätsstraße 30, 95447 Bayreuth, Germany

*correspondence to: meike.leiske@uni-bayreuth.de

Abstract

Polyelectrolytes gained significant attention for their unique, potentially specific association with living cells. Here, the synthesis of lysine- and phenylaniline-derived polyelectrolytes via post-polymerisation modification (PPM) is presented. These were chosen based on already shown active uptake of amino acid-derived polyelectrolytes by cancer cells and, following, potential for selective interactions with target cells. The amidation of activated ester prepolymers with protected basic amino acids and their subsequent deprotection yields tailored amino acid-functionalised polyzwitterions comprising side-chain chirality. Similarly, the use of achiral neutral amino acids results in polyanionic analogues of these polyzwitterions. Via this strategy, a small library of five polymers was created, which enables the careful evaluation of structure-property relationships of polyelectrolytes and their interactions with cells. In particular, we study the

influence of side-chain motifs: (i) aliphatic *vs*. aromatic side chains, (ii) permanent *vs*. non-permanent charge, and (iii) zwitterionic *vs*. anionic patterns. High performance liquid chromatography (HPLC) measurements are performed to investigate the influence of both the charge character and aromaticity on the hydrophilicity of the polyelectrolytes. Response to changes in the pH value is studied by dynamic light scattering (DLS) and electrophoretic light scattering (ELS) at different pH values. Furthermore, polyelectrolyte stability under biologically relevant conditions, i.e., in the presence of model proteins and more complex protein mixtures from foetal bovine serum (FBS) is assessed by DLS. Association with cells from different cancer and non-cancer cell lines provides information regarding structural driving forces for association efficiency and specificity. Furthermore, fluorescent imaging shows fast uptake of polyanions into targeted cells making them interesting candidates for drug-delivery applications.

1. Introduction

Limited stability of therapeutic compounds and loss of activity upon modification are major drawbacks of conventional medicine.[1,2] One strategy to overcome these limitations is the encapsulation into stable carriers perhaps possessing targeting ligands to facilitate the selective delivery to the target site.[2,3] Besides protecting the drug, these carriers (e.g., composed of synthetic polymers) must possess low-fouling properties and cell-specific moieties (*e.g.* proteins, peptides, aptamers, polysaccharides or small biomolecules).[4] Building blocks capable of fulfilling these tasks ought to be identified. The engineering of polyelectrolytes has proven to be a powerful strategy to tailor functional molecules for such biomedical application. By systematically varying charge density[5], backbone architecture[6], and side-chain functionality[7], polyelectrolytes can be designed to control (i) intermolecular interactions such as polymer-protein interactions (*i.e.* reduce aggregation with proteins)[8], (ii) self-assembly to form higher-level structures for stable drug transport in the biological environment, and (iii) responsiveness to external stimuli to facilitate cellular uptake. The latter is important since therapeutic compounds are often cell membrane-impermeable and polyelectrolytes may overcome the membrane barrier efficiently.[9] After membrane engulfment via endocytosis, a rapid release of the therapeutics (i.e., endosomal escape) is desired to minimize degradation of the

therapeutic compound.[10] In literature, non-ionic polymers based on polyethylene glycol (PEG) are described as performant tools for reducing protein aggregation.[11,12] However, tumour cell specificity of the polymer itself is comparatively low, thereby calling for decoration with additional targeting ligands (e.g., antibodies), which is both, costly and time-consuming. The targeting efficiency of non-ionic polymers without these ligands is mostly based on the enhanced permeability and retention (EPR) effect[13] – a passive cell targeting method – which is less efficient in larger tumours due to their cellular heterogeneity and thus, intracellular carrier accumulation is limited.[14]

Contrarily to PEGylated carrier systems, polyelectrolytes may be designed to tackle this challenge[15] and show superior suitability for the design of next-generation systems: polyelectrolytes combine synthetic precision with selective binding, controlled release properties, tuneable solubility and biocompatibility.[15,16] For example, Fuji *et al.* showed that certain polyelectrolyte building blocks, namely zwitterionic polybetaines and amino-acid-derived polyzwitterions can actively accumulate in tumours.[17,18] They pass the cell membrane by non-specific transporter-mediated mechanisms, which offer a new platform for targeted, biocompatible cancer nanomedicine. In addition, amino-acid-derived polyelectrolytes show beneficial features based on their biomimetic properties.[15,16] Thus, these polymers have *e.g.*, antifouling properties due to their high charge density which strongly binds a hydration layer *via* electrostatic interactions.[19] This layer is much more stable than the one associated *via* hydrogen bonding with non-ionic polymers (*e.g.*, poly(N-acryloylmorpholine) (PNAM) or PEG)[20,21] since it forms a significant barrier that biomolecules must overcome before attaching directly to the polymers.[22] Moreover, polyelectrolytes show pH-responsiveness by altering *e.g.*, side chain hydrophobicity,[23,24] ions[25] and backbone[6] to govern stable polymer performance and transportation in the body at physiological pH values (7.4), while triggering intracellular release mechanisms such as endosomal escape at acidic pH levels (5.0-6.8).[26] Hence, the functionality of polyelectrolytes can be used for introduction of targetability and transmembrane transfer efficiency which are important tools to modulate a polymer (complex) for potential medical applications such as drug delivery, gene transfection, and tissue engineering.[27,28] Synthetically, the design of polyelectrolytes from amino acids is a widely explored field, see, *e.g.*, the recent review on the synthesis and polymerisation of amino acid-derived monomers by Leiske *et al.*.[29] Others have shown that lysine- and ornithine-based brushed

polyelectrolytes show low fouling behaviour as they did not show any aggregation towards undiluted serum for 24 h. Furthermore, pH- and temperature responsiveness has been observed for isoleucine- or leucine- and serine-based polymers which are interesting functionalities for various applications as stated above.[30,31] We previously explored the introduction of permanent positive charges in the polymers to generate zwitterions with a fixed cationic centre. With that, we stabilised the zwitterionic character over a wider pH range.[32]

Driven by our previous study, which examined impact of the backbone chemistry of amino-acid-derived polyzwitterions on their cellular specificity, we were curious about the effect of the side-chain chemistry as well as alterations to the ionic moiety itself. Similar attempts were previously pursued by Fujii *et al.* were the internalisation of various polymethacrylamides into cancer cells was studied. These authors showed that their polymers were actively taken up by cancer cells with excellent biocompatibility.[27] Inspired by these observations, our research aims to enhance the comparability between the developed polymer systems. We intended to achieve this by synthesizing polyelectrolytes using activated esters as precursors, thereby mitigating the influence of polymerisation degree (X_n) and dispersity on the final product. Especially, we were interested in the influence of the positive charge (presence/absence) and hydrophobicity (aromatic/alkyl-side chain) on protein and cell interactions. Therefore, a small library was created where different amino acid or amino acid-like structures are substituted in the side chain to obtain zwitterionic or anionic analogue amino acid-derived polyelectrolytes. To summarise, this study aims to elucidate how charge (zwitterionic/anionic), side chain hydrophobicity (aliphatic/aromatic groups) and persistent positive charge influences physicochemical parameters. Moreover, specific parameters based on those building blocks and influencing cellular interactions provide insights for the development of novel polyelectrolytes for biological applications.

2. Results and Discussion

2.1. Synthesis and characterisation of amino-acid-derived polyelectrolytes

Post-polymerisation modification (PPM) is a powerful tool to create highly comparable polymer libraries with variations in the side chain only. It further offers the advantage to

incorporate fluorescent labels in a straightforward manner. Within this study, we aimed to investigate amino-acid-derived polyelectrolytes and their interaction with biological matter. Particular interest was placed on the impact of the side-chain chemistry (i.e., the nature of the zwitterion as well as the spacer between the ionic group and the polymer backbone). Our group has previously reported the synthesis of amino-acid-derived polyanions via PPM, allowing to draw valuable conclusions from the polymer side-chain structure towards their cellular interactions.[5] Here, we synthesized polyelectrolytes that were obtained *via* PPM of poly(N-acryloyl succinimide) (PNAS), which was obtained from reversible addition-fragmentation chain transfer (RAFT) polymerisation and subsequently reacted with different amino acids to design three different polyzwitterions: (i) aliphatic spacer and permanent positive charge, (ii) aliphatic spacer and non-permanent positive charge, and (iii) aromatic spacer and non-permanent positive charge as well as two corresponding polyanions with (iv) aliphatic and (v) aromatic spacer (**Scheme 1**). Consequently, the PPM of PNAS with five different reagents was conducted: (i) Me_3Lys-OMe-NH_2,[32] (ii) N-Boc-lysine-OH (Boc-Lys-OH),[32] (iii) Boc-4-aminophenylalanine (Boc-4-AmPhe-OH), (iv) 6-aminohexanoic acid (6-AmHex-OH), and (v) 3-(4-aminophenyl)propanoic acid (4-AmPhenylPr-OH). The successful PPM was verified via ^{1}H NMR measurements, showing the disappearance of the characteristic peak of NAS at δ = 2.8 ppm after the reaction, indicating full conversion (Fig 1A, B and S5). In case of the aliphatic polymers P(Me_3Lys-OMe-AAm), P(Boc-Lys-OH-AAm), and P(Hex-OH-AAm) a peak shift from 2.8 ppm in the ^{1}H NMR spectra of the starting compounds (Fig S4) to δ = 3.0 to 3.1 ppm in the polymer ^{1}H NMR spectra (Fig 1A and S5) is observed, indicating a change in environment for the methylene group adjacent to the amine (H3), now positioned adjacent to the amide (Fig S4-5). The aromatic polymers P(Boc-Phe-OH-AAm) and P(PhenylPr-OH-AAm) are characterised by the broadened aromatic peaks compared to the ^{1}H NMR spectra (Fig 1C and S5) indicating the different chemical environment each aromatic peak has, something typically observed in ^{1}H NMR spectra of polymers and therefore complementary, to disappearance of the characteristic NAS peak, confirming successful PPM.

The zwitterionic polymers P(Lys-OH-AAm) and P(Phe-OH-AAm) were obtained by acidic deprotection of P(Boc-Lys-AAm) and P(Boc-Phe-OH-AAm). Successful deprotection was verified via ^{1}H-NMR as the Boc group signal at δ = 1.4 ppm disappeared (H8 and H7,

respectively, Fig S6-7). P(Me_3Lys-OH-AAm) as obtained from P(Me_3Lys-OMe-AAm) after basic hydrolysis as previously shown.[32]

Aqueous size exclusion chromatography (SEC) measurements were conducted to obtain information about the integrity of the polymer chain during the PPM, deprotection and to verify the absence of unwanted chain coupling (e.g., caused by aminolysis of the chain-transfer agent (CTA)). All polymers showed monomodal molar mass distributions (Fig S8). Deprotection changed the dispersity (Đ) of P(Lys-OH-AAm) significantly from 2.25 to 3.27 which is probably caused by the increased charge density and thus, the enhanced interaction with the stationary phase of the column. This also resulted in a significantly later elution time and therefore high decrease in apparent molar mass ($M_{n,app}$) from 17.2 kDa to 2.0 kDa. This effect was not observed for P(Phe-OH-AAm) were Đ was constant (2.47 to 2.14) which can indicate that the aromatic groups prevent interactions with the stationary phase. Generally, all polymers showed increased Đ, with 2.0 < Đ < 3.3 (Fig S8-9), compared to PNAS (Đ = 1.9) (Fig S2). This broadening may be attributed to the use of a more polar eluent and high density of charged groups in the polymers, which promote hydrogen bonding and ionic interactions with the stationary phase, leading to broadening. P(Lys-OH-AAm) showed the lowest apparent molar mass ($M_{n,app}$ = 1.9 kDa) and the longest elution time, likely due to its stronger column interactions which consequentially also resulted in the highest Đ (Đ = 3.3). The remaining polymers have a more comparable $M_{n,app}$ in the range of 10 kDa.

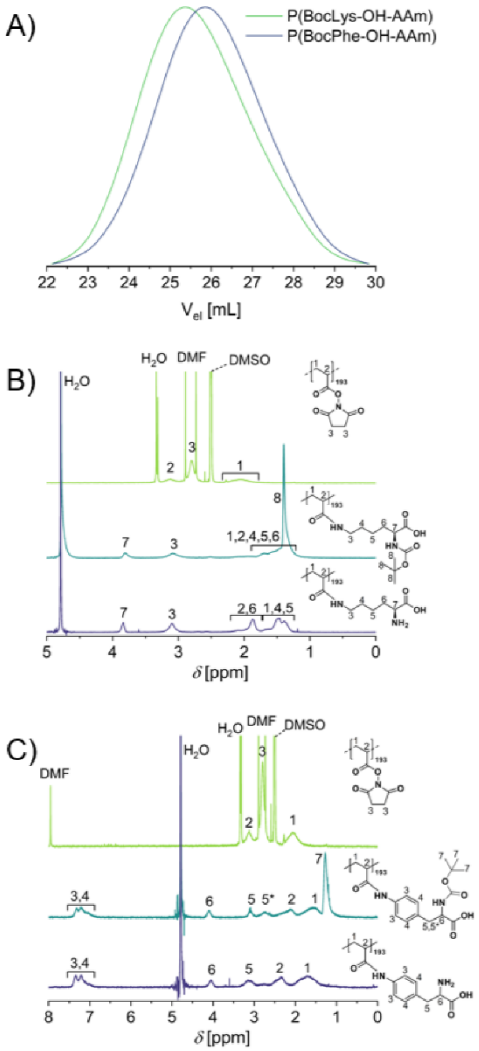
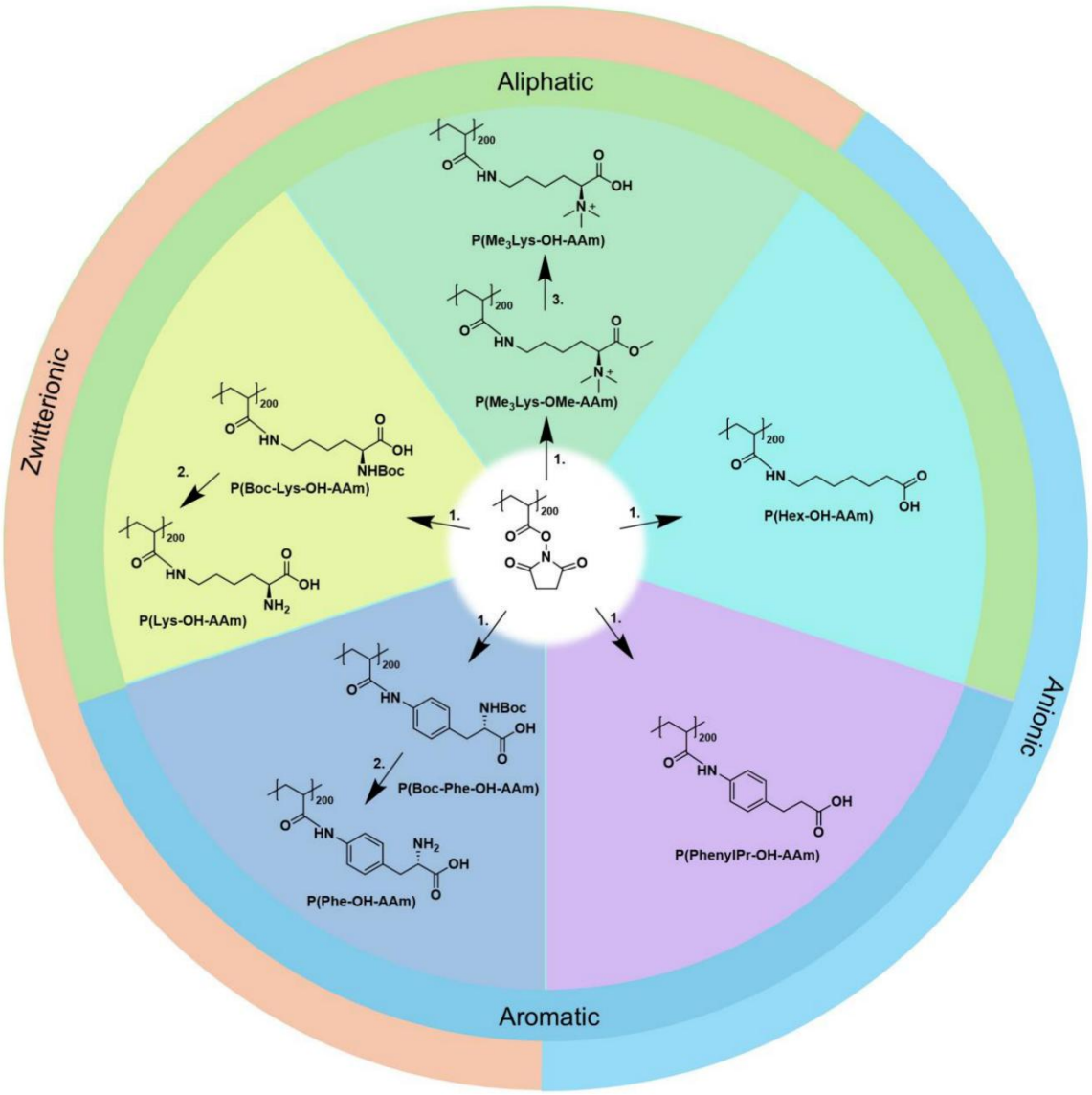


Figure 1: (A) Size-exclusion chromatograms (0.07 M aq. Na_2HPO_4) of P(BocLys-OH-AAm) (green) and P(BocPhe-OH-AAm) (blue). (B) ^{1}H NMR spectra (300 MHz) of poly(N-acryloyl succinimide) (green, DMSO), P(BocLys-OH-AAm) (cyan, D_2O) and P(Lys-OH-AAm) (blue, D_2O). (C) ^{1}H NMR spectra (300 MHz) of poly(N-acryloyl succinimide) (green, DMSO), P(BocPhe-OH-AAm) (cyan, D_2O) and P(Phe-OH-AAm) (blue, D_2O)

In addition, the cyanine-5 (Cy5)-labelled polymers (i.e., P(Lys-OH-AAm)-Cy5, P(Me_3Lys-OH-AAm)-Cy5, P(Hex-OH-AAm)-Cy5, P(Phe-OH-AAm)-Cy5 and P(PhenylPr-OH-AAm)-Cy5), which are needed for cell association experiments, were synthesised *via* sequential PPM with Cy5-amine and the respective amino acids. Those polymers were analysed as described above and the absence of unbound dye was verified by SEC measurements.[6]



Scheme 1: Synthesis of P(Boc-Lys-OH-AAm), P(Me_3Lys-OMe-AAm), P(Hex-OH-AAm), P(Boc-Phe-OH-AAm) and P(PhenylPr-OH-AAm) *via* PPM. (1) Et_3N, DMF and Boc-Lys-OH, Me_3Lys-Ome-NH_2, 6-AmHex-OH, Boc-4-AmPhe-OH and 4-AmPhenylPr-OH, respectively. 24 h at room temperatures (2) 50:50 v/v% [TFA/H2O], overnight at room temperature (3) 0.1 M NaOH, 24 h at room temperature.

Table 1: polymer characteristics.

Polymer	M^a [Da]	$X_{n,theo}{}^b$	$M_{n,theo}{}^b$ [kDa]	$M_{n,app}{}^c$ [kDa]	$Đ^c$	$t_{ret}{}^d$ [min.]
P(Lys-OH-AAm)	200.24	193	38.5	1.9	3.27	11.80
P(Me_3Lys-OH-AAm)	243.33	188	46.5	10.7[e]	1.96[e]	11.75
P(Hex-OH-AAm)	185.22	193	35.6	16.5	2.30	14.49
P(Phe-OH-AAm)	234.25	193	45.0	13.0	2.14	11.97
P(PhenylPr-OH-AAm)	219.24	193	42.1	11.0	2.71	15.94

[a]Molar mass (M) of repeating unit RU after deprotection. [b] $X_{n,theo}$ and $M_{n,theo}$ was calculated from ^{1}H-NMR. [c] $M_{n,app}$ and Đ was determined by aqueous SEC measurements (0.07M Na_2HPO_4) on a Suprema column set (PMA standard). [d] t_{ret} obtained from HPLC using a reversed phase column with a water/acetonitrile mixture + 0.1 vol% trifluoroacetic acid as eluent. [e]determined by aqueous SEC measurements (80/20 V% [H_2O/ACN] + 0.1M NaCl + 0.3% TFA) on a Novema column set (P2VP standard).).

2.2. pH-responsiveness and hydrophobicity

The application of polyelectrolytes in biological environments necessitates knowledge about their physicochemical properties, i.e., their hydrophobicity and responsiveness to changes in the pH value, which are important driving forces for interactions with cells and proteins. The Cy5-labelled polymers were subjected to HPLC measurements to gain information about their relative hydrophobicity. At eluent conditions (pH 2), chosen so the ionic state around the pK_a of the polymers cannot influence the elution time, the anionic polymers P(PhenylPr-OH-AAm)-Cy5 (polymeric retention time (t_{ret}) ~16 min) and P(Hex-OH-AAm)-Cy5 (t_{ret} ~15 min) were the most hydrophobic (Table 1 and Fig. 2A and S13). This increased hydrophobicity is explained by the protonation of the carboxylic acids[26] as the pH is below the reported pK_a (pH 4.88 for hexanoic acid and 4.37 for 3-phenylpropanoic acid) .[33] Furthermore, it was shown that the aromatic side chain influences the hydrophobicity of the polyanions. It is assumed that aromatic spacers feature an increased hydrophobicity due to the higher polarizability of the aromatic rings inducing stronger London dispersion forces with the C18 chains than a flexible alkyl group of similar size on the reversed phase column. In contrast, the zwitterionic polymers, P(Lys-OH-AAm)-Cy5, P(Me_3Lys-OH-AAm)-Cy5 and P(Phe-OH-AAm)-Cy5 showed a similar t_{ret} of ~12 min. Hence, side chain aromaticity or permanent positive charge has no influence

on the hydrophobicity of zwitterionic polymers at pH 2.0. Moreover, we calculated the theoretical partition coefficient (LogP) to obtain numerical values for comparison with the experimental data. All polymers except P(Lys-OH-AAm) exhibit a positive logP value which emphasizes the hydrophobic character of the polymers corroborating the HPLC data. Only P(Lys-OH-AAm) shows a negative logP value of -0.2319 indicating a slightly hydrophilic character. This could be attributed to the fact that the computational data is based on monomer calculations (one repeating unit per polymer). The algorithm of the trained machine learning model is designed for small molecules;[34] hence complete polymers were excluded from the calculation of logP and future application of algorithms for polymer-based systems could improve accuracy.

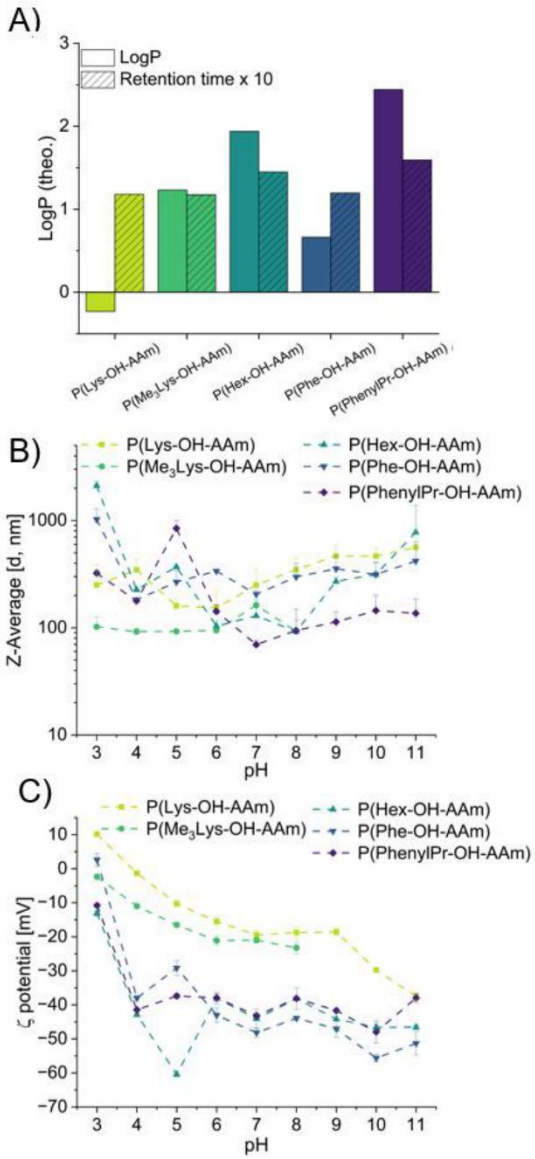


Figure 2: (A) Partition coefficients and retention time (x 10) of the polyelectrolytes. (B) Intensity weighted sizes and (C) ζ-potential of 2 mg mL^{-1} aqueous solutions at indicated pH values.

To support these findings, the effect of the pH on self-assembly was studied using DLS measurements performed at different pH values to get a general overview of its solubility behaviour at different pH. Additionally, changes in particle size serve as an indirect indicator of increased hydrophobicity, as hydrophobic interactions are expected to dominate upon protonation. This behaviour may be particularly relevant under biologically

relevant pH conditions (pH 6.0 – 7.5), even though the tested pH values exceed this range to give a general overview. With DLS measurements, we confirmed the decreased solubility of the polyanions by number size distributions (Fig S15C). For example, P(Hex-OH-AAm) showed hydrodynamic diameters (D_h) of > 1 000 nm at pH 3.0 and $D_h \approx$ 100 nm at pH 4.0 and 5.0. Moreover, number size distributions of P(PhenylPr-OH-AAm) (Fig S15E) showed a D_h between 1 and 10 nm at pH values between 6 and 11, as well as $D_h \approx$ 100 nm at pH 3.0 and 4.0. At pH 5.0, in comparison, the largest particles were present with diameters larger than 1000 nm. Visually, we could also see aggregation in the polymer solutions at pH values between 3 and 5 for P(Hex-OH-AAm) and P(PhenylPr-OH-AAm) (Fig S15). Those scenarios could be explained by the pK_a values of hexanoic acid, which is 4.88, and 3-phenylpropanoic acid, namely, 4.37.[33] Both values are close to the expected pK_a values of P(Hex-OH-AAm) and P(PhenylPr-OH-AAm), respectively, since the amide functional groups do not significantly influence the lower pK_a. As the polyanions are partially and fully protonated, around and below their pK_a it is also in agreement with our visual observation of aggregates and particle formation in light scattering measurements. The zwitterionic P(Lys-OH-AAm) showed an average particle diameter of around 10 nm across the whole measured pH range from pH 3.0 to pH 11.0 which was visually observed as a transparent solution. However, for the zwitterionic polymers with an aromatic motif in the side chain and permanent positive charge, aggregation was observed at pH 6.0 to 7.0 (P(Phe-OH-AAm)) and pH 7.0 (P(Me3Lys-OH-AAm)) with a D_h = 20 to 100 nm and $D_h \approx$160 nm, respectively.[35]

Additionally, ζ-potential measurements using electrophoretic light scattering (ELS) provided an insight into the surface charge of the polymers. ELS measurements (Fig 2C) showed that the zwitterionic amino acid side chains possessed a positive charge at pH 3.0 due to both the protonated carboxy group and the amine protonation at low pH values. This character changes to an overall negative net charge when the pH is raised to 4.0 or higher as both functional groups are deprotonated, and thus, the carboxyl group is present as an anion. The measurements for P(Lys-OH-AAm) are also in agreement with previous data of our group. We found that the isoelectric point (pI) is around pH = 4.3 which could be estimated by the expected pK_a. Previously derived amino-acid-derived polyzwitterions from the literature show similar values.[6,30,32] For P(Phe-OH-AAm), however, the pI observed by ELS was between pH 3.0 and 4.0 which is considerably lower than the amino

acid phenylalanine which is given to be approximately at pH = 5.5.[36] The lower apparent pI of P(Phe-OH-AAm) observed by ELS compared to free phenylalanine may result from preferential exposure of carboxylate groups at the particle surface, yielding a negative zeta potential at lower pH values. The aggregation detected by DLS near pH 6.0–7.0 further indicates that the polymer attains maximal hydrophobicity around the expected pI.

The side chains in both, P(Hex-OH-AAm) and P(PhenylPr-OH-AAm) only possess carboxyl groups that are mostly deprotonated. Even at pH 3.0, the particles were still negatively charged. But the moderate negative ζ-potentials at pH 3.0 (~ -10 mV) for both acid side chains indicated that most of the carboxyl acid groups were protonated and thus neutral. This results in a less negatively charged dispersion with reduced hydrophilic behaviour which can also be observed by the increased particle size of these polymers (from D_h 1 - 10 nm to ≈ 100 nm) during DLS measurement at the respective pH values (pH 3.0-5.0) (Fig S15C,E). It has already been shown that aggregation into larger structures under mildly acidic conditions, similar to extracellular pH values at tumour sites (pH ≈ 6.6),[37] can enhance retention within the tumour tissues as long as they exhibit a small hydrodynamic diameter under physiochemical conditions.

2.3. Interaction of amino-acid-derived polyelectrolytes with proteins

Our previous work demonstrated that both P(Lys-OH-AAm) and P(Me_3Lys-OH-AAm) exhibited minimal tendency for protein fouling when tested with model proteins such as lysozyme and bovine serum albumin (BSA) in phosphate-buffered saline (PBS) solution (pH 7.4).[32] Here, similarly, BSA was chosen as a negatively charged model protein, while lysozyme represented a positively charged model protein and tested in PBS solution.

To this extend, protein fouling tests were conducted here, as can be found in experimental section. DLS measurements were performed over 24 hours with the chosen model proteins in PBS solution at 37°C. Before the start of the measurement, the solution was mixed with promising candidates —P(Hex-OH-AAm), P(Phe-OH-AAm), and P(PhenylPr-OH-AAm)— which had not yet been tested for their protein fouling behaviour. Based on our previous results, it was expected that there would be strong interaction of the polyanions, P(Hex-OH-AAm) and P(PhenylPr-OH-AAm), with the positively charged

lysozyme.[5] P(Hex-OH-AAm), however, stayed stable (*e.g.* no aggregation observed) over the measured time period of 24 h while P(PhenylPr-OH-AAm) immediately formed large aggregates resulting in visible sedimentation at the bottom of the cuvette. Consequently, (almost) no particles were measured at the remaining time points as the sediment did not diffuse through the incident laser beam (Fig 3B). As expected, the polyanions did not form aggregates in the polymer-BSA mixture after 24 h. The fouling test of the zwitterionic, P(Phe-OH-AAm), did not show the formation of larger aggregates with either BSA or lysozyme (Fig S17 and S18). This is in line with previous findings from our group and other studies investigating zwitterionic polymers.[32,38] These results confirm the general trend that zwitterionic polymers or surfaces exhibit excellent resistance to biofouling, thereby being able to improve biocompatibility of coupled materials or cargo (*i.e.* drugs).[19,39–41]

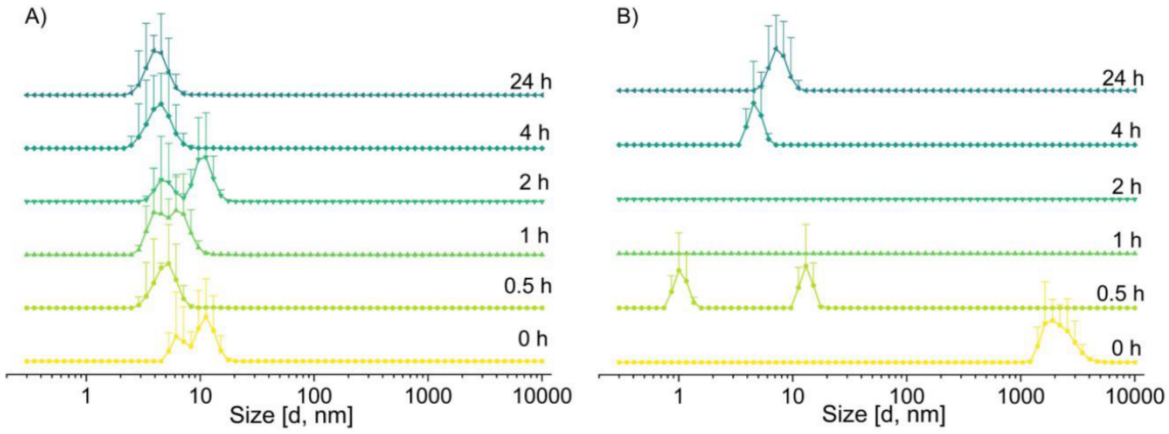


Figure 3: Number size distribution of A: P(Hex-OH-AAm) and B: P(PhenylPr-OH-AAm) (right)-Lysozyme-mixtures. The concentration of polymers and proteins was 0.5 mg mL^{-1} each in DPBS. Sizes were analysed by DLS measurements at 37 °C. Values (scatter) represent the mean and SD of five measurements with three runs each. lines do not represent measured values.

The interesting observation of non-aggregating aliphatic polyanions and instantly aggregating aromatic polyanions, could possibly be explained by the HPLC measurements for these polymers (Fig S13) and compared to the ones done in our previous work.[5] In our previous work, the more hydrophilic P(Gly-OH-AAm) showed smaller aggregates with lysozyme (D_h ≈ 150 nm), whereas the more hydrophobic, P(Nva-OH-AAm), showed the formation of larger (although stable) aggregates in combination with lysozyme (D_h ≈ 700 nm). Comparing, t_{ret} obtained by HPLC, the t_{ret} of P(Hex-OH-

AAm) (t_{ret} = 14.5 Min.) and P(PhenylPr-OH-AAm) (t_{ret} = 15.9 Min.) with P(Gly-OH-AAm) (t_{ret} = 13.2 Min.) and P(Nva-OH-AAm) (t_{ret} = 16.3 Min.), we observed a similar retention time for P(PhenylPr-OH-AAm) and P(Nva-OH-AAm) while P(Hex-OH-AAm) has a retention time between P(Nva-OH-AAm) and P(Gly-OH-AAm). Relating the fouling behaviour of the polyanions to their relative hydrophobicity is the most straightforward explanation for the immediate aggregation of the aromatic, more hydrophobic P(PhenylPr-OH-AAm). In comparison, the hydrophobicity of P(Hex-OH-AAm) is insufficient to induce aggregation with lysozyme. Building on these findings, further fouling experiments were conducted in PBS containing 10 % FBS to evaluate potential polymer aggregation under biologically relevant conditions that are later used during *in vitro* experiments. Here, the absence of an increase in particle size, over a measurement time of 5 hours, suggests that no polymer-protein aggregation takes place over the time period in which cell association experiments will be performed (Fig S20).

2.4. Interaction of amino-acid-derived polyelectrolytes with cells

The beforehand synthesized and tested polymers were tested on their biological compatibility and on their uptake behaviour in different cell lines to compare the influence of polymer on cell lines with cancer origin in comparison to non-cancer cells. To assure high biocompatibility of polymers, they have been tested in the breast cancer cell line MDA-MB-231 *via* 3-(4,5-dimethylthiazol-2-yl)-2,5-diphenyltetrazolium bromide (MTT) assay (Fig S21). All synthesized polymers were well tolerated by the MDA-MB-231 cells at concentrations up to 1 mg mL^{-1} (for 24 h). This concentration is 10-fold higher than the concentrations to be applied during cell association studies presented below. Moreover, the results were in line with our former study on amino-acid-derived polyanions where the cell viability was consistently ≥ 70% for concentrations up to 0.1 mg mL^{-1}.[5] These results demonstrate that cellular tolerance is unaffected by the side-chain spacer (aliphatic or aromatic), or the ionic character (permanent) zwitterion or anion) of the polymer.

In order to analyse the cell association of the polymers, they were functionalized with the dye Cy5 and then incubated on different cell lines. The evaluation was performed using flow cytometry. In the following experiments PNAM-Cy5 served as internal standard to determine the relative association to different cell types, as it has been reported that there is only unspecific association between cancer cells and non-ionic polymers.[6,32,42]Based

on the concentration-dependent association experiments, ranging from 0.04 – 2.5 µM, with P(Lys-OH-AAm)-Cy5 and MDA-MB-231 (Fig S23), a concentration of 2.5 µM was determined to be suitable for further comparative studies.

The cellular association experiments of all polymers have been performed on two human cancer cell lines (HCC 78 and MDA-MB-231) and a human mammary epithelial cell (MCF10a)[43]. Murine NIH 3T3 fibroblasts served as non-tumorigenic cell line for comparison. Generally, comparison with HCC-78 and MDA-MB-231 cells showed a statistically significant difference ($p < 0.05$) between association for P(Me_3Lys-OH-AAm)-Cy5 and P(PhenylPr-OH-AAm)-Cy5 while all other polymers showed similar association behaviour to lung and breast cancer cells (Fig 4A and S25).

When comparing these association results to the polymer association of MDA-MB-231 cells with NIH 3T3, it was observed that the overall polymer association for the fibroblasts was significantly lower than it was in MDA-MB-231 cells - except for P(Me_3Lys-OH-AAm)-Cy5, which showed higher association to the fibroblast. [44]For the non-tumorigenic human breast cells (MCF10A), the interaction between the permanently, positively charged P(Me_3Lys-OH-AAm)-Cy5 is statistically significantly lower compared to the other studied cell types ($p < 0.05$) (Fig 4A). The zwitterionic polymer variant P(Lys-OH-AAm)-Cy5 showed a ~2-fold higher association with MCF10A cells, however, the statistically significance indicated no difference to cancer cells such as MDA-MB-231. More interesting, we observed a ~5-fold stronger association between P(Hex-OH-AAm)-Cy5 and MCF10A. These results strongly indicate that specifically the polymeric anionic charge influences the interaction between human non-cancer cells and polyanions more drastically than to cancer cells. The same trend – however less pronounced – was observed for P(PhenylPr-OH-AAm)-Cy5. This phenomenon was even further reduced in case of P(Phe-OH-AAm)-Cy5.

We therefore assume that in addition to the ionic charge, the aromatic side chain inhibits the association with non-tumorigenic cell membranes. In summary, the permanently charged P(Me_3Lys-OH-AAm) exhibits the highest potential for further investigations of specific interaction with cancer cells without affecting healthy human cells.

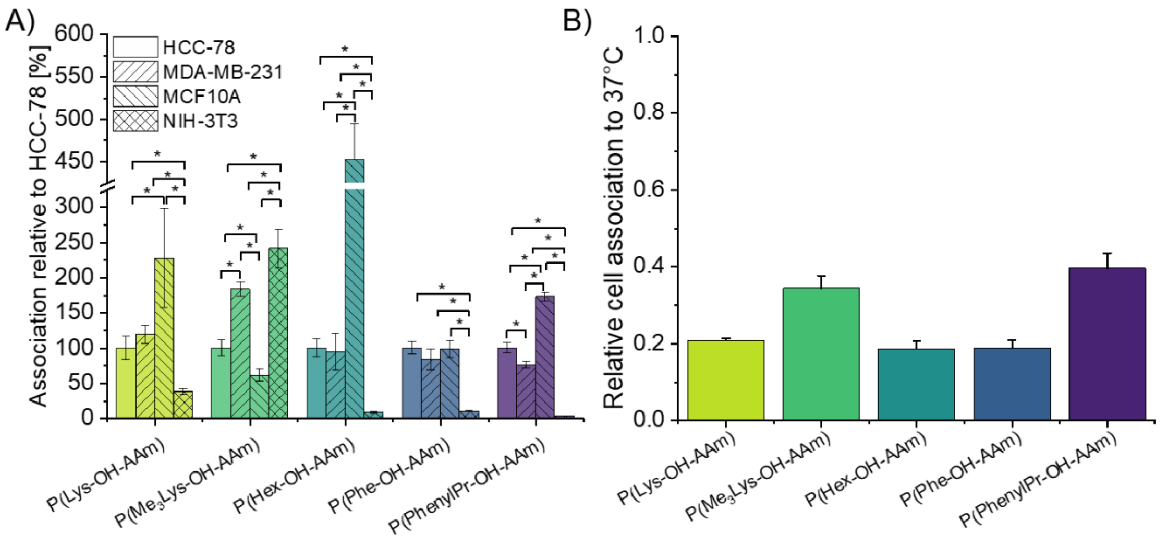


Figure 4: (A) Cellular association of polymers relative to HCC-78 determined by flow cytometry. The cells were seeded in 24-well plates (50,000 cells/well) and incubated with 2.5 µM polymer solutions (500 µL of FBS-containing cell culture media) at indicated temperatures for 4 h. Values represent mean and SD (n = 4). Statistical analysis (unpaired Welch's t-test) * Indicates a significance of $p < 0.05$ (B) Relative association of polymers on MDA-MB-231. Cells were seeded in 24-well plates (50,000 cells/well) and incubated with 2.5 µM polymer solutions at indicated temperatures at 4 and 37 °C for 4 h (Fig S26).

Further experiments were conducted to clarify whether polymers are taken up by the cells, *e.g.*, by including uptake studies. Since one goal of this study was to understand the specificity of polyelectrolytes toward human cancer cells, the following experiments were exclusively performed with MDA-MB 231 breast cancer cells. Clarification about the polymer uptake into cancer cells was sought by imaging via confocal laser scattering microscopy (CLSM) measurements of MDA-MB-231 cells in combination with the Cy5-labelled polymers after 1 hour of incubation time.

After 1 h of incubation, a strong intracellular fluorescence signal of the polyanions, P(Hex-OH-AAm)-Cy5 and P(PhenylPr-OH-AAm)-Cy5, was observed (Figure 5). Controls and single channels can be found in (Fig S34). This result indicated fast and efficient polymer uptake as already shown by flow cytometry measurements. Other previous studies demonstrated that carboxylated Cy5-labelled polymers can exhibit intracellular

mitochondrial colocalisation.[45] The deviating finding in the current study may be explained by the increased hydrophobicity of the polymers, which is assumed to impact the polymer association and uptake. In addition, a slow but significant accumulation of anionic polymers in the cell membrane has been reported. This is thought to be due to the combined effects of their anionic charge and hydrophobic properties, which promote membrane association with polyanions.[5] Anionic polymers typically show low cellular association, as the cell membrane consists of a phospholipid bilayer with a hydrophobic core and an anionic outer leaflet.[26] The rapid uptake observed for both polyanions examined in this study, (P(Hex-OH-AAm)-Cy5 and P(PhenylPr-OH-AAm)-Cy5), highlights the significant role of hydrophobicity in promoting cell interaction and accelerating internalisation.

After 1 h incubation time, the intracellular signal of the zwitterionic polymers P(Me_3Lys-OH-AAm)-Cy5, P(Lys-OH-AAm)-Cy5 and P(Phe-OH-AAm)-Cy5 was reduced compared to the polyanions. While this was in line with the flow cytometry results of the two Lys-derived polymers, a deviation for the Phe-derived polyzwitterion was observed. Live cell imaging after 4 h incubation (Fig S33), in turn, revealed an intracellular fluorescence signal for this polymer, suggesting a slower internalisation of the aromatic polyzwitterion than for the aliphatic polymers. Thus, it was demonstrated that the polymers were internalised by the cells depending on their characteristics of their sidechain.

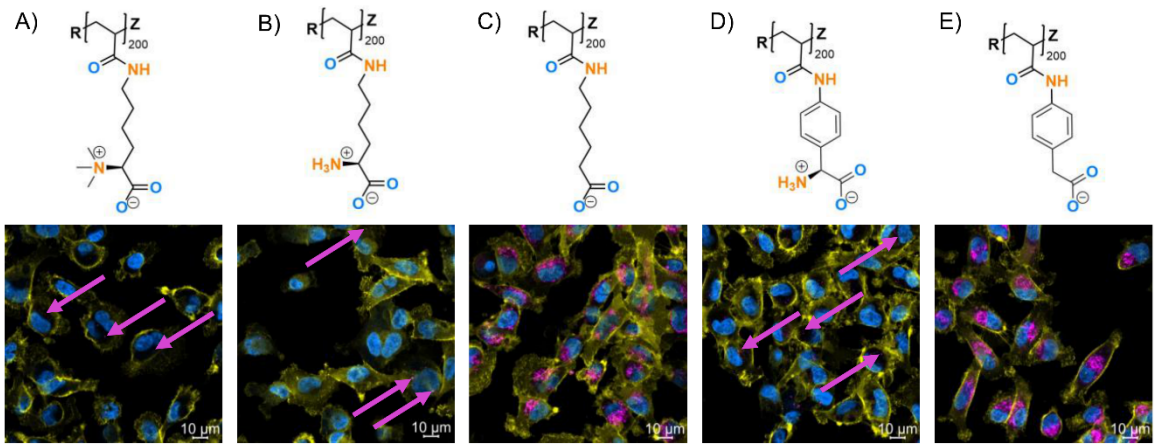


Figure 5. MDA-MB-231 cancer cells visualised by CLSM 1 h after treatment with polymers. Blue: Hoechst 33342/nucleus. Yellow: Cell membrane (CellMask™ Green Plasma Membrane stain). Magenta: Cy5/polymer channel. Cells were treated with Cy5 modified polymers A: P(Lys-OH-AAm)-Cy5. B: P(Me_3Lys-OH-AAm)-Cy5. C: P(Hex-OH-AAm)-Cy5. D: P(Phe-OH-AAm)-Cy5 E: P(PhenylPr-OH-AAm)-Cy5.

Several studies have reported that internalisation of macromolecules mainly follows active pathways.[46–48] Here, active uptake mechanisms were evaluated by cell incubation studies for 4 h at different temperatures, namely 37 °C and 4 °C. A reduction of the MFI by approximately 60 to 80% was observed at 4 °C compared to the respective control group incubated at 37°C (Fig 4B), showing lower polymer-cell interactions at decreased temperatures. The lower interactions at 4°C combined with the uptake shown in Fig 5 suggest uptake mainly takes place *via* active uptake pathways, which are often upregulated in cancer cells lines and facilitate enhanced cell growth.[49–51] Previous research by different groups has further suggested that the cell association of (amino-acid-derived) polyzwitterions is mainly driven by targeted (active) interactions with components on the cell surface of cancer cells (i.e. receptors or transporters).[27] Based on literature and decreased polymer-cell interaction at lower temperature, the driving forces behind the cellular association of the tested amino-acid-derived polymers were investigated with respect to potential selective interactions with cell-surface transporters. Therefore, competitive inhibitors for different amino acid transporters (AATs), which are overexpressed in MDA-MB-231 (i.e., SNAT1/2, ASCT1/2, LAT1/2, xCT and MCT4) were applied (Table 5).[52] Surprisingly, neither of the polymers showed an inhibitor-dependent decrease of uptake, as observed by constantly high MFI values (Fig S30). These results suggested an AAT interaction-independent cell association. As the inhibition of certain transporters can lead to starvation of the cell and, thus, overcompensation of other transporters could interfere the tests.[53] Complementary experiments with competitive amino acids (i.e., leucine (Leu, main substrate of LAT transporters)[54], phenylalanine (Phe, main substrate of LAT1)[55] and glutamic acid (Glu, main substrate of xCT)[51]) supported these findings (Fig S30). Here, only leucine showed a slight trend towards a decrease of polymer cell association. These results are generally in line with previously reported

results on CT26 cells, however, the inhibition was less pronounced.[27] This deviation may be caused by the use of different cell lines.

Based on the reported results, we conclude that the studied polymers do not strongly interact with specific AATs. The inhibited cellular interaction of all polymers at lower temperature and in the presence of leucine indicated active uptake mechanism and AAT involvement. Future studies will aim at examining the cellular association mechanisms in more detail, *e.g.,* by screening specific uptake mechanisms, for a better understanding of uptake and distribution of polymers inside the cell.

3. Conclusions

The synthesis of amino-acid-derived polyelectrolytes from lysine- and phenylalanine-derived motifs by PPM polymerisation was demonstrated. Defined polyzwitterions were prepared by using Boc-protected compounds and subsequent deprotection. Anionic structural analogues were synthesised likewise. *Via* this approach a library of five polymers was obtained which enabled a study of the effects of side chain alterations on the properties of amino-acid-derived polyelectrolytes. We investigated the influence of a (permanent) zwitterionic character compared to anionic motifs and, additionally, the influence of aliphatic and aromatic side chain spacers on both the physiochemical and the biological properties/behaviour. HPLC showed that aromaticity in the side chain increased the hydrophobicity, at pH ≈ 2, for anionic polymers while no influence was observed for the zwitterionic equivalents. pH-dependent DLS measurements were performed. Here aggregation around and below the pK_a was observed for the anionic polymers. Smaller aggregates were formed around the pI with both zwitterionic, P(Me_3Lys-OH-AAm) and P(Phe-OH-AAm), between pH 6-7 which can enhance retention within tumour tissue as the external pH at tumour sites is slightly lower. Furthermore, DLS measurements in combination with model proteins showed no aggregation with most polymers. Interestingly, the aromatic anionic polymer, which is more hydrophobic, showed aggregation with the formation of bigger segments while the aliphatic less hydrophobic polymer did not show any aggregation over time. No aggregation of the polymers in combination with FBS was observed, allowing further cell experiments. Here, all synthesised polymers were well tolerated by MDA-MB-231 breast cancer cells at concentrations up to 1 mg mL^{-1} (for 24 h). Cell association with different cell lines showed

general cell association of all polymers, however lower association with NIH 3T3 cells was observed. Further experiments to understand the uptake mechanism were performed by specific amino acid transporter inhibition and competitive uptake assays which revealed no dependence on the studied transporters; however, a strong energy dependent uptake was observed based on the presented results. The fast cellular uptake of the anionic polymers, that was observed by CLSM measurements, make them interesting candidates for further studies towards drug-delivery applications.

4. Experimental Part

4.1. Materials and instrumentation

4.1.1. Materials

Acetonitrile (99.9%), diethyl ether (99.5%), dimethylformamide (99.5%), methanol (99.9%) and sodium hydrogen carbonate (>99.7%) were purchased from FisherScientific. Chloroform (99.8%), dichloromethane (99.8%), isopropanol (99.9%), sodium hydroxide (99.5%), potassium hydroxide (99.5%), hydrochloric acid (32%), Dulbecco's PBS (DPBS), Bovine serum albumin (BSA) and lysozyme, from which the last two obtained as lyophilized powders, were purchased from VWR Chemicals. Triethylamine (99.5%), and potassium carbonate (99.0%) were purchased from Sigma Aldrich. Cyanin5-amine (95.0%) was purchased from Lumiprobe. 3-(4-aminophenyl)propanoic acid (98%), N-hydroxysuccinimide (98.0%), 2-Amino-2-norbornanecarboxylic acid (BCH, 95%), O-Benzyl-L-serine (BzlSer, 98%), Sulfasalazine (98%), 5-((5-Chloro-2-((5-ethoxyquinoline)-8-sulfonamido)phenyl)ethynyl)-4-methoxypicolinic acid (MSC-4381, 98%) and N-(tertbutoxycarbonyl)-4-amino-L-phenylalanine (98%) were purchased from BLD Pharmatech ltd. Trifluoroacetic acid (99.0%) was purchased from abcr. Acryloyl chloride (96%) was purchased from ThermoScientific. Boc-Lys-OH (98%) was purchased from Carbolution. 6-Aminohexanoic acid (6-AmHex-OH, >98.5%) was purchased from Fluka.

Azobis(isobutyronitril) (AIBN) (Fluka or Sigma Aldrich, 98.0%) was recrystallized from methanol before use. N-Acryloxysuccinimide (NAS)[56] and 2-{[(butylsulfanyl)-carbonothiosyl]sulfanyl}propanoic acid (PABTC)[57] were synthesised and characterised following known procedures in literature.

RPMI 1640 Medium (Sigma Aldrich), Dulbecco's Modified Eagle's Medium low glucose (Sigma Aldrich), Dulbecco's Modified Eagle's Medium (DMEM/F12; Sigma Aldrich), DMEM-LPSTA (Capricorn), Mammary Epithelial Cell Basal Medium (PromoCell) supplemented with BPE-26, hEGF-5, Insulin-2.5, and HC-250, foetal bovine serum (FBS; Bio&Sell), Penicillin/Streptomycin (Bio&Sell), Dulbecco's 1 x PBS (Capricorn), choleratoxin (Sigma Aldrich), NIH 3T3 (ACC 59, DSMZ), MDA-MB 231 (HTB-26, ATCC), HCC-78 (ACC 563, DSMZ), MCF10A ((#305026, Cytion)

DMEM-LPSTA (Capricorn), MDA-MB-231 ACC-732 (DSMZ), , CellMask™ Plasma Membrane Stain Green (Thermo Fisher Scientific), Hoechst33342, trihydrochloride, trihydrate (Thermo Fisher Scientific), Dulbecco's 1 x PBS (Capricorn), 4% Paraformaldehyde solution in PBS (Therrmo Fisher Scientific), µ-Plate 24 well (IBIDI), µ-Plate 96 well square (IBIDI), IBIDI Anti-Evaporation Oil (IBIDI).

4.1.2. Proton nuclear resonance (^{1}H NMR) spectroscopy

^{1}H- and spectra were recorded on a Bruker Avance 300 (300 MHz) spectrometer equipped with a BACS-120 autosampler and a ^{1}H, ^{13}C, ^{19}F and ^{31}P-BBO probe at room temperature.

4.1.3. Size-exclusion chromatography (SEC)

Aqueous SEC measurement of P(Boc-Lys-OH-AAm), P(Lys-OH-AAm), P(Hex-OH-AAm), P(Boc-Phe-OH-AAm), P(Phe-OH-AAm), P(PhenylPr-OH-AAm), P(Boc-Lys-OH-AAm)-Cy5, P(Lys-OH-AAm)-Cy5, P(Me_3Lys-OH-AAm)-Cy5, P(Hex-OH-AAm)-Cy5, P(Boc-Phe-OH-AAm)-Cy5, P(Phe-OH-AAm)-Cy5 and P(PhenylPr-OH-AAm)-Cy5 were performed on an instrument consisting of a column set with a Suprema precolumn (particle size = 5 µm) and three Suprema main columns (particle size = 5 µm, 1 × 30 Å; 2 × 1000 Å) with a separation range from 100 to 1 000 000 Da (PSS) together with a variable wavelength detector (1200 Series, Agilent Technologies). As solvent 0.07 M aqueous Na_2HPO_4 was used (for dissolving polymer and as eluting solvent) with a flow rate of 0.8 mL min^{-1} and the columns were maintained at room temperature. As internal standard ethylene glycol (HPLC grade) was used. The calibration was done with narrowly distributed poly(methacrylic acid) sodium salt homo-polymers (PMA Na salt; PSS calibration kit). An injection volume of 60 µL was used for the measurements. The samples were dissolved

with a concentration of 2 mg mL^{-1} and filtered through a 0.22 µm PTFE Nylon filter before analysis. The UV-detector was set to λ = 600 nm for measurements of Cy5-labeled polymers.
Reported molar masses of polymers in this study are based on the indicated standards and denoted as $M_{n,app}$.

Aqueous SEC measurements of P(Me_3Lys-OMe-AAm) and P(Me_3Lys-OMe-AAm)-Cy5 were performed on an instrument consisting of a column set with a NOVEMA Max precolumn (particle size = 10 µm) and three NOVEMA Max main columns (particle size = 10 µm, 1 × 100 Å; 2 × 3000 Å) with separation range from 100 to 3 000 000 Da (PSS, Mainz, Germany) together with a variable wavelength detector (1200 Series, Agilent Technologies). As solvent 80:20 Water/ACN mixture + 0.1 M NaCl + 0.1 V% TFA was used (for dissolving polymer and as eluting solvent) with a flow rate of 0.5 mL min^{-1} and the columns were maintained at room temperature. As internal standard ethylene glycol (HPLC grade) was used. The calibration was done with narrowly distributed Poly(2-vinylpyridine) (narrowly distributed P2VP homo-polymers, PSS calibration kit). An injection volume of 60 µL was used for the measurements. The samples were dissolved with a concentration of 2 mg mL^{-1} and filtered through a 0.22 µm PTFE Nylon filter before analysis. The UV-detector was set to λ = 600 nm for measurements of Cy5-labeled polymers

Size-exclusion chromatography of PNAS and PNAM was performed on an Agilent 1260 Infinity II system equipped with the MDS Refractive Index detector, MWD (UV), MDS Viscometer, PSS SLD 7100 multi angle light scattering detector and PSS GRAM 30 and 1000 column sets with DMAc (+ 5 g L^{-1} LiBr) as eluent. Measurements were conducted with 100 µL injection volume at a constant flow rate of 1 mL min^{-1}, with the column oven held at 40°C. All samples were filtered (PTFE 0.22 µm) before measurements. For calibration, narrowly distributed poly(ethylene oxide) (PEO) standards were used. The UV-detector was set to λ = 600 nm for measurements of Cy5-labeled polymers and λ = 310 nm for end-group removal.

4.1.4. High-performance liquid chromatography (HPLC)

HPLC measurements were conducted with a Jupiter 5 µm C18 300 Å LC column (250 × 4.6 mm). The run time was 35 min. A mixture of 0.1 v/v% TFA in water and acetonitrile served as eluent (Table 2). The fluorescence detected was set to λ_{ex} = 640 nm and λ_{em} = 680 nm with 1× gain. The ELSD detector was set to λ = 215 nm.

Table 2. Composition of HPLC eluent at indicated time points.

Time [min]	Fraction of 0.1 v/v% aqueous TFA [%]	Fraction of acetonitrile [%]
0	98.0	2.0
5	50.0	50.0
10	0.0	100.0
17	0.0	100.0
25	98.0	2.0
35	98.0	2.0

Data analysis of theoretical logP values

To obtain the theoretical partition coefficients (logP values), the cheminformatics tool RDkit with the descriptor MolLogP (based on Wildman and Crippen)[34,58] was used. The calculation was done for one repeating unit of each polymer. For this purpose, the following Simplified Molecular Input Line Entry System (SMILE) string were used:

P(PhenylPr-OH-AAm): C(C)CC(=O)Nc1ccc(CCC(=O)O)cc1

P(Phe-OH-AAm): C(C)CC(=O)Nc1ccc(CC([NH3+])C(=O)O)cc1

P(Hex-OH-AAm): C(C)CC(=O)NCCCCCCC(=O)O

P(Me3Lys-OH-AAm): C(C)CC(=O)NCCCCC(C(=O)O)[N+](C)(C)C

P(Lys-OH-AAm): C(C)CC(=O)NCCCCC([NH3+])C(=O)O

4.1.5. Dynamic light scattering (DLS)

DLS was measured on a Malvern Panalytical Zetasizer Ultra device using disposable folded capillary cuvettes. The excitation light source was a He–Ne laser at 633 nm and the intensity of the scattered light was measured at an angle of 173°. The light scattering was measured during an automatic measurement process from minimum 15 runs of 1.68 s run duration or 30 runs of 1.68 s each for each sample. Measurement parameters were set to an equilibrium time and temperature of 60 s and 37 °C. This method measures the

rate of intensity fluctuation, and the size of the particles is determined through the Stokes–Einstein equation. The concentration of the polymer solution was 2 mg mL^{-1}. For the pH-responsive measurements, a 2 mg mL^{-1} solution of the polymer in deionised water was prepared and 0.1 M aq. NaOH or aq. HCl were added until the desired pH-value was reached. Measurements were done with a Mettler Toledo digital pH meter.

4.1.6. Electrophoretic light scattering (ELS)

ELS was used to measure the zeta potential (ζ). The measurement was also performed on a Malvern Panalytical Zetasizer Ultra device using 1.5 mL semi-micro cuvettes or disposable folded capillary cuvettes by applying laser Doppler velocimetry. For each measurement, automatic measurements including min. 10 runs were carried out using the slow-field reversal and the fast-field reversal mode at 150 V. Each experiment was performed in triplicates at 37 °C after an equilibration time of 60 s. The zeta potential was calculated from the electrophoretic mobility (μ) according to the Henry equation. Henry coefficient f(ka) was calculated according to Ohshima.[59] The polymer solutions were similarly prepared as for during the DLS measurements.

4.2. Synthesis and characterization

4.2.1. Poly(N-acryloyl succinimide) (PNAS)

2 g of NAS (12 mmol, 200 equiv.) were transferred into a microwave tube (Biotage) equipped with a stirring bar. 0.984 mg (0.006 mmol, 0.1 equiv.) AIBN and 14.28 mg (0.06 mmol, 1 equiv.) PABTC were added, using stock solutions, followed by addition of DMF to reach a final volume of 4 mL. The tube was closed with a septum and vortexed until homogeneous before a sample was taken (t = 0h) for ^{1}H-NMR spectroscopy in DMSO-d6 in order to determine the conversion by comparing the sample with a sample at the end of the reaction. The reaction mixture was deoxygenated by putting the mixture under an argon flow for 30 min. after which it was placed in a preheated oil bath and stirred at 70 °C for 24 h. The reaction was terminated by cooling to RT and purging in air. A sample was taken and analysed *via* ^{1}H-NMR spectroscopy in DMSO-d6. The crude polymer was precipitated in diethyl ether (-80°C) twice. After centrifugation (5000 rpm, 5 min.), the supernatant was discarded, and the polymer was dried under reduced pressure overnight to obtain the product as a yellow viscous oil.

The X_n of the resulting polymer was calculated by using the signal of the vinyl CH_2-group at δ = 6.35 ppm and the reaction solvent at δ = 7.96 ppm both at t = 0h and 24h, suggesting a X_n of 188 for P(Me_3Lys-OH-AAm) and 193 for all others.

Polymers were analysed by DMAc SEC (standard: PEG).
Elugrams can be found in Fig S2.
PNAS for P(Me_3Lys-OH-AAm): $M_{n,app}$ = 4 700 g mol^{-1}; Đ = 1.84

PNAS for all others: $M_{n,app}$ = 8 100 g mol^{-1}; Đ = 1.87

4.2.2. Post-polymerisation modification of PNAS with Boc-Lys-OH, Me_3Lys-OMe-NH_2, 6-AmHex-OH, Boc-4-AmPhe-OH, 4-AmPhenylPr-OH

The post-polymerisation modification of PNAS is exemplary described for reactions with Boc-Lys-OH yielding P(Boc-Lys-OH-AAm). Quantities and moles are given relative to the single repeating unit NAS of the polymer and can be found in Table 3.
In a 5 mL reaction vessel (Biotage), PNAS (200 mg, 0.6 mmol, 1.00 equiv.) was dissolved in anhydrous DMF (9.5 mL). 500 µL triethylamine were added. After that, Boc-Lys-OH (296.5 mg, 1.204 mmol, 1.025 equiv.) was added, the reaction vial was closed with a septum, and the suspension was stirred at RT for 24 h. Then, the product was purified by dialysis (RC, MWCO 3.5 kDa, SpectraPor) against 1 L brine for one day followed by dialysis against 1 L deionised water for three days with daily water change. Upon lyophilisation, the product was yielded as an off-white powder. Polymers were analysed *via* ^{1}H NMR and aqueous SEC.

Table 3. Quantities of reagents used for the PPM of PNAS.

Amino acid	n [mmol]	m [mg]
Boc-Lys-OH	1.025	296.5
Me_3Lys-OMe-NH_2		
6-AmHex-OH		157.9
Boc-4-AmPhe-OH		337.4
4-AmPhenylPr-OH		198.8

Polymers were analysed by aqueous SEC (0.07 M aq. Na_2HPO_4 (standard: PMA Na salt)).
Elugrams can be found in Fig S8.
P(Boc-Lys-OH-AAm): $M_{n,app}$ = 17,200 g mol^{-1}; Đ = 2.25.

P(Hex-OH-AAm): $M_{n,app}$ = 16,500 g mol^{-1}; Đ = 2.30.
P(Boc-Phe-OH-AAm): $M_{n,app}$ = 12,800 g mol^{-1}; Đ = 2.48.
P(PhenylPr -OH-AAm): $M_{n,app}$ = 11,000 g mol^{-1}; Đ = 2.71.

4.2.3. Post-polymerisation modification of PNAS with Cy5-amine and Boc-Lys-OH, Me_3Lys-OMe-NH_2, 6-AmHex-OH, Boc-4-AmPhe-OH, 4-AmPhenylPr-OH

The post-polymerisation modification of PNAS is exemplary described for reactions with Boc-Lys-OH yielding P(Boc-Lys-OH-AAm)-Cy5. Quantities and moles are given relative to the single repeating unit NAS of the polymer and can be found in Table 4.
In a 5 mL reaction vessel (Biotage), PNAS (49 mg, 1.4 µmol, 1.00 equiv.) was dissolved in anhydrous DMF (900 µL). 1 mg Cy5-amine (1.5 µm, 1.1 equiv.) was added using a stock solution. After that, 7.6 µL of a 1:10 [triethylamine/DMF] mixture were added, and the reaction vessel was closed with a septum. The reaction mixture was stirred in the dark at RT for 24 h. Then, 52.6 µL triethylamine and Boc-Lys-OH (72.6 mg, 0.2949 mmol, 1.025 equiv.) were added with an additional 940 µL DMF. The reaction vial was closed with a septum, and the suspension was stirred at RT for 24 h. Then, the product was purified by dialysis (RC, MWCO 3.5 kDa, SpectraPor) against 1 L brine for one day followed by dialysis against 1 L deionised water for three days with daily water change. Upon lyophilisation, the product was obtained as a blue powder.

Table 4. Quantities of reagents used for the PPM of PNAS.

Amino acid	n [mmol]	m [mg]
Boc-Lys-OH	1.025	72.6
Me_3Lys-OMe-NH_2		
6-AmHex-OH		38.7
Boc-4-AmPhe-OH		82.7
4-AmPhenylPr-OH		48.7

Polymers were analysed by aqueous SEC (0.07 M aq. Na_2HPO_4 (standard: PMA Na salt)). Elugrams can be found in **Fig S11**.

P(Boc-Lys-OH-AAm)-Cy5: $M_{n,app}$ = 18,600 g mol^{-1}; Đ = 2.02.
P(Hex-OH-AAm)-Cy5: $M_{n,app}$ = 15,900 g mol^{-1}; Đ = 2.26.

P(Boc-Phe-OH-AAm)-Cy5: $M_{n,app}$ = 14,800 g mol^{-1}; Đ = 2.47.
P(PhenylPr -OH-AAm)-Cy5: $M_{n,app}$ = 15,700 g mol^{-1}; Đ = 2.54.

4.2.4. Acidic deprotection of P(Boc-Lys-AAm) and P(Boc-Phe-AAm) yielding P(Lys-AAm) and P(Phe-AAm), respectively.

100 mg P(Boc-Lys-AAm) and P(Boc-Phe-AAm) were stirred in a 10 mL 50/50 V% [TFA:water] mixture overnight. ± 30 mg P(Boc-Lys-AAm)-Cy5 and P(Boc-Phe-AAm)-Cy5 were stirred in the dark in a 4 mL 50/50 V% [TFA:water] mixture overnight. Subsequently, the reaction mixture was purified by dialysis (RC, MWCO 3.5 kDa, SpectraPor) against 1 L deionised water for one day with one water change after five hours followed by lyophilisation to obtain P(Lys-AAm), P(Phe-AAm), P(Lys-AAm)-Cy5 and P(Phe-AAm)-Cy5

Polymers were analysed by aqueous SEC (0.07 M aq. Na_2HPO_4 (standard: PMA Na salt)). Elugrams can be found in Fig S9.
P(Lys-OH-AAm): $M_{n,app}$ = 2,000 g mol^{-1}; Đ = 3.27.
P(Phe-OH-AAm): $M_{n,app}$ = 13,000 g mol^{-1}; Đ = 2.14.
P(Lys-OH-AAm)-Cy5: $M_{n,app}$ = 4,700 g mol^{-1}; Đ = 2.08.
P(Phe-OH-AAm)-Cy5: $M_{n,app}$ = 12,000 g mol^{-1}; Đ = 2.59.

4.2.5. Poly(N-acyrloylmorpholine) (PNAM)

1.78 mL of NAM (2 g, 14.2 mmol, 200 equiv.) were transferred into a microwave tube (Biotage) equipped with a stirring bar. 1.163 mg (0.0071 mmol, 0.1 equiv.) AIBN and 16.887 mg (0.071 mmol, 1 equiv.) PABTC were added, using stock solutions, followed by addition of DMF to reach a final volume of 4 mL. The tube was closed with a septum and vortexed until homogeneous before a sample was taken (t = 0 h) for ^{1}H-NMR spectroscopy in DMSO-d6 to determine the conversion by comparing the sample with a sample at the end of the reaction. The reaction mixture was deoxygenated by putting the mixture under an argon flow for 30 min. after which it was placed in a preheated oil bath and stirred at 70 °C for 24 h. The reaction was terminated by cooling to RT and purging in air. A sample was taken and analysed *via* ^{1}H-NMR spectroscopy in DMSO-d6. The crude polymer was precipitated in diethyl ether (-80 °C). After centrifugation (5000 rpm, 5 min.), the

supernatant was discarded, and the polymer was dried under reduced pressure overnight to obtain the product as a yellow viscous oil.

The X_n of the resulting polymer was calculated by using the signal of the vinyl CH_2-group at δ = 5.70 ppm and the reaction solvent at δ = 2.90 ppm both at t = 0 h and 24 h, suggesting a X_n of 198.

Polymer was analysed by DMAc SEC (standard: PEG).
Elugram can be found in Fig S22.
PNAM-CTA: $M_{n,app}$ = 8 300 g mol^{-1}; Đ = 1.48

4.2.6. CTA removal of PNAM

The end-group removal of trithiocarbonates was conducted according to a literature procedure.[60]

In a reaction vessel equipped with a stirrer bar, 1.5 g of P(NAM)-CTA (52.5 × 10^{-6} mol, 1.0 equiv), 173.02 mg of AIBN (1.05 mmol, 20.0 equiv), and 42 mg of Luperox (0.11 mmol, 2.0 equiv) were dissolved in 15 mL of toluene. The vessel was sealed with a septum, and the reaction mixture was deoxygenated with Argon for 30 min. Subsequently, the vial was placed in a preheated oil bath and heated to 80 °C for 2 h under continuous stirring. After cooling to RT, the crude mixture was precipitated in diethyl ether. After centrifugation (5000 rpm, 5 min.), the supernatant was discarded, and the polymer was dried under reduced pressure overnight to obtain the product as a transparent viscous oil. Complete removal of the trithiocarbonate end group was analysed by SEC measurements in DMAc using a UV detector (λ = 310 nm), showing the disappearance of the polymer UV trace (Elugram Fig S21)

PNAM-EGR: $M_{n,app}$ = 1 300 g mol^{-1}; Đ = 1.77

4.2.7. Cy5-labelling PNAM-EGR

In a small reaction vessel, 50 mg of PNAM-EGR (16.0 × 10^{-6} mol, 1.0 equiv.) and 14.47 mg of DMTMM·BF_4 (0.04 mmol, 2.5 equiv.) were dissolved in 20 mL anhydrous DMF and stirred at RT for 30 min. Subsequently, a 10 mg mL^{-1} solution of Cy5-amine (34.6 mg, 0.05 mol, 3.0 equiv.) in anhydrous DMF was added. The reaction was stirred at RT in the dark overnight. Then, the reaction mixture was precipitated in diethyl ether. After

centrifugation (5000 rpm, 5 min.), the supernatant was discarded. The crude product was redissolved in water. Then, the product was purified by dialysis (RC, MWCO 3.5 kDa, SpectraPor) against 1 L brine for one day followed by dialysis against 1 L deionised water for three days with daily water change. Upon lyophilisation, the product was yielded as a blue powder. Dye attachment and purity from unattached dye were confirmed by SEC (λ = 612 nm).

Polymer was analysed by DMAc SEC (standard: PEG).

Elugram can be found in Fig S22.

PNAM-Cy5: $M_{n,app}$ =18 900 g mol^{-1}; Đ = 1.31

4.3. Biological evaluation

4.3.1. Protein fouling

Aggregation of P(Lys-OH-AAm), P(Me$_3$Lys-OH-AAm), P(Hex-OH-AAm), P(Phe-OH-AAm) and P(PhenylPr-OH-AAm) after incubation with dedicated proteins (BSA and lysozyme) was analysed by DLS measurements. Stock solutions of the polymers and the proteins were prepared separately in DPBS (1 mg mL^{-1}) and mixed in a ratio of 1:1, resulting in final concentrations of c = 0.5 mg mL^{-1}. The samples were analysed immediately after mixing (t = 0 h) and at indicated time points (0.5 h, 1 h, 2 h, 4 h, 24 h) thereafter. In between measurements the samples were incubated at 37 °C whilst being shaken at 100 rpm on a thermostated shaker. Measurements were conducted at 37 °C with five measurements and three runs each. After the measurement, samples were placed back into the thermostated shaker immediately.

4.3.2. Polymer stability towards PBS+FBS

Aggregation of P(Lys-OH-AAm), P(Me$_3$Lys-OH-AAm), P(Hex-OH-AAm), P(Phe-OH-AAm) and P(PhenylPr-OH-AAm) after incubation in DPBS solution containing 10 V% FBS was analysed by DLS measurements. Polymers were weighed in and dissolved into the mixture to obtain a final concentrations of c = 0.1 mg mL^{-1}. The samples were analysed immediately after mixing (t = 0 h) and at indicated time points (0 h, 5 min, 10 min, 0.5h, 1 h, 2 h and 5 h) thereafter. In between measurements the samples were incubated at 37 °C without shaking. The light scattering was measured during 30 runs of 1.68 s each for

each sample. Measurement parameters were set to an equilibrium time and temperature of 60 s and 37 °C.

4.3.3. Cell culture

L929 cells were cultured in low-glucose Dulbecco's Modified Eagle Medium (DMEM) supplemented with 10% fetal bovine serum, 100 U mL^{-1} penicillin, and 100 µg mL^{-1} streptomycin. The cells were incubated at 37 °C using 5% CO_2 in a humidified incubator. MDA-MB-231 cells (HTB-26, ATCC) were maintained in DMEM/F12 cell culture medium, HCC 78 cells were cultured in RPMI 1640 medium, and NIH 3T3 were cultured in Dulbecco's Modified Eagle's Medium low glucose. All those media were supplemented with 10% fetal calf serum (FCS), 100 µg mL^{-1} streptomycin, and 100 U mL^{-1} penicillin each. MCF10A cells were maintained in Mammary Epithelial Cell Growth Medium with supplements and 100 ng mL^{-1} choleratoxin. All cells were cultivated at 37 °C in a humidified 5% CO_2 atmosphere.

4.3.4. Cell viability assay

The cell viability assay was slightly modified from our previous procedure.[32] The cytotoxicity of P(Lys-OH-AAm), P(Me_3Lys-OH-AAm), P(Hex-OH-AAm), P(Phe-OH-AAm) and P(PhenylPr-OH-AAm) were tested using MDA-MB-231 breast cancer cells. The polymers stock solutions were prepared at concentrations ≤ 20 mg mL^{-1} in demineralised water. The polymers were tested in a concentration range from 0 to 1.0 mg mL^{-1} MDA-MB-231 cells were cultured as described above. For the cell viability assay, cells (10^4 per well) were seeded in 96-well plates and allowed to adhere overnight. No cells were seeded in the outer wells. The media was subsequently removed and replaced by fresh polymer containing media. Then, the cells were incubated at 37 °C for an additional 24 h. After that, the media was removed, the cells were washed with 100 µL DPBS per well, and then fresh media containing thiazolyl blue tetrazolium bromide (MTT) (concentration: 1 mg mL^{-1}) was added (100 µL per well). Note: MTT (50 mg) was dissolved in 10 mL of sterile DPBS, filtrated (membrane, 0.22 µm), and 1 to 5 diluted in culture medium prior to use in this assay. After incubation for 3 h at 37 °C, the test medium was discarded, 100 µL per

well of *i*-PrOH were added to each well and the plates were gently shaken in the dark for 15 min to dissolve the formazan crystals. Quantification was done by measuring the absorbance at λ = 580 nm using a microplate reader (Genios Pro, Tecan). Untreated cells on the same plate served as negative control (100% viability), cells treated with 20% DMSO as positive control (0% viability), and wells without cells as background. Experiments were performed in triplicates on three different plates. Relative cell viability was calculated by using Equation (1).

$$\%\ Cell\ viability = \frac{Abs.sample - Abs.background}{Abs.negative\ control - Abs.background} \cdot 100 (1)$$

4.3.5. Cell association analysis via flow cytometry

Cell association assay I: Concentration-dependent polymer association with cells

The MDA-MB-231 cells were cultured as described above. For the experiments, 2 ×10^5 cells mL^{-1} were seeded in 2 mL of culture medium in a 6 well plate and cultivated for 24 h prior to treatment. 90 minutes before treatment, the medium was changed to 900 µL of fresh culture medium. The polymers were diluted in DPBS to a concentration of c = 0.2, 1, 5 and 25 µM and added to the wells (100 µL). The corresponding final concentrations of each polymer were c = 0.04, 0.2, 1.0 and 2.5 µM. As negative control (NC), cells were incubated with 100 µL DPBS. After 90 minutes of incubation at 37 °C in the cell culture incubator, the supernatant was discarded. After a washing step with DPBS cells were harvested by trypsinization, followed by centrifugation and resuspension in DPBS. Flow cytometry measurements were performed using a CytoFLEX S flow cytometer (Beckman Coulter, Krefeld, Germany) equipped with 405 nm, 488 nm and 561 nm lasers. Forward scatter (FSC), side scatter (SSC), Cy5 fluorescence (PC7 filter, 780/760 nm), and propidium iodide (PI) fluorescence (emission 620 nm) were recorded. Negative control samples (mock-treated cells) were used to set measurement parameters and define background fluorescence levels. For each sample, data from at least 10,000 events were collected. Cells were first gated based on FSC and SSC signals (linear scale) to select the non-apoptotic cell population and exclude debris and aggregates (Gate: “Cells”). Subsequently, FSC-A versus FSC-H gating (linear scale) was applied to exclude doublets (Gate: “Single cells”). The relative Cy5 fluorescence of the gated single-cell population was then quantified, enabling statistical analysis of Cy5-labelled polymer–cell interactions.

Cy5-positive cells were defined as those exhibiting fluorescence intensities exceeding the autofluorescence of the negative control cells. In parallel, PI fluorescence was used to assess cell viability. Fluorescence intensity histograms (logarithmic scale) were analyzed to quantify polymer–cell interactions, expressed as the mean fluorescence intensity (MFI).A detailed gating strategy is provided in Fig S24.

The mean fluorescence intensity (MFI) was normalised to the negative control using Equation (2).

$$Normalized\ MFI\ [a.u.] = \frac{MFI_{sample}}{MFI_{NC}} \times \frac{1}{rfluorescence_{sample}} \quad (2)$$

Cell association assay II: Time- and temperature-dependent polymer association with cells

The cell association assay was adapted from Leiske *et al.*[6] Polymers were investigated for their association with MDA-MB-231, NIH 3T3, HCC 78 and MCF10a. In detail, 4 ×10^5 MDA-MB-231 cells per well were seeded in a 6-well plate while 2 ×10^5 HCC 78 cells, 1.8 × 10^5 NIH 3T3 cells and 4 ×10^5 MCF10a cells per well were seeded in a 24-well plate and cultivated for 24 h. Then, the media were substituted with 450 µl per well fresh medium. After dilution of the polymers in DPBS to a concentration of c = 25 µM, 50 µL per well of the respective polymer was added and incubated for 4.0 h at 37 °C and in the cell culture incubator (final c = 2.5 µM). The NC contained only 50 µL DPBS. Moreover, an additional 6-well plate with MDA-MB-231 cells was treated identically, albeit for 4 h at 4 °C (refrigerator). After 4 h of incubation at 37 °C and in the cell culture incubator or 4°C, the cells were collected for flow cytometer measurements as described above (see Cell association assay I) (n = 4 (two duplicates)). A detailed gating strategy is provided in Figures S26-29.

The MFI was normalised to MFI of PNAM-treated cells using Equation (3).

$$Normalised\ MFI\ [a.u.] = \left(\frac{MFI_{sample}}{MFI_{NC}} \times \frac{1}{rfluorescence_{sample}}\right) \Big/ \left(\frac{MFI_{PNAM}}{MFI_{NC}} \times \frac{1}{rfluorescence_{PNAM}}\right) \quad (3)$$

Association relative to HCC-78 using Equation (4)

$$association\ relative\ to\ HCC-78[\%]\ = \left(Normalised\ MFI/_{Normalised\ MFI\ HCC-78}\right) \times 100 \quad (4)$$

The temperature-dependent reduction of cell association was calculated using Equation (5).

$$Relative\ cell\ association = 1 - \frac{MFI_{4\,°C}\ (normalized)}{MFI_{37\,°C}\ (normalized)}. \quad (5)$$

Cell association assay III: Polymer-cell association by blocking amino-acid transporters and competitive uptake

2×10^5 MDA-MB-231 cells per well were seeded in a 24-well plate and cultivated for 24 h. Afterward, the medium was replaced by fresh medium without FBS (225 µl per well). For the blocking of transporters, selected amino-acid transporter inhibitors were dissolved in DPBS with final concentrations of 100 mM (BzlSer), 100 mM (BCH), 1 mM (Sulfazaline), and 0.5 µM (MSC-4381) and added to the wells (25 µl per well).Inhibitor selectivity profile is provided in **Table 5**. After 15 min incubation, the medium was discarded and the cells washed with DPBS. Fresh medium was added (450 µl per well) and the prepared polymer solutions in DPBS (c = 25 µM) were added (50 µl per well).

Table 5. Inhibitor selectivity profile across amino acid and monocarboxylate transporters. Alanine/Serine/Cysteine Transporter 1 (ASCT1), Alanine/Serine/Cysteine Transporter 2 (ASCT2), L-type Amino Acid Transporter 1 (LAT1), L-type Amino Acid Transporter 2 (LAT2), Sodium-coupled Neutral Amino Acid Transporter 1 (SNAT1), Sodium-coupled Neutral Amino Acid Transporter 2 (SNAT2), Cystine/Glutamate Antiporter light chain (xCT; system xc-), and Monocarboxylate Transporter 4 (MCT4). “Yes” indicates reported inhibition/interaction in this dataset; “No” indicates no reported.

Inhibitor	ASCT1	ASCT2	LAT1	LAT2	SNAT1	SNAT2	xCT	MCT4
BzlSer	**Yes**	**Yes**	**Yes**	No	**Yes**	**Yes**	No	No
BCH	No	No	**Yes**	**Yes**	No	No	No	No
MSC-4381	No	No	No	No	No	No	No	**Yes**
Sulfasalazine	No	No	No	No	No	No	**Yes**	No

For assays with competitive amino acids, a 10 × stock of the corresponding compound was prepared in DPBS and then mixed with cell culture media to obtain the 1× concentration. Then, the media were substituted with 450 µL per well fresh medium containing the competiting amino acids. After dilution of the polymers in DPBS to a concentration of c = 25 µM, 50 µL per well of the respective polymer was added and incubated for 4 h at 37 °C in the cell culture incubator (final c = 2.5 µM). The NC contained only 50 µL DPBS. After an incubation time of 4 h at 37°C in the cell culture incubator, the cells were collected for flow cytometer measurements as described above (see Cell association assay I) (n = 2+2 in AAT blocking experiment and n = 2 in competitive uptake experiment). A detailed gating strategy is provided in Fig S32. The normalized MFI was calculated using Equation (2). The inhibitor-dependent reduction of cell association was calculated using Equation (6).

$$Reduction\ [\%] = 1 - \frac{MFI_{without\ inhibitor}\ (normalized)}{MFI_{with\ inhibitor}\ (normalized)} \cdot 100\% \qquad (6)$$

4.3.6. Confocal microscopy

For confocal laser scanning microscopy (CLSM), MDA-MB231 cells (DSMZ, ACC 732) were seeded with 2 × 10^5 cells mL^{-1} and cultured at 37 °C in humidified 5% v/v CO_2 atmosphere in Dulbecco's Modified Eagle Medium (DMEM) Low Glucose (1 g L^{-1}). The medium was supplemented with 10% v/v fetal bovine serum (FBS), 100 U mL^{-1} penicillin and 100 µg mL^{-1} streptomycin (culture medium). For the experiments the cells were seeded in 500 µL medium and incubated for 24 h in an IBIDI 24 well plate. 1 h prior to treatment the medium was changed to 450 µL fresh medium. 50 µL of the polymers solutions were added to the cells which were then incubated for another 1 h. After the incubation the cells were washed twice with warm 1 x Dulbecco's PBS, followed by a fixation step with a 2% prediluted paraformaldehyde solution in 1 x PBS. The fixation took place at room temperature for 10 min. Afterwards cells were washed twice with warm 1 x PBS. Hoechst33342 and CellMask Plasma Membrane Stain green were prediluted in warm cell culture medium and added to each well (0.5 µL of each stain per well). The staining was performed at 37 °C in humidified 5% v/v CO_2 atmosphere for 10 min. Afterwards the cells were washed again twice with 1 x PBS and then measured in 1 x PBS by CLSM. Imaging was performed using the LSM980 (Zeiss) The lasers had a wavelength

of 405 nm (0.2%) (detection wavelength 410 - 481 nm, detection of Hoechst), 488 nm (0.7%) (detection wavelength 492 - 527 nm, membrane) and 639 nm (1.1%) (detection wavelength 644 - 710 nm, detection of Cy5). All images were processed with ZEN software, version 3.7 (ZEN lite) (Zeiss). All measurements were performed at least twice, and the images presented in the paper are representative.

4.3.7. Statistical analysis

To assess the normal distribution of the data, a Lilliefors test was conducted using Origin2025 (OriginLab, Massachusetts, USA). Afterward a Levene's test was performed to analyse the homogeneity of the variances. In addition, the unequal variances were tested by the unpaired Welch's t-test. Statistical significance was defined as $p \leq 0.05$ for all tests.

5. Associated content

5.1. Supporting information

The supporting information is available free of charge and contains further analysis of the materials in this study, including ^{1}H spectra, fluorescence spectra, FTIR spectra, SEC data, cell viability data, cell association and uptake data.

6. Author information

6.1. Corresponding author

Meike N. Leiske – Macromolecular Chemistry, University of Bayreuth, Universitätsstraße 30, 95447 Bayreuth, Germany; Bavarian Polymer Institute, Universitätsstraße 30, 95447 Bayreuth, Germany; orcid.org/0000-0002-8525-2324; Email: meike.leiske@uni-bayreuth.de

6.2. Authors

Jonas De Breuck – Macromolecular Chemistry, University of Bayreuth, Universitätsstraße 30, 95447 Bayreuth, Germany; orcid.org/0009-0004-0248-9943

Theresa Lutz – Macromolecular Chemistry, University of Bayreuth, Universitätsstraße 30, 95447 Bayreuth, Germany

Christian Jahns – Macromolecular Chemistry, University of Bayreuth, Universitätsstraße 30, 95447 Bayreuth, Germany

Jonas Debbeler – Laboratory of Organic and Macromolecular Chemistry (IOMC), Friedrich Schiller University Jena, Humboldtstr. 10, 07743 Jena, Germany; Jena Center for Soft Matter (JCSM), Friedrich Schiller University Jena, Philosophenweg 7, 07743 Jena, Germany

Valérie Jérôme – Process Biotechnology, University of Bayreuth, Universitätsstraße 30, 95447 Bayreuth, Germany

Ruth Freitag – Process Biotechnology, University of Bayreuth, Universitätsstraße 30, 95447 Bayreuth, Germany; Bayreuth Center for Molecular Biosciences (BZMB), University of Bayreuth, Universitätsstraße 30, 95447 Bayreuth, Germany

Anja Traeger – Laboratory of Organic and Macromolecular Chemistry (IOMC), Friedrich Schiller University Jena, Humboldtstr. 10, 07743 Jena, Germany; Jena Center for Soft Matter (JCSM), Friedrich Schiller University Jena, Philosophenweg 7, 07743 Jena, Germany, Department of Pharmaceutical Chemistry, Institute of Pharmacy, Friedrich Schiller University, Philosophenweg 14, Jena, Germany

6.3. Notes

The authors declare no competing financial interest.

7. Acknowledgements

The authors would like to acknowledge Prof Johannes Brendel and Prof Thomas Scheibel for providing access to their laboratories and equipment. We thank Dr Martin Humenik for his help with the HPLC. We would like to thank Robert Bätz and Sebastian Städter for conducting size-exclusion chromatography measurements. This project was generously supported by the German Research Foundation (DFG; project number 535904448). M.N.L. acknowledges financial support from the “Fonds der Chemischen Industrie im Verband der Chemischen Industrie.” The authors gratefully acknowledge the Bundesministerium für Bildung und Forschung (BMBF, Germany, #13XP5034A PolyBioMik), the DFG Projects PolyTarget (SFB 1278, project B01, C06, project ID: 316213987) as well as the "Thüringer Aufbaubank (TAB)" (2021 FGI 0005), and the "Europäischer Fond für regionale Entwicklung (EFRE)" (2018FGI0025) for funding of flow cytometry devices at the Jena Center for Soft Matter (JCSM). This work was performed within the Joint Lab for Polymers Jena-Bayreuth. We thank the Microverse Imaging Center (and Aurélie Jost / Patrick Then) for providing microscope facility support for data

acquisition (and data analysis). The LSM 980 (used for producing images in Figure 5) was funded by the Free State of Thuringia with grant number 2019 FGI 0001. The Microverse Imaging Center is funded by the Deutsche Forschungsgemeinschaft (DFG, German Research Foundation) under Germany´s Excellence Strategy – EXC 2051 – Project-ID 390713860. We thank BioRender.com for the possibility of graphic creation. J.P.D. acknowledges funding through a scholarship from the Thüringer Aufbaubank and „Europäischen Sozialfonds Plus der Europäischen Union".

8. References

(1) Patil, J.; Pawde, D. M.; Bhattacharya, S.; Srivastava, S. Phospholipid Complex Formulation Technology for Improved Drug Delivery in Oncological Settings: A Comprehensive Review. *AAPS PharmSciTech 2024 255* **2024**, *25* (5), 91-. https://doi.org/10.1208/S12249-024-02813-X.

(2) Lim, S. B.; Banerjee, A.; Önyüksel, H. Improvement of Drug Safety by the Use of Lipid-Based Nanocarriers. *J. Control. Release* **2012**, *163* (1), 34–45. https://doi.org/10.1016/J.JCONREL.2012.06.002.

(3) Chandel, S.; Bioavailability Enhancement, A.; Kumar Bolla, P.; Bhalani, D. V; Nutan, B.; Kumar, A.; Singh Chandel, A. K. Bioavailability Enhancement Techniques for Poorly Aqueous Soluble Drugs and Therapeutics. *Biomed. 2022, Vol. 10, Page 2055* **2022**, *10* (9), 2055. https://doi.org/10.3390/BIOMEDICINES10092055.

(4) Zhong, Y.; Meng, F.; Deng, C.; Zhong, Z. Ligand-Directed Active Tumor-Targeting Polymeric Nanoparticles for Cancer Chemotherapy. *Biomacromolecules* **2014**, *15* (6), 1955–1969. https://doi.org/10.1021/BM5003009.

(5) De Breuck, J.; Streiber, M.; Ringleb, M.; Schröder, D.; Herzog, N.; Schubert, U. S.; Zechel, S.; Traeger, A.; Leiske, M. N. Amino-Acid-Derived Anionic Polyacrylamides with Tailored Hydrophobicity-Physicochemical Properties and Cellular Interactions. *ACS Polym. Au* **2024**, *4* (3), 222–234. https://doi.org/10.1021/acspolymersau.3c00048.

(6) Leiske, M. N.; De Geest, B. G.; Hoogenboom, R. Impact of the Polymer Backbone

Chemistry on Interactions of Amino-Acid-Derived Zwitterionic Polymers with Cells. *Bioact. Mater.* **2023**, *24* (January), 524–534. https://doi.org/10.1016/j.bioactmat.2023.01.005.

(7) Van Andel, E.; Lange, S. C.; Pujari, S. P.; Tijhaar, E. J.; Smulders, M. M. J.; Savelkoul, H. F. J.; Zuilhof, H. Systematic Comparison of Zwitterionic and Non-Zwitterionic Antifouling Polymer Brushes on a Bead-Based Platform. *Langmuir* **2018**, *35* (5), 1181–1191. https://doi.org/10.1021/ACS.LANGMUIR.8B01832.

(8) Uwaezuoke, O. J.; Kumar, P.; Pillay, V.; Choonara, Y. E. Fouling in Ocular Devices: Implications for Drug Delivery, Bioactive Surface Immobilization, and Biomaterial Design. *Drug Deliv. Transl. Res. 2021 115* **2021**, *11* (5), 1903–1923. https://doi.org/10.1007/S13346-020-00879-1.

(9) Zhang, Y.; Chan, H. F.; Leong, K. W. Advanced Materials and Processing for Drug Delivery: The Past and the Future. *Adv. Drug Deliv. Rev.* **2013**, *65* (1), 104–120. https://doi.org/10.1016/J.ADDR.2012.10.003.

(10) Pei, D.; Buyanova, M. Overcoming Endosomal Entrapment in Drug Delivery. *Bioconjug. Chem.* **2018**, *30* (2), 273–283. https://doi.org/10.1021/ACS.BIOCONJCHEM.8B00778.

(11) Gabizon, A. A. Liposome Circulation Time and Tumor Targeting: Implications for Cancer Chemotherapy. *Adv. Drug Deliv. Rev.* **1995**, *16* (2–3), 285–294. https://doi.org/10.1016/0169-409X(95)00030-B.

(12) Klibanov, A. L.; Maruyama, K.; Torchilin, V. P.; Huang, L. Amphipathic Polyethyleneglycols Effectively Prolong the Circulation Time of Liposomes. *FEBS Lett.* **1990**, *268* (1), 235–237. https://doi.org/10.1016/0014-5793(90)81016-H.

(13) Kang, H.; Rho, S.; Stiles, W. R.; Hu, S.; Baek, Y.; Hwang, D. W.; Kashiwagi, S.; Kim, M. S.; Choi, H. S. Size-Dependent EPR Effect of Polymeric Nanoparticles on Tumor Targeting. *Adv. Healthc. Mater.* **2020**, *9* (1), 1901223. https://doi.org/10.1002/ADHM.201901223;WEBSITE:WEBSITE:ADVANCED;CTYPE:STRING:JOURNAL.

(14) Fang, J.; Nakamura, H.; Maeda, H. The EPR Effect: Unique Features of Tumor

Blood Vessels for Drug Delivery, Factors Involved, and Limitations and Augmentation of the Effect. *Adv. Drug Deliv. Rev.* **2011**, *63* (3), 136–151. https://doi.org/10.1016/J.ADDR.2010.04.009.

(15) Traeger, A.; Leiske, M. N. The Whole Is Greater than the Sum of Its Parts – Challenges and Perspectives in Polyelectrolytes. *Biomacromolecules* **2024**, *26* (1), 5–32. https://doi.org/10.1021/ACS.BIOMAC.4C01061.

(16) Li, M.; Zhang, W.; Li, J.; Qi, Y.; Peng, C.; Wang, N.; Fan, H.; Li, Y. Zwitterionic Polymers: Addressing the Barriers for Drug Delivery. *Chinese Chem. Lett.* **2023**, *34* (11), 108177. https://doi.org/10.1016/j.cclet.2023.108177.

(17) Fujii, S.; Sakurai, K. Zwitterionic Amino Acid Polymer-Grafted Core-Crosslinked Particle toward Tumor Delivery. *Biomacromolecules* **2022**, *23* (9), 3968–3977. https://doi.org/10.1021/acs.biomac.2c00803.

(18) Fujii, S.; Takano, S.; Nakazawa, K.; Sakurai, K. Impact of Zwitterionic Polymers on the Tumor Permeability of Molecular Bottlebrush-Based Nanoparticles. *Biomacromolecules* **2022**, *23* (7), 2846–2855. https://doi.org/10.1021/acs.biomac.2c00216.

(19) Schlenoff, J. B. Zwitteration: Coating Surfaces with Zwitterionic Functionality to Reduce Nonspecific Adsorption. **2014**. https://doi.org/10.1021/la500057j.

(20) He, M.; Gao, K.; Zhou, L.; Jiao, Z.; Wu, M.; Cao, J.; You, X.; Cai, Z.; Su, Y.; Jiang, Z. Zwitterionic Materials for Antifouling Membrane Surface Construction. *Acta Biomater.* **2016**, *40*, 142–152. https://doi.org/10.1016/J.ACTBIO.2016.03.038.

(21) Bernstein, R.; Belfer, S.; Freger, V. Bacterial Attachment to RO Membranes Surface-Modified by Concentration-Polarization-Enhanced Graft Polymerization. *Environ. Sci. Technol.* **2011**, *45* (14), 5973–5980. https://doi.org/10.1021/ES1043694.

(22) Sarker, P.; Lu, T.; Liu, D.; Wu, G.; Chen, H.; Jahan Sajib, M. S.; Jiang, S.; Chen, Z.; Wei, T. Hydration Behaviors of Nonfouling Zwitterionic Materials. *Chem. Sci.* **2023**, *14* (27), 7500–7511. https://doi.org/10.1039/d3sc01977b.

(23) Chen, R.; Eccleston, M. E.; Yue, Z.; Slater, N. K. H. Synthesis and PH-Responsive Properties of Pseudo-Peptides Containing Hydrophobic Amino Acid Grafts. *J. Mater. Chem.* **2009**, *19* (24), 4217–4224. https://doi.org/10.1039/B902822F.

(24) Chen, S.; Wang, S.; Kopytynski, M.; Bachelet, M.; Chen, R. Membrane-Anchoring, Comb-Like Pseudopeptides for Efficient, PH-Mediated Membrane Destabilization and Intracellular Delivery. *ACS Appl. Mater. Interfaces* **2017**, *9* (9), 8021–8029. https://doi.org/10.1021/acsami.7b00498.

(25) Laschewsky, A. Structures and Synthesis of Zwitterionic Polymers. *Polymers (Basel).* **2014**, *6* (5), 1544–1601. https://doi.org/10.3390/polym6051544.

(26) Wang, S. PH-Responsive Amphiphilic Carboxylate Polymers: Design and Potential for Endosomal Escape. *Front. Chem.* **2021**, *9* (March), 1–8. https://doi.org/10.3389/fchem.2021.645297.

(27) Takano, S.; Sakurai, K.; Fujii, S. Internalization into Cancer Cells of Zwitterionic Amino Acid Polymers via Amino Acid Transporter Recognition. *Polym. Chem.* **2021**, *12* (42), 6083–6087. https://doi.org/10.1039/d1py01010g.

(28) Theodorou, I.; Anilkumar, P.; Lelandais, B.; Clarisse, D.; Doerflinger, A.; Gravel, E.; Ducongé, F.; Doris, E. Stable and Compact Zwitterionic Polydiacetylene Micelles with Tumor-Targeting Properties. *Chem. Commun.* **2015**, *51* (80), 14937–14940. https://doi.org/10.1039/c5cc05333a.

(29) Leiske, M. N.; Kempe, K. A Guideline for the Synthesis of Amino-Acid-Functionalized Monomers and Their Polymerizations. *Macromol. Rapid Commun.* **2022**, *43* (2), 1–24. https://doi.org/10.1002/marc.202100615.

(30) Maji, T.; Banerjee, S.; Biswas, Y.; Mandal, T. K. Dual-Stimuli-Responsive l -Serine-Based Zwitterionic UCST-Type Polymer with Tunable Thermosensitivity. *Macromolecules* **2015**, *48* (14), 4957–4966. https://doi.org/10.1021/acs.macromol.5b01099.

(31) Bauri, K.; Roy, S. G.; Pant, S.; De, P. Controlled Synthesis of Amino Acid-Based PH-Responsive Chiral Polymers and Self-Assembly of Their Block Copolymers. *Langmuir* **2013**, *29* (8), 2764–2774. https://doi.org/10.1021/la304918s.

(32) De Breuck, J.; Jérôme, V.; Freitag, R.; Leiske, M. N. Zwitterionic Amino-Acid-Derived Polyacrylamides with a Betaine Twist – Synthesis and Characterization. *Macromol. Rapid Commun.* **2025**, *46* (1), 2400623. https://doi.org/10.1002/MARC.202400623;JOURNAL:JOURNAL:01732803;WGROUP:STRING:PUBLICATION.

(33) Namazian, M.; Halvani, S. Calculations of PKa Values of Carboxylic Acids in Aqueous Solution Using Density Functional Theory. *J. Chem. Thermodyn.* **2006**, *38* (12), 1495–1502. https://doi.org/10.1016/J.JCT.2006.05.002.

(34) Wildman, S. A.; Crippen, G. M. Prediction of Physicochemical Parameters by Atomic Contributions. *J. Chem. Inf. Comput. Sci.* **1999**, *39* (5), 868–873. https://doi.org/10.1021/CI990307L.

(35) Kord Forooshani, P.; Lee, B. P. Recent Approaches in Designing Bioadhesive Materials Inspired by Mussel Adhesive Protein. *J. Polym. Sci. Part A Polym. Chem.* **2017**, *55* (1), 9–33. https://doi.org/10.1002/POLA.28368;REQUESTEDJOURNAL:JOURNAL:10990518;JOURNAL:JOURNAL:15429350;WGROUP:STRING:PUBLICATION.

(36) Dawson, M. C.; Elliott, D. C.; Elliott, W. H.; Jones, K. M. DATA FOR BIOCHEMICAL RESEARCH EDITED BY OXFORD AT THE CLARENDON PRESS 1959.

(37) van Sluis, R.; Bhujwalla, Z. M.; Raghunand, N.; Ballesteros, P.; Alvarez, J.; Cerd□n, S.; Galons, J.-P.; Gillies, R. J. In Vivo Imaging of Extracellular PH Using1H MRSI. *Magn. Reson. Med.* **1999**, *41* (4), 743–750. https://doi.org/10.1002/(SICI)1522-2594(199904)41:4<743::AID-MRM13>3.0.CO;2-Z.

(38) Dinda, P.; Anas, M.; Banerjee, P.; Mandal, T. K. Dual Thermoresponsive Boc-Lysine-Based Acryl Polymer: RAFT Kinetics and Anti-Protein-Fouling of Its Zwitterionic Form. *Macromolecules* **2022**, *55* (10), 4011–4024. https://doi.org/10.1021/acs.macromol.2c00633.

(39) Chou, Y. N.; Ou, M. Z. Zwitterionic Surface Modification of Aldehydated

Sulfobetaine Copolymers for the Formation of Bioinert Interfaces. *ACS Appl. Polym. Mater.* **2023**, *5* (7), 5411–5428. https://doi.org/10.1021/acsapm.3c00762.

(40) Wang, Z.; Ma, G.; Zhang, J.; Lin, W.; Ji, F.; Bernards, M. T.; Chen, S. Development of Zwitterionic Polymer-Based Doxorubicin Conjugates: Tuning the Surface Charge To Prolong the Circulation and Reduce Toxicity. *Langmuir* **2014**, *30* (13), 3764–3774. https://doi.org/10.1021/LA5000765.

(41) Ou, H.; Cheng, T.; Zhang, Y.; Liu, J.; Ding, Y.; Zhen, J.; Shen, W.; Xu, Y.; Yang, W.; Niu, P.; Liu, J.; An, Y.; Liu, Y.; Shi, L. Surface-Adaptive Zwitterionic Nanoparticles for Prolonged Blood Circulation Time and Enhanced Cellular Uptake in Tumor Cells. *Acta Biomater.* **2018**, *65*, 339–348. https://doi.org/10.1016/J.ACTBIO.2017.10.034.

(42) Leiske, M. N.; Mazrad, Z. A. I.; Zelcak, A.; Wahi, K.; Davis, T. P.; McCarroll, J. A.; Holst, J.; Kempe, K. Zwitterionic Amino Acid-Derived Polyacrylates as Smart Materials Exhibiting Cellular Specificity and Therapeutic Activity. *Biomacromolecules* **2022**, *23* (6), 2374–2387. https://doi.org/10.1021/acs.biomac.2c00143.

(43) Qu, Y.; Han, B.; Yu, Y.; Yao, W.; Bose, S.; Karlan, B. Y.; Giuliano, A. E.; Cui, X. Evaluation of MCF10A as a Reliable Model for Normal Human Mammary Epithelial Cells. *PLoS One* **2015**, *10* (7), e0131285. https://doi.org/10.1371/JOURNAL.PONE.0131285.

(44) Kitchen, J. R.; Cysyk, R. L. Synthesis and Release of Hyaluronic Acid by Swiss 3T3 Fibroblasts. *Biochem. J.* **1995**, *309* (2), 649–656. https://doi.org/10.1042/bj3090649.

(45) Mahmoud, A. M.; de Jongh, P. A. J. M.; Briere, S.; Chen, M.; Nowell, C. J.; Johnston, A. P. R.; Davis, T. P.; Haddleton, D. M.; Kempe, K. Carboxylated Cy5-Labeled Comb Polymers Passively Diffuse the Cell Membrane and Target Mitochondria. *ACS Appl. Mater. Interfaces* **2019**, *11* (34), 31302–31310. https://doi.org/10.1021/acsami.9b09395.

(46) Bareford, L. M.; Swaan, P. W. ENDOCYTIC MECHANISMS FOR TARGETED

DRUG DELIVERY. *Adv. Drug Deliv. Rev.* **2007**, *59* (8), 748. https://doi.org/10.1016/J.ADDR.2007.06.008.

(47) Kaźmierczak, Z.; Szostak-Paluch, K.; Przybyło, M.; Langner, M.; Witkiewicz, W.; Jędruchniewicz, N.; Dąbrowska, K. Endocytosis in Cellular Uptake of Drug Delivery Vectors: Molecular Aspects in Drug Development. *Bioorg. Med. Chem.* **2020**, *28* (18), 115556. https://doi.org/10.1016/J.BMC.2020.115556.

(48) Sousa De Almeida, M.; Susnik, E.; Drasler, B.; Taladriz-Blanco, P.; Petri-Fink, A.; Rothen-Rutishauser, B. Understanding Nanoparticle Endocytosis to Improve Targeting Strategies in Nanomedicine. *Chem. Soc. Rev.* **2021**, *50* (9), 5397–5434. https://doi.org/10.1039/D0CS01127D.

(49) Bröer, S. Amino Acid Transporters as Targets for Cancer Therapy: Why, Where, When, and How. *Int. J. Mol. Sci.* **2020**, *21* (17), 1–20. https://doi.org/10.3390/ijms21176156.

(50) Fuchs, B. C.; Bode, B. P. Amino Acid Transporters ASCT2 and LAT1 in Cancer: Partners in Crime? *Semin. Cancer Biol.* **2005**, *15* (4), 254–266. https://doi.org/10.1016/j.semcancer.2005.04.005.

(51) Cha, Y. J.; Kim, E. S.; Koo, J. S. Amino Acid Transporters and Glutamine Metabolism in Breast Cancer. *Int. J. Mol. Sci. 2018, Vol. 19, Page 907* **2018**, *19* (3), 907. https://doi.org/10.3390/IJMS19030907.

(52) Morotti, M.; Zois, C. E.; El-Ansari, R.; Craze, M. L.; Rakha, E. A.; Fan, S. J.; Valli, A.; Haider, S.; Goberdhan, D. C. I.; Green, A. R.; Harris, A. L. Increased Expression of Glutamine Transporter SNAT2/SLC38A2 Promotes Glutamine Dependence and Oxidative Stress Resistance, and Is Associated with Worse Prognosis in Triple-Negative Breast Cancer. *Br. J. Cancer 2020 1242* **2020**, *124* (2), 494–505. https://doi.org/10.1038/s41416-020-01113-y.

(53) van Geldermalsen, M.; Quek, L.-E.; Turner, N.; Freidman, N.; Pang, A.; Guan, Y. F.; Krycer, J. R.; Ryan, R.; Wang, Q.; Holst, J. Benzylserine Inhibits Breast Cancer Cell Growth by Disrupting Intracellular Amino Acid Homeostasis and Triggering Amino Acid Response Pathways. *BMC Cancer* **2018**, *18* (1), 689.

https://doi.org/10.1186/s12885-018-4599-8.

(54) Kim, D. K.; Kim, I. J.; Hwang, S.; Kook, J. H.; Lee, M. C.; Shin, B. A.; Bae, C. S.; Yoon, J. H.; Ahn, S. G.; Kim, S. A.; Kanai, Y.; Endou, H.; Kim, J. K. System L-Amino Acid Transporters Are Differently Expressed in Rat Astrocyte and C6 Glioma Cells. *Neurosci. Res.* **2004**, *50* (4), 437–446. https://doi.org/10.1016/J.NEURES.2004.08.003.

(55) Yanagida, O.; Kanai, Y.; Chairoungdua, A.; Kim, D. K.; Segawa, H.; Nii, T.; Cha, S. H.; Matsuo, H.; Fukushima, J. ichi; Fukasawa, Y.; Tani, Y.; Taketani, Y.; Uchino, H.; Kim, J. Y.; Inatomi, J.; Okayasu, I.; Miyamoto, K. ichi; Takeda, E.; Goya, T.; Endou, H. Human L-Type Amino Acid Transporter 1 (LAT1): Characterization of Function and Expression in Tumor Cell Lines. *Biochim. Biophys. Acta - Biomembr.* **2001**, *1514* (2), 291–302. https://doi.org/10.1016/S0005-2736(01)00384-4.

(56) Paul, T. J.; Strzelczyk, A. K.; Feldhof, M. I.; Schmidt, S. Temperature-Switchable Glycopolymers and Their Conformation-Dependent Binding to Receptor Targets. *Biomacromolecules* **2020**, *21* (7), 2913–2921. https://doi.org/10.1021/ACS.BIOMAC.0C00676/SUPPL_FILE/BM0C00676_SI_001.PDF.

(57) Ferguson, C. J.; Hughes, R. J.; Nguyen, D.; Pham, B. T. T.; Gilbert, R. G.; Serelis, A. K.; Such, C. H.; Hawkett, B. S. Ab Initio Emulsion Polymerization by RAFT-Controlled Self-Assembly. *Macromolecules* **2005**, *38* (6), 2191–2204. https://doi.org/10.1021/ma048787r.

(58) Leiske, M. N.; Kuenneth, C.; De Breuck, J.; De Geest, B. G.; Hoogenboom, R. Amphiphilic Zwitterionic Bioderived Block Copolymers from Glutamic Acid and Cholesterol – Ability to Form Nanoparticles and Serve as Vectors for the Delivery of 6-Mercaptopurine. *Macromol. Chem. Phys.* **2023**, *224* (24), 1–11. https://doi.org/10.1002/macp.202300200.

(59) Ohshima, H. A Simple Expression for Henry's Function for the Retardation Effect in Electrophoresis of Spherical Colloidal Particles. *J. Colloid Interface Sci.* **1994**, *168* (1), 269–271. https://doi.org/10.1006/jcis.1994.1419.

(60) Chong, Y. K.; Moad, G.; Rizzardo, E.; Thang, S. H. Thiocarbonylthio End Group Removal from RAFT-Synthesized Polymers by Radical-Induced Reduction. *Macromolecules* **2007**, *40* (13), 4446–4455. https://doi.org/10.1021/MA062919U.

Impact of the polymer side-chain chemistry on interactions of amino-acid-derived polyelectrolytes with cells

Jonas De Breuck,[a] Theresa M. Lutz,[a] Christian Jahns,[a] Jonas Debbeler,[b,c] Valérie Jérôme,[d] Ruth Freitag,[d,e] Anja Traeger,[b,c] Meike N. Leiske[a,f,*]

[a]Macromolecular Chemistry, University of Bayreuth, Universitätsstraße 30, 95447 Bayreuth, Germany

[b]Laboratory of Organic and Macromolecular Chemistry (IOMC), Friedrich Schiller University Jena, Humboldtstr. 10, 07743 Jena, Germany

[c]Jena Center for Soft Matter (JCSM), Friedrich Schiller University Jena, Philosophenweg 7, 07743 Jena, Germany

[d]Process Biotechnology, University of Bayreuth, Universitätsstraße 30, 95447 Bayreuth, Germany

[e]Bayreuth Center for Molecular Biosciences (BZMB), University of Bayreuth, Universitätsstraße 30, 95447 Bayreuth, Germany

[f]Bavarian Polymer Institute, Universitätsstraße 30, 95447 Bayreuth, Germany

*correspondence to: meike.leiske@uni-bayreuth.de

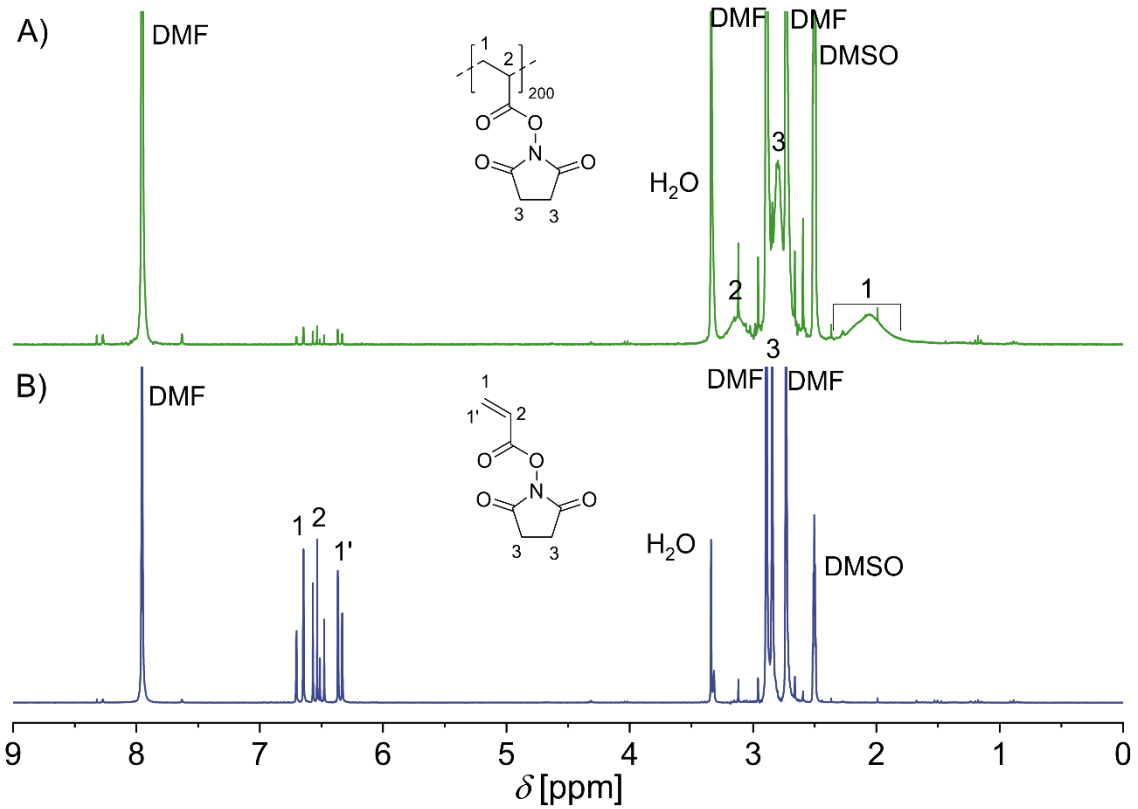


Figure S1. ^{1}H NMR (DMSO-d6, 300 MHz) spectra of polymerization mixture PNAS A: t=24h. B: 0h

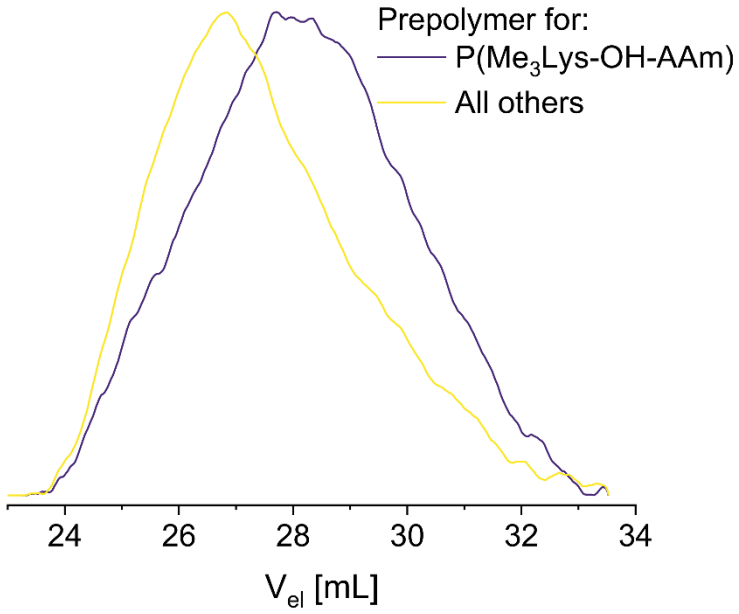


Figure S2. SEC (DMAc) elugram of PNAS.

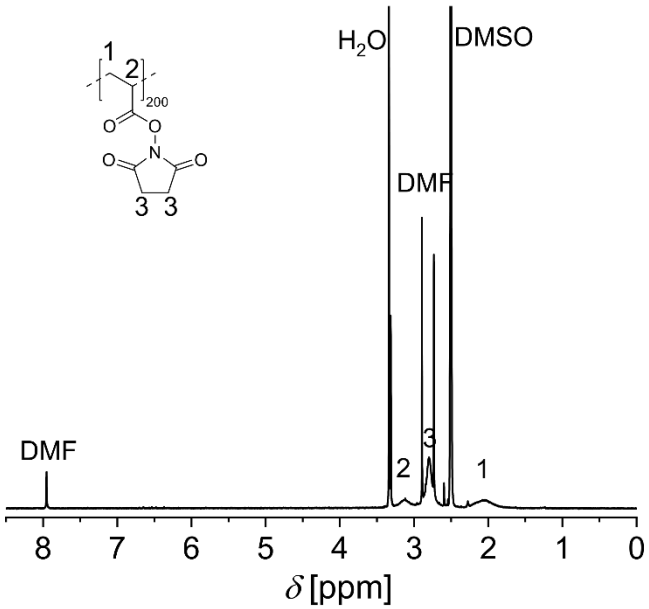


Figure S3. ^{1}H NMR (DMSO-d6, 300 MHz) PNAS

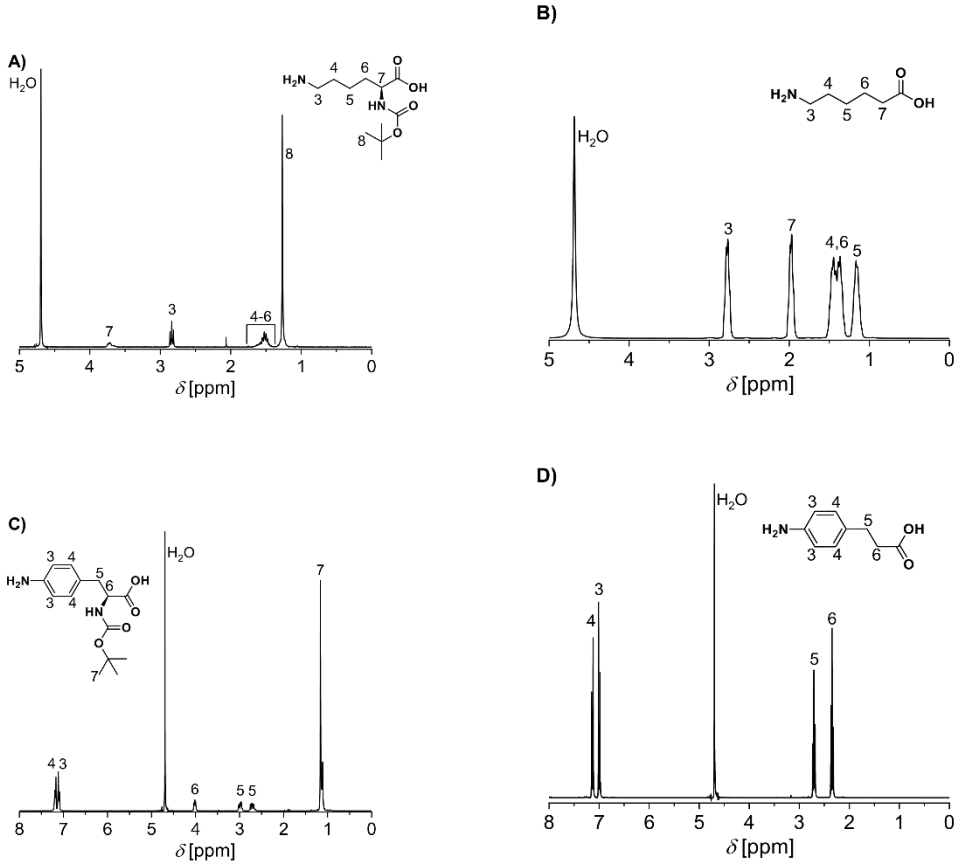


Figure S4. ^{1}H NMR (D_2O, 300 MHz) spectra of A: Boc-Lys-OH. B: 6-AmHex-OH. C: Boc-4-AmPhe-OH. D: 4-AmPhenylPr-OH.

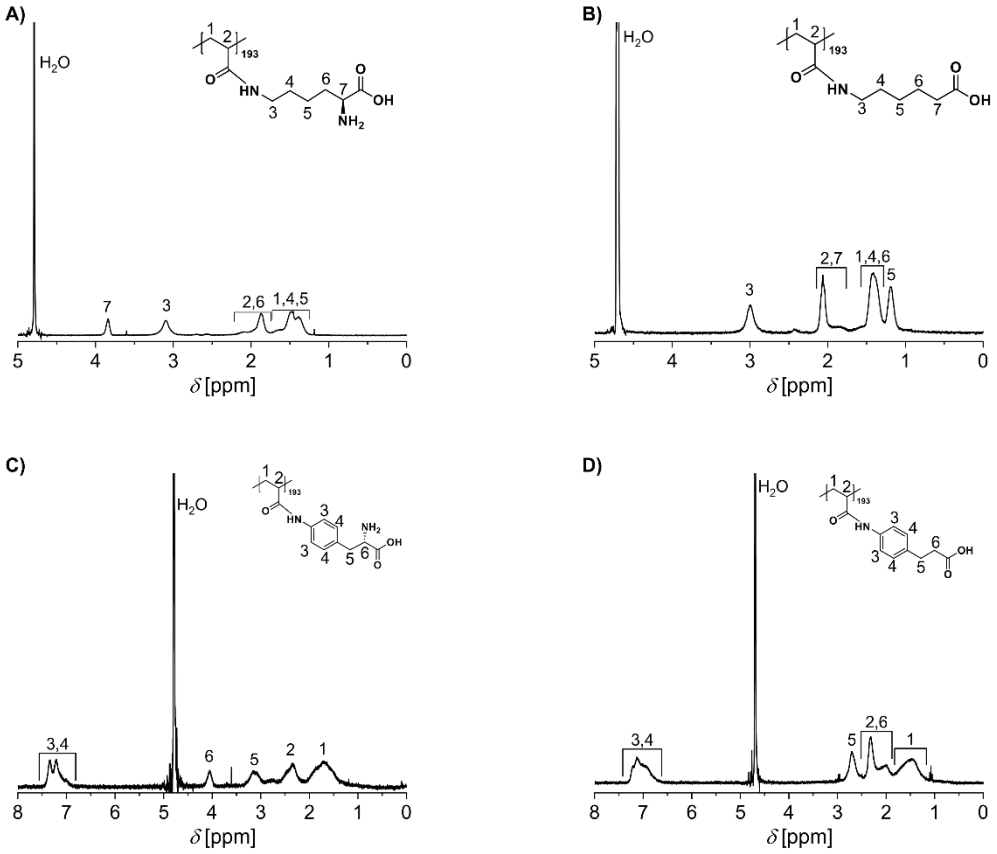


Figure S5. ^{1}H NMR (D_2O, 300 MHz) spectra of A: P(Lys-OH-AAm). B: P(Hex-OH-AAm). C: P(Phe-OH-AAm). D: P(PhenylPr-OH-AAm).

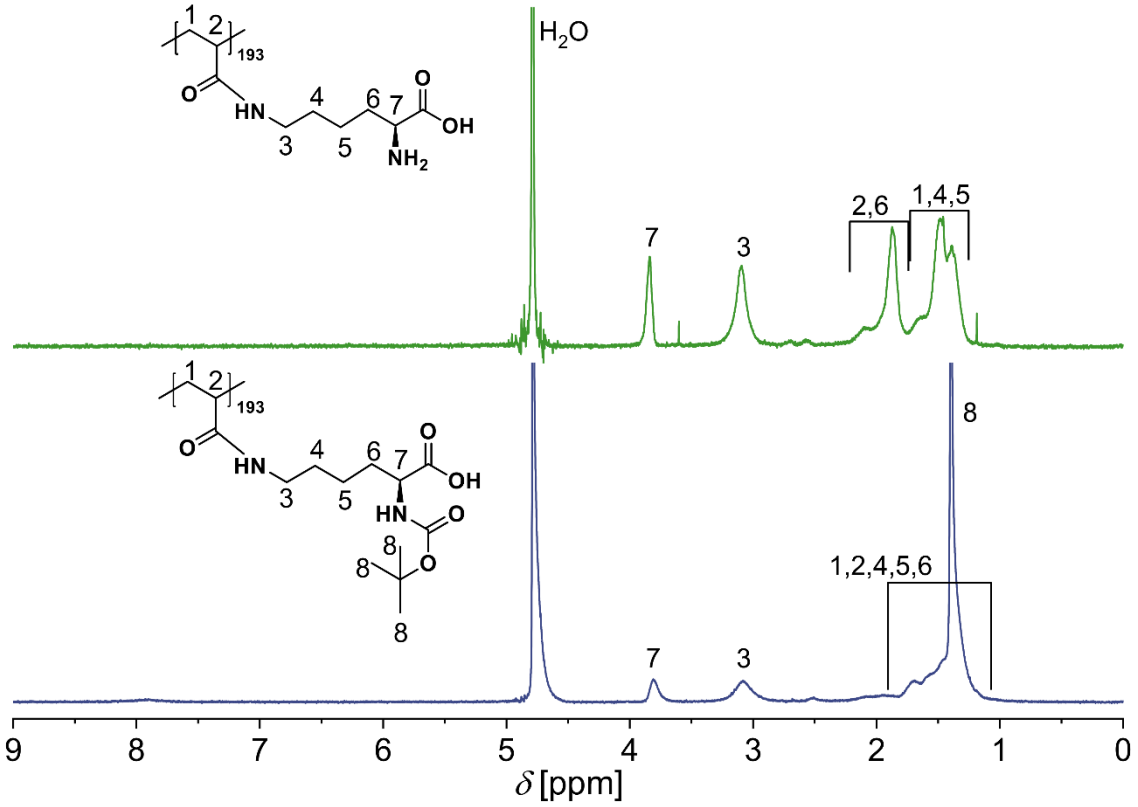


Figure S6. ^{1}H NMR (D_2O, 300 MHz) spectra of P(Boc-Lys-OH-AAm) (bottom) and P(Boc-Lys-OH-AAm) (top)

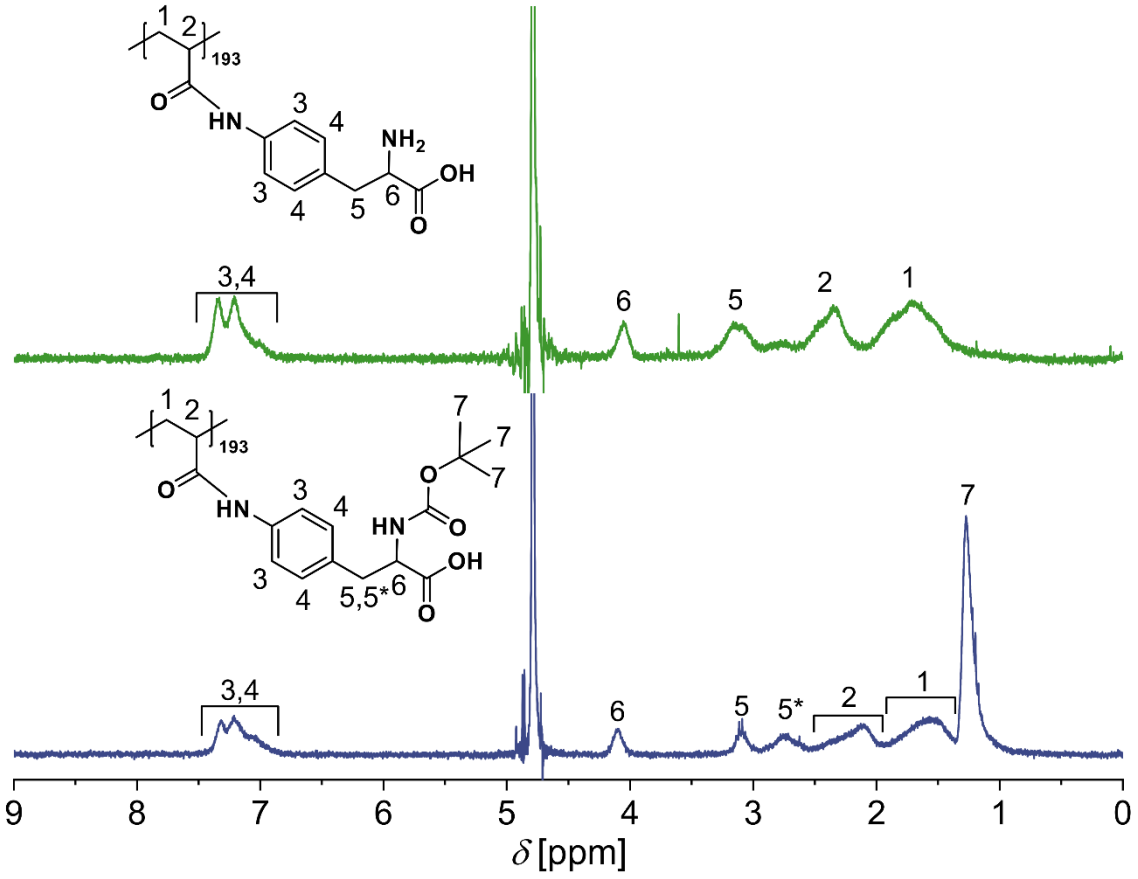


Figure S7. ^{1}H NMR (D_2O, 300 MHz) spectra of P(Boc-Phe-OH-AAm) (bottom) and P(Phe-OH-AAm) (top)

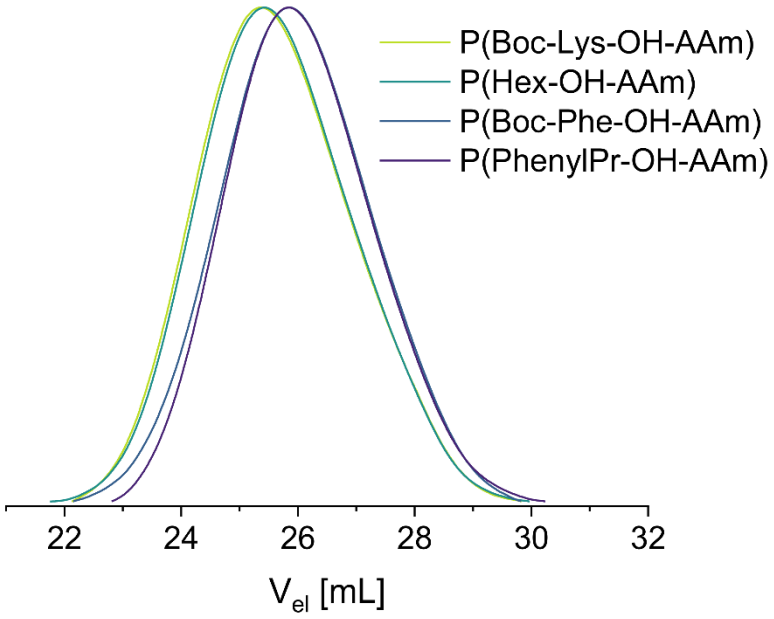


Figure S8. Size-exclusion chromatograms (0.07 M aq. Na_2HPO_4) of P(BocLys-OH-AAm), P(Hex-OH-AAm), P(Boc-Phe-OH-AAm) and P(PhenylPr-OH-AAm)

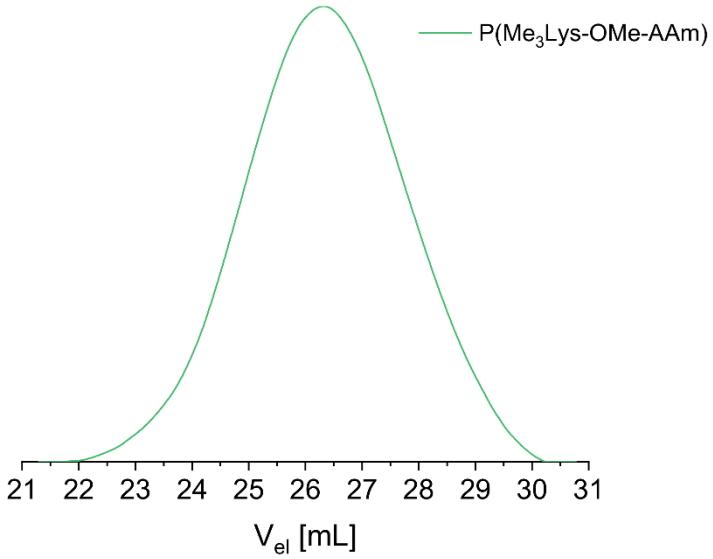


Figure S9. Size-exclusion chromatograms (0.07 M aq. Na_2HPO_4) of P(Lys-OH-AAm) and P(Phe-OH-AAm)

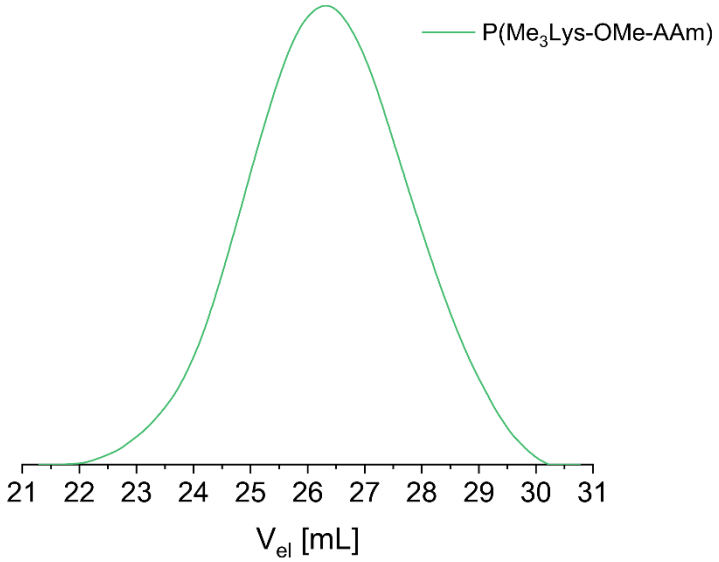


Figure S10. Size-exclusion chromatogram (80:20 [H_2O/ACN]+0.1M NaCl+0.1V% TFA) of P(Me_3Lys-OMe-AAm)

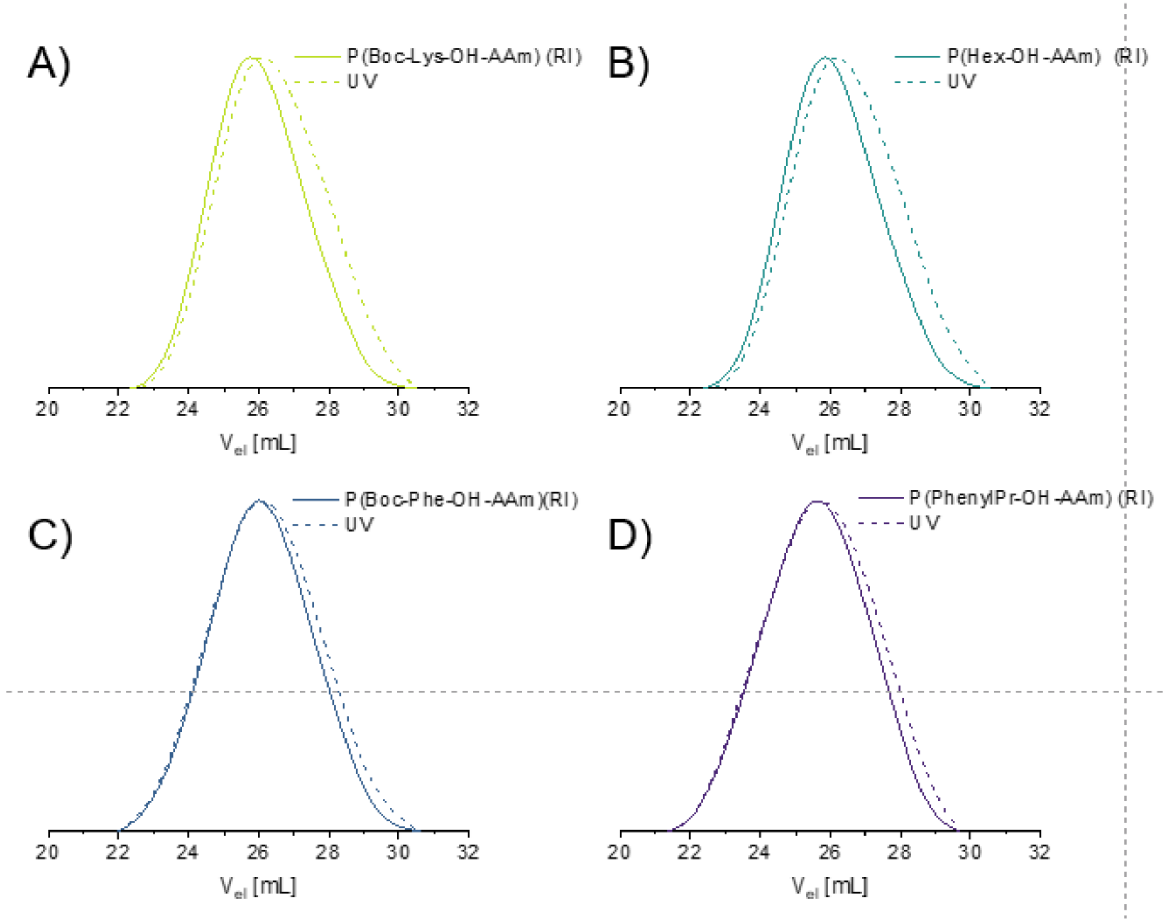


Figure S11. Size-exclusion chromatograms (0.07 M aq. Na_2HPO_4) of Cyanine5-amine (Cy5)-labelled (A) P(BocLys-OH-AAm)-Cy5, (B) P(Hex-OH-AAm)-Cy5, (C) P(Boc-Phe-OH-AAm)-Cy5 and (D) P(PhenylPr-OH-AAm)-Cy5. Refractive index (line) and λ = 600 nm (dashed)

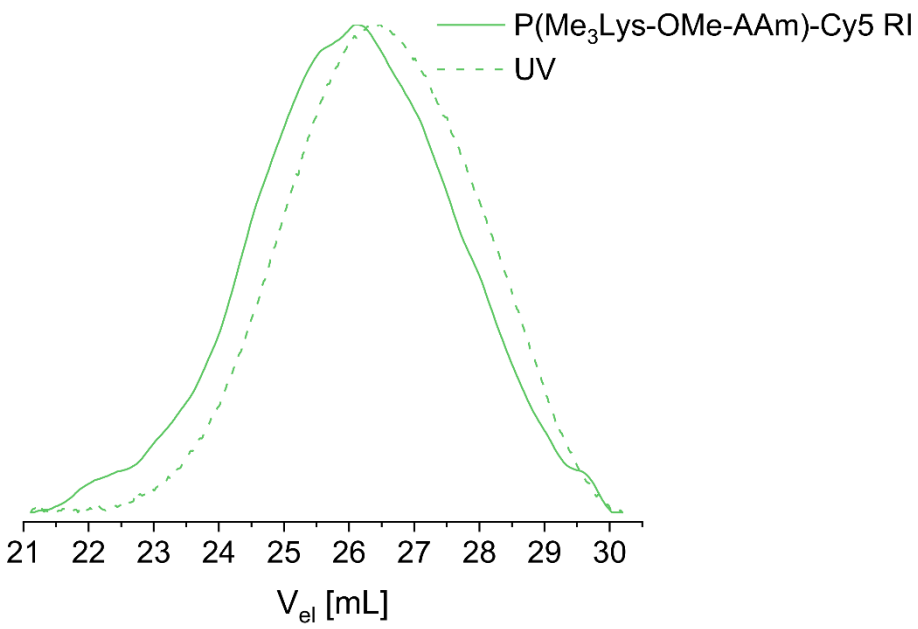


Figure S12. Size-exclusion chromatograms (80:20 [H_2O/ACN]+0.1M NaCl+0.1V% TFA) of P(Me_3Lys-OMe-AAm)-Cy5. Refractive index (line) and λ = 600 nm (dashed)

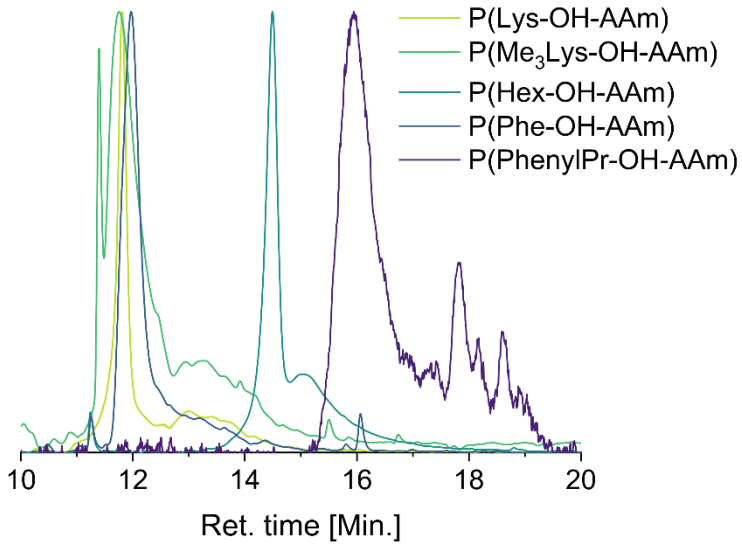


Figure S13. HPLC chromatograms (acetonitrile/water gradient, 0.1v% TFA). Spectra show the normalised UV-absorption (at 215 nm) for eluting P(Lys-OH-AAm)-Cy5, P(Me_3Lys-OH-AAm)-Cy5, P(Hex-OH-AAm)-Cy5, P(Phe-OH-AAm)-Cy5 and normalised fluorescence intensity of eluting P(PhenylPr-OH-AAm)-Cy5 (λ_{ex} = 640 nm; λ_{em} = 680 nm)

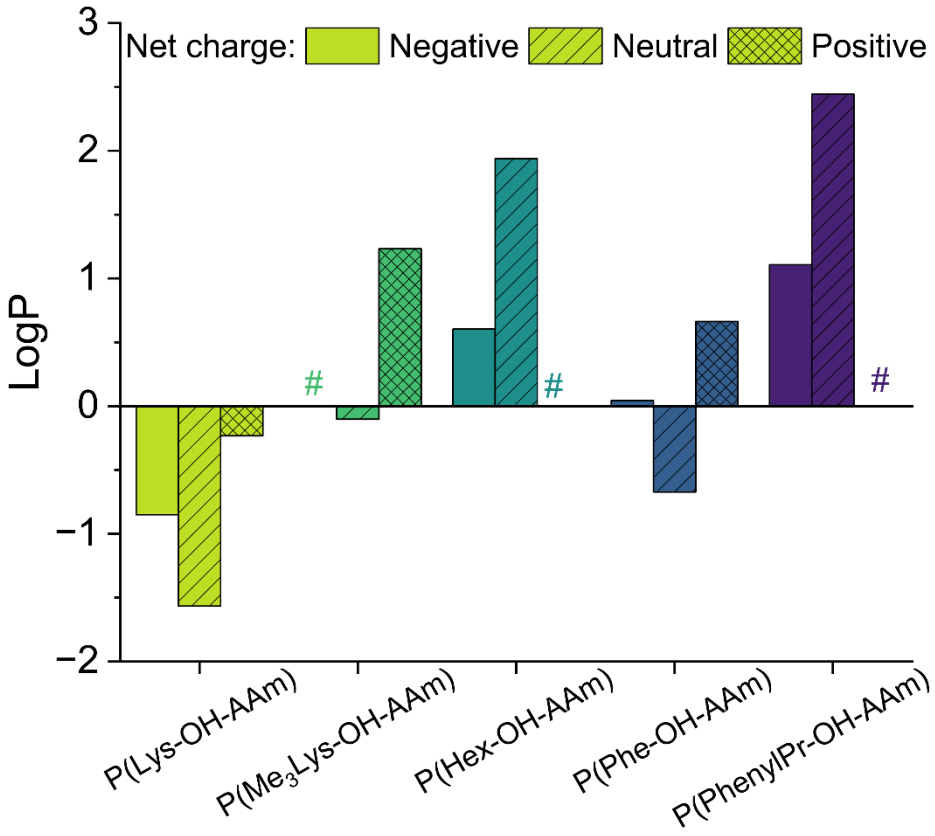


Figure S14. Theoretical partition coefficient of polyelectrolytes at negative, neutral and positive charge. # depicts polymers which do not exist in the corresponding state.

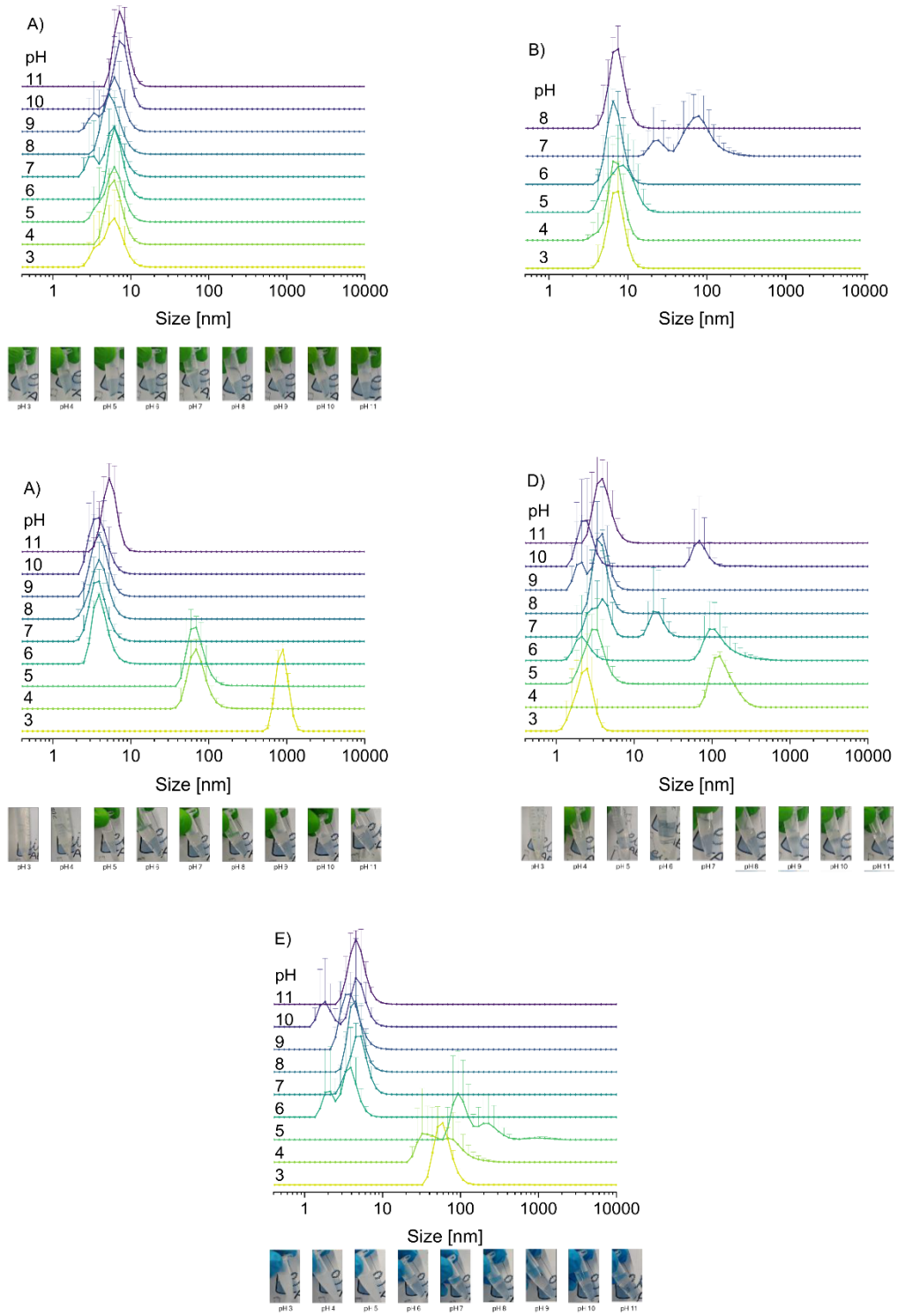


Figure S15. pH dependent number size distribution of A: P(Lys-OH-AAm). B: P(Me_3Lys-OH-Aam). C: P(Hex-OH-AAm). D: P(Phe-OH-AAm). E: P(PhenylPr-OH-AAm) in water (2 mg mL^{-1}) determined by DLS measurements. Values (scatter) represent the mean

and SD of five measurements with three runs each. Dashed lines do not represent measured values.

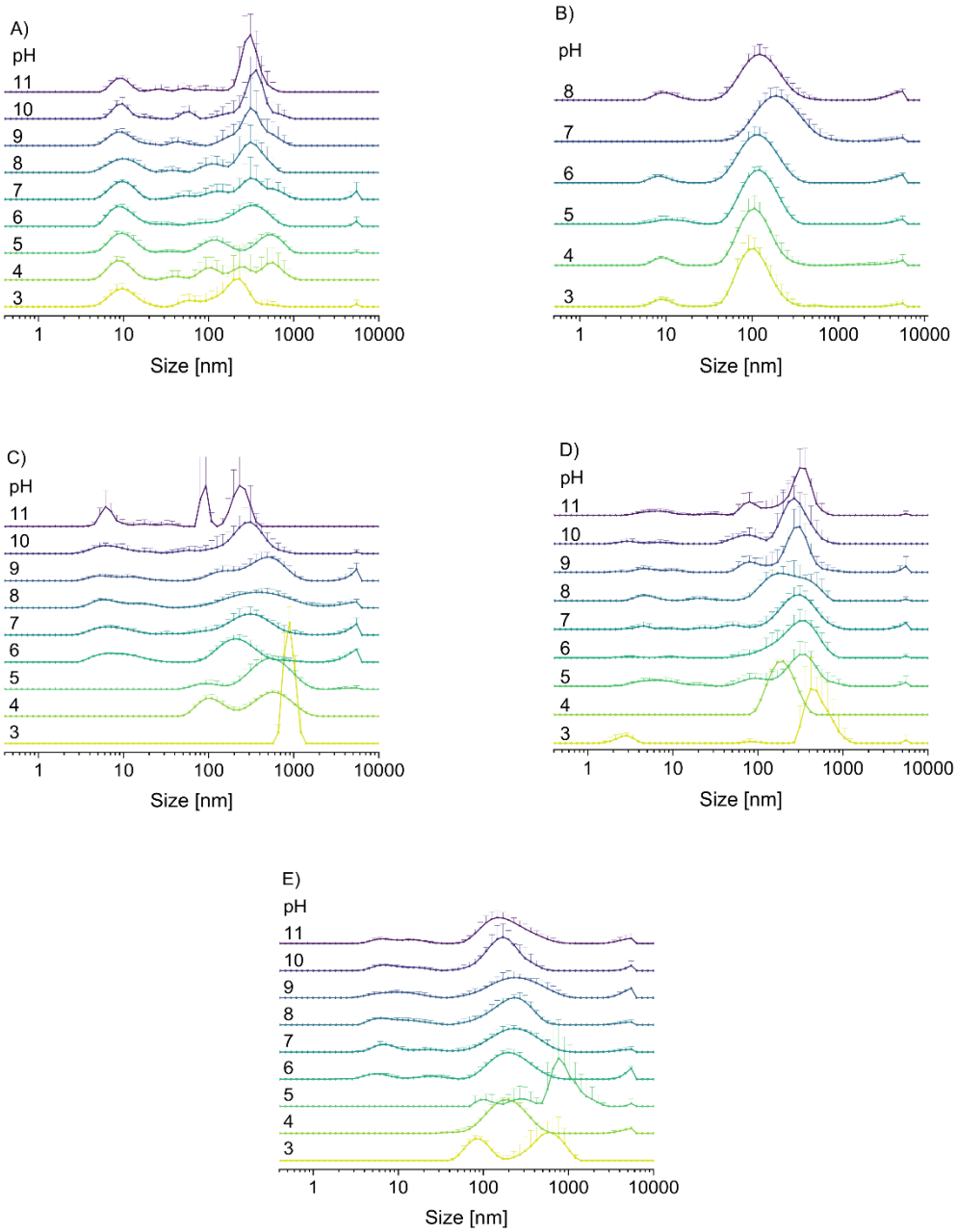


Figure S16. pH dependent intensity size distribution of A: P(Lys-OH-AAm). B: P(Me_3Lys-OH-Aam). C: P(Hex-OH-AAm). D: P(Phe-OH-AAm). E: P(PhenylPr-OH-AAm) in water (2 mg mL^{-1}) determined by DLS measurements. Values (scatter) represent the mean and SD

of five measurements with three runs each. Dashed lines do not represent measured values.

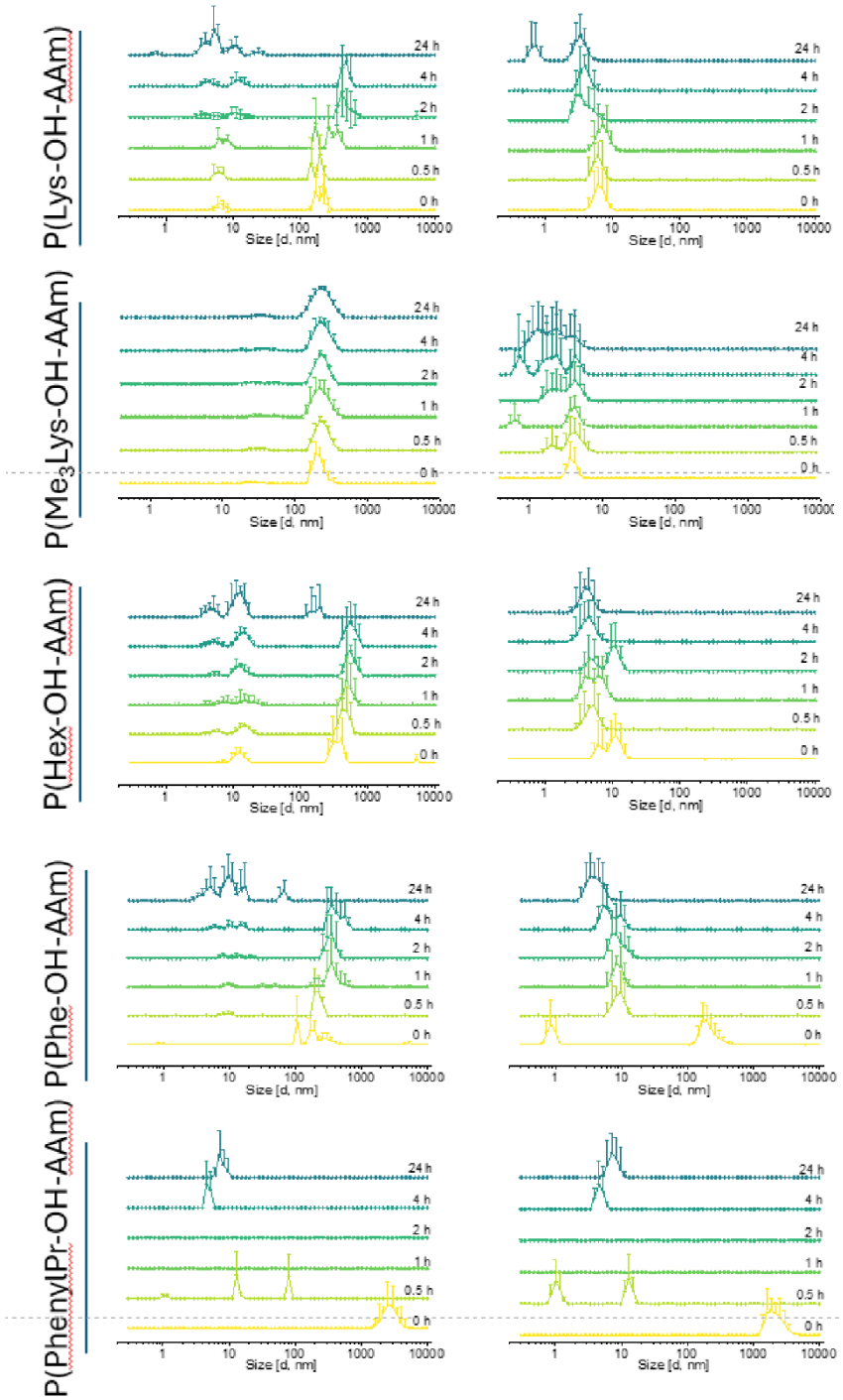


Figure S17. Intensity (left) and number (right) size distribution of polymer-Lysozyme-mixtures. The concentration of polymers and proteins was 0.5 mg mL^{-1} each in DPBS.

Sizes were analysed by DLS measurements at 37 °C. Values (scatter) represent the mean and SD of five measurements with three runs each. Dashed lines do not represent measured values.

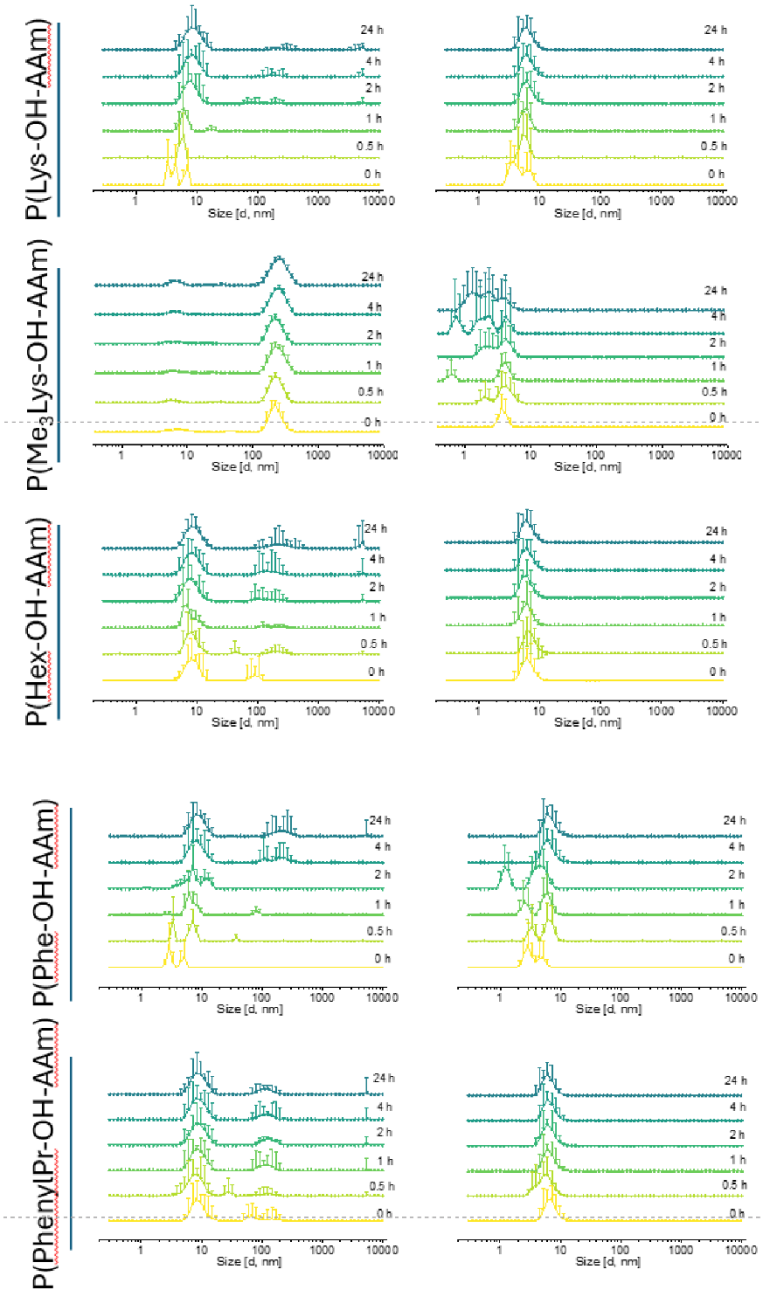


Figure S18. Intensity (left) and number (right) size distribution of polymer-BSA-mixtures. The concentration of polymers and proteins was 0.5 mg mL^{-1} each in DPBS. Sizes were analysed by DLS measurements at 37 °C. Values (scatter) represent the mean and SD of five measurements with three runs each. Dashed lines do not represent measured values.

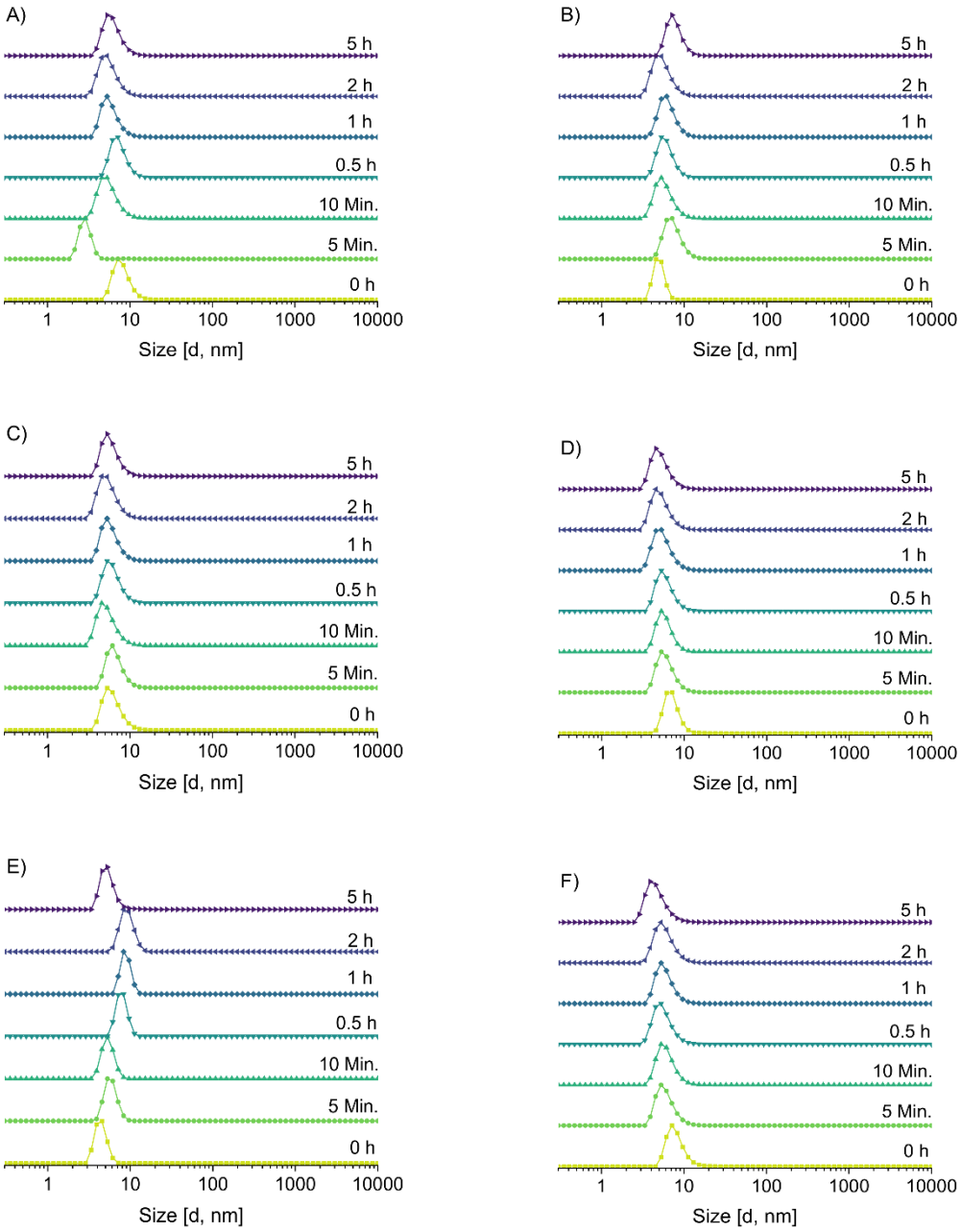


Figure S19. time dependent number size distribution of A: P(Lys-OH-AAm). B: P(Me_3Lys-OH-Aam). C: P(Hex-OH-AAm). D: P(Phe-OH-AAm). E: P(PhenylPr-OH-AAm). F: blank. In 90:10 V% [DPBS/FBS] (0.1 mg mL^{-1}) determined by DLS measurements. Values (scatter) represent the mean of six measurements with five runs each. Dashed lines do not represent measured values.

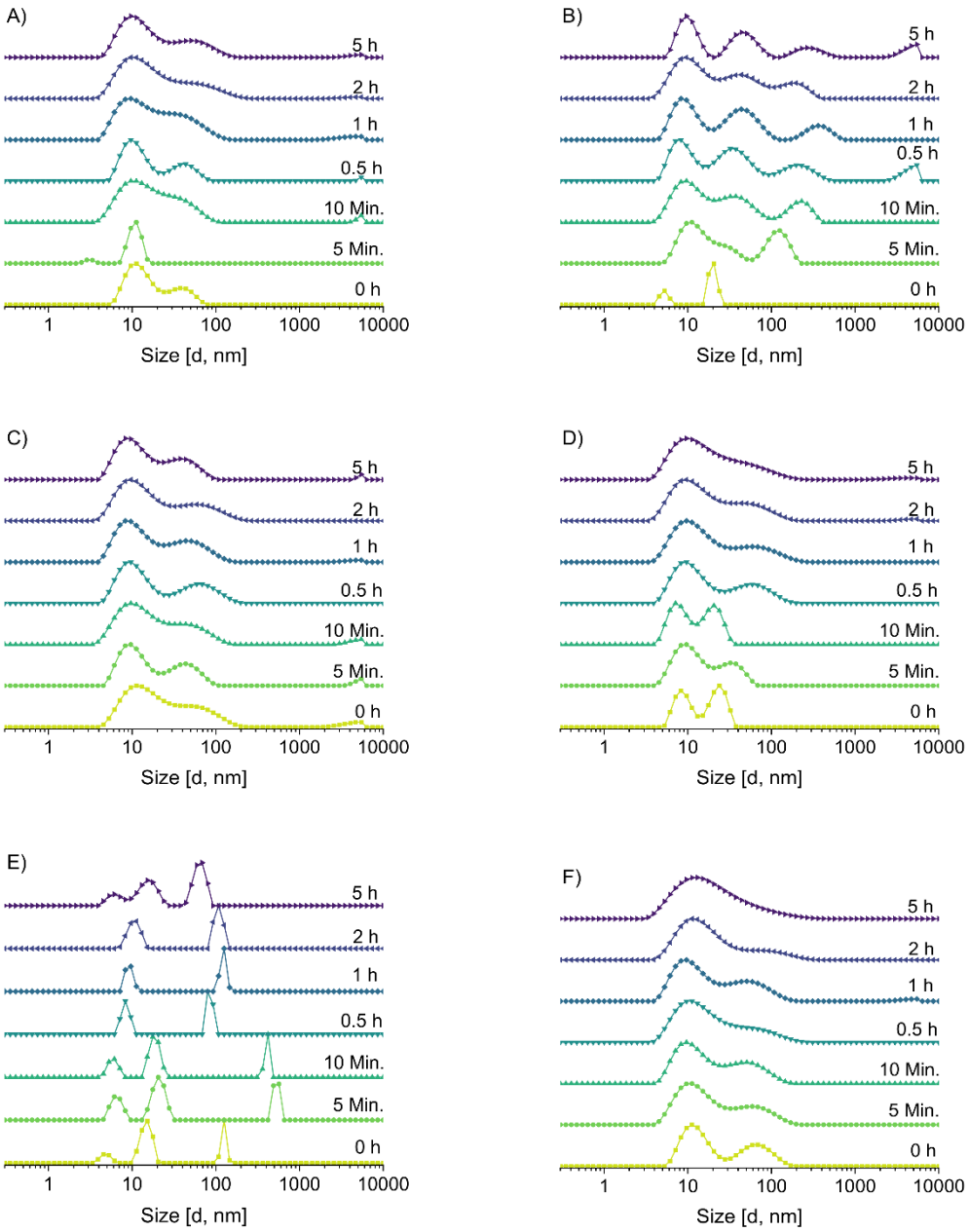


Figure S20. time dependent intensity based size distribution of A: P(Lys-OH-AAm). B: P(Me_3Lys-OH-Aam). C: P(Hex-OH-AAm). D: P(Phe-OH-AAm). E: P(PhenylPr-OH-AAm). F: blank. In 90:10 [DPBS/FBS] (0.1 mg mL^{-1}) determined by DLS measurements. Values (scatter) represent the mean of six measurements with five runs each. Dashed lines do not represent measured values.

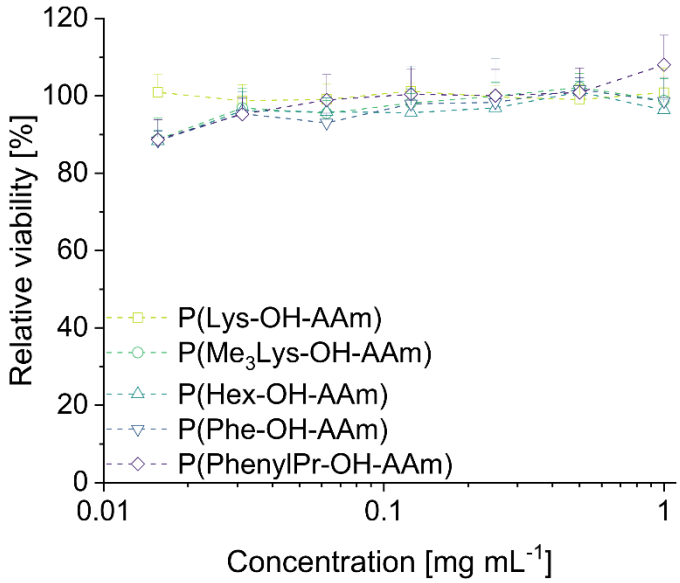


Figure S21. Cell viability of MDA-MB-231 breast cancer cells after incubation with P(Lys-OH-AAm), P(Me$_3$Lys-OH-Aam), P(Hex-OH-AAm), P(Phe-OH-AAm), P(PhenylPr-OH-AAm) for 24 h. Cell viability was determined by MTT assay. Cells without polymer treatment served as negative control (NC, 100% cell viability). Values shown are relative to the NC. Cells treated with 20% DMSO served as positive control (PC, 0% cell viability, data not shown)

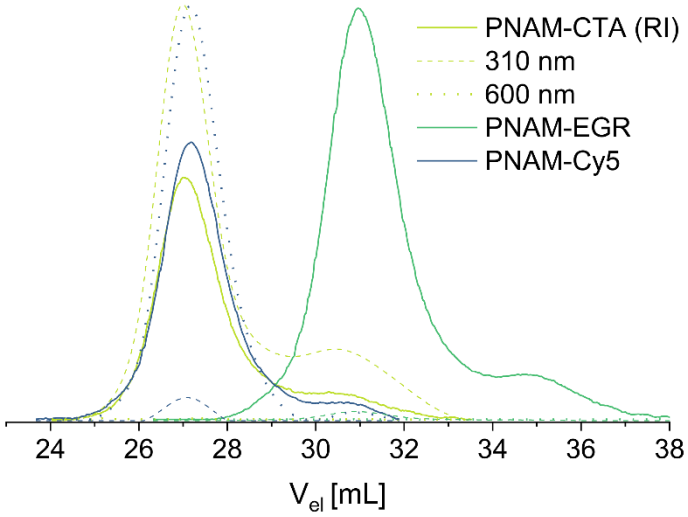


Figure S22. SEC (DMAc) elugram of P(NAM)-CTA, P(NAM)-EGR and P(NAM)-Cy5. Refractive index (line), λ = 310 nm (dashed) and λ = 600 nm (dotted)

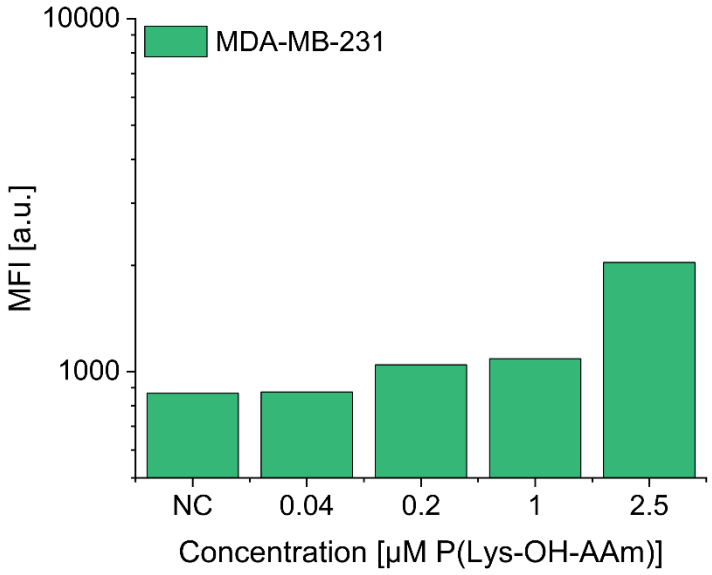


Figure S23. Dependence of the cellular association of P(Lys-OH-AAm)-Cy5 with MDA-MB-231 breast cancer cells depending on the polymer concentration. Cells were incubated with polymers in cell culture media and incubated at 37 °C for 1.5 h. MFI (columns) was determined using flow cytometry.

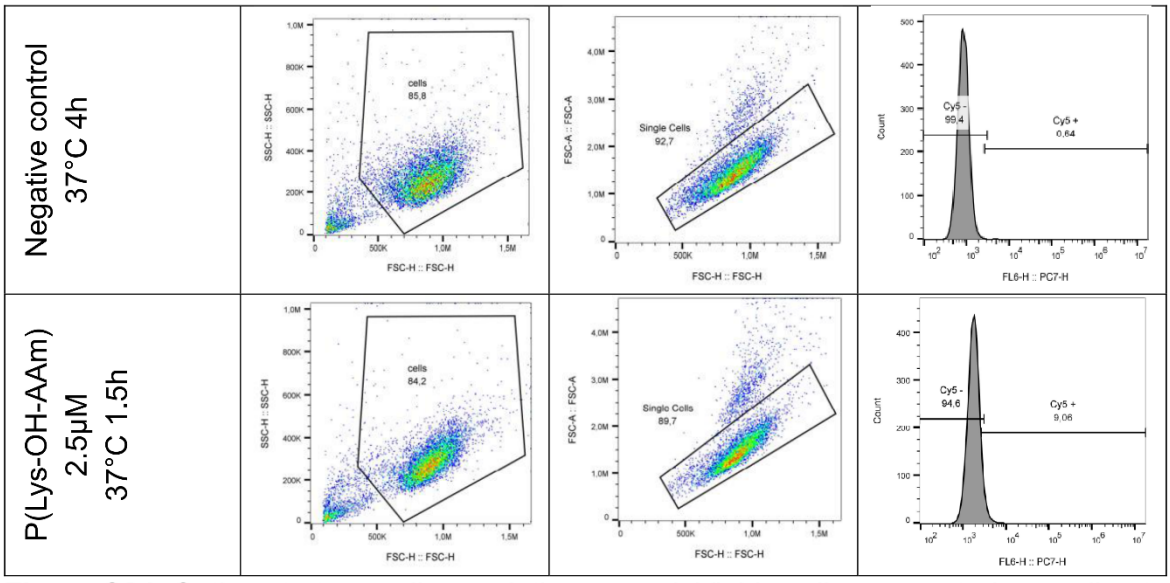


Figure S24. Gating strategy cell association assay I. Viable cells were gated according to the FSC/SCC pattern. Subsequently the single cells were discriminated from doublets in the sample using the area of FSC signal plotted against the FSC height. Cy5 positive cells were identified by the single cells to the negative control

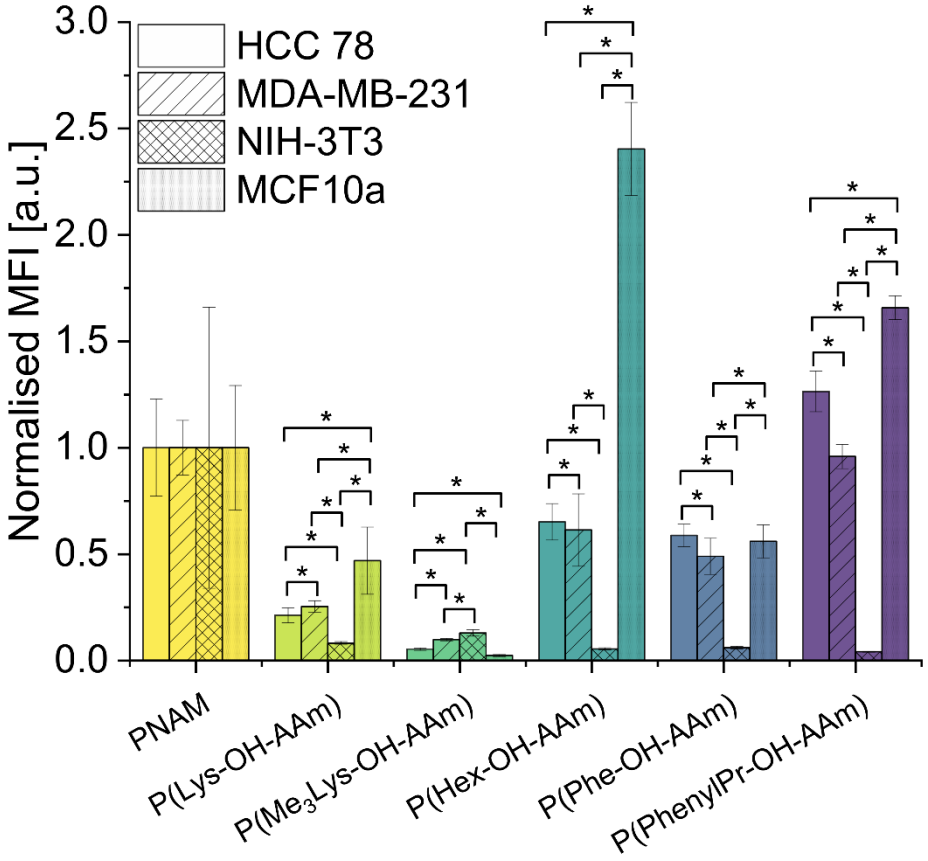
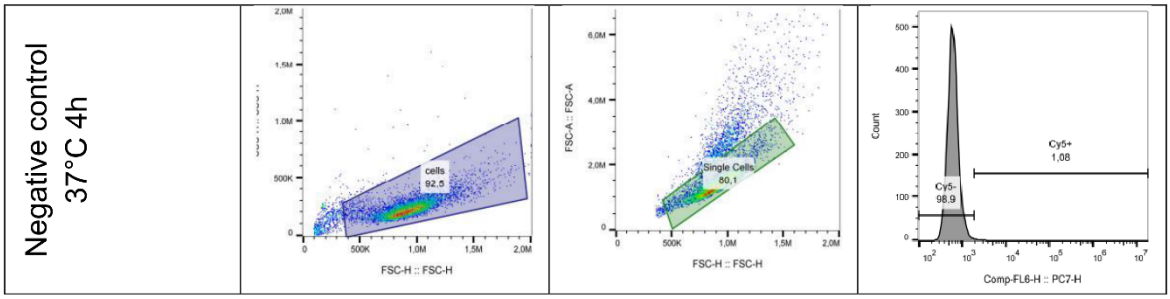


Figure S25. Cellular association of Cy5-labelled polymers with HCC-78, MDA-MB-231, NIH 3T3, and MCF10a as determined by flow cytometry. The cells were seeded in 24-well plates (50,000 cells/well) and incubated with 2.5 μM polymer solutions (500 μL of FBS-containing cell culture media) at indicated temperatures for 4 h. Values represent mean and SD (n = 4). *Indicates a significance of $p < 0.05$



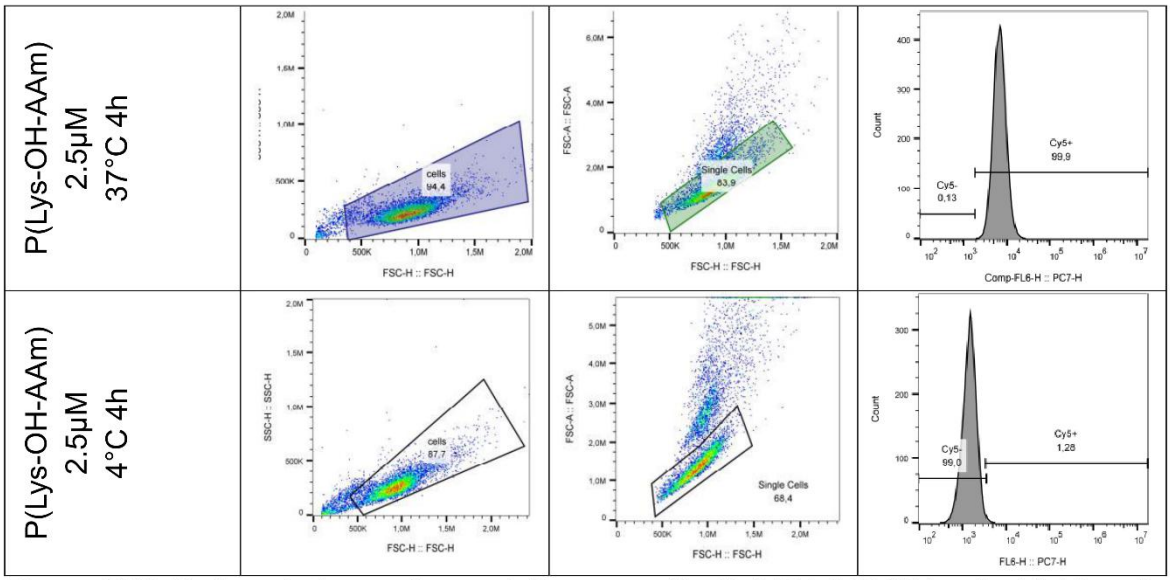


Figure S26. Gating strategy cell association assay II with MDA-MB-231 cells. Viable cells were gated according to the FSC/SCC pattern. Subsequently the single cells were discriminated from doublets in the sample using the area of FSC signal plotted against the FSC height. Cy5 positive cells were identified by the single cells to the negative control

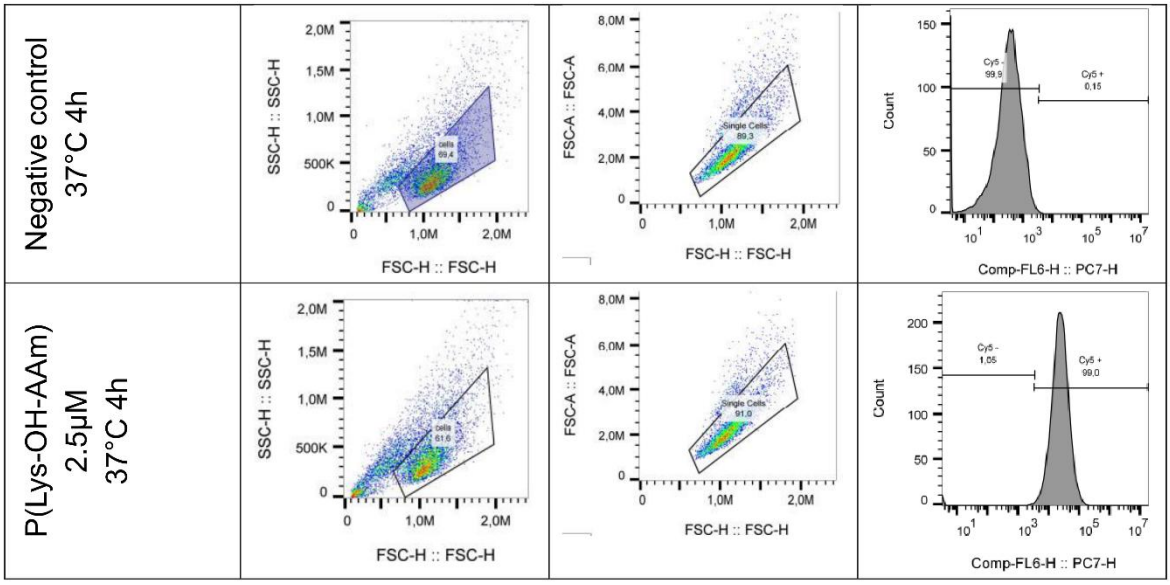


Figure S27. Gating strategy cell association assay II with HCC 78 cells. Viable cells were gated according to the FSC/SCC pattern. Subsequently the single cells were discriminated from doublets in the sample using the area of FSC signal plotted against the FSC height. Cy5 positive cells were identified by the single cells to the negative

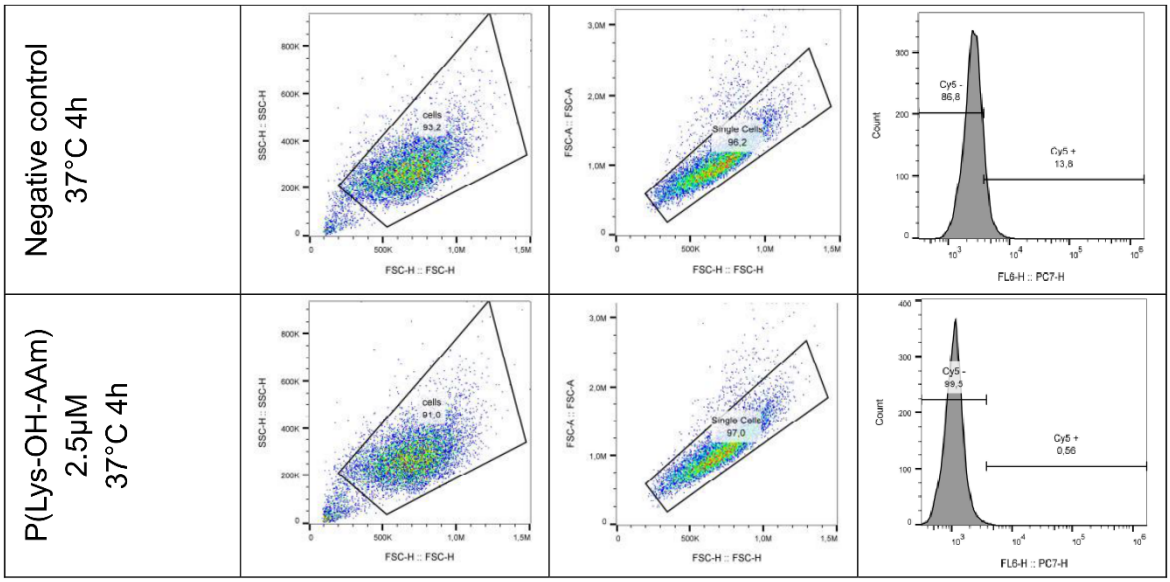
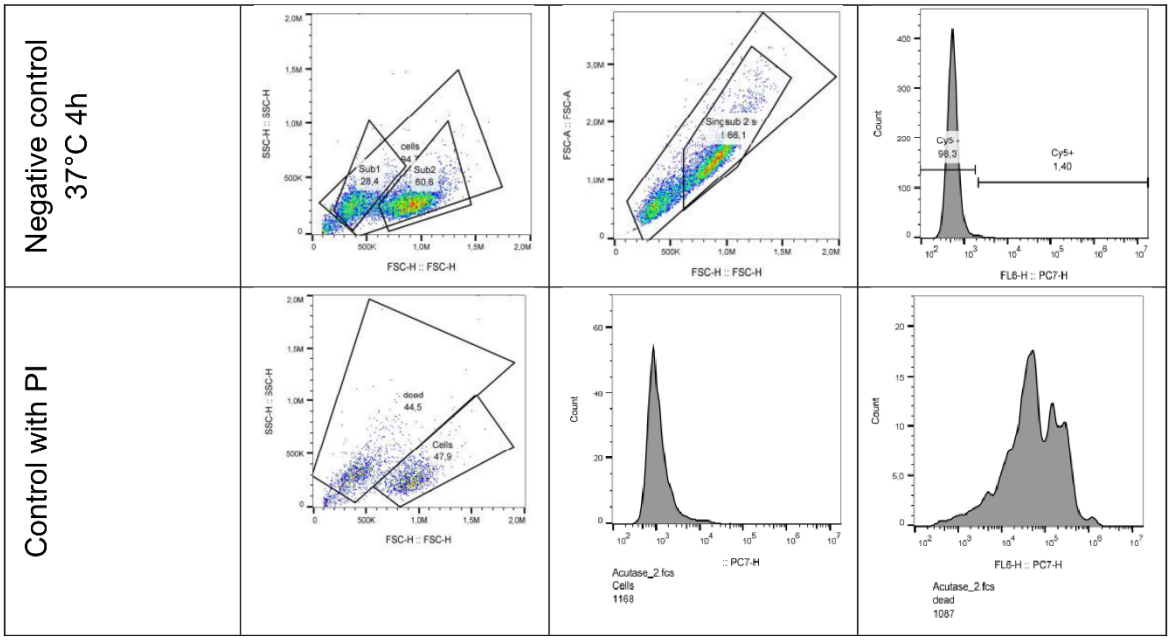


Figure S28. Gating strategy cell association assay II with NIH 3T3 cells. Viable cells were gated according to the FSC/SCC pattern. Subsequently the single cells were discriminated from doublets in the sample using the area of FSC signal plotted against the FSC height. Cy5 positive cells were identified by the single cells to the negative control



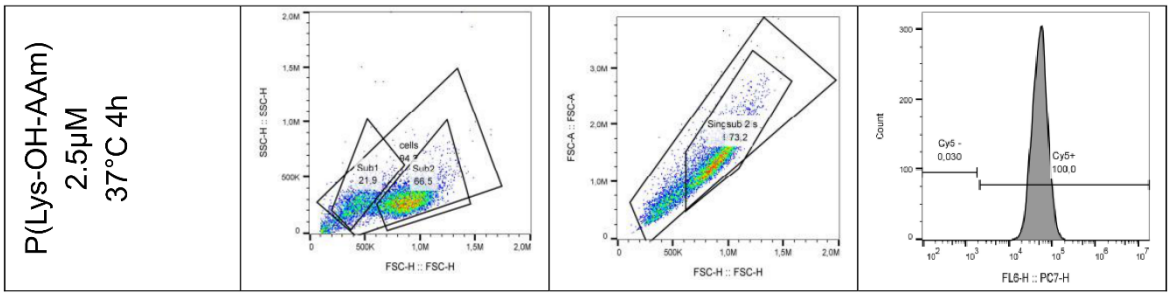


Figure S29. Gating strategy cell association assay II with MCF10a cells. Viable cells were gated according to the FSC/SCC pattern. Subsequently the single cells were discriminated from doublets in the sample using the area of FSC signal plotted against the FSC height. Cy5 positive cells were identified by the single cells to the negative control

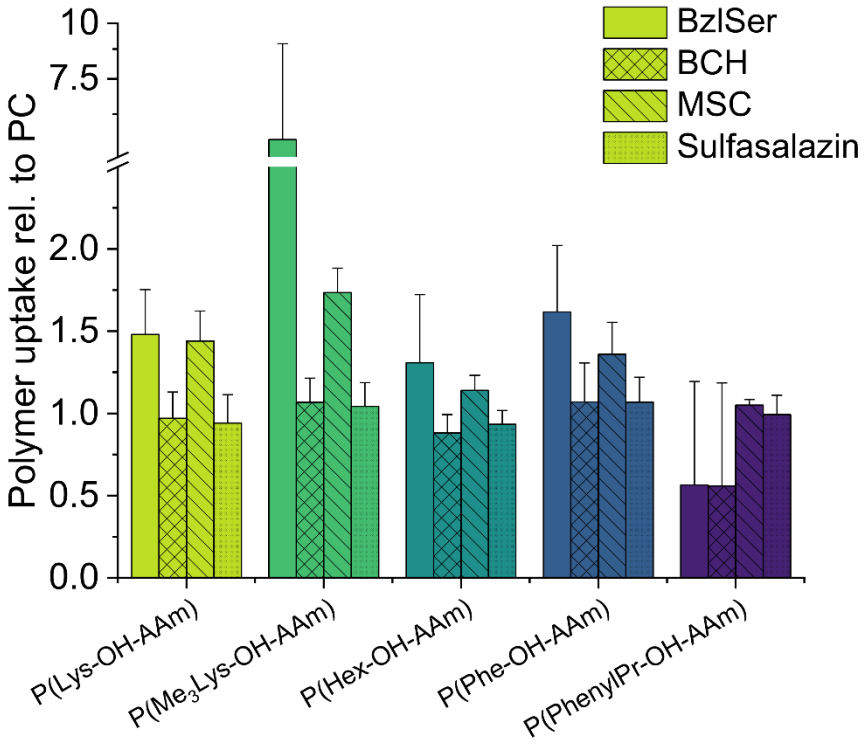


Figure S30. Cellular association of Cy5-labelled polymers with MDA-MB-231 breast cancer cells in the absence and presence of inhibitors determined via flow cytometry measurements. PC: No inhibitor was used. The cells were seeded in 24-well plates (50,000 cells/well) and incubated with 2.5 µM polymer solutions (500 µL of FBS-containing cell culture media) at indicated temperatures for 1 h. Values represent mean and SD (n=4).

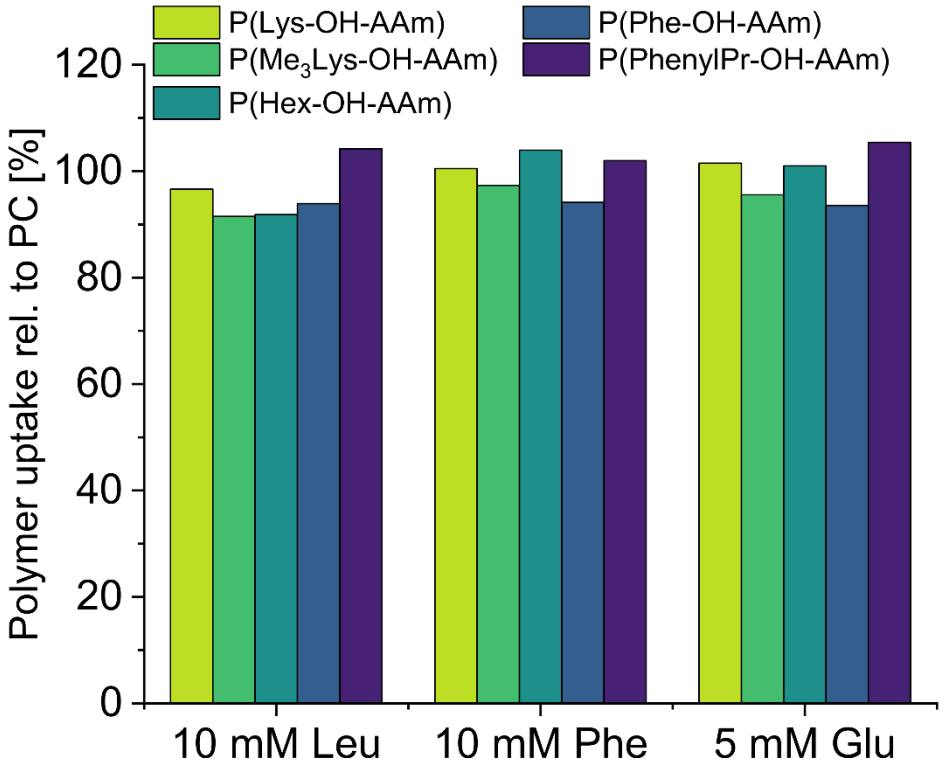


Figure S31. Cellular association of Cy5-labelled polymers with MDA-MB-231 breast cancer cells in the absence and presence of competitive amino acids determined via flow cytometry measurements. PC: No competitive amino acid was used. The cells were seeded in 24-well plates (50,000 cells/well) and incubated with 2.5 µM polymer solutions (500 µL of FBS-containing cell culture media) at indicated temperatures for 1 h. Values represent mean (n=2)

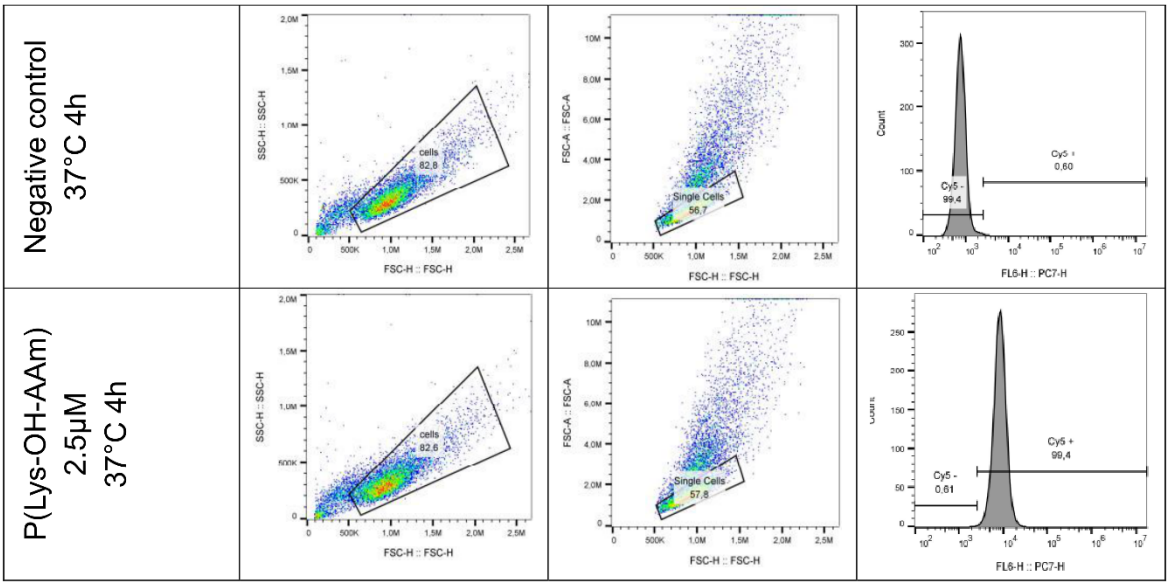


Figure S32. Gating strategy cell association assay III with MDA-MB-231 cells. Viable cells were gated according to the FSC/SCC pattern. Subsequently the single cells were discriminated from doublets in the sample using the area of FSC signal plotted against the FSC height. Cy5 positive cells were identified by the single cells to the negative control

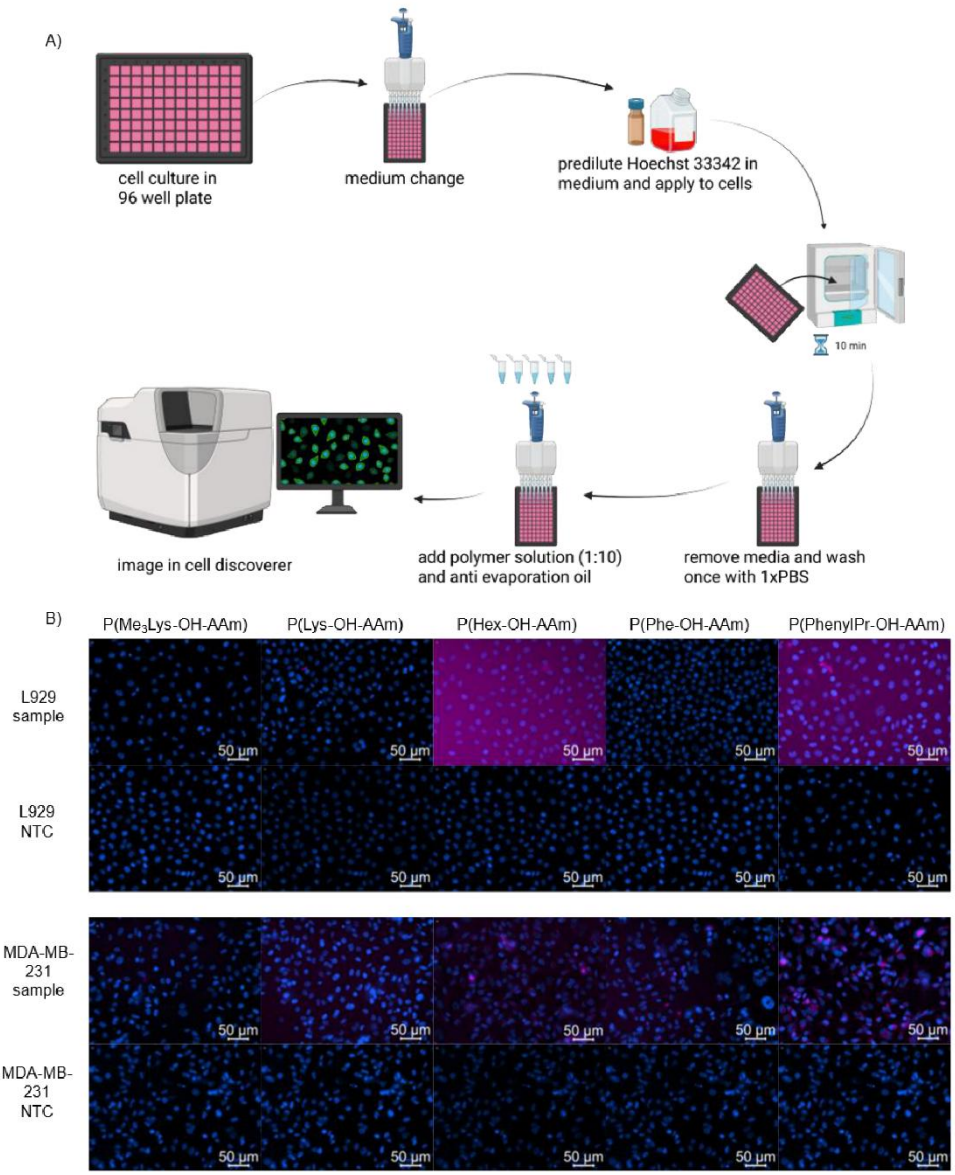


Figure S33. A) Workflow for the measurement of cells via Cell Discoverer 7. B) Extracted 4 h time point of Cell Discoverer 7 measurement. Sample measured under same settings. Image settings for polymers were individualized. Image settings for the non-treated control (NTC) have been the same as for respective polymer image settings. Upper row shows L929 cells treated with different polymer samples. Second row shows untreated L929 cells at 4 h timepoint. Third row shows MDA-MB-231 cells treated with different polymers and fourth row shows untreated MDA-MB-231 cells. The different polymers were added from left to right (P(Me$_3$Lys-OH-AAm)-Cy5, P(Lys-OH-AAm)-Cy5, P(Hex-OH-AAm)-Cy5, P(Phe-OH-AAm)-Cy5 and P(PhenylPr-OH-AAm))-Cy5.

1. Material and methods

L929 (mouse fibroblast cell line) and MDA-MB-231 (triple-negative human breast adenocarcinoma cell line) were cultured in DMEM (1 g × L^{-1} glucose, supplemented with 10% (v/v) FBS, 100 U × mL^{-1} penicillin, 100 µg × mL^{-1} streptomycin) in an IBIDI 96-well square plate. All cell lines were cultivated at 37 °C in a humidified 5% (v/v) CO_2 incubator. 24 h prior to treatment, cells were seeded at cell densities of 0.1 and 0.2 × 10^6 cells per mL respectively. 1 h prior to treatment medium has been replaced by 100 µL of fresh medium. 1 h after medium change, medium got exchanged by prewarmed medium supplemented with Hoechst 33342, trihydrochloride, trihydrate to reach a final amount of 0.1 µL of Hoechst solution per well. This solution was then incubated for 10 min in the incubator at 37 °C. Afterwards, the solution has been discarded and the cells were washed once with 100 µL prewarmed 1 × concentrated Dulbecco's PBS and immediately afterwards, 90 µL of prewarmed medium has been added to the cells, followed by 10 µL of different polymer solutions (P(Lys-OH-AAM), P(Me_3Lys-OH-AAm), P(Phe-OH-AAm), P(Phenyl-OH-AAm), P(Hex-OH-AAm) except for the control well, where 100 µL of medium were added. Final polymer solutions on cells were 2.5 µM. After adding of polymers all treated wells were covered with 100 µL IBIDI anti evaporation oil sterile for cell culture to reduce medium evaporation during experimentation. With finalization of cell preparation, the well has been moved to Carl Zeiss Cell Discoverer 7. Cells were cultivated further at 37 °C at 5% CO_2 and humidified atmosphere. From the first measurement on an image has been made every 1 h for a period of 24 h. For this purpose, the autofocus function of the machine has been used to find cells on basis of nucleus signal. The following laser settings were applied: Hoechst33342 has been measured at 352 nm excitation and 455 nm emission with a laser LED power of 20 % for 2 ms. CY5 signals have been measured at 650 nm excitation and 673 nm of emission at a laser LED power of 12.1% for 3 ms. Brightfield measurement took place at 10% laser power for 2.5 ms. All samples were measured with plan-apochromat 20 × /0.95 objective and 1 × tubulens. The created image settings were identical for each polymer throughout different cell lines and control samples, to obtain comparable results. The measurement has been performed at least twice, and the images are representative.

2. Results and Discussion

2.1. Uptake behaviour of Cy5 labelled polymers in L929 and MDA-MB231 cells

In line with previously measured data *via* flow cytometry, different polymer uptakes have been observed after 4 h of incubation. Polymer uptake was dependent on different

polymers as well as on different cell lines. All samples were measured under the same settings. Image settings were adapted individually for each polymer throughout the different cell lines and controls. Visibly, a higher overall polymer uptake could be achieved in MDA-MB-231 cells in comparison to L929 mouse fibroblast cells. These results are also in line with the tested fibroblast cells in flow cytometry measurements. Furthermore, the uptake of the polymers P(Hex-OH-AAm)-Cy5 and P(Phenyl-OH-AAm)-Cy5 showed the strongest uptake signals, followed by P(Phe-OH-AAm)-Cy5 in MDA-MB231, which could also be shown in the CLSM measurement after 1 h of uptake. The other two polymers (P(Lys-OOH-AAm)-Cy5 and P(Me_3Lys-OOH-AAm))-Cy5 showed low number of signals in both cell lines MDA-MB-231 and L929 cells, which could also be seen in the flow cytometry data for P(Me_3Lys-OOH-AAm))-Cy5. The overall reduced uptake behavior in these experiments for L929 cells has already been described elsewhere.

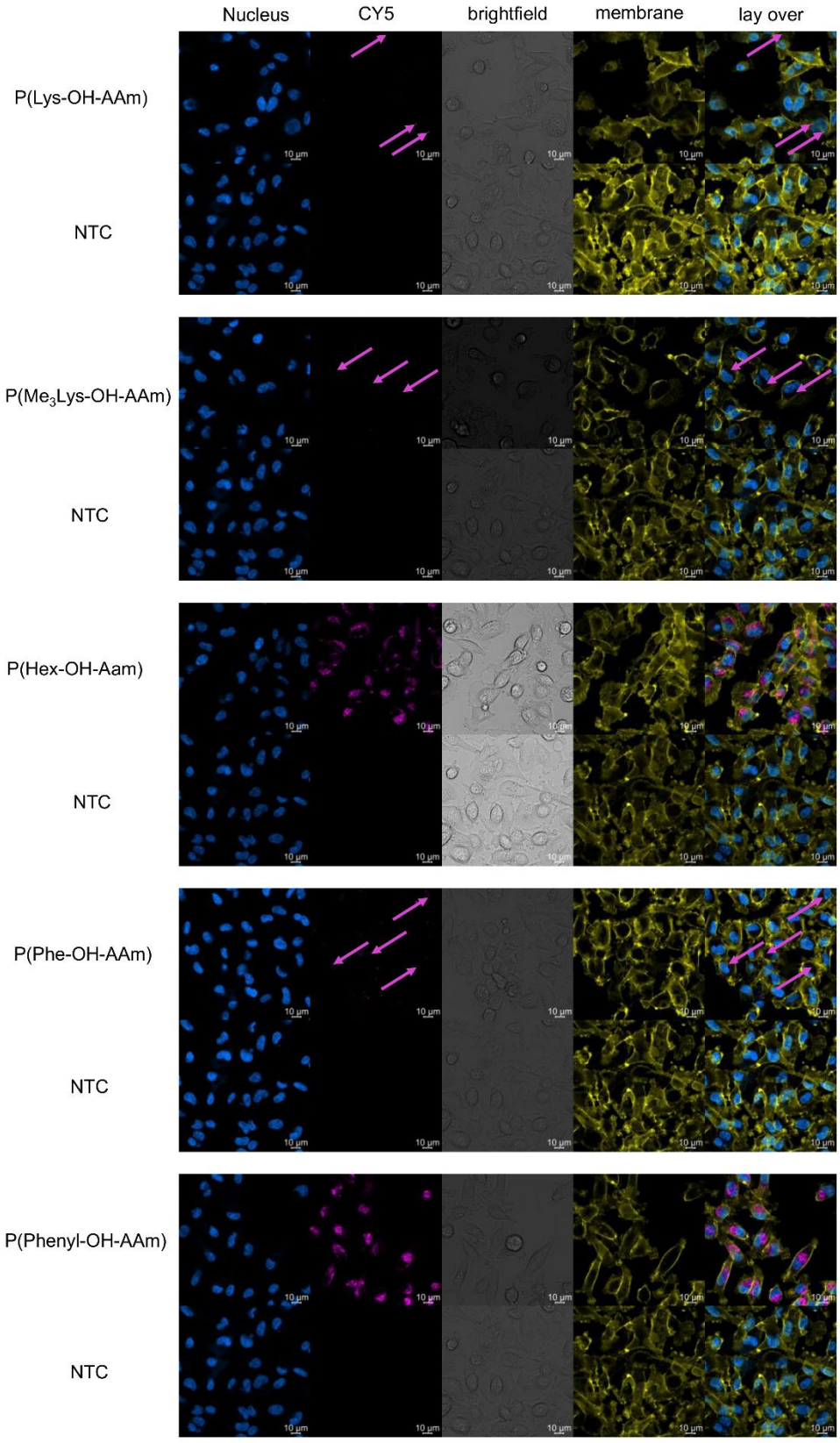

Nucleus
CY5
brightfield
membrane
lay over
P(Lys-OH-AAm)
NTC
P(Me3Lys-OH-AAm)
NTC
P(Hex-OH-Aam)
NTC
P(Phe-OH-AAm)
NTC
P(Phenyl-OH-AAm)
NTC

Figure S34. CLSM measurement of MDA-MB-231 cells after 1 h of incubation with different polymers in comparison to the non-treated control (NTC) with individual settings used for each polymer. Tested polymers from top to bottom: P(Lys-OOH-AAm), P(Me_3Lys-OOH-AAm), PP(Hex-OH-AAm), P(Phe-OH-AAm) and P(Phenyl-OH-AAm).

5 Danksagung

As first I would like to thank my supervisor, Prof Dr Meike N. Leiske or Meike for the trust she putted in me to do this PhD research after getting to know each other in the lab in Ghent. Without your trust and guidance the whole research process, including, the papers and thesis would not be written as smooth as they have gotten now. For this, I am thankful as for the short line of communication we had as a starting group while still having the freedom to develop my own research ideas. I found it extremely pleasant to do my PhD research as the first PhD student in your group as it started next to the labs of Prof Dr Schmidt who is retired by now. When we arrived, Prof Schmidt and his PhD students have accepted really fast at the chair, which a lot I can call my friends by now. I specially want to thank Florian, Julian, Dennis, Francesco, Nora, Jannik, Melina, Andi and Simon.

For the financial support I would like to thank the German research foundation just as the Graduate School of the University of Bayreuth

.As our group got pleasantly bigger over time, Dr Theresa Lutz joined our group who I also want to thank for her help in the writing and scientific process of two papers. Our (almost) endless discussions about our research and writing were very enjoyable and I learned a lot. Also a huge thank you for setting up the biolab and keeping it running.

In terms of bio-experiments, I also have to thank Dr Valérie Jérôme for introducing and guiding me during my first steps into the biolab. You're a very pleasant person to cooperate with and your expertise together with your work ethics are inspiring. Thanks for being there whenever I had a question or problem related to my bio experiment or results.

I also want to thank Rika Schneider for her countless SEC measurements. Annette and Dr. Dennis Schröder for their help introducing me to the NMR device. Jannik Petry for his help to get the GC device running.

A special thanks goes to my office partner, Martina, for the enjoyable Wednesdays till Fridays, and other members of Leiske lab for the scientific discussions, help and support. For support in the lab, I also want to thank all practical students which I had the pleasure of supervising.

Going further, I want to thank the people that got me and supported me towards this point in my life which is my foundation — my home, my parents and my family.

I want to thank my parents for making me the person I am today; for showing me that it's not about going to work every day just to make a living, but about doing something you are passionate about every day. You showed me that being happy with what you do each day makes you happier—and often successful—in the long run. You didn't show me the conventional or the easiest way, but the way where you have to put effort into achieving something. You showed me how it is to fail, and more importantly, how to cope with it and keep your motivation, even when it sometimes seems like everything that can go bad is moving in your direction. These are the work ethics I feel privileged to have grown up close to, and to see two passionate parents living what they love to do. It gave me confidence to choose the

rather unconventional path of studying natural sciences and moving to a city to do a doctoral thesis that only people from Belgium who love Richard Wagner have heard of. Something I'll never regret and will be forever thankful for.

Apart from that, I'm thankful for the caring parents you are. Supporting me during my studies in the best way you could, even without having experience in it yourselves. Bringing my lunch (almost every week), because I forgot it at home (again). Supporting me in doing my sport, teaching me how to ski (and après-ski 😊). Letting me fail (a lot) and being forgiving about it, even though you shouldn't always have been. You taught me more important lessons by being forgiving than any actual punishment ever could have. I'm thankful for giving me the freedom to develop myself, letting me go out into the world and explore. Starting with letting me go to summer camps and school trips, letting me go (with friends) to festivals and on holidays, and with that letting me choose my friends.

Those friends, who I don't want to name all, because I am afraid to forget one of them, made a part my personality since my adolescence. It is crazy and inspiring to see how such different people who, based on career and life choices, went in such different directions can still see each other on weekends, and be open about feelings, issues, opinions, experiences, and stories. They still teach and impress me every time I see them, with their (sometimes different) life visions, which make them so inspiring, unique, and one-for-one perfect at the same time. I wouldn't know who I would be if I hadn't met every single one of them. They made me feel loved and unique every time I see them. They made me feel missed with their random texts saying they will be happy when I'm back in Belgium as they miss me (although I'm still wondering if those were drunk texts on a Thursday evening). They were always interested in everything that was happening in my life although it is sometimes so far away from theirs. They are therefore one of the reasons I'm moving back to the place where I have my roots. They made this friendship extra special by taking time out of their own lives to visit me here, in a city that none of them had on their bingo card for 2024. Things like that, and being the people they are, give them a special place in my heart.

It is crazy and inspiring to see how such a different people who, based on carrier and life choices, went is such a different directions can still see each other during the weekends, be open towards about feelings, issues, opinions, experiences and stories. They still teach and impress me every time I see them with their (sometimes different) life visions which make them so inspiring, unique and one for one perfect at the same time. I wouldn't know who I would be if I wouldn't have met ever single one of them. They made me feel loved and unique every time I see them. Made me feel missed by their random text saying that they missed me and would be back in Belgium (although I'm still wondering if those were drunk texts on a Thursday evening). They were always interested in everything what was happening in my life and are one of the reasons I'm moving back to the place I have my roots. They made this friendship extra special by having taken time out of their own life to visit me here in a city that none of them had on their bingo card of 2024. Such things and being the persons they are, gives them a special place in my heart.

Lastly, I want to thank my parents for giving me two beautiful sisters (for the last one, I also have to thank Cindy). It is difficult to describe in words what comes to my mind when I think of them. One of

them is, at this time, a young adolescent who is finding her way in life, and it is incredible to see how she is doing that. I am thankful that she lets me be so close to her life and be part of the journey she is going through as a young woman, even though we were separated by such a big distance for the last three years. Our Wednesday calls or “yap session” made the distance go away and let me be the present brother I want to be. Although you are considerably younger, you’ve already taught me important things in life. Love you!

My older, but shorter, sister is as extraordinary as they come. At the moment, she’s finishing a master that no-one would have thought she would have been able to do 10 years ago. Speaking about people with incredible passion and work ethic, she is at the top of my list. It is amazing to see what she is achieving and how confident and grounded she is in life. I appreciate a lot how you open up your insecure side to me and are willing to discuss all the doubts you have in life. We’ve lived the longest time of our lives together and no one will be able to understand the path we went through in life like we do. Therefore, you’re one of the most valuable people in my life. I love spending time with you and appreciate you as you’’ll always (try) to understand me even though it is sometimes difficult. I’ll cherish you for the rest of my life. Looking at my two incredible sisters makes me feel the underperformer of the family, although they probably look at me the same way. I’m incredibly proud to call them my sister and I am and always will be happy to have them in my life.

About Bayreuth. If I’m looking back at it now, and I’m quite sure I’ll think the same later, I’m happy about the fact that I’ve made the decision to do my doctoral thesis in Bayreuth. I’ve met a lot of people that would otherwise have never been in my life, learned a (the Bayern) culture that I would otherwise never have. I’ve learned and still try to appreciate the beer, just as everyone tried to appreciate the ones I brought once a year with me.

During my time people like Dennis, Marius, Rika, Roman and Sebastian took me to my first beer fest, and my second, and my third which also got joined by Emilia and Marvin who joined later. Off course not too much can be said about these events as this will be once printed out, but this was the beginning of a special friendship and an incredible three years where I grew both inside and outside the lab. Without those people this journey wouldn’t have been the same, they made me feel welcome and part of their friends group as if I was always in there. Once I’ve moved from NWII to B6, I got Dennis convinced to join and a new colleague–Marvin–joined the lab. This was one of the most productive and fun times I had as I finally had a colleagues where I could share my ideas and coffee with (@Dennis, learn how to drink coffee). Me and Martina were also able to introduce Schlager Freitag, which at one exception changed to Blasmusik during the Bayrische Woche. One day a week where all doors in the lab were closed except ours. As new people come and go at university, I got Jiaxin at one point as my colleague and had to say goodbye to Dennis. In her own way, she made herself a very enjoyable colleague who until now, never told me I was wrong.

I also shortly want to thank the ‘fun’ students we had in the group during my time. Especially, Natascha, Katja and Lena made the breaks and working atmosphere very enjoyable. Knowing that the three of you will be coming back to the lab makes me feel like a bit of a legacy that I leave behind, although we all know that you are coming back because Meike is an amazing supervisor.

At last I’m thankful for the unique environment that a university offers. This gave me the opportunity to get to know a lot of visiting students. Rita, Lina, Masylia and Brandon I love you all.

If you came this far, a final thank you for reading this far, or the last page 😊

(Eidesstattliche) Versicherungen und Erklärungen

(§ 9 Satz 2 Nr. 3 PromO BayNAT)

Hiermit versichere ich eidesstattlich, dass ich die Arbeit selbstständig verfasst und keine anderen als die von mir angegebenen Quellen und Hilfsmittel benutzt habe (vgl. Art. 97 Abs. 1 Satz 8 BayHIG).

(§ 9 Satz 2 Nr. 3 PromO BayNAT)

Hiermit erkläre ich, dass ich die Dissertation nicht bereits zur Erlangung eines akademischen Grades eingereicht habe und dass ich nicht bereits diese oder eine gleichartige Doktorprüfung endgültig nicht bestanden habe.

(§ 9 Satz 2 Nr. 4 PromO BayNAT)

Hiermit erkläre ich, dass ich Hilfe von gewerblichen Promotionsberatern bzw. -vermittlern oder ähnlichen Dienstleistern weder bisher in Anspruch genommen habe noch künftig in Anspruch nehmen werde.

(§ 9 Satz 2 Nr. 7 PromO BayNAT)

Hiermit erkläre ich mein Einverständnis, dass die elektronische Fassung meiner Dissertation unter Wahrung meiner Urheberrechte und des Datenschutzes einer gesonderten Überprüfung unterzogen werden kann.

(§ 9 Satz 2 Nr. 8 PromO BayNAT)

Hiermit erkläre ich mein Einverständnis, dass bei Verdacht wissenschaftlichen Fehlverhaltens Ermittlungen durch universitätsinterne Organe der wissenschaftlichen Selbstkontrolle stattfinden können.

Sint-Niklaas, 30/07/2026

……

Ort, Datum, Unterschrift